PERIPHERAL REGULATORS OF OBESITY

EDITED BY: Andrew J. McAinch, Deanne H. Hryciw and Sudip Bajpeyi
PUBLISHED IN: Frontiers in Endocrinology

frontiers Research Topics

ISSN 1664-8714
ISBN 978-2-88963-020-2
DOI 10.3389/978-2-88963-020-2

About Frontiers

Frontiers is more than just an open-access publisher of scholarly articles: it is a pioneering approach to the world of academia, radically improving the way scholarly research is managed. The grand vision of Frontiers is a world where all people have an equal opportunity to seek, share and generate knowledge. Frontiers provides immediate and permanent online open access to all its publications, but this alone is not enough to realize our grand goals.

Frontiers Journal Series

The Frontiers Journal Series is a multi-tier and interdisciplinary set of open-access, online journals, promising a paradigm shift from the current review, selection and dissemination processes in academic publishing. All Frontiers journals are driven by researchers for researchers; therefore, they constitute a service to the scholarly community. At the same time, the Frontiers Journal Series operates on a revolutionary invention, the tiered publishing system, initially addressing specific communities of scholars, and gradually climbing up to broader public understanding, thus serving the interests of the lay society, too.

Dedication to Quality

Each Frontiers article is a landmark of the highest quality, thanks to genuinely collaborative interactions between authors and review editors, who include some of the world's best academicians. Research must be certified by peers before entering a stream of knowledge that may eventually reach the public - and shape society; therefore, Frontiers only applies the most rigorous and unbiased reviews.
Frontiers revolutionizes research publishing by freely delivering the most outstanding research, evaluated with no bias from both the academic and social point of view. By applying the most advanced information technologies, Frontiers is catapulting scholarly publishing into a new generation.

What are Frontiers Research Topics?

Frontiers Research Topics are very popular trademarks of the Frontiers Journals Series: they are collections of at least ten articles, all centered on a particular subject. With their unique mix of varied contributions from Original Research to Review Articles, Frontiers Research Topics unify the most influential researchers, the latest key findings and historical advances in a hot research area! Find out more on how to host your own Frontiers Research Topic or contribute to one as an author by contacting the Frontiers Editorial Office: researchtopics@frontiersin.org

PERIPHERAL REGULATORS OF OBESITY

Topic Editors:
Andrew J. McAinch, Victoria University, Australia
Deanne H. Hryciw, Griffith University and Victoria University, Australia
Sudip Bajpeyi, University of Texas at El Paso, United States

Citation: McAinch, A. J., Hryciw, D. H., Bajpeyi, S., eds. (2019). Peripheral Regulators of Obesity. Lausanne: Frontiers Media. doi: 10.3389/978-2-88963-020-2

Table of Contents

frontiers in Endocrinology

EDITORIAL
published: 04 June 2019
doi: 10.3389/fendo.2019.00357

Editorial: Peripheral Regulators of Obesity

Andrew J. McAinch[1,2]*, *Deanne H. Hryciw*[1,3] *and Sudip Bajpeyi*[4]

[1] *Institute for Health and Sport, College of Health and Biomedicine, Victoria University, Melbourne, VIC, Australia,* [2] *Australian Institute for Musculoskeletal Science, Victoria University, Melbourne, VIC, Australia,* [3] *School of Environment and Science, Griffith Sciences, Griffith University, Nathan, QLD, Australia,* [4] *Department of Kinesiology, College of Health Sciences, University of Texas at El Paso, El Paso, TX, United States*

Keywords: obesity, diabetes, adipose tissue, body composition, TRPV1 - transient receptor potential vanilloid type 1 receptor, PPAR gamma, HIV, hepatocyte growth factor (HGF)

Editorial on the Research Topic

Peripheral Regulators of Obesity

The incidence of obesity is increasing significantly worldwide and is considered one of the most significant public health challenges due to the associated disease states increasing morbidity and mortality and reducing quality of life. Despite the impact (both social and economic) of obesity little is known of the complex physiology that dictates the maintenance of the obese state and resistance to weight loss, and the link between obesity and complex diseases, including type 2 diabetes. Understanding the peripheral abnormalities that are present in obesity are essential to our development of treatments for these conditions. This special issue aimed to elucidate at least some of the complex interactions that occur particularly in the periphery. The special issue contained a mix of 4 review articles and 6 original manuscripts ranging from cell culture studies to clinical trials and large cross sectional observations.

The review by Christie et al. discusses TRPV1 structure and function, how this is linked to the endocannabinoid system, energy homeostasis, appetite control, and gastrointestinal vagal afferents. The review concluded with how TRPV1 activation may stimulate energy expenditure particularly via brown adipose tissue thermogenesis and its role in β-cell function in diabetes. However, despite TRPV1's potential roles in energy expenditure and blood glucose regulation, it has complex interactions with many signaling pathways. Thus further research to provide fundamental physiological understanding of TRPV1 to enable targeted treatment options for obesity and associated metabolic diseases is required.

Peroxisome proliferator-activated receptor γ (PPARγ) and its role in adipocytes via dynamic change of transcription was reviewed by Ma et al. PPARγ plays a key role in adipogenesis through ligand binding and selective interaction with transcriptional corepressors or coactivators. Of note, PPARγ plays a critical role in the determination of the brown and beige adipocytes. Ma et al. conclude via the discussion of the role of specific PPARγ phosphorylation sites and how stimulation of phosphorylation at different sites results in potentially different physiological outcomes.

The special issue continues with the review investigating insulin resistance induced by antiretroviral drugs in HIV-Patients by Pedro et al. This review discusses the increase in circulating proinflammatory cytokines and bacterial lipopolysaccharides resulting in downregulation of insulin signaling. Through discussion of what is known about the molecular signaling associated with antiretroviral induced insulin resistance as well as the link with gut microbiota and obesity and dyslipidemia, this review highlights the need for further research into this condition to enable the next generation of targeted medications to ensure the long term quality of life of HIV patients.

OPEN ACCESS

Edited and reviewed by:
Konstantinos Tziomalos, Aristotle University of Thessaloniki, Greece

***Correspondence:**
Andrew J. McAinch
andrew.mcainch@vu.edu.au

Specialty section:
This article was submitted to Obesity, a section of the journal Frontiers in Endocrinology

Received: *12 March 2019*
Accepted: *20 May 2019*
Published: *04 June 2019*

Citation:
McAinch AJ, Hryciw DH and Bajpeyi S (2019) Editorial: Peripheral Regulators of Obesity. Front. Endocrinol. 10:357. doi: 10.3389/fendo.2019.00357

The theme of insulin resistance is also continued in the review by Oliveira et al. which discusses the role of hepatocyte growth factor (HGF) in insulin resistance and diabetes. This review discusses the structure and function of HGF and its role in the regulation of glucose metabolism in different cells and tissues. It then continues to provide insight into the involvement of HGF in inflammatory responses as well as cancer therapy and thus the complexity of targeting HGF in obesity or diabetes.

The reviews captured in this special issue provide an interesting snapshot of the current state of research into several signaling cascades that are associated with obesity and insulin resistance as well as the influence of other disease states on these signaling cascades in a number of tissues, including adipose tissue. The special issue then continues with a study by Merlin et al. which demonstrates that cultured white adipocytes derived from regions such as inguinal white adipose tissue (iWAT) with adequate sympathetic innervation respond efficiently to agonists, but only in combination with an additional priming stimulus such as rosiglitazone. This contrasts with *in vivo* iWAT depots in which chronic sympathetic tone is sufficient to maintain the capacity for brite (or beige) activation. This study emphasized the importance of activating both browning and thermogenic programs in cultured white adipocytes in order to reach maximum browning capacity.

Understanding the impact of not just obesity, but also how our body stores and distributes fat mass can have important implications on our health. Cui et al., determined that in Qingdao, China, being classified as overweight or having abdominal obesity as determined by waist circumference was associated with depression whereas waist-to-hip ratio was not. The impact of body composition not just body weight was also investigated by Colleluori et al. which observed a U-shaped distribution of fat mass when correlated to estradiol (Serum E_2) levels in postmenopausal women which was different to the linear increase seen when only looking at body weight or body mass index (BMI). This study raises some speculations regarding E_2 sensitivity and fat mass regulation in postmenopausal women. An inverse association with circulating SIRT1 and adiposity levels across the body weight range (underweight to obese) was also observed by Mariani et al. This inverse association was also associated with liver fat content, insulin and other markers of metabolic phenotype.

Even in the healthy weight range, according to BMI, Park et al. determined that young women classified as plump (around 55 kg) compared to slim (around 46 kg) young women showed more atherogenic features in LDL and HDL as well as elevated oxidation and glycation with loss of antioxidant ability and apoA-I. Despite these observations, interventions can improve the health outcomes, as determined in this special issue's final manuscript by Telles et al. In this study Telles et al. demonstrated an age effect, with women with central obesity between 30 and 45 years of age having a greater reduction in measures such as waist circumference and BMI following 12 weeks of yoga compared to the control group who just received nutritional advice. This reduction was not seen in the 46–59 year age range, which demonstrates that early interventions may have better health outcomes.

AUTHOR CONTRIBUTIONS

All authors listed have made a substantial, direct and intellectual contribution to the work, and approved it for publication.

Conflict of Interest Statement: The authors declare that the research was conducted in the absence of any commercial or financial relationships that could be construed as a potential conflict of interest.

frontiers in Endocrinology

REVIEW
published: 31 July 2018
doi: 10.3389/fendo.2018.00420

Involvement of TRPV1 Channels in Energy Homeostasis

Stewart Christie[1], *Gary A. Wittert*[1,2], *Hui Li*[1,2] *and Amanda J. Page*[1,2]*

[1] *Vagal Afferent Research Group, Centre for Nutrition and Gastrointestinal Disease, Adelaide Medical School, University of Adelaide, Adelaide, SA, Australia,* [2] *Nutrition and Metabolism, South Australian Health and Medical Research Institute, Adelaide, SA, Australia*

The ion channel TRPV1 is involved in a wide range of processes including nociception, thermosensation and, more recently discovered, energy homeostasis. Tightly controlling energy homeostasis is important to maintain a healthy body weight, or to aid in weight loss by expending more energy than energy intake. TRPV1 may be involved in energy homeostasis, both in the control of food intake and energy expenditure. In the periphery, it is possible that TRPV1 can impact on appetite through control of appetite hormone levels or via modulation of gastrointestinal vagal afferent signaling. Further, TRPV1 may increase energy expenditure via heat production. Dietary supplementation with TRPV1 agonists, such as capsaicin, has yielded conflicting results with some studies indicating a reduction in food intake and increase in energy expenditure, and other studies indicating the converse. Nonetheless, it is increasingly apparent that TRPV1 may be dysregulated in obesity and contributing to the development of this disease. The mechanisms behind this dysregulation are currently unknown but interactions with other systems, such as the endocannabinoid systems, could be altered and therefore play a role in this dysregulation. Further, TRPV1 channels appear to be involved in pancreatic insulin secretion. Therefore, given its plausible involvement in regulation of energy and glucose homeostasis and its dysregulation in obesity, TRPV1 may be a target for weight loss therapy and diabetes. However, further research is required too fully elucidate TRPV1s role in these processes. The review provides an overview of current knowledge in this field and potential areas for development.

Keywords: TRPV1, appetite regulation, metabolism, obesity, endovanilloid, endocannabinoid

OPEN ACCESS

Edited by:
Andrew J. McAinch,
Victoria University, Australia

Reviewed by:
Denis P. Blondin,
Université de Sherbrooke, Canada
Thomas Alexander Lutz,
Universität Zürich, Switzerland

***Correspondence:**
Amanda J. Page
Amanda.page@adelaide.edu.au

Specialty section:
This article was submitted to Obesity, a section of the journal Frontiers in Endocrinology

Received: *30 March 2018*
Accepted: *04 July 2018*
Published: *31 July 2018*

Citation:
Christie S, Wittert GA, Li H and Page AJ (2018) Involvement of TRPV1 Channels in Energy Homeostasis. Front. Endocrinol. 9:420. doi: 10.3389/fendo.2018.00420

INTRODUCTION

Obesity has become the fifth leading cause of death, and the second leading cause of preventable death worldwide, closely following tobacco smoking (1, 2). There are multiple hormonal, neurotransmitter, and receptor systems involved in the regulation of energy balance. Pharmacological attempts to favorably modulate these systems to encourage weight loss have been somewhat effective, although not without adverse side effects. This has led to the search for more suitable targets. One such group of receptors/ion channels gaining attention for their possible role in energy homeostasis are the Transient Receptor Potential (TRP) channels.

TRP channels are a superfamily of about 28 non-selective cation channels divided into 7 subfamilies including TRP vanilloid (TRPV), and TRP ankyrin (TRPA) (3). They were first identified in 1969 from an irregular electroretinogram in a mutant strain of the *Drosophila* fly (4). The electroretinogram presented a short increase in retinal potential which gave rise to the name "transient receptor potential" (5). Since their discovery, TRP channels have been identified as osmo- and mechano-sensitive (6). For example, TRPA1 is associated with pain sensations and inflammation (7), and TRPV1 is associated with pain and temperature regulation (8).

Endotherms use energy to create heat to maintain body temperature and in colder climates it has been shown that humans expend more energy for thermoregulation compared to warmer climates (9). Given the high energy costs of generating heat to maintain an optimal cellular environment thermoregulation can also play an important role in energy homeostasis. TRPV1 channels are involved in thermoregulation, making them a possible target for the modulation of energy expenditure. Further, it is becoming apparent that TRPV1 may be involved in the regulation of appetite via the modulation of appetite hormones and/or by acting on gastrointestinal vagal afferents. This is a process that may involve interaction with the endocannabinoid system considering that endocannabinoids such as anandamide (AEA), produced in the gastrointestinal tract are also endogenous TRPV1 agonists. In addition, there are suggestions that TRPV1 may be involved in the regulation of insulin secretion in the pancreas. Studies in obese individuals have suggested that TRPV1 may be dysfunctional or dysregulated due to loss of effect on energy homeostasis. For this reason TRPV1 may be a potential target for pharmacological manipulation to aid in weight loss with recent studies suggesting selective blockade or activation of specific functions of TRPV1. However, due to its complexity this may prove difficult. This review explores TRPV1 structure and modulation and will focus on its involvement in energy homeostasis, diabetes, and possible pharmacological manipulation.

TRPV1 CHANNELS

TPRV1, the first channel in the vanilloid family, is highly permeable to calcium and was discovered in 1997 by cloning dorsal root ganglia expressed genes in human embryonic kidney cells (10). It is expressed in a wide range of central and peripheral tissues. Centrally, TRPV1 is highly expressed in the brain stem, mid-brain, hypothalamus and limbic system (11). Peripherally it is expressed in many tissues including the vagal and spinal sensory nerves (12), stomach (13), and adipose tissue (14).

TRPV1 Structure

The TRPV1 channel consists of four identical subunits located in the plasma membrane with each subunit (**Figure 1**) consisting of an N-terminus, a transmembrane region, and a C-terminus (15, 16). The N-terminus contains an ankyrin repeating domain consisting of 6 ankyrin subunits (16) which in its tertiary structure forms six α-helices connected by finger loops (15). Sites on the N-terminus are capable of phosphorylation by protein kinases with the S116 phosphorylation site being one of functionality (17). A linker section connects the N-terminus to the transmembrane region via the pre-helical segment (pre-S1), and connects TPRV1 subunits together (15–18).

The transmembrane region of each TRPV1 subunit comprises 6 helical segments (S1–S6), where S1–S4 contribute to the voltage-sensing domain, and S5–S6 contribute to the pore-forming domain (16). S1-S4 are connected to S5-S6 by a linker segment, and act as a foundation which allows the linker segment to move, contributing to pore opening and TRPV1 activation. The transmembrane region also contains binding sites for several ligands. For example, vanilloids (e.g., capsaicin) are capable of binding to S3 and S4, and protons (H^+) are capable of binding to S5 and the S5–S6 linker (pore helix) (15).

Lastly, the C-terminus consists of a TRP domain (TRP-D) which interacts with pre-S1 suggesting a structural role (16). Following the TRP domain are several protein kinase A (PKA) and protein kinase C (PKC) phosphorylation sites, and sites for binding calmodulin and phosphatidylinositol-4,5-bisphosphate (PIP_2) (15, 16).

TRPV1 Channel Activation or Modulation

TRPV1 is activated by a wide variety of different stimuli including heat, protons ($pH < 5.9$) (8, 19), capsaicin the irritant compound in hot chilies (10), allicin and diallyl sulfides from garlic (20, 21), peperine from black pepper (22), and gingerol from ginger (23). Spider and jellyfish venom-derived toxins are also TRPV1 agonists (24, 25).

Endogenous agonists are referred to as endovanilloids. To qualify as an endovanilloid the compound should be produced and released in sufficient amount to evoke a TRPV1-mediated response by direct binding and subsequent activation of the channel. Further, to permit regulation of the channel the signal should have a short half-life. Therefore, the mechanisms for synthesis and breakdown of the endovanilloid should be in close proximity to TRPV1. As the binding sites for endogenous ligands of TRPV1 are intracellular (26, 27) then the ligand could also be produced within the cell or there should be a mechanism to bring it into the cell. Three different classes of lipid are known to activate TRPV1 i.e., N-acyl-ethanolamines [NAEs, e.g., AEA (28)], some lipoxygenase products of arachidonic acid and N-acyl-dopamines (e.g., N-arachidonoyldopamine, N-oleoyldopamine) (29). Further, adipose tissue B lymphocytes (B1 cells) that regulate local inflammatory responses produce leukotrienes including leukotriene B4 which is also a TRPV1 agonist (30).

Abbreviations: AC, adenylyl cyclase; AEA, anandamide; AMPK, adenosine monophosphate kinase; BAT, brown adipose tissue; BGL, blood glucose level; BMP, bone morphogenic protein; CAMK, calmodulin dependent kinase; CB, cannabinoid; DMV, dorsal motor nucleus of the vagus; GI, gastrointestinal; GLP, glucagon like peptide; PGC, PPAR gamma coactivator; PI3K, phosphatidylinositol 4-5 bisphosphate 3-kinase; PIP2, phosphatidylinositol-4,5-bisphosphate; PKA, protein kinase A; PKC, protein kinase C; PLC, phospholipase C; PPAR, peroxisome proliferator activated receptor; PRDM, positive regulatory domain; SIRT, sirtuin; SNS, somatic nervous system; TRPV, transient receptor potential vanilloid; UCP, uncoupling protein; WAT, white adipose tissue.

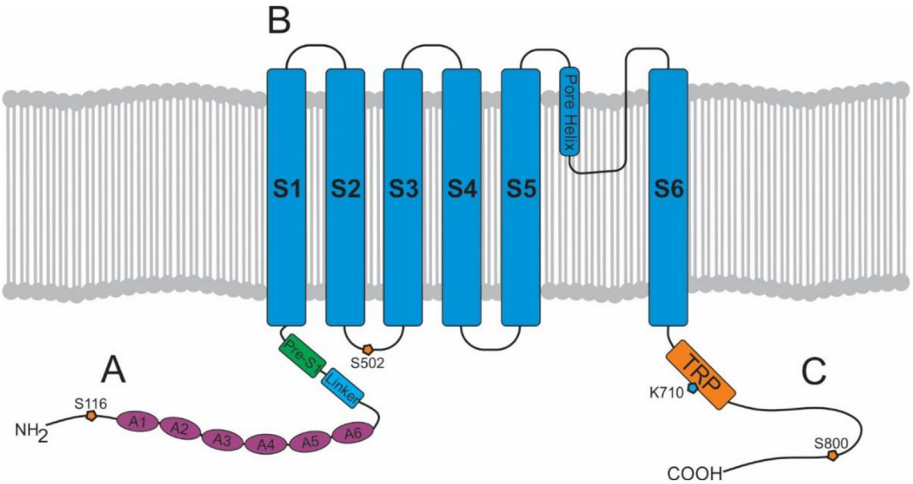

FIGURE 1 | Structure of a TRPV1 subunit. **(A)** N-terminus containing 6 ankyrin subunits (A1–A6) and a linking region consisting of a linker and a Pre-S1 helix segment. **(B)** Transmembrane region with 6 helical segments (S1–S6). **(C)** C-terminus containing a TRP domain and binding sites for PKA, PKC, PIP_2, and calmodulin.

Intracellularly, calmodulin, a calcium-binding messenger, mediates the negative feedback loop formed by calcium (31). Calcium binds and activates calmodulin allowing it to bind to the N-terminus or C-terminus of TRPV1 inhibiting TRPV1 activity (15). Other secondary messengers such as PKA, PKC, and PIP_2 are also capable of modulating TRPV1 activity. PKA can enhance or activate TRPV1 through phosphorylation of sites (S116 and T370) on the N-terminal (32) and may play a role in the capsaicin induced Ca^{2+} dependent desensitization of TRPV1 activation, a phenomenon which has been extensively reviewed elsewhere (33). PKC directly activates TRPV1 through phosphorylation of the S2–S3 linker region (S502) and C-terminal sites (S800), and also potentiates the effect of other ligands such as protons (34, 35). PIP_2 is a negative regulator, inhibiting TRPV1 activity when bound to the C-terminal sites (TRP domain: K710) (36).

Interactions Between TRPV1 and the Endocannabinoid System

The Endocannabinoid System

The endocannabinoid system consists of endocannabinoids, their receptors and the enzymes involved in endocannabinoid synthesis and degradation. This system is involved in many physiological processes including memory, mood, and relevant to this review promotion of food intake (37). Endocannabinoids are endogenous lipid messengers (e.g., AEA and 2-arachydonoyl-glycerol) which activate their receptors, cannabinoid receptor-1 (CB1) and cannabinoid receptor-2 (CB2) (38, 39).

These endogenous lipid messengers are synthesized on demand and degraded by cellular uptake and enzymatic hydrolysis [see review (40) and **Figure 2**]. Briefly, the first step in the synthesis of AEA and NAEs is the transacylation of membrane phosphatidyethanolamine-containing phospholipids to N-acylphosphatidyl-ethanolamines (NAPEs) (41, 42). There are a number of ways that NAPEs are metabolized to their corresponding NAE including catalyzed hydrolysis by the NAPE-hydrolysing enzyme phospholipase D (NAPE-PLD) (43). In contrast, diacylglycerol lipase (DAGL) is responsible for the formation of 2-AG (44). There is still some controversy on whether there is an endocannabinoid membrane transporter [See reviews (45, 46)]. Nonetheless, endocannabinoids can be cleared from the extracellular space. Further, there are intracellular proteins that can shuttle these lipids to specific intracellular locations (e.g., TRPV1 for AEA) (47, 48), the best characterized of these are the fatty acid-binding proteins (FABP e.g., FABP5 and 7) (49). The enzymes responsible for the breakdown of AEA and NAEs are fatty acid amide hydrolase (FAAH) and N-acylethanolamine-hydrolysing acid-amidase (NAAA). NAAA is predominantly located in the lungs where it is localized to the lysosomes of macrophages (50, 51). FAAH is more ubiquitous and FAAH-1 is located on the endoplasmic reticulum whereas FAAH-2 (not found in rodents) is located in the lipid rafts (52, 53). Monoacylglycerol lipase (MAGL) is the enzyme responsible for the majority of 2-AG hydrolysis in most tissues (54–56).

The receptors for endocannabinoids, CB1 and CB2 are members of the G-protein coupled receptor family, being predominantly coupled to the $G_{i/o}\alpha$ proteins that inhibit adenylyl cyclase thereby reducing cellular cAMP levels (57, 58). However, coupling to other effector proteins has also been reported, including activation of G_q and G_s proteins, inhibition of voltage-gated calcium channels, activation of inwardly rectifying potassium channels, β-arrestin recruitment and activation of mitogen-activated protein kinase (MAPK) signaling pathways (59). As a result of CB receptor signaling through multiple effector proteins the probability of biased signaling (ligand-dependent selectivity for specific signal transduction pathways) increases. Biased signaling is thought to occur when different ligands bind to the receptor causing different conformational changes to the receptor enabling the receptor to preferentially signal one pathway over the other (60, 61). This is attractive, in

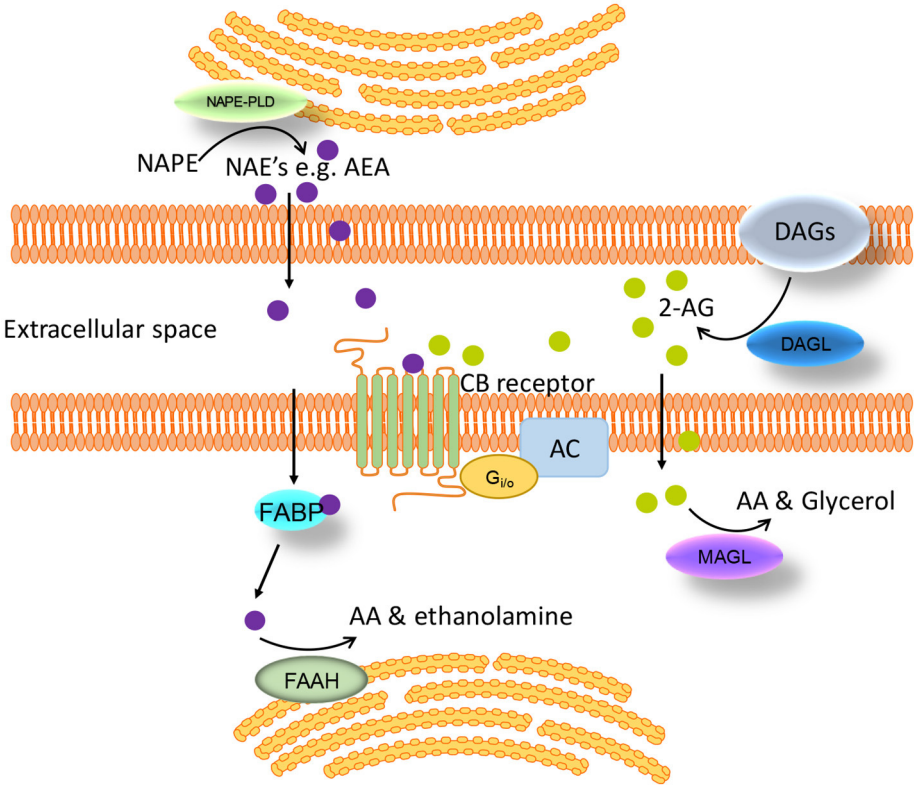

FIGURE 2 | Schematic of the synthesis, degradation and action of endocannabinoids at cannabinoid receptors. Endogenous lipid messengers, such as AEA and 2-AG, act on cannabinoid receptors. AEA and 2-AG are synthesized on demand and degraded by cellular uptake and enzymatic hydrolysis by FAAH and MAGL respectively. FABP carries AEA from the cell membrane to the endoplasmic reticulum where it is finally converted to AA by FAAH. AA, arachidonic acid; AC, adenylate cyclase; AEA, anandamide; 2-AG, 2-arachidonoylglycerol; CB, cannabinoid; DAGs, diacylglycerols; DAGL, diacylglycerol lipase; FAAH, fatty acid amide hydrolase; FABP, fatty acid-binding protein; MAGL, monoacylglycerol lipase; NAE, *N*-acylethanolamines; NAPE, *N*-acylphosphatidylethanolamine; NAPE-PLD, NAPE-specific phospholipase D.

terms of development of pharmacotherapies for various diseases, as it suggests the possibility of being able to design a drug that will activate/inhibit a specific intracellular pathway.

The endocannabinoid system drives food intake via CB1 (62). Administration of CB1 agonists induces feeding in rodents (63) and humans (64), while blocking CB1 reduces food intake (65). Further, overactivity of the endocannabinoid system perpetuates the problems associated with obesity (62) and drugs targeting CB1 have been used therapeutically to manage obesity but withdrawn due to CNS side effects (66). New evidence indicates the endocannabinoid system can control food intake by a peripheral mechanism of action (66). Peripherally-restricted CB1 antagonists, with no direct central effects, reduce food intake and body weight in rodents (67, 68).

The Endocannabinoid System and TRPV1

Endocannabinoids, such as AEA, are also endogenous ligands for TRPV1 (69). Capsaicin, an agonist of TRPV1, has an anti-obesity effect in rodents (14) and reduces food intake in humans (70). Therefore, the effects of endocannabinoids on food intake will depend on the site of action (**Figure 3**). This is complicated further as effects may be mediated via cross talk between TRPV1 and CB1. It has been demonstrated that CB1 can enhance or inhibit TRPV1 channel activity depending on whether it activates the phospholipase C (PLC)-PKC or inhibits the adenylate cyclase (AC)-PKA pathways respectively (71) (**Figure 3**). This interaction appears to be dose-dependent. Moderate to high concentrations of AEA (1–10 μM) have been shown to activate TRPV1 in a PKC dependent manner (34, 35). Conversely, low doses of AEA (3–30 nM) inhibit TRPV1 activity (72, 73), presumably through CB1 mediated inhibition of AC (74). Therefore, enzymatic synthesis and breakdown of endocannabinoids are potentially important determinants of TRPV1 activity in tissue, such as neuronal tissue, that co-express TRPV1 and CB1 (71). A clearer understanding of the role endocannabinoids play in food intake regulation in health and obesity is required to determine the physiological relevance of these different interactions. In mice, the levels of AEA in the small intestinal mucosa and plasma were elevated in high fat diet-induced obese mice compared to controls (68) but still within the low dose range (3–30 nM) shown to inhibit TRPV1 (72, 73). Consistent with these observations food intake was reduced by treatment with a peripherally restricted CB1 antagonist (68). Similar observations were made in humans

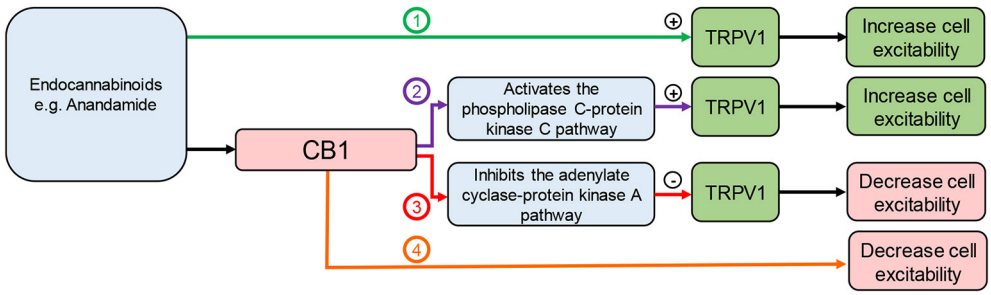

FIGURE 3 | Interaction between endocannabinoids, TRPV1, and CB1. Endocannabinoids can: (1) directly activate TRPV1 leading to cannabinoid receptor 1 (CB1)-independent effects; (2) activate CB1 leading to activation of the phospholipase C pathway enhancing TRPV1 activity; (3) activate CB1 leading to inhibition of the adenylate cyclase pathway inhibiting TRPV1 activity; (4) activate CB1 leading to TRPV1-independent effects.

with plasma anandamide levels elevated in obese compared to overweight or lean individuals, again to levels consistent with TRPV1 inhibition. Therefore, the physiological significance of TRPV1 activation observed at moderate to high concentrations of AEA remain to be determined.

INVOLVEMENT OF TRPV1 IN ENERGY HOMEOSTASIS

Reports on TRPV1 mediated regulation of energy intake and expenditure are conflicting. Nonetheless, epidemiological data indicate that consumption of food containing capsaicin is associated with a lower prevalence of obesity (75, 76). Further, in a clinical trial capsinoid supplementation for 12 weeks decreased body weight in overweight individuals compared to the placebo control group (77). In a separate trial, capsinoid supplementation for only 4 weeks resulted in a trend toward a decrease in body weight (78). Under laboratory conditions, dietary capsaicin supplementation had no effect on body weight (14) in mice fed a standard laboratory diet. However, in high-fat diet-induced obese mice, dietary supplementation of capsaicin significantly reduced weight gain (14, 79, 80). Further, reduced weight gain was also observed in high fat diet mice after topical application of capsaicin (81). This appears to be consistent across species as a study in rabbits, fed a standard laboratory diet supplemented with cholesterol and corn oil, demonstrated that dietary capsaicin reduced weight gain (82). In contrast, it has been shown that a 6 week dietary capsaicin treatment had no effect on body weight in high fat diet mice (83). Weight gain in TRPV1-knockout (KO) mice has been reported to be reduced (84), increased (85) or unchanged (86, 87) compared to wild type mice. This variability may reflect the study design. For example, TRPV1 channels can be activated by the endogenous ligand AEA (69). The production of AEA is dependent on dietary fat and therefore even slight changes in diet will impact on research outcomes. A summary of the effect of TRPV1 on energy homeostasis in humans can be found in **Table 1**. The following sections integrate the data on energy intake and expenditure from human and animal studies in an attempt to draw some clear conclusions and directions for further study.

Role of TRPV1 in Energy Intake

The effects of capsaicin supplementation on satiety and food intake are illustrated in **Table 1**. In human studies, dietary supplementation of a TRPV1 agonist such as capsaicin, or the less pungent sweet form capsiate, caused a short-term trend or significant decrease in energy intake along with an increase in satiety (88, 89, 91, 92, 97). These effects could at least in part be due to the effect of TRPV1 on appetite hormones and/or gastrointestinal vagal afferents. This will be discussed in detail below.

Conversely, other data from human (90, 92) and animal studies (82, 105–108) suggest that dietary supplementation of capsaicin has no effects on energy intake. This could be due to capsaicin mediated TRPV1 desensitization where food intake is initially reduced, due to capsaicin activation of the TRPV1 channel, but shortly returns to normal, due to a desensitization of the channel following the initial transient activation (14). In a Chinese adult cohort study, it has been shown that energy intake depends on the amount of chili consumed with individuals with chili consumption below 20 g per day and above 50 mg per day having reduced and increased energy intake respectively, compared to non-consumers (76). Therefore, it is possible that at low levels of consumption capsaicin activates TRPV1 leading to a reduction in food intake and at high levels it could be desensitizing TRPV1 leading to an increase in food intake. However, this is highly speculative and requires further investigation.

Dietary supplementation of capsaicin can also influence nutrient preference. It has been demonstrated that capsaicin ingestion reduced the desire for and subsequent intake of fatty foods (91, 97, 98), whilst also increasing the desire for and intake of carbohydrates (92, 97). Conversely, in other studies, capsaicin ingestion reduced the desire for and consumption of carbohydrates, and increased the desire for salt rich foods (91, 102). The sensory mechanisms responsible for the changes in food preferences remain to be determined.

TRPV1 and Appetite Hormones

There is evidence to indicate that TPRV1 interacts with appetite regulating hormones, most notably, ghrelin, leptin, and glucagon-like peptide-1 (GLP-1). Ghrelin is an orexigenic

TABLE 1 | Effects of Capsaicin Supplementation on food intake and metabolism in Humans.

Capsaicin dosage	Duration	Appetite effects	Metabolic effects			References
			Energy expenditure	RQ value	Blood glucose	
Capsaicin (7.68 mg/day)	36 h	↓ Energy intake trend ↑ Satiety	–	–	–	(88)
Chili (1.03 g/meal)	24 h	↑ Satiety	↑ Thermogenesis	–	–	(89)
Capsaicin (7.68 mg/meal)	24 h	No effects	↑ Energy expenditure ↑ Fat oxidation	↓	–	(90)
Chili (1 g/meal)	1 meal	↓ Energy intake ↑ Satiety trend	↑ Energy expenditure	↓	–	(91)
Chili (0.3 g/meal)	5 meals	No effects	–	–	–	(92)
Chili (1.03 g/meal)	1 meal	↑ Plasma GLP-1 ↓ Plasma ghrelin trend	No effect	–	–	(93)
Capsaicin 26.6 mg	1 meal	–	–	–	↓	(94)
Capsaicin + green tea	3 weeks	↓ Energy intake ↑ Satiety	–	–	–	(95)
Chili 3 g + caffeine 200 mg	24 h	↓ Energy intake ↓ Fat intake	↑ Energy expenditure ↑ SNS activity	–	–	(70)
Capsaicin 150 mg	1 meal	–	↑ Fat oxidation	↓	–	(96)
Chili 0.9 g/meal	2 days	↓ Energy intake ↑ Satiety	–	–	–	(97)
Chili with meal	1 meal	↓ Energy intake trend ↓ Fat intake	–	–	–	(98)
Capsaicin 3.5 mg with glucose drink	1 meal	–	–	–	↓	(99)
Capsaicin 135 mg/day	3 months	↓ Plasma leptin (likely due to weight loss)	↑ Fat oxidation	↓	↓	(100)
Capsaicin 3 mg/meal	1 meal	–	↑ Energy expenditure ↑ SNS activity effects lost in obesity	–	–	(101)
Chili 6 g in appetizer	1 meal	↓ Energy intake ↓ Carbohydrate intake	↑ SNS activity	–	–	(102)
Chili 10 g/meal	1 meal	↓ Energy intake trend ↓ Protein and fat Intake	↑ Thermogenesis ↑ Fat oxidation	↓	–	(102)
Chili 10 g before meal	1 meal	–	No effect	↑	No effect	(103)
Chili 10 g/meal	1 meal	–	No effect	↑	–	(104)

peptide mainly expressed in the stomach as an endogenous ligand for the growth hormone secretagogue receptor (GHSR) (109). It is involved in many processes including appetite regulation, secretion of gastric acid, gastrointestinal motility, and regulation of energy storage (110). It has been reported that TRPV1 activation reduced plasma ghrelin levels (93), which may account for the reduced food intake observed after capsaicin supplementation (88, 89, 91, 92, 97). However, this requires more intensive investigation. Within the stomach ghrelin maybe involved in the interaction between the endocannabinoid system and TRPV1. CB1 receptors co-expressed with ghrelin in specialized cells within the stomach wall (111). Ghrelin reduces gastric vagal afferent mechanosensitivity, in a manner dependent on nutritional status, via action at GHSR expressed on vagal afferents (112–115). Therefore, although the eating stimulatory effects of ghrelin are not thought to be mediated by vagal afferents (113), ghrelin acting on vagal afferents may impact on the amount of food consumed after the initiation of a meal. Inhibition of CB1 decreases gastric ghrelin secretion with subsequent, vagal afferent mediated, reductions in food intake (111). Therefore, part of the effect of endocannabinoids on vagal afferent activity maybe mediated indirectly via the activation of CB1 on ghrelin-producing cells. It is conceivable that the inhibitory effects of ghrelin are mediated via TRPV1 considering that, in the CNS, ghrelin effects on supraoptic magnocellular neurons are mediated via TRPV1 (116). Similar, interactions with the endocannabinoid system are observed centrally in areas associated with appetite regulation, including the hypothalamic arcuate and paraventricular nuclei (117). A comprehensive investigation of the interactions between the endocannabinoid system, ghrelin and TRPV1 is required to fully understand their role in appetite regulation.

Leptin is a satiety hormone produced and secreted in proportion to the amount of white adipose tissue (WAT). Data suggests that it is also secreted by gastric cells (118). There is evidence to suggest that TRPV1 and leptin may interact, since TRPV1 -/- mice exhibit increased basal leptin levels, even when normalized to WAT mass (85). Exogenous administration of

leptin normally results in decreased food intake; however, this was not observed in TPRV1 -/- mice (85). Furthermore, there is evidence for direct interactions between leptin and TRPV1 in certain brain stem regions. For example, TRPV1 activation increased the frequency of miniature excitatory synaptic currents in leptin receptor containing neurons of gastric-related dorsal motor nucleus of the vagus (DMV) (119). These data suggest that TRPV1 may mediate the effects of leptin; however, further research is needed to substantiate these claims and to determine if leptin effects in the periphery are also mediated through TRPV1.

GLP-1 is a peptide hormone secreted by intestinal L-cells, pancreatic α-cells, and neurons in the brainstem and hypothalamus (120). Evidence suggests it is involved in appetite regulation, gastric emptying, gastrointestinal motility (121), insulin secretion, and glucagon inhibition (122). Capsaicin supplementation enhanced the increase in plasma GLP-1 levels observed after a meal (93) suggesting TRPV1 channel activation may play a role in GLP-1 secretion. This requires further investigation but has the potential to be a peripheral target for the treatment of obesity and/or diabetes.

TRPV1 and Gastrointestinal Vagal Afferents

Gastrointestinal vagal afferents are an important link between the gut and brain. They relay information on the arrival, amount and nutrient composition of a meal to the hindbrain where it is processed and gastrointestinal reflexes are coordinated with behavioral responses and sensations such as satiety and fullness (123–125). The role of gastrointestinal vagal afferents in the control of food intake has been extensively reviewed previously (126). Briefly, as food is ingested the vagal afferents innervating the stomach respond to mechanical stimulation as undigested food enters, fills and distends the stomach wall. There are two fundamental classes of mechanosensitive vagal afferent ending in the stomach according to location and response to mechanical stimulation (127, 128): mucosal receptors respond to fine tactile stimulation and tension receptors respond to distension and contraction of the stomach wall. Gastric mechanosensitive vagal afferents can be modulated by gut hormones and adipokines in a nutritional status dependent manner (114, 129, 130). As gastric emptying occurs, nutrients enter the small intestine and interact with nutrient receptors on the surface of specialized cells within the intestinal mucosa. This initiates an intracellular cascade that culminates in the release of gut hormones (126). These hormones can act in a paracrine fashion on vagal afferent endings innervating the small intestine and/or act as true hormones by coordinating activities within the gut or by entering the circulation and acting in the brain.

It has been demonstrated that TRPV1 is expressed in rat duodenal (131), mouse jejunal (132) and mouse gastric vagal afferents (13, 87). Activation of TRPV1, by oleoylethanolamide (OEA), caused depolarisation of nodose neurons and decreased short-term food intake (133). Further, OEA increased gastric vagal afferent tension receptor mechanosensitivity in lean but not high fat diet-induced obese mice (87). In standard laboratory diet fed TRPV1$^{-/-}$ mice, the response of gastric vagal afferent tension (but not mucosal) receptors to mechanical stimulation was reduced compared to TRPV1$^{+/+}$ mice (13, 87). This was associated with an increase in food intake in the standard laboratory diet fed TRPV1$^{-/-}$ mice (87). However, the increase in food intake could also be due to the involvement of TRPV1 in gut hormone release (93, 97) or its interaction with leptin in central regions, such as the DMV (119), as described in detail above. Nonetheless, this data suggests that TRPV1 is involved in gastric vagal afferent signaling.

In high fat diet-induced obese mice the response of gastric tension receptors to distension was dampened (87) an effect also observed in jejunal vagal afferents (134). Gastric tension receptor mechanosensitivity in high fat diet-fed TRPV1$^{-/-}$ mice was not significantly different compared to standard laboratory diet fed TRPV1$^{-/-}$ mice (87). This suggests that disrupted TRPV1 signaling plays a role in the dampened vagal afferent signaling observed in high fat diet-induced obesity, however, this requires further investigation. Interestingly, CB1 receptors are also expressed in vagal afferent neurons (135, 136) and therefore it is conceivable that there is an interaction between TRPV1 and CB1 in gastric vagal afferent signaling, however, this has yet to be confirmed.

Role of TRPV1 in Energy Expenditure

There is increasing evidence that capsaicin ingestion may have desirable metabolic outcomes such as increased metabolic rate and fat oxidation. It was reported that dietary capsaicin supplementation lowered the respiratory quotient indicating decreased carbohydrate oxidation and increased fat oxidation (90, 91, 96, 100). In contrast, there is data demonstrating that dietary capsaicin increased the respiratory quotient (103, 104). The differences in study design, which may account for the different outcomes, include method of ingestion (capsule vs. meal), active ingredient (capsinoid vs. capsaicin) and the population studied (habitual chili consumers, non-habitual, normal weight, overweight, fitness level). For example, the study by Lim et al. specifically used "runners" for their investigation (103). There is some evidence that capsaicin can elevate energy expenditure by action on the sympathetic nervous system (SNS) or adipose tissue; this is discussed below.

TRPV1 and the Sympathetic Nervous System

The SNS is involved in many processes and is probably best known for its involvement in the "flight or fight" response. Dietary supplementation of capsaicin increases postprandial SNS activity (70, 101, 102). Capsaicin excites TRPV1 containing afferent nerves, carrying a signal to the spinal cord (137). Efferent nerves are then excited by the central nervous system leading to elevated catecholamine (e.g., epinephrine, norepinephrine, and dopamine) release from the adrenal medulla (137–139). Catecholamines can bind β-adrenergic receptors increasing expenditure and thermogenic activity (104, 140). This suggests that TRPV1 may directly stimulate heat production. Further, these effects of TRPV1 on SNS activity are lost in obese subjects suggesting TRPV1 dysfunction in obesity (101).

TRPV1 and Adipose Tissue

Adipose tissue plays a key role in energy homeostasis (141). WAT generally stores excess energy as lipids, and oxidizes these

stores when required, whereas, brown adipose tissue (BAT) is specialized for energy dissipation (142, 143). TRPV1 has been shown to be expressed in 3T3-L1 and HB2 adipocyte cell lines, brown adipocytes, BAT and WAT (144–147). Data indicate that TRPV1 may prevent the development of mature adipocytes from pre-adipocytes, and decrease their lipid content by increasing lipolysis (14). This may partially explain the decreased lipid accumulation during dietary supplementation of capsaicin. Further, it has been demonstrated that capsaicin induces browning in differentiating 3T3-L1 preadipocytes (145). Therefore, TRPV1 could be involved in the browning of WAT and the thermogenic activity of brown adipose tissue (BAT). The levels of TRPV1 mRNA in BAT and WAT are reduced in HFD-induced obesity and leptin receptor deficient mice (147) suggesting possible involvement in the development of obesity.

Browning is a process whereby WAT becomes thermogenic in nature, similar to BAT. The calcium influx from TRPV1 activation may mediate this process by activating the peroxisome proliferator-activated receptor gamma (PPARγ) and positive regulatory domain containing 16 (PRDM16) pathways (107). Calcium binds and activates calmodulin-dependent protein kinase II (CaMKII) leading to the subsequent activation of adenosine monophosphate activated protein kinase (AMPK) and sirtuin-1 (SIRT-1). SIRT-1 deacetylates PRDM and PPARγ causing browning events such as thermogenesis (**Figure 4**) (107).

TRPV1 activation may also promote BAT thermogenesis either through modulation of the SNS or via direct activation of BAT. However, research in this area is limited. The PPARγ and PRDM16 pathway, previously mentioned in WAT, has been shown to be activated by TRPV1, via SIRT1, in BAT (107, 108). Further, SIRT1 also activates peroxisome proliferator-activated receptor gamma coactivator 1-α (PGC-1α). PGC-1α transcriptionally activates PPARα subsequently leading to the production of uncoupling protein-1 (UCP-1) (108). UCP-1 is a mitochondrial protein that uncouples the respiratory chain triggering a more efficient substrate oxidation and thus heat generation (148). Lastly, TRPV1 activates bone morphogenic protein 8b in BAT, which also contributes to thermogenesis (**Figure 5**) (108).

Regulation of BAT by TRPV1 can also be via an indirect mechanism through modulation of the SNS. Activation of TRPV1 in the gastrointestinal tract, by capsaicin or its analogs, has been shown to enhance thermogenesis and activate UCP-1 in BAT in mice (149, 150) via a mechanism mediated via extrinsic nerves innervating the gastrointestinal tract (149). This is consistent with reports that TRPV1 ligands (capsaicin and acid) increase gastrointestinal afferent activity (151, 152) via TRPV1 (152). Further, it has been demonstrated that ingestion of capsinoids increases energy expenditure through activation of BAT in humans (153). Gastrointestinal vagal afferents have central endings in the nucleus tractus solitaries (NTS). The NTS has projections to BAT (154) where it regulates the sympathetic tone to BAT (155) and has been directly implicated in the control of thermogenesis (156, 157). Lipid activation of duodenal vagal afferents has been shown to increase BAT temperature via a cholecystokinin dependent mechanism (158). In contrast, it has been reported that vagal afferent activation decreases BAT sympathetic nerve activity and BAT thermogenesis in rats (159). Further, glucagon-like peptide-1 activation of gastrointestinal vagal afferents leads to a reduction in energy expenditure and BAT thermogenesis in mice (160). It is possible that different subtypes of gastrointestinal vagal afferent have different roles in the control of BAT thermogenesis, however, this requires further investigation along with the role of TRPV1 in this gut-brain-BAT pathway.

Capsaicin can also evoke a heat-loss response which could conceivably result in compensatory thermogenesis to maintain thermal homeostasis. Capsaicin evoked complex heat-loss responses have been shown in various mammals including the rat, mouse, guinea-pig, rabbit, dog, goat, and humans (161). In humans, cutaneous vasodilation and sweating in response to hot chili consumption is well recognized (161). In the rat it has

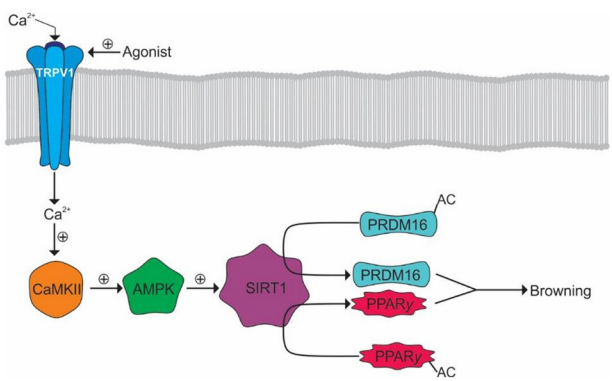

FIGURE 4 | Browning of WAT by TRPV1 activation. Activation of TRPV1 results in Ca^{2+} influx and the subsequent activation of CaMKII. CaMKII facilitates the subsequent activation of AMPK and SIRT1 allowing the deacetylation of PRDM16 and PPARγ allowing their interaction and promotion of WAT browning.

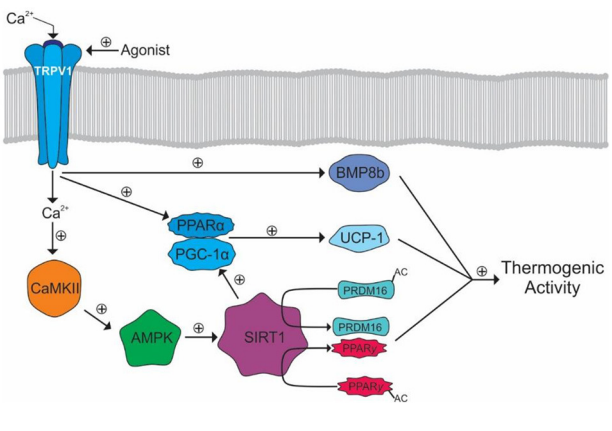

FIGURE 5 | TRPV1 mediated activation of thermogenic activity in BAT. The calcium influx activates CaMKII leading to the eventual activation of SIRT1 and deacetylation of PRDM16 and PPARγ. SIRT1 also activates PGC-1α leading to the activation of PPARα. PGC-1α and PPARα transcriptionally activate UCP-1. TRPV1 also activates BMP8b which, along with UCP-1, PRDM, and PPARγ, cause increased thermogenic activity.

been demonstrated that capsaicin elicited cutaneous vasodilation resulting in a reduction in core body temperature (162). Simultaneously, capsaicin also enhanced heat production (162). In these experiments, it appeared that capsaicin independently activated pathways for heat production and heat loss and therefore the observed thermogenesis may not be a simple compensatory mechanism in response to heat loss, however, this requires further investigation.

INVOLVEMENT OF TRPV1 IN DIABETES

Type 1 Diabetes

Insulin is a hormone, secreted by β-cells of the pancreatic islets, which regulates blood glucose levels. Type 1 diabetes is an autoimmune disease involving T cell-targeted destruction of pancreatic β-cells. TRPV1 is expressed in sensory nerves innervating the pancreas. Chemical denervation of these TRPV1 containing pancreatic afferents, using high doses of capsaicin (approximately 150 mg/kg body weight), significantly reduced blood glucose levels and increased plasma insulin (163), suggesting that TRPV1 containing pancreatic afferents negatively regulate insulin secretion. Further, chemical destruction of TRPV1 expressing neurons in neonatal mice (164) was able to protect the mice from autoimmune diabetes (165). Chemical denervation of TRPV1 containing pancreatic afferents significantly reduced the levels of pre-type 1 diabetes immune markers such as $CD4^+$ and $CD25^+$ T-regulatory cells in pancreatic lymph tissue and reduced the infiltration of CD8-CD69 positive effector T-cells (165, 166); immune cells implicated in the destruction of pancreatic islets in type 1 diabetes. However, as the afferents are destroyed and the treatment is not selective for TRPV1, it is plausible that the observed effects have nothing to do with TRPV1. Pancreatic islets also include resident dendritic cells which are generally believed to express TRPV1 (167–169) although there is some controversy (170). Activation of TRPV1 channels on dentritic cells could activate cell function including antigen presentation to $CD4^+$ T cells. Further, TRPV1 channels have been shown to be expressed on rat pancreatic β-cells where they control the release of insulin leading to reduced blood glucose levels (171) and capsaicin has been shown to reduce blood glucose by increasing insulin levels in a streptozotocin-induced diabetic rat model (172). Taken together, these data suggest that TRPV1 may influence insulin secretion and type 1 diabetes acting via a number of different cell types within the pancreas.

Type 2 Diabetes

Insulin resistance, closely linked to obesity (173), occurs when cells are less responsive to insulin. As a consequence there is reduced blood glucose uptake leading to increased blood glucose levels. Pancreatic β-cells normally respond to this by increasing output of insulin to meet the needs of the tissues. Development of type 2 diabetes stems from a failure of the β-cells to adequately compensate for insulin resistance (174). It has been demonstrated that postprandial insulin levels were lower after the consumption of a standardized meal seasoned with cayenne pepper (175). As the plasma glucose levels were not significantly different from the control group the authors suggested that glucose clearance occurred similarly with lower levels of insulin, implying increased insulin sensitivity after the consumption of the hot meal. Further, consumption of chili has been shown to decrease postprandial insulin levels in obese subjects (176). In support of these studies, $TRPV1^{-/-}$ mice have been shown to be more insulin resistant than wild type mice (85).

Type 2 diabetes is believed to be associated with inflammation (177, 178). It is believed that inflammation in the pancreas leads to an increase in the activity of TRPV1 which contributes to increasing levels of calcitonin gene-related peptide (CGRP) (179). CGRP is known to promote insulin resistance and obesity by decreasing insulin release from β-cells (180).

TRPV1 AS A PHARMACOLOGICAL TARGET FOR OBESITY AND DIABETES

Behavioral interventions (e.g., diet and exercise) alone are seldom sufficient for the intervention of obesity and diabetes. Combining behavioral and pharmacological approaches is becoming increasingly more attractive. However, pharmacological interventions can have hard to access targets and/or adverse side effects. TRPV1 is present in the periphery making it an easily accessible target compared to drugs that target the central nervous system. However, TRPV1 interacts with other systems and shares pathways commonly used by other signaling molecules. Therefore, without a clear understanding of the interactions of TRPV1 with other systems, the targeting TRPV1 for the treatment of obesity and diabetes is unlikely to be successful, as evident from the numerous contradictory studies looking at the effect of capsaicin analogs on food intake and weight gain. Data suggest that manipulation of TRPV1 may be possible in such a way to reduce or eliminate any unwanted side effects. For example, three different TRPV1 ligands known to antagonize TRPV1 had different effects on thermoregulation (e.g., hyperthermia, hypothermia, or no effect) (181). In fact, TRPV1 can be manipulated in such a way, by action at different domains, to eliminate some functions of the TRPV1 channels without affecting others. For example, some antagonists block activation by capsaicin and high temperatures but not activation by low pH (182), and other antagonists block activation by capsaicin but not the activation by high temperature (183). However, this raises further questions on whether, for example, the observed effects are cell type specific. Again, this highlights the lack of fundamental knowledge on the role of TRPV1 in energy homeostasis and therefore the current challenges of targeting TRPV1 for the treatment of obesity.

CONCLUSION

TRPV1 appears to be involved in energy homeostasis at a number of levels. In the periphery, TRPV1 activation or inhibition can have an impact of appetite and food intake through the control of appetite hormone levels or via the modulation of gastrointestinal vagal afferents, important for determining meal size and meal duration. In addition, TRPV1 plays a role

in energy expenditure via heat production, either via direct thermogenesis or as a compensatory mechanism in response to TRPV1 induced heat-loss. Dietary supplementation with TRPV1 analogs, such as capsaicin, has yielded conflicting results with some studies demonstrating a decrease in food intake and increase in energy expenditure and others indicating the converse. This is probably reflective of the involvement of TRPV1 in a multitude of processes regulating food intake and energy expenditure. The story is complicated further by the interaction TRPV1 has with other systems involved in energy homeostasis, such as the endocannabinoid system. In addition, TRPV1 appears to be dysregulated in obesity, possibly due to alterations in the interaction with other systems. Therefore, although it is clear that TRPV1 plays a role in energy homeostasis without improved knowledge of the fundamental physiological mechanisms involved and the interactions with other systems it is impossible to target this system for the treatment of obesity, the maintenance of weight loss and the metabolic diseases associated with obesity.

AUTHOR CONTRIBUTIONS

SC wrote the review under the supervision of GW and AP. HL edited the article and along with GW and AP provided assistance with the structure of the review.

FUNDING

AP and GW were awarded a Diabetes Australia Research Trust grant.

REFERENCES

1. Gupta N, Goel K, Shah P, Misra A. Childhood obesity in developing countries: epidemiology, determinants, and prevention. *Endocrine Rev.* (2012) 33:48–70. doi: 10.1210/er.2010-0028
2. Smith KB, Smith MS. Obesity statistics. *Prim Care* (2016) 43:121–35. doi: 10.1016/j.pop.2015.10.001
3. Venkatachalam K, Montell C. TRP channels. *Annu Rev Biochem.* (2007) 76:387–417. doi: 10.1146/annurev.biochem.75.103004.142819
4. Cosens DJ, Manning A. Abnormal electroretinogram from a Drosophila mutant. *Nature* (1969) 224:285–7. doi: 10.1038/224285a0
5. Montell C, Rubin GM. Molecular characterization of the Drosophila trp locus: a putative integral membrane protein required for phototransduction. *Neuron* (1989) 2:1313–23. doi: 10.1016/0896-6273(89)90069-X
6. Tracey W. D. Jr, Wilson RI, Laurent G, Benzer S. Painless, a Drosophila gene essential for nociception. *Cell* (2003) 113:261–73. doi: 10.1016/S0092-8674(03)00272-1
7. Asgar J, Zhang Y, Saloman JL, Wang S, Chung MK, Ro JY. The role of TRPA1 in muscle pain and mechanical hypersensitivity under inflammatory conditions in rats. *Neuroscience* (2015) 310:206–15. doi: 10.1016/j.neuroscience.2015.09.042
8. Cao E, Cordero-Morales JF, Liu B, Qin F, Julius D. TRPV1 channels are intrinsically heat sensitive and negatively regulated by phosphoinositide lipids. *Neuron* (2013) 77:667–79. doi: 10.1016/j.neuron.2012.12.016
9. Ocobock C. Human energy expenditure, allocation, and interactions in natural temperate, hot, and cold environments. *Am J Phys Anthropol.* (2016) 161:667–5. doi: 10.1002/ajpa.23071
10. Caterina MJ, Schumacher MA, Tominaga M, Rosen TA, Levine JD, Julius D. The capsaicin receptor: a heat-activated ion channel in the pain pathway. *Nature* (1997) 389:816–24. doi: 10.1038/39807
11. Edwards JG. TRPV1 in the central nervous system: synaptic plasticity, function, and pharmacological implications. *Prog Drug Res.* (2014) 68:77–104. doi: 10.1007/978-3-0348-0828-6_3
12. Eid SR, Cortright DN. (2009). Transient receptor potential channels on sensory nerves. *Handb Exp Pharmacol.* 194:261–81. doi: 10.1007/978-3-540-79090-7_8
13. Bielefeldt K, Davis BM. Differential effects of ASIC3 and TRPV1 deletion on gastroesophageal sensation in mice. *Am J Physiol Gastrointest Liver Physiol.* (2008) 294:G130–8. doi: 10.1152/ajpgi.00388.2007
14. Zhang LL, Yan Liu D, Ma LQ, Luo ZD, Cao TB, Zhong J, et al. Activation of transient receptor potential vanilloid type-1 channel prevents adipogenesis and obesity. *Circ Res.* (2007) 100:1063–70. doi: 10.1161/01.RES.0000262653.84850.8b
15. Cao E, Liao M, Cheng Y, Julius D. TRPV1 structures in distinct conformations reveal activation mechanisms. *Nature* (2013) 504:113–8. doi: 10.1038/nature12823
16. Liao M, Cao E, Julius D, Cheng Y. Structure of the TRPV1 ion channel determined by electron cryo-microscopy. *Nature* (2013) 504:107–12. doi: 10.1038/nature12822
17. Bhave G, Zhu W, Wang H, Brasier DJ, Oxford GS, Gereau RWT. cAMP-dependent protein kinase regulates desensitization of the capsaicin receptor (VR1) by direct phosphorylation. *Neuron* (2002) 35:721–31. doi: 10.1016/S0896-6273(02)00802-4
18. Lishko PV, Procko E, Jin X, Phelps CB, Gaudet R. The ankyrin repeats of TRPV1 bind multiple ligands and modulate channel sensitivity. *Neuron* (2007) 54:905–18. doi: 10.1016/j.neuron.2007.05.027
19. Dhaka A, Uzzell V, Dubin AE, Mathur J, Petrus M, Bandell M, et al. TRPV1 is activated by both acidic and basic pH. *J Neurosci.* (2009) 29:153–8. doi: 10.1523/JNEUROSCI.4901-08.2009
20. Salazar H, Llorente I, Jara-Oseguera A, Garcia-Villegas R, Munari M, Gordon SE, et al. A single N-terminal cysteine in TRPV1 determines activation by pungent compounds from onion and garlic. *Nat Neurosci.* (2008) 11:255–61. doi: 10.1038/nn2056
21. Koizumi K, Iwasaki Y, Narukawa M, Iitsuka Y, Fukao T, Seki T, et al. Diallyl sulfides in garlic activate both TRPA1 and TRPV1. *Biochem Biophys Res Commun.* (2009) 382:545–8. doi: 10.1016/j.bbrc.2009.03.066
22. Okumura Y, Narukawa M, Iwasaki Y, Ishikawa A, Matsuda H, Yoshikawa M, et al. Activation of TRPV1 and TRPA1 by black pepper components. *Biosci Biotechnol Biochem.* (2010) 74:1068–72. doi: 10.1271/bbb.90964
23. Iwasaki Y, Morita A, Iwasawa T, Kobata K, Sekiwa Y, Morimitsu Y, et al. A nonpungent component of steamed ginger–[10]-shogaol–increases adrenaline secretion via the activation of TRPV1. *Nutr Neurosci.* (2006) 9:169–78. doi: 10.1080/110284150600955164
24. Siemens J, Zhou S, Piskorowski R, Nikai T, Lumpkin EA, Basbaum AI, et al. Spider toxins activate the capsaicin receptor to produce inflammatory pain. *Nature* (2006) 444:208–12. doi: 10.1038/nature05285
25. Cromer BA, Mcintyre P. Painful toxins acting at TRPV1. *Toxicon* (2008) 51:163–73. doi: 10.1016/j.toxicon.2007.10.012
26. De Petrocellis L, Bisogno T, Maccarrone M, Davis JB, Finazzi-Agro A, Di Marzo V. The activity of anandamide at vanilloid VR1 receptors requires facilitated transport across the cell membrane and is limited by intracellular metabolism. *J Biol Chem.* (2001a) 276:12856–63. doi: 10.1074/jbc.M008555200
27. Jordt SE, Julius D. Molecular basis for species-specific sensitivity to "hot" chili peppers. *Cell* (2002) 108:421–30. doi: 10.1016/S0092-8674(02)00637-2
28. Smart D, Gunthorpe MJ, Jerman JC, Nasir S, Gray J, Muir AI, et al. The endogenous lipid anandamide is a full agonist at the human vanilloid receptor (hVR1). *Br J Pharmacol.* (2000) 129:227–30. doi: 10.1038/sj.bjp.0703050
29. Van Der Stelt M, Di Marzo V. Endovanilloids. Putative endogenous ligands of transient receptor potential vanilloid 1 channels. *Eur J Biochem.* (2004) 271:1827–34. doi: 10.1111/j.1432-1033.2004.04081.x

30. Vigna SR, Shahid RA, Nathan JD, Mcvey DC, Liddle RA. Leukotriene B4 mediates inflammation via TRPV1 in duct obstruction-induced pancreatitis in rats. *Pancreas* (2001) 40:708–14. doi: 10.1097/MPA.0b013e318214c8df
31. Rosenbaum T, Gordon-Shaag A, Munari M, Gordon SE. Ca2+/calmodulin modulates TRPV1 activation by capsaicin. *J General Physiol.* (2004) 123:53–62. doi: 10.1085/jgp.200308906
32. De Petrocellis L, Harrison S, Bisogno T, Tognetto M, Brandi I, Smith GD, et al. The vanilloid receptor (VR1)-mediated effects of anandamide are potently enhanced by the cAMP-dependent protein kinase. *J Neurochem.* (2001b) 77:1660–63. doi: 10.1046/j.1471-4159.2001.00406.x
33. Vyklicky L, Novakova-Tousova K, Benedikt J, Samad A, Touska F, Vlachova V. Calcium-dependent desensitization of vanilloid receptor TRPV1: a mechanism possibly involved in analgesia induced by topical application of capsaicin. *Physiol Res.* (2008) 57(Suppl. 3):S59–68.
34. Premkumar LS, Ahern GP. Induction of vanilloid receptor channel activity by protein kinase C. *Nature* (2000) 408:985–90. doi: 10.1038/35050121
35. Vellani V, Mapplebeck S, Moriondo A, Davis JB, Mcnaughton PA. Protein kinase C activation potentiates gating of the vanilloid receptor VR1 by capsaicin, protons, heat and anandamide. *J Physiol.* (2001) 534:813–25. doi: 10.1111/j.1469-7793.2001.00813.x
36. Chuang HH, Prescott ED, Kong H, Shields S, Jordt SE, Basbaum AI, et al. Bradykinin and nerve growth factor release the capsaicin receptor from PtdIns(4,5)P2-mediated inhibition. *Nature* (2001) 411:957–62. doi: 10.1038/35082088
37. Lu Y, Anderson HD. Cannabinoid signaling in health and disease. *Can J Physiol Pharmacol.* (2017) 95:311–27. doi: 10.1139/cjpp-2016-0346
38. Harrold JA, Williams G. The cannabinoid system: a role in both the homeostatic and hedonic control of eating? *Br J Nutr.* (2003) 90:729–34. doi: 10.1079/BJN2003942
39. Cristino L, Becker T, Di Marzo V. Endocannabinoids and energy homeostasis: an update. *Biofactors* (2014) 40:389–97. doi: 10.1002/biof.1168
40. Fowler CJ, Doherty P, Alexander SPH. Endocannabinoid turnover. *Adv Pharmacol.* (2017) 80:31–66. doi: 10.1016/bs.apha.2017.03.006
41. Natarajan V, Reddy PV, Schmid PC, Schmid HH. N-Acylation of ethanolamine phospholipids in canine myocardium. *Biochim Biophys Acta* (1982) 712:342–55. doi: 10.1016/0005-2760(82)90352-6
42. Natarajan V, Schmid PC, Reddy PV, Zuzarte-Augustin ML, Schmid HH. Biosynthesis of N-acylethanolamine phospholipids by dog brain preparations. *J Neurochem.* (1983) 41:1303–12. doi: 10.1111/j.1471-4159.1983.tb00825.x
43. Schmid PC, Reddy PV, Natarajan V, Schmid HH. Metabolism of N-acylethanolamine phospholipids by a mammalian phosphodiesterase of the phospholipase D type. *J Biol Chem.* (1983) 258:9302–6.
44. Bisogno T, Howell F, Williams G, Minassi A, Cascio MG, Ligresti A, et al. Cloning of the first sn1-DAG lipases points to the spatial and temporal regulation of endocannabinoid signaling in the brain. *J Cell Biol.* (2003) 163:463–8. doi: 10.1083/jcb.200305129
45. Fowler CJ. Transport of endocannabinoids across the plasma membrane and within the cell. *FEBS J.* (2013) 280:1895–904. doi: 10.1111/febs.12212
46. Nicolussi S, Gertsch J. Endocannabinoid transport revisited. *Vitam Horm.* (2015) 98:441–85. doi: 10.1016/bs.vh.2014.12.011
47. Kaczocha M, Glaser ST, Deutsch DG. Identification of intracellular carriers for the endocannabinoid anandamide. *Proc Natl Acad Sci USA.* (2009) 106:6375–80. doi: 10.1073/pnas.0901515106
48. Oddi S, Fezza F, Pasquariello N, D'agostino A, Catanzaro G, De Simone C, et al. Molecular identification of albumin and Hsp70 as cytosolic anandamide-binding proteins. *Chem Biol.* (2009) 16:624–32. doi: 10.1016/j.chembiol.2009.05.004
49. Sanson B, Wang T, Sun J, Wang L, Kaczocha M, Ojima I, et al. Crystallographic study of FABP5 as an intracellular endocannabinoid transporter. *Acta Crystallogr D Biol Crystallogr.* (2014) 70:290–8. doi: 10.1107/S1399004713026795
50. Ueda N, Yamanaka K, Yamamoto S. Purification and characterization of an acid amidase selective for N-palmitoylethanolamine, a putative endogenous anti-inflammatory substance. *J Biol Chem.* (2001) 276:35552–7. doi: 10.1074/jbc.M106261200
51. Tsuboi K, Zhao LY, Okamoto Y, Araki N, Ueno M, Sakamoto H, et al. Predominant expression of lysosomal N-acylethanolamine-hydrolyzing acid amidase in macrophages revealed by immunochemical studies. *Biochim Biophys Acta* (2007) 1771:623–32. doi: 10.1016/j.bbalip.2007.03.005
52. Wei BQ, Mikkelsen TS, Mckinney MK, Lander ES, Cravatt BF. A second fatty acid amide hydrolase with variable distribution among placental mammals. *J Biol Chem.* (2006) 281:36569–78. doi: 10.1074/jbc.M606646200
53. Kaczocha M, Glaser ST, Chae J, Brown DA, Deutsch DG. Lipid droplets are novel sites of N-acylethanolamine inactivation by fatty acid amide hydrolase-2. *J Biol Chem.* (2010) 285:2796–806. doi: 10.1074/jbc.M109.058461
54. Blankman JL, Simon GM, Cravatt BF. A comprehensive profile of brain enzymes that hydrolyze the endocannabinoid 2-arachidonoylglycerol. *Chem Biol.* (2007) 14:1347–56. doi: 10.1016/j.chembiol.2007.11.006
55. Pan B, Wang W, Zhong P, Blankman JL, Cravatt BF, Liu QS. Alterations of endocannabinoid signaling, synaptic plasticity, learning, and memory in monoacylglycerol lipase knock-out mice. *J Neurosci.* (2011) 31:13420–30. doi: 10.1523/JNEUROSCI.2075-11.2011
56. Zhong P, Pan B, Gao XP, Blankman JL, Cravatt BF, Liu QS. Genetic deletion of monoacylglycerol lipase alters endocannabinoid-mediated retrograde synaptic depression in the cerebellum. *J Physiol.* (2011) 589:4847–55. doi: 10.1113/jphysiol.2011.215509
57. Howlett AC. Reverse pharmacology applied to the cannabinoid receptor. *Trends Pharmacol Sci.* (1990) 11:395–7. doi: 10.1016/0165-6147(90)90142-U
58. Howlett AC. Pharmacology of cannabinoid receptors. *Annu Rev Pharmacol Toxicol.* (1995) 35:607–34. doi: 10.1146/annurev.pa.35.040195.003135
59. Ibsen MS, Connor M, Glass M. Cannabinoid CB1 and CB2 receptor signaling and bias. *Cannabis Cannabinoid Res.* (2017) 2:48–60. doi: 10.1089/can.2016.0037
60. Khajehali E, Malone DT, Glass M, Sexton PM, Christopoulos A, Leach K. Biased agonism and biased allosteric modulation at the CB1 cannabinoid receptor. *Mol Pharmacol.* (2015) 88:368–79. doi: 10.1124/mol.115.099192
61. Laprairie RB, Bagher AM, Kelly ME, Denovan-Wright EM. Biased type 1 cannabinoid receptor signaling influences neuronal viability in a cell culture model of Huntington disease. *Mol Pharmacol.* (2016) 89:364–75. doi: 10.1124/mol.115.101980
62. Sharkey KA, Pittman QJ. Central and peripheral signaling mechanisms involved in endocannabinoid regulation of feeding: a perspective on the munchies. *Sci STKE* (2005) 2005:pe15. doi: 10.1126/stke.2772005pe15
63. Jarbe TU, Dipatrizio NV. Delta9-THC induced hyperphagia and tolerance assessment: interactions between the CB1 receptor agonist delta9-THC and the CB1 receptor antagonist SR-141716 (rimonabant) in rats. *Behav Pharmacol.* (2005) 16:373–80. doi: 10.1097/00008877-200509000-00009
64. Foltin RW, Brady JV, Fischman MW. Behavioral analysis of marijuana effects on food intake in humans. *Pharmacol Biochem Behav.* (1986) 25:577–82. doi: 10.1016/0091-3057(86)90144-9
65. Scheen AJ, Finer N, Hollander P, Jensen MD, Van Gaal LF, Group, RI-DS. Efficacy and tolerability of rimonabant in overweight or obese patients with type 2 diabetes: a randomised controlled study. *Lancet* (2006) 368:1660–72. doi: 10.1016/S0140-6736(06)69571-8
66. Shrestha N, Cuffe JSM, Hutchinson DS, Headrick JP, Perkins AV, Mcainch AJ, et al. Peripheral modulation of the endocannabinoid system in metabolic disease. *Drug Discov Today* (2018) 23:592–604. doi: 10.1016/j.drudis.2018.01.029
67. Cluny NL, Vemuri VK, Chambers AP, Limebeer CL, Bedard H, Wood JT, et al. A novel peripherally restricted cannabinoid receptor antagonist, AM6545, reduces food intake and body weight, but does not cause malaise, in rodents. *Br J Pharmacol.* (2010) 161:629–42. doi: 10.1111/j.1476-5381.2010.00908.x
68. Argueta DA, Dipatrizio NV. Peripheral endocannabinoid signaling controls hyperphagia in western diet-induced obesity. *Physiol Behav.* (2017) 171:32–9. doi: 10.1016/j.physbeh.2016.12.044
69. Ross RA. Anandamide and vanilloid TRPV1 receptors. *Br J Pharmacol.* (2003) 140:790–801. doi: 10.1038/sj.bjp.0705467
70. Yoshioka M, Doucet E, Drapeau V, Dionne I, Tremblay A. Combined effects of red pepper and caffeine consumption on 24 h energy balance in subjects given free access to foods. *Br J Nutr.* (2001) 85:203–11. doi: 10.1079/BJN2000224
71. Hermann H, De Petrocellis L, Bisogno T, Schiano Moriello A, Lutz B, Di Marzo V. Dual effect of cannabinoid CB1 receptor stimulation on a

vanilloid VR1 receptor-mediated response. *Cell Mol Life Sci.* (2003) 60:607–16. doi: 10.1007/s000180300052
72. Mahmud A, Santha P, Paule CC, Nagy I. Cannabinoid 1 receptor activation inhibits transient receptor potential vanilloid type 1 receptor-mediated cationic influx into rat cultured primary sensory neurons. *Neuroscience* (2009) 162:1202–11. doi: 10.1016/j.neuroscience.2009.05.024
73. Santha P, Jenes A, Somogyi C, Nagy I. The endogenous cannabinoid anandamide inhibits transient receptor potential vanilloid type 1 receptor-mediated currents in rat cultured primary sensory neurons. *Acta Physiol Hung.* (2010) 97:149–58. doi: 10.1556/APhysiol.97.2010.2.1
74. Matsuda LA, Lolait SJ, Brownstein MJ, Young AC, Bonner TI. Structure of a cannabinoid receptor and functional expression of the cloned cDNA. *Nature* (1990) 346:561–4. doi: 10.1038/346561a0
75. Wahlqvist ML, Wattanapenpaiboon N. Hot foods–unexpected help with energy balance? *Lancet* (2001) 358:348–9. doi: 10.1016/S0140-6736(01)05586-6
76. Shi Z, Riley M, Taylor AW, Page A. Chilli consumption and the incidence of overweight and obesity in a Chinese adult population. *Int J Obes.* (2017) 41:1074–9. doi: 10.1038/ijo.2017.88
77. Snitker S, Fujishima Y, Shen H, Ott S, Pi-Sunyer X, Furuhata Y, et al. Effects of novel capsinoid treatment on fatness and energy metabolism in humans: possible pharmacogenetic implications. *Am J Clin Nutr.* (2009) 89:45–50. doi: 10.3945/ajcn.2008.26561
78. Inoue N, Matsunaga Y, Satoh H, Takahashi M. Enhanced energy expenditure and fat oxidation in humans with high BMI scores by the ingestion of novel and non-pungent capsaicin analogues (capsinoids). *Biosci Biotechnol Biochem.* (2007) 71:380–9. doi: 10.1271/bbb.60341
79. Baboota RK, Murtaza N, Jagtap S, Singh DP, Karmase A, Kaur J, et al. Capsaicin-induced transcriptional changes in hypothalamus and alterations in gut microbial count in high fat diet fed mice. *J Nutr Biochem.* (2014a) 25:893–902. doi: 10.1016/j.jnutbio.2014.04.004
80. Shen W, Shen M, Zhao X, Zhu H, Yang Y, Lu S, et al. Anti-obesity effect of capsaicin in mice fed with high-fat diet is associated with an increase in population of the gut bacterium *Akkermansia muciniphila*. *Front Microbiol.* (2017) 8:272. doi: 10.3389/fmicb.2017.00272
81. Lee GR, Shin MK, Yoon DJ, Kim AR, Yu R, Park NH, et al. Topical application of capsaicin reduces visceral adipose fat by affecting adipokine levels in high-fat diet-induced obese mice. *Obesity* (2013) 21:115–22. doi: 10.1002/oby.20246
82. Yu Q, Wang Y, Yu Y, Li Y, Zhao S, Chen Y, et al. Expression of TRPV1 in rabbits and consuming hot pepper affects its body weight. *Mol Biol Rep.* (2012) 39:7583–9. doi: 10.1007/s11033-012-1592-1
83. Song JX, Ren H, Gao YF, Lee CY, Li SF, Zhang F, et al. Dietary capsaicin improves glucose homeostasis and alters the gut microbiota in obese diabetic ob/ob mice. *Front Physiol.* (2017) 8:602. doi: 10.3389/fphys.2017.00602
84. Motter AL, Ahern GP. TRPV1-null mice are protected from diet-induced obesity. *FEBS Lett.* (2008) 582:2257–62. doi: 10.1016/j.febslet.2008.05.021
85. Lee E, Jung DY, Kim JH, Patel PR, Hu X, Lee Y, et al. Transient receptor potential vanilloid type-1 channel regulates diet-induced obesity, insulin resistance, and leptin resistance. *FASEB J.* (2015) 29:3182–92. doi: 10.1096/fj.14-268300
86. Marshall NJ, Liang L, Bodkin J, Dessapt-Baradez C, Nandi M, Collot-Teixeira S, et al. A role for TRPV1 in influencing the onset of cardiovascular disease in obesity. *Hypertension* (2013) 61:246–52. doi: 10.1161/HYPERTENSIONAHA.112.201434
87. Kentish SJ, Frisby CL, Kritas S, Li H, Hatzinikolas G, O'donnell TA, et al. TRPV1 channels and gastric vagal afferent signalling in lean and high fat diet induced obese mice. *PLoS ONE* (2015) 10:e0135892. doi: 10.1371/journal.pone.0135892
88. Janssens PL, Hursel R, Westerterp-Plantenga MS. Capsaicin increases sensation of fullness in energy balance, and decreases desire to eat after dinner in negative energy balance. *Appetite* (2014) 77:44–9. doi: 10.1016/j.appet.2014.02.018
89. Smeets AJ, Janssens PL, Westerterp-Plantenga MS. Addition of capsaicin and exchange of carbohydrate with protein counteract energy intake restriction effects on fullness and energy expenditure. *J Nutr.* (2013) 143:442–7. doi: 10.3945/jn.112.170613
90. Janssens PL, Hursel R, Martens EA, Westerterp-Plantenga MS. Acute effects of capsaicin on energy expenditure and fat oxidation in negative energy balance. *PLoS ONE* (2013) 8:e67786. doi: 10.1371/journal.pone.0067786
91. Ludy MJ, Mattes RD. The effects of hedonically acceptable red pepper doses on thermogenesis and appetite. *Physiol Behav.* (2011) 102:251–8. doi: 10.1016/j.physbeh.2010.11.018
92. Reinbach HC, Martinussen T, Moller P. Effects of hot spices on energy intake, appetite and sensory specific desires in humans. *Food Quality Preference* (2010) 21:655–61. doi: 10.1016/j.foodqual.2010.04.003
93. Smeets A, Westerterp-Plantenga M. The acute effects of a lunch containing capsaicin on energy and substrate utilization, hormones, and satiety. *Eur J Nutr.* (2009) 48:229–34. doi: 10.1007/s00394-009-0006-1
94. Chaiyasit K, Khovidhunkit W, Wittayalertpanya S. Pharmacokinetic and the effect of capsaicin in *Capsicum frutescens* on decreasing plasma glucose level. *J Med Assoc Thai* (2009) 92:108–113.
95. Reinbach HC, Smeets A, Martinussen T, Moller P, Westerterp-Plantenga MS. Effects of capsaicin, green tea and CH-19 sweet pepper on appetite and energy intake in humans in negative and positive energy balance. *Clin Nutr.* (2009) 28:260–5. doi: 10.1016/j.clnu.2009.01.010
96. Shin KO, Moritani T. Alterations of autonomic nervous activity and energy metabolism by capsaicin ingestion during aerobic exercise in healthy men. *J Nutr Sci Vitaminol.* (2007) 53:124–32. doi: 10.3177/jnsv.53.124
97. Westerterp-Plantenga MS, Smeets A, Lejeune MP. Sensory and gastrointestinal satiety effects of capsaicin on food intake. *Int J Obes.* (2005) 29:682–8. doi: 10.1038/sj.ijo.0802862
98. Yoshioka M, Imanaga M, Ueyama H, Yamane M, Kubo Y, Boivin A, et al. Maximum tolerable dose of red pepper decreases fat intake independently of spicy sensation in the mouth. *Br J Nutr.* (2004) 91:991–5. doi: 10.1079/BJN20041148
99. Chaiyata P, Puttadechakum S, Komindr S. Effect of chili pepper (*Capsicum frutescens*) ingestion on plasma glucose response and metabolic rate in Thai women. *J Med Assoc Thai* (2003) 86:854–60.
100. Lejeune MP, Kovacs EM, Westerterp-Plantenga MS. Effect of capsaicin on substrate oxidation and weight maintenance after modest body-weight loss in human subjects. *Br J Nutr.* (2003) 90:651–9. doi: 10.1079/BJN2003938
101. Matsumoto T, Miyawaki C, Ue H, Yuasa T, Miyatsuji A, Moritani T. Effects of capsaicin-containing yellow curry sauce on sympathetic nervous system activity and diet-induced thermogenesis in lean and obese young women. *J Nutr Sci Vitaminol.* (2000) 46:309–15. doi: 10.3177/jnsv.46.309
102. Yoshioka M, St-Pierre S, Drapeau V, Dionne I, Doucet E, Suzuki M, et al. Effects of red pepper on appetite and energy intake. *Br J Nutr.* (1999) 82:115–23.
103. Lim K, Yoshioka M, Kikuzato S, Kiyonaga A, Tanaka H, Shindo M, et al. Dietary red pepper ingestion increases carbohydrate oxidation at rest and during exercise in runners. *Med Sci Sports Exerc.* (1997) 29:355–61. doi: 10.1097/00005768-199703000-00010
104. Yoshioka M, Lim K, Kikuzato S, Kiyonaga A, Tanaka H, Shindo M, et al. Effects of red-pepper diet on the energy metabolism in men. *J Nutr Sci Vitaminol.* (1995) 41:647–56. doi: 10.3177/jnsv.41.647
105. Ohnuki K, Haramizu S, Oki K, Watanabe T, Yazawa S, Fushiki T. Administration of capsiate, a non-pungent capsaicin analog, promotes energy metabolism and suppresses body fat accumulation in mice. *Biosci Biotechnol Biochem.* (2001) 65:2735–40. doi: 10.1271/bbb.65.2735
106. Kang JH, Goto T, Han IS, Kawada T, Kim YM, Yu R. Dietary capsaicin reduces obesity-induced insulin resistance and hepatic steatosis in obese mice fed a high-fat diet. *Obesity* (2010) 18:780–7. doi: 10.1038/oby.2009.301
107. Baskaran P, Krishnan V, Ren J, Thyagarajan B. Capsaicin induces browning of white adipose tissue and counters obesity by activating TRPV1 channel-dependent mechanisms. *Br J Pharmacol.* (2016) 173:2369–89. doi: 10.1111/bph.13514
108. Baskaran P, Krishnan V, Fettel K, Gao P, Zhu Z, Ren J, et al. TRPV1 activation counters diet-induced obesity through sirtuin-1 activation and PRDM-16 deacetylation in brown adipose tissue. *Int J Obes.* (2017) 41:739–49. doi: 10.1038/ijo.2017.16
109. Kojima M, Hosoda H, Date Y, Nakazato M, Matsuo H, Kangawa K. Ghrelin is a growth-hormonereleasing acylated peptide from stomach. *Nature* (1999) 402:656–60. doi: 10.1038/45230

110. Sato T, Nakamura Y, Shiimura Y, Ohgusu H, Kangawa K, Kojima M. Structure, regulation and function of ghrelin. *J Biochem.* (2012) 151:119–28. doi: 10.1093/jb/mvr134
111. Senin LL, Al-Massadi O, Folgueira C, Castelao C, Pardo M, Barja-Fernandez S, et al. The gastric CB1 receptor modulates ghrelin production through the mTOR pathway to regulate food intake. *PLoS ONE* (2013) 8:e80339. doi: 10.1371/journal.pone.0080339
112. Date Y, Murakami N, Toshinai K, Matsukura S, Niijima A, Matsuo H, et al. The role of the gastric afferent vagal nerve in ghrelin-induced feeding and growth hormone secretion in rats. *Gastroenterology* (2002) 123:1120–8. doi: 10.1053/gast.2002.35954
113. Arnold M, Mura A, Langhans W, Geary N. Gut vagal afferents are not necessary for the eating-stimulatory effect of intraperitoneally injected ghrelin in the rat. *J Neurosci.* (2006) 26:11052–60. doi: 10.1523/JNEUROSCI.2606-06.2006
114. Page AJ, Slattery JA, Milte C, Laker R, O'donnell T, Dorian C, et al. Ghrelin selectively reduces mechanosensitivity of upper gastrointestinal vagal afferents. *Am J Physiol Gastrointest Liver Physiol.* (2007) 292:G1376–84. doi: 10.1152/ajpgi.00536.2006
115. Kentish S, Li H, Philp LK, O'donnell TA, Isaacs NJ, Young RL, et al. Diet-induced adaptation of vagal afferent function. *J. Physiol.* (2012) 590:209–21. doi: 10.1113/jphysiol.2011.222158
116. Yokoyama T, Saito T, Ohbuchi T, Suzuki H, Otsubo H, Okamoto T, et al. Ghrelin potentiates miniature excitatory postsynaptic currents in supraoptic magnocellular neurones. *J Neuroendocrinol.* (2009) 21:910–20. doi: 10.1111/j.1365-2826.2009.01911.x
117. Kola B, Farkas I, Christ-Crain M, Wittmann G, Lolli F, Amin F, et al. The orexigenic effect of ghrelin is mediated through central activation of the endogenous cannabinoid system. *PLoS ONE* (2008) 3:e1797. doi: 10.1371/journal.pone.0001797
118. Sobhani I, Bado A, Vissuzaine C, Buyse M, Kermorgant S, Laigneau J, et al. Leptin secretion and leptin receptor in the human stomach. *Gut* (2000) 47:178–83. doi: 10.1136/gut.47.2.178
119. Zsombok A, Jiang Y, Gao H, Anwar IJ, Rezai-Zadeh K, Enix CL, et al. Regulation of leptin receptor-expressing neurons in the brainstem by TRPV1. *Physiol Rep.* (2014) 2:e12160. doi: 10.14814/phy2.12160
120. Baggio LL, Drucker DJ. Biology of incretins: GLP-1 and GIP. *Gastroenterology* (2007) 132:2131–57. doi: 10.1053/j.gastro.2007.03.054
121. Torekov SS, Madsbad S, Holst JJ. Obesity–an indication for GLP-1 treatment? Obesity pathophysiology and GLP-1 treatment potential. *Obesity Rev.* (2011) 12:593–601. doi: 10.1111/j.1467-789X.2011.00860.x
122. Ryan D, Acosta A. GLP-1 receptor agonists: nonglycemic clinical effects in weight loss and beyond. *Obesity* (2015) 23:1119–29. doi: 10.1002/oby.21107
123. Broberger C. Brain regulation of food intake and appetite: molecules and networks. *J Intern Med.* (2005) 258:301–27. doi: 10.1111/j.1365-2796.2005.01553.x
124. Berthoud HR. The vagus nerve, food intake and obesity. *Regul Pept* (2008) 149:15–25. doi: 10.1016/j.regpep.2007.08.024
125. Hameed S, Dhillo WS, Bloom SR. Gut hormones and appetite control. *Oral Dis.* (2009) 15:18–26. doi: 10.1111/j.1601-0825.2008.01492.x
126. Page AJ, Kentish S. Plasticity of gastrointestingal vagal afferent satiety signals. *Neurogastroenterol Motil.* (2016) 29:e12973. doi: 10.1111/nmo.12973
127. Page AJ, Blackshaw LA. An *in vitro* study of the properties of vagal afferent fibres innervating the ferret oesophagus and stomach. *J Physiol.* (1998b) 512:907–16. doi: 10.1111/j.1469-7793.1998.907bd.x
128. Page AJ, Martin CM, Blackshaw LA. Vagal mechanoreceptors and chemoreceptors in mouse stomach and esophagus. *J Neurophysiol.* (2002) 87:2095–103. doi: 10.1152/jn.00785.2001
129. Kentish SJ, O'donnell TA, Isaacs NJ, Young RL, Li H, Harrington AM, et al. Gastric vagal afferent modulation by leptin is influenced by food intake status. *J Physiol.* (2013) 591:1921–34. doi: 10.1113/jphysiol.2012.247577
130. Kentish SJ, Li H, Frisby CL, Page AJ. Nesfatin-1 modulates murine gastric vagal afferent mechanosensitivity in a nutritional state dependent manner. *Peptides* (2017) 89:35–41. doi: 10.1016/j.peptides.2017.01.005
131. Zhoa H, Sprunger LK, Simasko SM. Expression of transient receptor potential channels and two-pore potassium channels in subtypes of vagal afferent neurons in rat. *Am J Physiol Gastrointest Liver Physiol.* (2009) 298:G212–21. doi: 10.1152/ajpgi.00396.2009
132. Tan LL, Bornstein JC, Anderson CR. Neurochemical and morphological phenotypes of vagal afferent neurons innervating the adult mouse jejunum. *Neurogastroenterology Motil.* (2009) 21:994–1001. doi: 10.1111/j.1365-2982.2009.01322.x
133. Wang X, Miyares RL, Ahern GP. Oleoylethanolamide excites vagal sensory neurones, induces visceral pain and reduces short-term food intake in mice via capsaicin receptor TRPV1. *J Physiol.* (2005) 564:541–7. doi: 10.1113/jphysiol.2004.081844
134. Daly DM, Park SJ, Valinsky WC, Beyak MJ. Impaired intestinal afferent nerve satiety signalling and vagal afferent excitability in diet induced obesity in the mouse. *J Physiol.* (2011) 589:2857–70. doi: 10.1113/jphysiol.2010.204594
135. Partosoedarso ER, Abrahams TP, Scullion RT, Moerschbaecher JM, Hornby PJ. Cannabinoid1 receptor in the dorsal vagal complex modulates lower oesophageal sphincter relaxation in ferrets. *J Physiol.* (2003) 550:149–58. doi: 10.1113/jphysiol.2003.042242
136. Burdyga G, Lal S, Varro A, Dimaline R, Thompson DG, Dockray GJ. Expression of cannabinoid CB1 receptors by vagal afferent neurons is inhibited by cholecystokinin. *J Neurosci.* (2004) 24:2708–15. doi: 10.1523/JNEUROSCI.5404-03.2004
137. Longhurst JC, Kaufman MP, Ordway GA, Musch TI. Effects of bradykinin and capsaicin on endings of afferent fibers from abdominal visceral organs. *Am J Physiol.* (1984) 247:R552–9. doi: 10.1152/ajpregu.1984.247.3.R552
138. Watanabe T, Kawada T, Yamamoto M, Iwai K. Capsaicin, a pungent principle of hot red pepper, evokes catecholamine secretion from the adrenal medulla of anesthetized rats. *Biochem Biophys Res Commun.* (1987) 142:259–64. doi: 10.1016/0006-291X(87)90479-7
139. Watanabe T, Kawada T, Kurosawa M, Sato A, Iwai K. Adrenal sympathetic efferent nerve and catecholamine secretion excitation caused by capsaicin in rats. *Am J Physiol.* (1988) 255:E23–27. doi: 10.1152/ajpendo.1988.255.1.E23
140. Kawada T, Watanabe T, Takaishi T, Tanaka T, Iwai K. Capsaicin-induced beta-adrenergic action on energy metabolism in rats: influence of capsaicin on oxygen consumption, the respiratory quotient, and substrate utilization. *Proc Soc Exp Biol Med.* (1986) 183:250–6. doi: 10.3181/00379727-183-42414
141. Spiegelman BM, Flier JS. Adipogenesis and obesity: rounding out the big picture. *Cell* (1996) 87:377–89. doi: 10.1016/S0092-8674(00)81359-8
142. Nedergaard J, Ricquier D, Kozak LP. Uncoupling proteins: current status and therapeutic prospects. *EMBO Rep.* (2005) 6:917–21. doi: 10.1038/sj.embor.7400532
143. Feldmann HM, Golozoubova V, Cannon B, Nedergaard J. UCP1 ablation induces obesity and abolishes diet-induced thermogenesis in mice exempt from thermal stress by living at thermoneutrality. *Cell Metab.* (2009) 9:203–9. doi: 10.1016/j.cmet.2008.12.014
144. Bishnoi M, Kondepudi KK, Gupta A, Karmase A, Boparai RK. Expression of multiple transient receptor potential channel genes in murine 3T3-L1 cell lines and adipose tissue. *Pharmacol Rep.* (2013) 65:751–5. doi: 10.1016/S1734-1140(13)71055-7
145. Baboota RK, Singh DP, Sarma SM, Kaur J, Sandhir R, Boparai RK, et al. Capsaicin induces "brite" phenotype in differentiating 3T3-L1 preadipocytes. *PLoS ONE* (2014b) 9:e103093. doi: 10.1371/journal.pone.0103093
146. Kida R, Yoshida H, Murakami M, Shirai M, Hashimoto O, Kawada T, et al. Direct action of capsaicin in brown adipogenesis and activation of brown adipocytes. *Cell Biochem Funct.* (2016) 34:34–41. doi: 10.1002/cbf.3162
147. Sun W, Li C, Zhang Y, Jiang C, Zhai M, Zhou Q, et al. Gene expression changes of thermo-sensitive transient receptor potential channels in obese mice. *Cell Biol Int.* (2017) 41:908–13. doi: 10.1002/cbin.10783
148. Brondani LDA, Assmann TS, Coutinho G, Duarte K, Gross JL, Canani LH, et al. The role of the uncoupling protein 1 (UCP1) on the development of obesity and type 2 diabetes mellitus. *Arq Bras Endocrinol Metab.* (2012) 56:215–25. doi: 10.1590/S0004-27302012000400001
149. Kawabata F, Inoue N, Masamoto Y, Matsumura S, Kimura W, Kadowaki M, et al. Non-pungent capsaicin analogs (capsinoids) increase metabolic rate and enhance thermogenesis via gastrointestinal TRPV1 in mice. *Biosci Biotechnol Biochem.* (2009) 73:2690–7. doi: 10.1271/bbb.90555
150. Okamatsu-Ogura Y, Tsubota A, Ohyama K, Nogusa Y, Saito M, Kimura K. Capsinoids suppress diet-induced obesity through uncoupling protein 1-dependent mechanism in mice. *J Funct Foods* (2015) 19:1–9. doi: 10.1016/j.jff.2015.09.005

151. Page AJ, Blackshaw LA. An *in vitro* study of the properties of vagal afferent fibres innervating the ferret oesophagus and stomach. *J Physiol.* (1998a). 512 (Pt 3):907–16.
152. Rong W, Hillsley K, Davis JB, Hicks G, Winchester WJ, Grundy D. Jejunal afferent nerve sensitivity in wild-type and TRPV1 knockout mice. *J Physiol.* (2004) 560:867–81. doi: 10.1113/jphysiol.2004.071746
153. Yoneshiro T, Aita S, Kawai Y, Iwanaga T, Saito M. Nonpungent capsaicin analogs (capsinoids) increase energy expenditure through the activation of brown adipose tissue in humans. *Am J Clin Nutr.* (2012) 95:845–50. doi: 10.3945/ajcn.111.018606
154. Bamshad M, Song CK, Bartness TJ. CNS origins of the sympathetic nervous system outflow to brown adipose tissue. *Am J Physiol.* (1999) 276:R1569–78. doi: 10.1152/ajpregu.1999.276.6.R1569
155. Madden CJ, Morrison SF. Hypoxic activation of arterial chemoreceptors inhibits sympathetic outflow to brown adipose tissue in rats. *J Physiol.* (2005) 566:559–73. doi: 10.1113/jphysiol.2005.086322
156. Skibicka KP, Grill HJ. Hypothalamic and hindbrain melanocortin receptors contribute to the feeding, thermogenic, and cardiovascular action of melanocortins. *Endocrinology* (2009) 150:5351–61. doi: 10.1210/en.2009-0804
157. Cao WH, Madden CJ, Morrison SF. Inhibition of brown adipose tissue thermogenesis by neurons in the ventrolateral medulla and in the nucleus tractus solitarius. *Am J Physiol Regul Integr Comp Physiol.* (2010) 299:R277–90. doi: 10.1152/ajpregu.00039.2010
158. Blouet C, Schwartz GJ. Duodenal lipid sensing activates vagal afferents to regulate non-shivering brown fat thermogenesis in rats. *PLoS ONE* (2012) 7:e51898. doi: 10.1371/journal.pone.0051898
159. Madden CJ, Santos Da Conceicao EP, Morrison SF. Vagal afferent activation decreases brown adipose tissue (BAT) sympathetic nerve activity and BAT thermogenesis. *Temperature* (2017) 4:89–96. doi: 10.1080/23328940.2016.1257407
160. Krieger JP, Santos Da Conceicao EP, Sanchez-Watts G, Arnold M, Pettersen KG, Mohammed M, et al. Glucagon-like peptide-1 regulates brown adipose tissue thermogenesis via the gut-brain axis in rats. *Am J Physiol Regul Integr Comp Physiol*. (2018). doi: 10.1152/ajpregu.00068.2018. [Epub ahead of print].
161. Szolcsanyi J. Capsaicin-type pungent agents producing pyrexia. In: Milton AS, editor. *Handbook of Experimental Pharmacology*. Berlin: Springer Verlag. (1982). p. 437–78.
162. Kobayashi A, Osaka T, Namba Y, Inoue S, Lee TH, Kimura S. Capsaicin activates heat loss and heat production simultaneously and independently in rats. *Am J Physiol.* (1998) 275:R92–8. doi: 10.1152/ajpregu.1998.275.1.R92
163. Gram DX, Ahren B, Nagy I, Olsen UB, Brand CL, Sundler F, et al. Capsaicin-sensitive sensory fibers in the islets of Langerhans contribute to defective insulin secretion in Zucker diabetic rat, an animal model for some aspects of human type 2 diabetes. *Eur J Neurosci.* (2007) 25:213–23. doi: 10.1111/j.1460-9568.2006.05261.x
164. Jancso G, Kiraly E, Jancso-Gabor A. Pharmacologically induced selective degeneration of chemosensitive primary sensory neurones. *Nature* (1977) 270:741–3. doi: 10.1038/270741a0
165. Razavi R, Chan Y, Afifiyan FN, Liu XJ, Wan X, Yantha J, et al. TRPV1+ sensory neurons control beta cell stress and islet inflammation in autoimmune diabetes. *Cell* (2006) 127:1123–35. doi: 10.1016/j.cell.2006.10.038
166. Diaz-Garcia CM, Morales-Lazaro SL, Sanchez-Soto C, Velasco M, Rosenbaum T, Hiriart M. Role for the TRPV1 channel in insulin secretion from pancreatic beta cells. *J Membr Biol.* (2014) 247:479–91. doi: 10.1007/s00232-014-9658-8
167. Basu S, Srivastava P. Immunological role of neuronal receptor vanilloid receptor 1 expressed on dendritic cells. *Proc Natl Acad Sci USA*. (2005) 102:5120–5. doi: 10.1073/pnas.0407780102
168. Toth BI, Benko S, Szollosi AG, Kovacs L, Rajnavolgyi E, Biro T. Transient receptor potential vanilloid-1 signaling inhibits differentiation and activation of human dendritic cells. *FEBS Lett.* (2009) 583:1619–24. doi: 10.1016/j.febslet.2009.04.031
169. Szollosi AG, Olah A, Toth IB, Papp F, Czifra G, Panyi G, et al. Transient receptor potential vanilloid-2 mediates the effects of transient heat shock on endocytosis of human monocyte-derived dendritic cells. *FEBS Lett.* (2013) 587:1440–5. doi: 10.1016/j.febslet.2013.03.027
170. O'connell PJ, Pingle SC, Ahern GP. Dendritic cells do not transduce inflammatory stimuli via the capsaicin receptor TRPV1. *FEBS Lett.* (2005) 579:5135–9. doi: 10.1016/j.febslet.2005.08.023
171. Akiba Y, Kato S, Katsube K, Nakamura M, Takeuchi K, Ishii H, et al. Transient receptor potential vanilloid subfamily 1 expressed in pancreatic islet beta cells modulates insulin secretion in rats. *Biochem Biophys Res Commun.* (2004) 321:219–25. doi: 10.1016/j.bbrc.2004.06.149
172. Zhang S, Ma X, Zhang L, Sun H, Liu X. Capsaicin reduces blood glucose by increasing insulin levels and glycogen content better than capsiate in streptozotocin-induced diabetic rats. *J Agric Food Chem.* (2017) 65:2323–30. doi: 10.1021/acs.jafc.7b00132
173. Kahn SE, Hull RL, Utzschneider KM. Mechanisms linking obesity to insulin resistance and type 2 diabetes. *Nature* (2006) 444:840–6. doi: 10.1038/nature05482
174. Fonseca VA. Defining and characterizing the progression of type 2 diabetes. *Diabetes Care* (2009) 32(Suppl. 2):S151–6. doi: 10.2337/dc09-S301
175. Ahuja KD, Robertson IK, Geraghty DP, Ball MJ. Effects of chili consumption on postprandial glucose, insulin, and energy metabolism. *Am J Clin Nutr.* (2006) 84:63–9. doi: 10.1093/ajcn/84.1.63
176. Kroff J, Hume DJ, Pienaar P, Tucker R, Lambert EV, Rae DE. The metabolic effects of a commercially available chicken peri-peri (African bird's eye chilli) meal in overweight individuals. *Br J Nutr.* (2017) 117:635–44. doi: 10.1017/S0007114515003104
177. Festa A, D'agostino R Jr, Howard G, Mykkanen L, Tracy RP, Haffner SM. Chronic subclinical inflammation as part of the insulin resistance syndrome: the Insulin Resistance Atherosclerosis Study (IRAS). *Circulation* (2000) 102:42–7. doi: 10.1161/01.CIR.102.1.42
178. Wu T, Dorn JP, Donahue RP, Sempos CT, Trevisan M. Associations of serum C-reactive protein with fasting insulin, glucose, and glycosylated hemoglobin: the third national health and nutrition examination survey, 1988-1994. *Am J Epidemiol.* (2002) 155:65–71. doi: 10.1093/aje/155.1.65
179. Gram DX, Hansen AJ, Wilken M, Elm T, Svendsen O, Carr RD, et al. Plasma calcitonin gene-related peptide is increased prior to obesity, and sensory nerve desensitization by capsaicin improves oral glucose tolerance in obese Zucker rats. *Eur J Endocrinol.* (2005) 153:963–9. doi: 10.1530/eje.1.02046
180. Pettersson M, Ahren B, Bottcher G, Sundler F. Calcitonin gene-related peptide: occurrence in pancreatic islets in the mouse and the rat and inhibition of insulin secretion in the mouse. *Endocrinology* (1986) 119:865–9. doi: 10.1210/endo-119-2-865
181. Gomtsyan A, Mcdonald HA, Schmidt RG, Daanen JF, Voight EA, Segreti JA, et al. TRPV1 ligands with hyperthermic, hypothermic and no temperature effects in rats. *Temperature* (2015) 2:297–301. doi: 10.1080/23328940.2015.1046013
182. Gavva NR, Tamir R, Klionsky L, Norman MH, Louis JC, Wild KD, et al. Proton activation does not alter antagonist interaction with the capsaicin-binding pocket of TRPV1. *Mol Pharmacol.* (2005) 68:1524–33. doi: 10.1124/mol.105.015727
183. Lehto SG, Tamir R, Deng H, Klionsky L, Kuang R, Le A, et al. Antihyperalgesic effects of (R,E)-N-(2-hydroxy-2,3-dihydro-1H-inden-4-yl)-3-(2-(piperidin-1-yl)-4-(trifluorom ethyl)phenyl)-acrylamide (AMG8562), a novel transient receptor potential vanilloid type 1 modulator that does not cause hyperthermia in rats. *J Pharmacol Exp Ther.* (2008) 326:218–29. doi: 10.1124/jpet.107.132233

Conflict of Interest Statement: The authors declare that the research was conducted in the absence of any commercial or financial relationships that could be construed as a potential conflict of interest.

frontiers in Endocrinology

REVIEW
published: 21 August 2018
doi: 10.3389/fendo.2018.00473

Deciphering the Roles of PPARγ in Adipocytes via Dynamic Change of Transcription Complex

*Xinran Ma, Dongmei Wang, Wenjun Zhao and Lingyan Xu**

Shanghai Key Laboratory of Regulatory Biology, Institute of Biomedical Sciences and School of Life Sciences, East China Normal University, Shanghai, China

Peroxisome proliferator-activated receptor γ (PPARγ), a ligand-dependent transcription factor highly expressed in adipocytes, is a master regulator of adipogenesis and lipid storage, a central player in thermogenesis and an active modulator of lipid metabolism and insulin sensitivity. As a nuclear receptor governing numerous target genes, its specific signaling transduction relies on elegant transcriptional and post-translational regulations. Notably, in response to different metabolic stimuli, PPARγ recruits various cofactors and forms distinct transcriptional complexes that change dynamically in components and epigenetic modification to ensure specific signal transduction. Clinically, PPARγ activation via its full agonists, thiazolidinediones, has been shown to improve insulin sensitivity and induce browning of white fat, while undesirably induce weight gain, visceral obesity and other adverse effects. Thus, deciphering the combinatorial interactions between PPARγ and its transcriptional partners and their preferential regulatory network in the processes of development, function and senescence of adipocytes would provide us the molecular basis for developing novel partial agonists that promote benefits of PPARγ signaling without detrimental side effects. In this review, we discuss the dynamic components and precise regulatory mechanisms of the PPARγ-cofactors complexes in adipocytes, as well as perspectives in treating metabolic diseases via specific PPARγ signaling.

Keywords: PPAR gamma, adipocytes, transcription complex, obesity, metabolic diseases

OPEN ACCESS

Edited by:
Andrew J. McAinch,
Victoria University, Australia

Reviewed by:
Pawel K. Olszewski,
University of Waikato, New Zealand
Claire Joanne Stocker,
University of Buckingham, United Kingdom

****Correspondence:***
Lingyan Xu
lyxu@bio.ecnu.edu.cn

Specialty section:
This article was submitted to Obesity, a section of the journal Frontiers in Endocrinology

Received: *04 April 2018*
Accepted: *31 July 2018*
Published: *21 August 2018*

Citation:
Ma X, Wang D, Zhao W and Xu L (2018) Deciphering the Roles of PPARγ in Adipocytes via Dynamic Change of Transcription Complex. Front. Endocrinol. 9:473. doi: 10.3389/fendo.2018.00473

INTRODUCTION

Adipose tissue is critical in maintaining energy homeostasis and insulin sensitivity in vertebrate organisms by directing energy fluxes toward triglyceride synthesis for storage or fuel mobilization for utilization in response to different metabolic requirements. Genetic, dietary, pathological, or aging-related disruption of adipose tissue function is one of the underlying causes of the current pandemics of metabolic diseases including obesity and type 2 diabetes. Adipose tissue exerts its normal physiological function via a complicated and delicate network of transcription factors to orchestrate and fine-tune various molecular events in adipocytes development, functionality, and senescence, among which peroxisome proliferator activated receptor γ (PPARγ) holds special importance for its unique and indispensable role in adipogenesis, lipid metabolism and insulin sensitivity (1). Moreover, evidences from murine and *Caenorhabditis elegans* models indicate that PPARγ is also a key driver in promoting longevity (2, 3). As a ligand dependent transcription factor, PPARγ exerts pleiotropic functions through its vast sets of downstream transcriptional targets. Mechanistic

studies reveal that, under different stimuli or physiopathological status, PPARγ forms distinct transcription complex with different set of cofactors and transcription partners to regulate specific transcriptional circuit. Though the upstream regulators of PPARγ transcription is well studied and documented, from an empirical standpoint, it would be intriguing to decipher the detailed molecular events during which PPARγ integrates and transduces diverse signals toward specific clusters of downstream targets. In this review, we aim to discuss our current understanding of the combinatorial interactions between PPARγ and its interaction partners and how their dynamic changes impact PPARγ downstream target gene transactivation under different metabolic scenario and during the aging process in adipose tissues, thus potentially provide us with more elaborate and precise strategies to screen novel therapeutic targets that target PPARγ and its cofactors in treating adipocyte dysfunctions and metabolic diseases.

DISTINCT ROLES OF ADIPOCYTES IN ENERGY HOMEOSTASIS

Three distinct types of fat (white, brown, and beige adipose tissue) exist based on different anatomic locations and functions (4). White adipocytes feature a single large lipid droplet and store excess energy in forms of triglycerides. In sharp contrast to white adipocytes, brown adipocytes, characteristically contain multiple lipid droplets and packed with mitochondrial, are vital in defending body temperature through activation of uncoupling protein 1 (UCP1) and uncoupling the mitochondrial respiratory chain to produce heat, thus contribute greatly for energy expenditure and adaptive thermogenesis. Interspersed within white fat, the newly discovered beige adipocytes share functional similarities with both white and brown adipocytes. Briefly speaking, beige adipocytes are indistinguishable from white adipocytes morphologically under basal condition. While upon cold or adrenogenic signaling stimulation, beige adipocytes are activated (referred to as the "browning of white fat" effect) and take on a brown adipocyte-like look with multiple small lipid droplets and rich mitochondria content. Similar to brown fat, activated beige adipocytes have high UCP1 expression and enhanced thermogenic capacity and energy expenditure (5–7). Importantly, upon activation, brown, and beige adipocytes uptake high levels of lipid and glucose for heat production, thus serve as a metabolic sink to clear excess nutrients in blood and contribute to insulin sensitivity and whole body lipid/glucose metabolism (8), in addition to the lowing body weight effect. Together, white, brown and beige adipocytes maintain the whole-body energy homeostasis.

Though rise from different precursors, white, brown and beige adipocytes all go through a finely tuned differentiation process (referred to as "adipogenesis") to mature and become fully functional (9). Then, mature adipocytes can respond to different metabolic stimuli to store or utilize energy, as well as crosstalk with other cell types via various adipokines, cytokines or lipid/glucose fluxes (10). Eventually, adipocytes undergo senescence and gradually lose their differentiation or thermogenic capability (11, 12). During various stages of the adipocyte lifespan, PPARγ is a well-established central player in orchestrating the numerous molecular events that ensure the normal physiological function of white, brown and beige adipocytes. PPARγ, a member of the nuclear receptor PPARs family, shares the common PPAR domain structures that feature a highly conserved DNA-binding domain (DBD) and a transactivation domain (AF1) at the N-terminal region, and a ligand-binding domain (LBD) and a ligand-dependent transactivation domain (AF2) at the C-terminal region. PPARγ has two isoforms, PPARγ1 and PPARγ2, the latter contains an additional NH2-terminal region composed of 30 amino acids due to different promoter usage and alternative splicing (13). PPARγ1 expresses ubiquitously while PPARγ2 expresses the highest in adipose tissues and is highly inducible in other tissues under high fat diet (HFD) (14). By forming distinct transcription complexes with different interaction partners or through epigenetic modifications, PPARγ exerts critical and pleiotropic functions in adipose tissues that include: (I) adipocyte differentiation and lipid storage, (II) acquisition of brown/beige adipocyte identity (III) maintenance of brown/beige adipocyte thermogenic capacity, (IV) brown/beige adipocyte functional decline in aging, and (V) regulation of diabetic gene program (15). The dynamics beween PPARγ and its transcription partners in these physiological processes are discussed below.

PPARγ/Corepressors/Coactivators Dynamics Controls Adipocyte Differentiation

PPARγ is considered the master regulator for adipogenesis since ectopic expression of PPARγ alone in fibroblasts could successfully drive the adipogenesis program and no other factors could induce adipogenesis without the presence of PPARγ (16–18). *In vivo* studies reveal PPARγ is vital in controlling adipogenesis and lipid/glucose metabolism. For instance, aP2- and adiponectin-driven loss of PPARγ in adipose tissues consistently lead to impaired adipocyte differentiation and reduced fat weights or lipodystrophy, though different animal models show improved or worsen insulin sensitivity depend on the extent of PPARγ deficiency (19–21). In adult mice, PPARγ ablation in adipose tissues with tamoxifen-dependent Cre-ER(T2) recombination system leads to adipocyte death and subsequent renewal, suggesting that PPARγ is required for the survival of mature adipocyte (22, 23). In clinic, patients with heterozygous PPARγ mutation show partial lipodystrophy and insulin resistance (24). PPARγ is also a critical thrifty gene that governs hoarding gene programs for energy storage mostly in white adipocytes (25).

Adipocytes differentiation is a closely regulated process that rises in response to physiological needs, i.e., adipocytes turnover and excess nutrient influx. Though it may function differently in aging (26), during development and in adulthood, PPARγ controls the transcriptional activation of the adipogenesis process through ligand binding and selective interaction with transcription corepressors or coactivators (17). Corepressors

bind to transcription factor/DNA complexes to recruit histone deacetylases (HDAC) and make the target DNA region less accessible for transcription. On the contrary, coactivators possess intrinsic histone acetyltransferase (HAT) activity or recruit other proteins with HAT activity to acetylate histones and loosen the chromatin in a limited region, allowing for increased basal transcription machinery accessibility (27). PPARγ constitutively forms a heterodimer with retinoid X receptor (RXR) and binds to a specific DNA sequence termed PPAR response elements (PPRE). In basal condition, unliganded PPARγ forms a complex with transcription corepressors such as silencing mediator of retinoid and thyroid hormone receptors (SMRT), the nuclear receptor corepressor (NCoR), and HDACs, which blocks its transactivation activity. Upon ligand binding, PPARγ undergoes a conformational change, dissociates corepressors and recruits coactivators i.e., CREB-binding protein (CBP), histone acetyltransferase p300 (p300) and PPAR-binding protein (PBP), thus initiates the adipogenic gene programs including Fatty Acid Binding Protein 4 (Fabp4), Cluster of differentiation 36 (Cd36), Adiponectin, Fatty Acid Synthase (Fasn), etc. (28, 29). It has been shown that coactivators deficiency in fibroblasts hinders adipocyte differentiation while adipocytes lack corepressors accumulate more lipids, which demonstrates the dynamic competition between activating vs. suppressive PPARγ-cofactors transcriptional complexes in adipogenesis (30, 31).

PPARγ/PRDM16/EBF2/EHMT1 Complex Determines Brown/Beige Adipocyte Identity

It is demonstrated that brown adipocytes and skeletal muscle cells rise from the common *Myf5*+ Dermomyotomal precursors while beige adipocytes and white adipocytes share the common *Pdgfra*+ mesodermal stem cells (32). Besides its indispensable role in promoting differentiation of white, brown and beige adipocytes, another critical function of PPARγ resides in the determination of brown and beige adipocyte identity. To achieve this, PPARγ recruits PRDM16, EBF2, and EHMT1 to coordinate the transcriptional circuits toward the brown/beige lineage (33).

For brown/beige adipocytes to acquire their identity and become thermogenic poised adipocytes, PPARγ recruits PR (PRD1-BF1-RIZ1 homologous)-domain-containing 16 (PRDM16) to form a core transcription complex that determines the transition of brown adipocyte from skeletal muscle cell or beige adipocyte from white adipocyte. Mass spectrometry analysis indicates PPARγ as the only DNA binding transcription factor interacts with PRDM16 in a near stoichiometric manner (34). This is further proved when full length GST-PPARγ2 fusion protein binds to *in vitro* translated PRDM16. PRDM16 is a powerful inducer and maintainer of the thermogenic phenotype in both brown adipocyte development and the browning process (35, 36). Mechanistic studies show that PRDM16 binds to PPREs on the promoter and/or enhancer of brown fat-selective genes and highly stimulates the activity of a PPRE luciferase reporter. Besides, PRDM16 fails to promote adipogenesis in PPARγ-deficient fibroblasts (37), indicating it at least partially exerts function via PPARγ. In myocytes, in the presence of PPARγ agonists, PRDM16 induces multiple PPARγ target genes in adipogenesis like aP2 and adiponectin, as well as brown fat-selective gene program, including Ucp1 and Cidea. Later, it is revealed that PPARγ agonists could induce a white-to-brown fat conversion through stabilization of PRDM16 protein, suggesting the existence of a positive regulatory loop to strengthen the interaction of the PPARγ/PRDM16 complex to maintain the thermogenic capacity in beige adipocytes (38). *In vivo* studies echo the results from *in vitro* studies. Transgenic and tissue specific animal models show that increased expression of PRDM16 in rodent inguinal white adipose tissue (iWAT) and in mature adipocytes promotes beige adipocyte commitment and prevents HFD-provoked weight gain and systemic insulin resistance (39). Conversely, deletion of Prdm16 in adipocytes causes a profound loss of beige adipocytes in mice, leading to aggravated metabolic deregulation upon exposure to HFD (40).

Two other factors, Histone-lysine N-methyltransferase (EHMT1) and Early B-cell factor (EBF2), present in the PPARγ/PRDM16 complex and facilitate its function in brown/beige fat identity determination (41). EHMT1 is the only methyltransferase purified specifically with PRDM16 by mass spectrum. It induces the inhibitory H3K9me2 and H3K9me3 at PRDM16-resident myogenic gene promoter regions, thus enables the PPARγ/PRDM16/EHMT1 to promote the common $Myf5^{+}$ precursors toward brown adipocytes linage instead of muscle linage. EHMT1 also controls thermogenesis by stabilizing PRDM16 and extending its half-life. Similar to PRDM16, EHMT1 fat-specific deficient mice show obesity and insulin resistance (41). Moreover, it has been reported that activation of brown adipocytes in the adult human perirenal depot is highly correlated with PRDM16–EHMT1 complex expression (42).

On the other hand, it is demonstrated that PPARγ recruits EBF2 to its brown-selective binding site and coactivates the expression of brown fat-selective genes such as Ucp1, Pparα, and Prdm16 (43). Genome-wide ChIP-sequencing and motif analyses of the consensus binding site for EBF2 reveal that it is highly enriched in brown adipocytes compared to white and beige fat. Consistent with its function in coactivating PPARγ downstream brown fat-selective gene program, EBF2 deficient mice fail to thrive due to severe defects in brown fat development and themogenesis (43). Intriguingly, transcription regulator ZFP423 maintains white fat identify via inhibition of EBF2 and PRDM16 activity (44), further suggesting the critical role of PPARγ/PRDM16/EBF2 in brown adipocyte development.

Overall, the PPARγ/PRDM16/EBF2/EHMT1 complex determines the identity of brown/beige adipocytes. It has been shown that the loss of brown and beige fat may predispose the obese and aging population to metabolic dysfunction, thus future extensive study of this complex is fundamental for developing compounds that could drive precursor cells to undergo brown/beige adipocytes fate and potentially achieve enhanced thermogenesis and energy expenditure.

PPARγ/PRDM16/PGC1α Modulates Brown/Beige Adipocyte Functionality

After the thermogenic endowment of brown/beige fat, the PPARγ/PRDM16 complex recruits another distinct set of cofactors to promote brown/beige fat function in adaptive thermogenesis and energy homeostasis, among which PPARγ-coactivator PGC1α plays a central role. PGC1α is first cloned from murine brown fat cell cDNA library through yeast two-hybrid system using PPARγ partial protein as bait (45). As a coactivator, PGC1α is capable of binding to and coactivating many nuclear receptors and transcription factors to exhibit different functions, such as PPARα, β/δ for fatty acid β-oxidation, thyroid receptor and IRF4 for thermogenesis, HSF1 for heat shock responses, NRF1 and NRF2 for mitochondrial biogenesis (46–48). In brown fat, PGC1α promotes mitochondrial biogenesis and thermogenesis at least partially by coactivating PPARγ and enhancing PPARγ's transcription activity on the thermogenic gene program, including Cidea, Elovl3, and Ucp1 (49). Moreover, it has been found that PRDM16 directly interacts with PGC1α, which increases PGC1α expression and promotes PGC1α transactivation activity (50). These data suggest the existence of a PPARγ/PRDM16//PGC1α thermogenic transcription complex in the regulation of brown/beige functionality. This core complex in turn recruits other cofactors or undergoes various modifications to fine tune thermogenesis and energy homeostasis.

For example, MED1 is found to be enriched along with PPARγ/PRDM16 complex on the promoters of brown fat-selective genes (51). As a component of mediator complex, MED1 plays a crucial role in regulating transcription in part through bridging the transcription factor-bound enhancer regions with the general transcriptional machinery and RNA Pol II at gene promoters. In the brown/beige adipocytes context, MED1 physically binds to PRDM16 and is then recruited to super enhancers at brown fat-selective genes. Consistently, MED1 binding at PRDM16 target sites reduces in PRDM16 deficiency BAT, causing a fundamental change in chromatin architecture at key brown fat-selective genes (52).

The SRCs family, also known as p160 proteins, includes SRC-1/NCoA-1, SRC-2/GRIP1/TIF2/NCoA2, and SRC-3/p/CIP/AIB1. They are transcriptional coactivators that interact with nuclear receptors and enhance their transactivation in a ligand-dependent manner (27, 53). In the metabolic context, they work as cofactors for PPARγ/PGC1α to influence brown/beige function and energy homeostasis. For Instance, SRC-$1^{-/-}$ mice showed partially impaired PPARγ function in the brown fat and are prone to obesity due to reduced energy expenditure and fatty acid oxidation upon HFD feeding (54, 55). Mechanistic study reveals that SRC-1 stabilizes PPARγ/PGC1α interaction and thus increases PGC1α-mediated adaptive thermogenesis (54). On the contrary, SRC-$2^{-/-}$ mice are protected against obesity. In white fat, PPARγ preferentially recruits SRC-2 as its coactivator to transactivate downstream fat uptake and storage pathways while in the brown fat SRC-2 competes with SRC-1 for PPARγ binding and disrupts SRC-1-induced interaction between PPARγ and PGC1α (56, 57). Meanwhile, in SRC-$3^{-/-}$ mice, HFD feeding causes a depot-selective decrease in PPARγ2 level, resulting in body weight reduction, fat mass decrease and fat redistribution in knockout mice (58, 59). Besides, SRC-3 induces PGC1α acetylation and consequently inhibits its activity in brown fat (60). SRC-3 also cooperates with SRC-2 to attenuate PPARγ phosphorylation at S114, which in turn increase PPARγ transcriptional activity and adipogenesis (61). Collectively, these data summarize the crucial roles of SRC family members that cooperate or antagonize with each other to regulate the interaction of PPARγ/PGC1α complex and its transactivation activity on the thermogenic network.

The stability of PPARγ/PRDM16 complex also impacts the induction of brown fat gene programs and thus the brown/beige fat function. It is well demonstrated that SirT1-dependent deacetylation of PPARγ Lys268 and Lys293 facilitate the close interaction between PPARγ and PRDM16 and is essential for the selective induction of brown fat-selective genes and repression of visceral white fat-selective genes (62). Silencing SIRT1 in 3T3-L1 preadipocytes leads to their hyperplasia and increased expression of white fat and inflammatory markers with a parallel decrease in brown fat markers (63). Specific genetic ablation of SIRT1 in WAT leads to obesity, increased inflammatory infiltration, and insulin resistance similar to that observed in HFD induced obesity, further suggesting SIRT1 deficiency leads to whitening effects of mature adipocytes (64). Conversely, SirT1 pharmacologic activators, i.e., resveratrol is shown to be effective in inducing the browning of white fat, weight loss, and improved insulin sensitivity in mice, though possibly through multiple mechanisms in addition to SirT1 activation (65). On the other hand, a few negative regulators of browning work through disrupting PPARγ/PRDM16 interactions. For example, TLE3 is a white-selective cofactor that competes with PRDM16 for PPARγ interaction to specify lipid storage or thermogenic gene programs (66). In addition to transcriptional factors and cofactors, PexRAP, a peroxisomal lipid synthetic enzyme interacts with PPARγ and PRDM16 and disrupts PRDM16-mediated gene expression (67). Last but not least, it has to be noted that nuclear factor I-A (NFIA) is recently reported to co-localize with PPARγ at the brown fat specific enhancers and facilitate PPARγ chromatin accessibility for induction of brown fat gene programs through mechanisms independent of the PPARγ/PRDM16 complex (68).

Collectively, these findings extend our understanding on how the PPARγ/PRDM16/PGC1α thermogenic transcriptional complex ensures delicate regulation on brown/beige fat functions by fine tuning its various components and modification status. The fact that the thermogenic transcriptional complex is required for brown/beige adipocytes to be fully functional supports the notion of targeting it for future potential drug discoveries to treat obesity and metabolic diseases, while inhibition of the negative regulators of this complex provides alternative strategies of inducing browning for energy expenditure.

PPARγ/Cofactors Complex in Aging

Life expectancy increases with the advancement in modern medicine and the improvement in life quality, bringing forward an aging society. It has been well accepted that energy

homeostasis is tightly controlled by the central nervous system, most prominently in the hypothalamus and brainstem areas that receive and integrate peripheral signals such as insulin and leptin, and in turn regulate food intake and energy metabolism in peripheral organs including adipose tissues, livers, and muscle (69). Thus it is not surprising that metabolic dysfunction occurs in line with aging due to the gradual deterioration in brain function. In both rodents and humans, advanced aging features significant weight loss due to anhedonia, anorexia, lipodystrophy, and muscle atrophy caused by the deregulations in brain (70). Intriguingly, during aging, peripheral organs such as adipose tissues undergo programmed functional loss and senescence as well. It is well documented that during aging, adipose tissues undergo a gradual exhaustion in progenitor pool, impaired proliferation and differentiation capability in preadipocytes and programmed functional loss in mature adipocytes (71, 72), resulting in disrupted lipid and glucose metabolism and impaired energy homeostasis. The aging trajectory begins around middle age after the peak fertility is passed. Compared to the phase of advanced aging, this phase often features an increase in body weight and fat mass, impaired metabolic fitness, and deregulated lipid profiles, during which the senescence and dysfunction of adipose tissues play a profound role. Indeed, midlife weight gain is one of the major risk factors for metabolic syndrome such as Type 2 diabetes, cardiovascular diseases, hypertension, hyperlipidemia, hepatic steatosis, and certain types of cancer, which poses a serious burden on public health management nowadays (73, 74). Thus, how aging affects adipocyte function and its intrinsic mechanism attract great attentions in the recent years (75).

As the master regulator in adipocytes, with the triumph of specific cre/loxP recombination system, the *in vivo* roles of PPARγ and its cofactors in fat biology during development or in young adult animals have been extensively studied. However, the existing aP2-Cre/loxP or adiponectin-Cre/loxP system deletes gene in fat tissues in early stages of life, the results of which are hard to extrapolate to the aging process. It has been shown that the PPARγ agonist rosiglitazone (TZD) treatment rescues shortened lifespan in *C. elegans* and induces a transcriptional signature that overlaps with longevity-associated genes (3). Besides, hypomorphic PPARγ mice and PPARγ2 heterozygous mice both show reduced lifespan (2), indicating an important role of PPARγ in aging. Considering the metabolic derangement in adipose tissues during aging and the critical role of PPARγ in adipocytes, it merits further investigation on the dynamics of PPARγ and its cofactors specifically in the aging process and how they impact the functional decline in adipose tissues.

Using the adenoviral delivery strategy, Ma et al. reported the surprising finding that loss of PPARγ specifically in subcutaneous fat in aging mice (12-month-old) is sufficient to increase body weight and insulin resistance by accelerating the decay of browning effects of white fat and disrupting energy homeostasis. Detailed analysis reveals that in aging adipose tissues, PPARγ preferentially binds to the promoters of browning vs. whitening gene program, thus maintains browning capability of subcutaneous fat of aging mice rather than lipid storage,

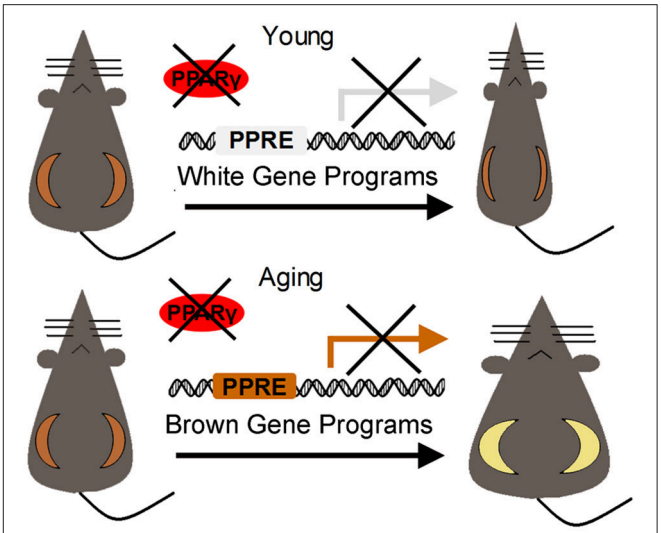

FIGURE 1 | Preferential regulation of white and brown gene programs by PPARγ in beige fat during aging.

as shown by gene program expression array and *in vivo* ChIP analysis (**Figure 1**). Meanwhile, although the total PPARγ levels do not change, PPARγ Ser273 phosphorylation increases during aging, which may potentially affect PPARγ affinity with its cofactors and rewire its metabolic circuitry toward brown gene program (26). Additionally, in rodent and human adipose tissues, SRC-1 expression levels decrease during aging, which may disrupt PPARγ/SRC-1 complex and its function in insulin sensitivity and adipogenic activity (76). These works offer novel insights on the unique combinatorial organization of the PPARγ/cofactors complex and the resulting target gene sets under the aging scenario, which might be largely different than previously reported PPARγ function in young animal models. From a therapeutic point of view, these results emphasize the need of personalized treatment when targeting PPARγ to treat metabolic disorders in patients of different ages. It would also be of importance to further investigate the potential benefits of targeting PPARγ in preventing age-associated metabolic diseases and promoting longevity.

PPARγ Phosphorylation in Diabetic/Adipogenic/Osteogenic Gene Program

In addition to recruitment of different cofactors, the post-translational regulations of PPARγ add another layer of regulation for the PPARγ/cofactors complex to selectively transactivate different gene circuits. In clinic, the full PPARγ agonists TZDs are very effective in glycemic control but have multiple adverse effects such as obesity, water retention, and increased risk of cardiovascular diseases and bone fractions. The opportunity for improvement emerges when Spiegelman's lab identifies the distinguish role of PPARγ Ser273 phosphorylation in lipid metabolism and insulin sensitivity (77–79). Briefly, in HFD induced obesity, protein kinase cyclin-dependent kinase 5

(Cdk5) is activated and in turn phosphorylates PPARγ at Ser273. This form of post-translational modified PPARγ selectively transactivates target genes involved in insulin resistance, without significant changes in adipogenic or osteogenic gene program (77). Consistently, Ma et al. report increased PPARγ Ser273 phosphorylation in iWAT of 12-month-old mice, which may contribute to impaired insulin sensitivity during aging (26).

PPARγ Ser273 phosphorylation is regulated by its interacting cofactors, which specifies a regulatory role of PPARγ/cofactors complex on the diabetic gene program. For example, PPARγ corepressor NcoR functions as an adaptor to enhance Cdk5 activity on interacting and phosphorylating PPARγ Ser273. Consistently, when fed a HFD, compared to wild type mice, fat-specific NCoR-deficient mice are prone to obesity yet have enhanced insulin sensitivity (80). Upon PPARγ Ser273 phosphorylation, phosphorylated PPARγ recruits thyroid hormone receptor-associated protein 3 (thrap3) to facilitate the expression of the diabetic gene programs (78). These data establish a delicate control of diabetic genes by PPARγ/cofactor complex through PPARγ Ser273 phosphorylation, as well as the potential of targeting PPARγ Ser273 phosphorylation to improve insulin sensitivity while eliminating the disadvantage of side effects. Of therapeutic significance, ERK have been shown to phosphorylate PPARγ Ser273 and induce insulin resistance in the absence of Cdk5, rendering ERK as promising anti-diabetic targets (79). Moreover, novel PPARγ partial ligands such as SR1664, F12016, and antibiotic ionomycin are designed or screened to inhibit PPARγ Ser273 phosphorylation, which show effective glycemic control with minimal side effects (81–83).

Aside from its numerous functions in adipocytes, PPARγ also plays vital role in controlling the balance between bone marrow adipogenesis and bone formation. For instance, PPARγ phosphorylation at Ser112 by mitogen-activated protein kinases (MAPKs) inhibits adipogenesis while promoting osteogenesis (84). A non-phosphorylatable Ser112 PPARγ mutation drives adipogenic differentiation and inhibited osteoblastogenesis *in vitro*. Consistently, mice carrying this homozygous PPARγ mutation (PPARγ-S112A mice) show increased bone marrow adipose tissue with reduced bone volume. In another study, PPARγ phosphorylation at different sites exhibits osteoblastic (pS112) or osteoclastic (pS273) activity thus regulates bone formation and absorption in a delicate balance. These collective data, along with the role of PPARγ Ser273 phosphorylation in promoting diabetic gene program, show the advantage of using PPARγ agonists against selective phosphorylation sites. For instance, SR10171, a PPARγ S273 phosphorylation blocker, increases both insulin sensitivity and osteoclastogenesis (85) while PPARγ partial agonist Telmisartan, which decreases PPARγ S273 without altering pS112 phosphorylation, promotes browning effects and improves insulin sensitivity without altering bone mass or bone biomechanical properties in mice (86). Thus, it would be desirable to develop pharmacologic agents targeting specific PPARγ phosphorylation sites, especially ones that dephosphorylate S273 while maintaining pS112 phosphorylation, to maximize their beneficial activities.

PERSPECTIVES

In clinic, PPARγ Pro12Ala polymorphism is identified as one of the common risk polymorphisms for Type 2 diabetes in multiple GWAS studies (87). Indeed, the thiazolidinedione class of drugs, the PPARγ full agonists, has a long history of use in treating Type 2 diabetes mellitus for its insulin sensitizing effects, though multiple side effects exist including obesity, water retention, increased risk of cardiovascular diseases and bone fractions. Besides, recent studies indicate PPARγ play an important role in antiretroviral treatment related adipocyte dysfunction and lipodystrophy in HIV-infected patients. These studies potentiate the importance of developing PPARγ partial agonists to selectively activate a specific set of its numerous target genes in order to avoiding possible side effects. To date, various PPARγ partial agonists are in different stages of drug development yet none has progressed into clinic due to insufficient efficacy and potential adverse effects, which merits a close examination to gain more mechanistic insights of PPARγ.

Of note, when developing PPARγ agonists, it is necessary to put the interaction between PPARγ and its cofactors into the equation since after ligand binding, PPARγ recruits transcription partners and cofactors to form a transcription complex to achieve selective target gene transactivation. In this review, we highlight a comprehensive review of the dynamics in transcription partners, coregulators, and post-translational modifications of PPARγ in adipose tissues during various stages of the adipocyte life cycle and the resulting regulatory function on fat development, thermogenesis and adipocyte senescence (**Figure 2**). PPARγ dissociates corepressors (e.g., NCoR, HDAC, SMRT) and binds with coactivators including CPB, p300, and PBP to initiate adipocyte differentiation in white, brown and beige adipocytes. In brown and beige adipocytes, PPARγ complexes with PRDM16/EBF2/EHMT1 for brown/beige cell linage determination while their unique functions in adaptive thermogenesis and energy homeostasis are maintained and modulated by the PPARγ/PRDM16//PGC1α complex as well as their interaction with various cofactors i.e., MED1, SRC1/2/3, and TLE3. Of therapeutic relevance, under aging scenario, PPARγ may complex with different cofactors due to different post-translational modifications or cofactor expression levels and thus exert distinct function as compared to its function in young animals. Last but not least, modulation of phosphorylation status of PPARγ selectively activates the diabetic or adipogenic circuits in adipocytes, which serves as an attractive strategy for therapeutic development. In recent years, the triumph of high-throughput sequencing technology has offered us the whole picture of the binding profiles of PPARγ on the genome-wide scale in white, brown and beige adipocytes under different metabolic conditions, which enable us to gain a deeper understanding of the common and distinct target gene sets regulated by PPARγ in different fat depots, under different diet regimes or ages, or in response to different environmental or drug stimulus. However, challenge remains as how PPARγ achieves differential regulatory patterns in different scenarios. To achieve this, multiple ChIP sequence analyses using various PPARγ cofactors are needed to link the dynamics of PPARγ and

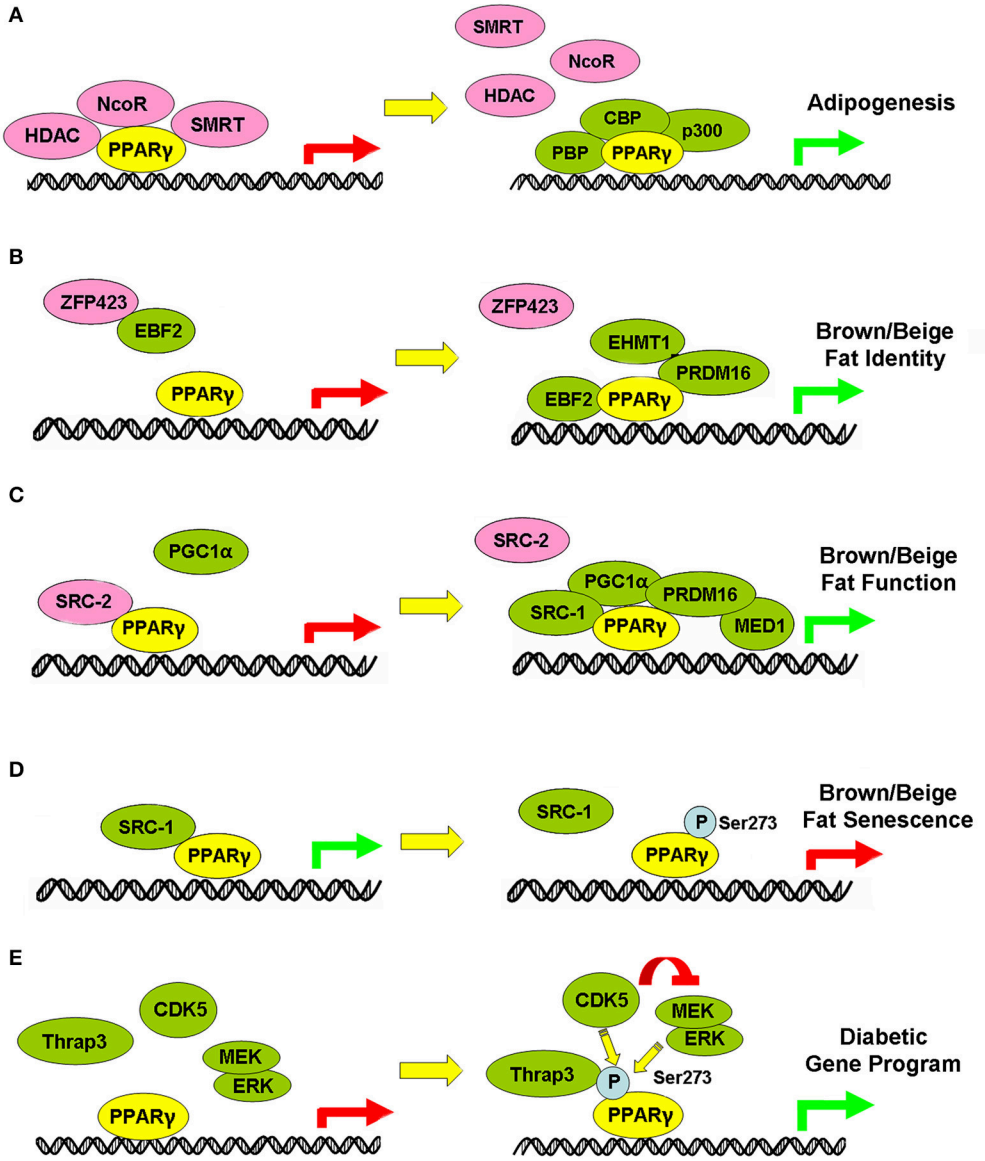

FIGURE 2 | Illustration of dynamic regulation of PPARγ-centered complex in different physiological processes of adipocytes. Green arrows indicate activation, while red arrows indicate suppression of transcriptional gene programs. Green and Pink circle indicates proteins in cooperation with PPARγ to activate and suppress specific gene programs. **(A-E)** PPARγ-centered complex in the regulation of Adipogenesis **(A)**, Brown/beige fat identity **(B)**, Brown/beige fat function **(C)**, Brown/beige fat senescence **(D)** and Diabetic gene program **(E)**.

its transcription partners with specific transactivation circuits and functionality.

During gene transcription, upon transcription factor binding, cofactors add an extra layer of transcriptional regulation on target genes and endow enhanced regulatory complexity. To combat the high prevalence of metabolic diseases worldwide, the needs for novel PPARγ agonists that feature maximum beneficial effects i.e., efficient glycemic control or enhanced "browning" effects while avoid undesirable side effects are heightened. With the crystal structure of PPARγ fully resolved and the accumulating data on its conformational changes upon full or partial agonists binding, a large body of works focuses on finding potential novel PPARγ agonists via computational predictions and virtual screening strategies. However, despite binding to the PPARγ ligand binding domain with high affinity as predicted, these compounds often face the problem of low transactivation activity *in vitro*, which hinders their progression into clinic. In this regard, the importance of cofactors during PPARγ transactivation events is underappreciated. It would be more informative to resolve the structure changes of PPARγ in the presence of various cofactors i.e., PRDM16 and PGC1α and take the dynamics between PPARγ and its cofactors into

consideration when designing new PPARγ agonists in the future. For example, strategies could be developed to screen for agonists that could strengthen the interaction between PPARγ and specific coactivators or block PPARγ phosphorylation at specific sites.

In previous reports, specific PPARγ deletion in adipose tissues in young adult animals results in lipodystrophy or massive adipocyte death, indicting an indispensable role of PPARγ in adipose tissue development and survival. Unexpectedly, PPARγ deletion in a temporal-specific manner in inguinal fat of aging animals causes significant increases in body weight and fat mass, which is in sharp contrast to young control animals (26). Further analyses show PPARγ has unique spectrums of interaction partners and target genes in aging, which is in consistent with previous reports of PPARγ as a potential driver for increased longevity (2, 3, 26). These findings shed first light on the potential of using PPARγ agonists in aged population to promote healthspan and lifespan. As a transcription factor with pleiotropic functions, targeting PPARγ could have multiple benefits against various aspects of aging. Firstly, aging features metabolic derangement, toward which PPARγ agonists show high efficacy in glycemic control, thus promoting metabolic fitness during aging. Secondly, caloric restriction (CR) is a well-established nutritional intervention that increases longevity and promotes metabolic health in various species from *C. elegance* to primates (88). It is reported that PPARγ expression levels are dramatically induced by CR treatment in metabolic organs, especially in inguinal fat for browning of white fat, suggesting that PPARγ activation might mimic CR effects at least in fat tissues (89). Thirdly, recent reports show compounds classically functioning through glycemic control (i.e., metformin) or immunosuppression (i.e., rapamycin) are effective in promoting longevity (90, 91). Considering the dual function of PPARγ in glucose metabolism and inflammation control, it would be interesting to test its agonists in longevity.

Overall, although PPARγ has been recognized as a promising target in preventing and treating metabolic diseases, challenges remain in finding the suitable agonists with high therapeutic efficacy and low side effects. Understanding how PPARγ dynamically complexes with its cofactors to transactivating specific downstream target gene sets in different metabolic conditions might provide a novel angle in search of new therapeutic compounds against various aspects of obese- and aging-associated metabolic diseases.

AUTHOR CONTRIBUTIONS

XM and LX conceived, drafted and revised the review. DW and WZ drafted the review.

FUNDING

This project was supported by funding from National Natural Science Foundation of China (31770840 to XM), Shanghai Pujiang Program (17PJ1402600 to XM and 17PJ1402700 to LX), the China Postdoctoral Science Foundation (2017M611499 to DW), and the Program for Professor of Special Appointment (Eastern Scholar) at Shanghai Institutions of Higher Learning to XM.

REFERENCES

1. Tontonoz P, Spiegelman BM. Fat and beyond: the diverse biology of PPARγ. *Annu Rev Biochem.* (2008) 77:289–312. doi: 10.1146/annurev.biochem.77.061307.091829
2. Argmann C, Dobrin R, Heikkinen S, Auburtin A, Pouilly L, Cock TA, et al. Ppargamma2 is a key driver of longevity in the mouse. *PLoS Genet.* (2009) 5:e1000752. doi: 10.1371/journal.pgen.1000752
3. McCormack S, Polyak E, Ostrovsky J, Dingley SD, Rao M, Kwon YJ, et al. Pharmacologic targeting of sirtuin and PPAR signaling improves longevity and mitochondrial physiology in respiratory chain complex I mutant *Caenorhabditis elegans*. *Mitochondrion* (2015) 22:45–59. doi: 10.1016/j.mito.2015.02.005
4. Farmer SR. Molecular determinants of brown adipocyte formation and function. *Genes Dev.* (2008) 22:1269–75. doi: 10.1101/gad.1681308
5. Nedergaard J, Cannon B. The browning of white adipose tissue: some burning issues. *Cell Metab.* (2014) 20:396–407. doi: 10.1016/j.cmet.2014.07.005
6. Wu J, Bostrom P, Sparks LM, Ye L, Choi JH, Giang AH, et al. Beige adipocytes are a distinct type of thermogenic fat cell in mouse and human. *Cell* (2012) 150:366–76. doi: 10.1016/j.cell.2012.05.016
7. Sharp LZ, Shinoda K, Ohno H, Scheel DW, Tomoda E, Ruiz L, et al. Human BAT possesses molecular signatures that resemble beige/brite cells. *PLoS ONE* (2012) 7:e49452. doi: 10.1371/journal.pone.0049452
8. Kajimura S, Spiegelman BM, Seale P. Brown and beige fat: physiological roles beyond heat generation. *Cell Metab.* (2015) 22:546–59. doi: 10.1016/j.cmet.2015.09.007
9. Vegiopoulos A, Rohm M, Herzig S. Adipose tissue: between the extremes. *EMBO J.* (2017) 36:1999–2017. doi: 10.15252/embj.201696206
10. Villarroya F, Cereijo R, Villarroya J, Giralt M. Brown adipose tissue as a secretory organ. *Nat Rev Endocrinol.* (2017) 13:26–35. doi: 10.1038/nrendo.2016.136
11. Rogers NH, Landa A, Park S, Smith RG. Aging leads to a programmed loss of brown adipocytes in murine subcutaneous white adipose tissue. *Aging Cell* (2012) 11:1074–83. doi: 10.1111/acel.12010
12. Armani A, Berry A, Cirulli F, Caprio M. Molecular mechanisms underlying metabolic syndrome: the expanding role of the adipocyte. *FASEB J.* (2017) 31:4240–55. doi: 10.1096/fj.201601125RRR
13. Zhu Y, Qi C, Korenberg JR, Chen XN, Noya D, Rao MS, et al. Structural organization of mouse peroxisome proliferatoractivated receptor γ (mPPARγ) gene: alternative promoter use and different splicing yield two mPPARγ isoforms. *Proc Natl Acad Sci USA.* (1995) 92:7921–5. doi: 10.1073/pnas.92.17.7921
14. Lehrke M, Lazar MA. The many faces of PPARgamma. *Cell* (2005) 123:993–9. doi: 10.1016/j.cell.2005.11.026
15. Gross B, Pawlak M, Lefebvre P, Staels B. PPARs in obesity-induced T2DM, dyslipidaemia and NAFLD. *Nat Rev Endocrinol.* (2017) 13:36–49. doi: 10.1038/nrendo.2016.135
16. Tontonoz P, Hu E, Spiegelman BM. Stimulation of adipogenesis in fibroblasts by PPAR gamma 2, a lipid-activated transcription factor. *Cell* (1994) 79:1147–56. doi: 10.1016/0092-8674(94)90006-X
17. Rosen ED, MacDougald OA. Adipocyte differentiation from the inside out. *Nat Rev Mol Cell Biol.* (2006) 7:885–96. doi: 10.1038/nrm2066
18. Farmer SR. Transcriptional control of adipocyte formation. *Cell Metab.* (2006) 4:263–73. doi: 10.1016/j.cmet.2006.07.001
19. He W, Barak Y, Hevener A, Olson P, Liao D, Le J, et al. Adipose-specific peroxisome proliferator-activated receptor gamma knockout causes insulin resistance in fat and liver but not in muscle. *Proc Natl Acad Sci USA.* (2003) 100:15712–7. doi: 10.1073/pnas.2536828100

20. Jones JR, Barrick C, Kim KA, Lindner J, Blondeau B, Fujimoto Y, et al. Deletion of PPARgamma in adipose tissues of mice protects against high fat diet-induced obesity and insulin resistance. *Proc Natl Acad Sci USA.* (2005) 102:6207–12. doi: 10.1073/pnas.0306743102
21. Wang SE, Mullican JR, DiSpirito LC, Peed MA, Lazar MA. Lipoatrophy and severe metabolic disturbance in mice with fat-specific deletion of PPARγ. *Proc Natl Acad Sci USA.* (2013) 110:18656–61. doi: 10.1073/pnas.1314863110
22. Imai T, Takakuwa R, Marchand S, Dentz E, Bornert JM, Messaddeq N, et al. Peroxisome proliferator-activated receptor gamma is required in mature white and brown adipocytes for their survival in the mouse. *Proc Natl Acad Sci USA.* (2004) 101:4543–7. doi: 10.1073/pnas.0400356101
23. Wang QA, Zhang F, Jiang L, Ye R, An Y, Shao M, et al. PPARγ and its role in adipocyte homeostasis and thiazolidinedione-mediated insulin sensitization. *Mol Cell Biol.* (2018) 38:e00677-17. doi: 10.1128/MCB.00677-17
24. Semple RK, Chatterjee VK, O'Rahilly S. PPAR gamma and human metabolic disease. *J Clin Invest.* (2006) 116:581–9. doi: 10.1172/JCI28003
25. Auwerx J. PPARgamma, the ultimate thrifty gene. *Diabetologia* (1999) 42:1033–49. doi: 10.1007/s001250051268
26. Xu L, Ma X, Verma NK, Wang D, Gavrilova O, Proia RL, et al. Ablation of PPARγ in subcutaneous fat exacerbates age-associated obesity and metabolic decline. *Aging Cell* (2018) 17:e12721. doi: 10.1111/acel.12721
27. Spiegelman BM, Heinrich R. Biological control through regulated transcriptional coactivators. *Cell* (2004) 119:157–67. doi: 10.1016/j.cell.2004.09.037
28. Takahashi N, Kawada T, Yamamoto T, Goto T, Taimatsu A, Aoki N, et al. Overexpression and ribozymemediated targeting of transcriptional coactivators CREB-binding protein and p300 revealed their indispensable roles in adipocyte differentiation through the regulation of peroxisome proliferator-activated receptor gamma. *J Biol Chem.* (2002) 277:16906–12. doi: 10.1074/jbc.M200585200
29. Salma N, Xiao H, Mueller E, Imbalzano AN. Temporal recruitment of transcription factors and SWI/SNF chromatin-remodeling enzymes during adipogenic induction of the peroxisome proliferator-activated receptor gamma nuclear hormone receptor. *Mol Cell Biol.* (2004) 24:4651–63. doi: 10.1128/MCB.24.11.4651-4663.2004
30. Qi C, Surapureddi S, Zhu YJ, Yu S, Kashireddy P, Rao MS, et al. Transcriptional coactivator PRIP, the peroxisome proliferator-activated receptor γ (PPARγ)-interacting protein, is required for PPARγ-mediated adipogenesis. *J Biol Chem.* (2003) 278:25281–4. doi: 10.1074/jbc.C300175200
31. Mouchiroud L, Eichner LJ, Shaw RJ, Auwerx J. Transcriptional coregulators: fine-tuning metabolism. *Cell Metab.* (2014) 20:26–40. doi: 10.1016/j.cmet.2014.03.027
32. Sidossis L, Kajimura S. Brown and beige fat in humans: thermogenic adipocytes that control energy and glucose homeostasis. *J Clin Invest.* (2015) 125:478–86. doi: 10.1172/JCI78362
33. Lynes MD, Tseng YH. Deciphering adipose tissue heterogeneity. *Ann N Y Acad Sci.* (2018) 1411:5–20. doi: 10.1111/nyas.13398
34. Frühbeck G, Sesma P, Burrell MA. PRDM16: the interconvertible adipo-myocyte switch. *Trends Cell Biol.* (2009) 19:141–6. doi: 10.1016/j.tcb.2009.01.007
35. Ishibashi J, Seale P. Functions of Prdm thermogenic fat cells. *Temperature* (2015) 2:65–72. doi: 10.4161/23328940.2014.974444
36. Seale P, Conroe HM, Estall J, Kajimura S, Frontini A, Ishibashi J, et al. Prdm16 determines the thermogenic program of subcutaneous white adipose tissue in mice. *J Clin Invest.* (2011) 121:96–105. doi: 10.1172/JCI44271
37. Seale P, Bjork B, Yang W, Kajimura S, Chin S, Kuang S, et al. PRDM16 controls a brown fat/skeletal muscle switch. *Nature* (2008) 454:961–7. doi: 10.1038/nature07182
38. Ohno H, Shinoda K, Spiegelman BM, Kajimura S. PPARγ agonists induce a white-to-brown fat conversion through stabilization of PRDM16 protein. *Cell Metab.* (2012) 15:395–404. doi: 10.1016/j.cmet.2012.01.019
39. Moreno-Navarrete JM, Ortega F, Moreno M, Xifra G, Ricart W, Fernández-Real JM. PRDM16 sustains white fat gene expression profile in human adipocytes in direct relation with insulin action. *Mol Cell Endocrinol.* (2015) 405:84–93. doi: 10.1016/j.mce.2015.01.042
40. Cohen P, Levy JD, Zhang Y, Frontini A, Kolodin DP, Svensson KJ, et al. Ablation of PRDM16 and beige adipose causes metabolic dysfunction and a subcutaneous to visceral fat switch. *Cell* (2014) 156:304–16. doi: 10.1016/j.cell.2013.12.021
41. Ohno H, Shinoda K, Ohyama K, Sharp LZ, Kajimura S. EHMT1 controls brown adipose cell fate and thermogenesis through the PRDM16 complex. *Nature* (2013) 504:163–7. doi: 10.1038/nature12652
42. Nagano G, Ohno H, Oki K, Kobuke K, Shiwa T, Yoneda M, et al. Activation of classical brown adipocytes in the adult human perirenal depot is highly correlated with PRDM16-EHMT1 complex expression. *PLoS ONE* (2015) 10:e0122584. doi: 10.1371/journal.pone.0122584
43. Rajakumari S, Wu J, Ishibashi J, Lim HW, Giang AH, Won KJ, et al. EBF2 determines and maintains brown adipocyte identity. *Cell Metab.* (2013) 17:562–74. doi: 10.1016/j.cmet.2013.01.015
44. Shao M, Ishibashi J, Kusminski CM, Wang QA, Hepler C, Vishvanath L, et al. Zfp423 maintains white adipocyte identity through suppression of the beige cell thermogenic gene program. *Cell Metab.* (2016) 23:1167–84. doi: 10.1016/j.cmet.2016.04.023
45. Puigserver P, Wu Z, Park CW, Graves R, Wright M, Spiegelman BM. A cold-inducible coactivator of nuclear receptors linked to adaptive thermogenesis. *Cell* (1998) 92:829–39. doi: 10.1016/S0092-8674(00)81410-5
46. Wu Z, Puigserver P, Andersson U, Zhang C, Adelmant G, Mootha V, et al. Mechanisms controlling mitochondrial biogenesis and respiration through the thermogenic coactivator PGC-1. *Cell* (1999) 98:115–24. doi: 10.1016/S0092-8674(00)80611-X
47. Kong X, Banks A, Liu T, Kazak L, Rao RR, Cohen P, et al. IRF4 is a key thermogenic transcriptional partner of PGC-1α. *Cell* (2014) 158:69–83. doi: 10.1016/j.cell.2014.04.049
48. Ma X, Xu L, Alberobello AT, Gavrilova O, Bagattin A, Skarulis M, et al. Celastrol protects against obesity and metabolic dysfunction through activation of a HSF1-PGC1α transcriptional axis. *Cell Metab.* (2015) 22:695–708. doi: 10.1016/j.cmet.2015.08.005
49. Spiegelman BM, Puigserver P, Wu Z. Regulation of adipogenesis and energy balance by PPARgamma and PGC-1. *Int J Obes Relat Metab Disord.* (2000) 24(Suppl. 4):S8–10. doi: 10.1038/sj.ijo.0801492
50. Seale P, Kajimura S, Yang W, Chin S, Rohas LM, Uldry M, et al. Transcriptional control of brown fat determination by PRDM16. *Cell Metab.* (2007) 6:38–54. doi: 10.1016/j.cmet.2007.06.001
51. Iida S, Chen W, Nakadai T, Ohkuma Y, Roeder RG. PRDM16 enhances nuclear receptor-dependent transcription of the brown fat-specific Ucp1 gene through interactions with mediator subunit MED1. *Genes Dev.* (2015) 29:308–21. doi: 10.1101/gad.252809.114
52. Harms MJ, Lim HW, Ho Y, Shapira SN, Ishibashi J, Rajakumari S, et al. PRDM16 binds MED1 and controls chromatin architecture to determine a brown fat transcriptional program. *Genes Dev.* (2015) 29:298–307. doi: 10.1101/gad.252734.114
53. Smith CL, O'Malley BW. Coregulator function: a key to understanding tissue specificity of selective receptor modulators. *Endocr Rev.* (2004) 25:45–71. doi: 10.1210/er.2003-0023
54. Qi C, Zhu Y, Pan J, Yeldandi AV, Rao MS, Maeda N, et al. Mouse steroid receptor coactivator-1 is not essential for peroxisome proliferator-activated receptor α-regulated gene expression. *Proc Natl Acad Sci USA.* (1999) 96:1585–90. doi: 10.1073/pnas.96.4.1585
55. Wang Z, Qi C, Krones A, Woodring P, Zhu X, Reddy JK, et al. Critical roles of the p160 transcriptional coactivators p/CIP and SRC energy balance. *Cell Metab.* (2006) 3:111–22. doi: 10.1016/j.cmet.2006.01.002
56. Picard F, Géhin M, Annicotte J, Rocchi S, Champy MF, O'Malley BW, et al. SRC-1 and TIF2 control energy balance between white and brown adipose tissues. *Cell* (2002) 111:931–41. doi: 10.1016/S0092-8674(02)01169-8
57. Jeong JW, Kwak I, Lee KY, White LD, Wang XP, Brunicardi FC, et al. The genomic analysis of the impact of steroid receptor coactivators ablation on hepatic metabolism. *Mol Endocrinol.* (2006) 20:1138–52. doi: 10.1210/me.2005-0407
58. Louet JF, Coste A, Amazit L, Tannour-Louet M, Wu RC, Tsai SY, et al. Oncogenic steroid receptor coactivator-3 is a key regulator of the white adipogenic program. *Proc Natl Acad Sci USA.* (2006) 103:17868–73. doi: 10.1073/pnas.0608711103

59. Xu L, Ma X, Li J, Li X, Xu J, Wang S, et al. SRC-3 deficient mice developed fat redistribution under high-fat diet. *Endocrine* (2010) 38:60–6. doi: 10.1007/s12020-010-9344-2
60. Coste A, Louet JF, Lagouge M, Lerin C, Antal MC, Meziane H, et al. The genetic ablation of SRC-3 protects against obesity and improves insulin sensitivity by reducing the acetylation of PGC-1{alpha}. *Proc Natl Acad Sci USA.* (2008) 105:17187–92. doi: 10.1073/pnas.0808207105
61. Hartig SM, He B, Long W, Buehrer BM, Mancini MA. Homeostatic levels of SRC-2 and SRC-3 promote early human adipogenesis. *J Cell Biol.* (2011) 192:55–67. doi: 10.1083/jcb.201004026
62. Qiang L, Wang L, Kon N, Zhao W, Lee S, Zhang Y, et al. Brown remodeling of white adipose tissue by SirT1-dependent deacetylation of Pparγ. *Cell* (2012) 150:620–32. doi: 10.1016/j.cell.2012.06.027
63. Mayoral R, Osborn O, McNelis J, Johnson AM, Oh DY, Izquierdo CL, et al. Adipocyte SIRT1 knockout promotes PPARγ activity, adipogenesis and insulin sensitivity in chronic-HFD and obesity. *Mol Metab.* (2015) 4:378–91. doi: 10.1016/j.molmet.2015.02.007
64. Abdesselem H, Madani A, Hani A, Al-Noubi M, Goswami N, Ben Hamidane H, et al. SIRT1 limits adipocyte hyperplasia through c-Myc inhibition. *J Biol Chem.* (2016) 291:2119–35. doi: 10.1074/jbc.M115.675645
65. Chalkiadaki A, Guarente L. Sirtuins mediate mammalian metabolic responses to nutrient availability. *Nat Rev Endocrinol.* (2012) 8:287–96. doi: 10.1038/nrendo.2011.225
66. Villanueva CJ, Vergnes L, Wang J, Drew BG, Hong C, Tu Y, et al. Adipose subtype-selective recruitment of TLE3 or Prdm16 by PPARγ specifies lipid storage versus thermogenic gene programs. *Cell Metab.* (2013) 17:423–35. doi: 10.1016/j.cmet.2013.01.016
67. Lodhi IJ, Dean JM, He A, Park H, Tan M, Feng C, et al. PexRAP inhibits PRDM16-mediated thermogenic gene expression. *Cell Rep.* (2017) 20:2766–74. doi: 10.1016/j.celrep.2017.08.077
68. Hiraike Y, Waki H, Yu J, Nakamura M, Miyake K, Nagano G, et al. NFIA co-localizes with PPARγ and transcriptionally controls the brown fat gene program. *Nat Cell Biol.* (2017) 19:1081–92. doi: 10.1038/ncb3590
69. Bruce KD, Zsombok A, Eckel RH. Lipid processing in the brain: a key regulator of systemic metabolism. *Front Endocrinol.* (2017) 8:60. doi: 10.3389/fendo.2017.00060
70. Yin F, Boveris A, Cadenas E. Mitochondrial energy metabolism and redox signaling in brain aging and neurodegeneration. *Antioxid Redox Signal.* (2014) 20:353–71. doi: 10.1089/ars.2012.4774
71. Kirkland JL, Dobson DE. Preadipocyte function and aging: links between age-related changes in cell dynamics and altered fat tissue function. *J Am Geriatr Soc.* (1997) 45:959–67. doi: 10.1111/j.1532-5415.1997.tb02967.x
72. Berry DC, Jiang Y, Arpke RW, Close EL, Uchida A, Reading D, et al. Cellular aging contributes to failure of cold-induced beige adipocyte formation in old mice and humans. *Cell Metab.* (2017) 25:166–81. doi: 10.1016/j.cmet.2016.10.023
73. Bray GA. Medical consequences of obesity. *J Clin Endocrinol Metab.* (2004) 89:2583–9. doi: 10.1210/jc.2004-0535
74. Chadid S, Singer MR, Kreger BE, Bradlee ML, Moore LL. Midlife weight gain is a risk factor for obesity-related cancer. *Br J Cancer* (2018) 118:1665–71. doi: 10.1038/s41416-018-0106-x
75. Ma X, Xu L, Gavrilova O, Mueller E. Role of forkhead box protein A age-associated metabolic decline. *Proc Natl Acad Sci USA.* (2014) 111:14289–94. doi: 10.1073/pnas.1407640111
76. Miard S, Dombrowski L, Carter S, Boivin L, Picard F. Aging alters PPARgamma in rodent and human adipose tissue by modulating the balance in steroid receptor coactivator-1. *Aging Cell* (2009) 8:449–59. doi: 10.1111/j.1474-9726.2009.00490.x
77. Choi JH, Banks AS, Estall JL, Kajimura S, Boström P, Laznik D, et al. Anti-diabetic drugs inhibit obesity-linked phosphorylation of PPARgamma by Cdk5. *Nature* (2010) 466:451–6. doi: 10.1038/nature09291
78. Choi JH, Choi SS, Kim ES, Jedrychowski MP, Yang YR, Jang HJ, et al. Thrap3 docks on phosphoserine 273 of PPARγ and controls diabetic gene programming. *Genes Dev.* (2014) 28:2361–9. doi: 10.1101/gad.249367.114
79. Banks AS, McAllister FE, Camporez JP, Zushin PJ, Jurczak MJ, Laznik-Bogoslavski D, et al. An ERK/Cdk5 axis controls the diabetogenic actions of PPARγ. *Nature* (2015) 517:391–5. doi: 10.1038/nature13887
80. Li P, Fan W, Xu J, Lu M, Yamamoto H, Auwerx J, et al. Adipocyte NCoR knockout decreases PPARγ phosphorylation and enhances PPARγ activity and insulin sensitivity. *Cell* (2011) 147:815–26. doi: 10.1016/j.cell.2011.09.050
81. Choi JH, Banks AS, Kamenecka TM, Busby SA, Chalmers MJ, Kumar N, et al. Antidiabetic actions of a non-agonist PPARγ ligand blocking Cdk5-mediated phosphorylation. *Nature* (2011) 477:477–81. doi: 10.1038/nature10383
82. Liu C, Feng T, Zhu N, Liu P, Han X, Chen M, et al. Identification of a novel selective agonist of PPARγ with no promotion of adipogenesis and less inhibition of osteoblastogenesis. *Sci Rep.* (2015) 5:9530. doi: 10.1038/srep09530
83. Zheng W, Feng X, Qiu L, Pan Z, Wang R, Lin S, et al. Identification of the antibiotic ionomycin as an unexpected peroxisome proliferator-activated receptor γ (PPARγ) ligand with a unique binding mode and effective glucose-lowering activity in a mouse model of diabetes. *Diabetologia* (2013) 56:401–11. doi: 10.1007/s00125-012-2777-9
84. Ge C, Zhao G, Li B, Li Y, Cawthorn WP, MacDougald OA, Franceschi RT. Genetic inhibition of PPARγ S112 phosphorylation reduces bone formation and stimulates marrow adipogenesis. *Bone* (2018) 107:1–9. doi: 10.1016/j.bone.2017.10.023
85. Stechschulte LA, Czernik PJ, Rotter ZC, Tausif FN, Corzo CA, Marciano DP, et al. PPARG post-translational modifications regulate bone formation and bone resorption. *EBioMedicine* (2016) 10:174–84. doi: 10.1016/j.ebiom.2016.06.040
86. Kolli V, Stechschulte LA, Dowling AR, Rahman S, Czernik PJ, Lecka-Czernik B. Partial agonist, telmisartan, maintains PPARγ serine 112 phosphorylation, and does not affect osteoblast differentiation and bone mass. *PLoS ONE* (2014) 9:e96323. doi: 10.1371/journal.pone.0096323
87. Ruchat SM, Rankinen T, Weisnagel SJ, Rice T, Rao DC, Bergman RN, et al. Improvements in glucose homeostasis in response to regular exercise are influenced by the PPARG Pro12Ala variant: results from the HERITAGE family study. *Diabetologia* (2010) 53:679–89. doi: 10.1007/s00125-009-1630-2
88. Anton S, Leeuwenburgh C. Fasting or caloric restriction for healthy aging. *Exp Gerontol.* (2013) 48:1003–5. doi: 10.1016/j.exger.2013.04.011
89. Masternak MM1, Bartke A. PPARs in calorie restricted and genetically long-lived mice. *PPAR Res.* (2007) 2007:28436. doi: 10.1155/2007/28436
90. Martin-Montalvo A, Mercken EM, Mitchell SJ, Palacios HH, Mote PL, Scheibye-Knudsen M, et al. Metformin improves healthspan and lifespan in mice. *Nat Commun.* (2013) 4:2192. doi: 10.1038/ncomms3192
91. Ehninger D, Neff F, Xie K. Longevity, aging and rapamycin. *Cell Mol Life Sci.* (2014) 71:4325–46. doi: 10.1007/s00018-014-1677-1

Conflict of Interest Statement: The authors declare that the research was conducted in the absence of any commercial or financial relationships that could be construed as a potential conflict of interest.

frontiers in Endocrinology

REVIEW
published: 05 September 2018
doi: 10.3389/fendo.2018.00514

Insulin Resistance in HIV-Patients: Causes and Consequences

Marcelo N. Pedro[1†], Guilherme Z. Rocha[1†], Dioze Guadagnini[1], Andrey Santos[1], Daniela O. Magro[2], Heloisa B. Assalin[1], Alexandre G. Oliveira[1,3], Rogerio de Jesus Pedro[1] and Mario J. A. Saad[1]*

[1] Department of Internal Medicine, Faculty of Medical Sciences, State University of Campinas-UNICAMP, Campinas, Brazil,
[2] Department of Surgery, Faculty of Medical Sciences, State University of Campinas-UNICAMP, Campinas, Brazil,
[3] Biosciences Institute, São Paulo State University (UNESP), Rio Claro, Brazil

Here we review how immune activation and insulin resistance contribute to the metabolic alterations observed in HIV-infected patients, and how these alterations increase the risk of developing CVD. The introduction and evolution of antiretroviral drugs over the past 25 years has completely changed the clinical prognosis of HIV-infected patients. The deaths of these individuals are now related to atherosclerotic CVDs, rather than from the viral infection itself. However, HIV infection, cART, and intestinal microbiota are associated with immune activation and insulin resistance, which can lead to the development of a variety of diseases and disorders, especially with regards to CVDs. The increase in LPS and proinflammatory cytokines circulating levels and intracellular mechanisms activate serine kinases, resulting in insulin receptor substrate-1 (IRS-1) serine phosphorylation and consequently a down regulation in insulin signaling. While lifestyle modifications and pharmaceutical interventions can be employed to treat these altered metabolic functions, the mechanisms involved in the development of these chronic complications remain largely unresolved. The elucidation and understanding of these mechanisms will give rise to new classes of drugs that will further improve the quality of life of HIV-infected patients, over the age of 50.

Keywords: insulin resistance, diabetes, HIV, CVD, cART, LPS

OPEN ACCESS

Edited by:
Andrew J. McAinch,
Victoria University, Australia

Reviewed by:
Caterina Conte,
Università Vita-Salute San Raffaele, Italy
Kathleen Grace Mountjoy,
University of Auckland, New Zealand

****Correspondence:***
Mario J. A. Saad
msaad@fcm.unicamp.br

† These authors have contributed equally to this work

Specialty section:
This article was submitted to Obesity, a section of the journal Frontiers in Endocrinology

Received: *28 May 2018*
Accepted: *16 August 2018*
Published: *05 September 2018*

Citation:
Pedro MN, Rocha GZ, Guadagnini D, Santos A, Magro DO, Assalin HB, Oliveira AG, Pedro RdJ and Saad MJA (2018) Insulin Resistance in HIV-Patients: Causes and Consequences. Front. Endocrinol. 9:514. doi: 10.3389/fendo.2018.00514

INTRODUCTION

The introduction and evolution of antiretroviral drugs over the past 25 years has completely changed the clinical prognosis of HIV-infected patients (1). These drugs have transformed the disease into a chronic condition, and increased life expectancy, which is similar to the general uninfected population (2). Nowadays, the deaths of HIV-infected individuals, who appropriately follow their therapy regimen, are related to non-communicable and HIV-related chronic diseases, mainly atherosclerotic cardiovascular disease (CVD) (3–6). Some of the mechanisms responsible for this increased cardiovascular risk, in HIV-infected patients, involve HIV infection and inflammation, dyslipidemia, insulin resistance, as well as metabolic, and body composition changes induced by antiretroviral therapy (7–11). Moreover, non-HIV related risk factors, such as aging, can also contribute to the development of these metabolic alterations and risk factors (12–15).

Here we review how immune activation and insulin resistance contribute to the metabolic alterations observed in HIV-infected patients, and how these alterations increase the risk of developing CVD. In section Sources of Immune Activation and Insulin Resistance in HIV Patients, we discuss how HIV infection and inflammation, combination antiretroviral therapy (cART), and

gut microbiota contribute to immune activation and insulin resistance. In section Consequences of Immune Activation and Insulin Resistance in HIV-Infected Patients, we review the clinical consequences of immune activation and insulin resistance, as well as how these processes are involved in the development of age-related metabolic diseases in HIV patients.

SOURCES OF IMMUNE ACTIVATION AND INSULIN RESISTANCE IN HIV PATIENTS

The immune activation of HIV-infected patients, whether on cART or not, is usually accompanied by insulin resistance (16). In this section, the role of HIV infection and inflammation, cART, and gut microbiota in immune activation and molecular mechanism of insulin resistance are discussed.

Effect of HIV Infection and Inflammation on Insulin Resistance

It is generally accepted that there is a correlation between innate immune system activation and insulin resistance, which contributes to glucose metabolism dysregulation and dyslipidemia (8). Immune activation results in chronic inflammation, that varies in severity, and has been observed in untreated HIV patients and patients undergoing cART (17). However, untreated HIV-patients display an enhanced inflammatory state, which is characterized by high levels of proinflammatory cytokines, like tumor necrosis factor alpha (TNF-α), and interleukins (IL-6 and IL-1β), and is associated with a procoagulant state (12). Under these conditions, the insulin resistance is probably severe and could occur in the liver, muscle, and adipose tissue. In fact, severe insulin resistance in the adipose tissue (as observed in HIV untreated patients), may prevents adipose mass gain as described in mice (18–20) (**Figure 1A**).

In patients undergoing antiretroviral drug therapy, there is a decrease in proinflammatory cytokines, which do not completely return to normal, thus indicating that some level of inflammation persists (21). A variety of factors, such as: virus production, cytomegalovirus infection, regulatory T-cell loss, and/or lymphoid structure damage could contribute to this persistent inflammation (22, 23). There is still insulin resistance, but it is mild or moderate. As previously demonstrated in animal models of obesity (24, 25), less severe insulin resistance in adipose tissue allows normal or increased glucose uptake and lipid conversion in this tissue, favoring weight gain and contributing to explain the increase in visceral adipose tissue (VAT) in these patients (26, 27) (**Figure 1A**).

In HIV-treated patients, the activation of the innate immune system and insulin resistance is similar to what has been described in obesity and type 2 diabetes mellitus (DM2) (28, 29). The innate immune system and insulin signaling are integrated and toll-like receptors (TLRs), inducible nitric oxide synthase (iNOS), protein kinase R (PKR), c-Jun N-terminal kinases (JNK), and NF-κB are connected to the insulin receptor (IR) and its downstream signaling pathway IRS/PI3K/Akt. Upon activation of the innate immune system, proteins involved in insulin signaling pathways become posttranscriptionally modified, resulting in reduced insulin action (**Figure 1B**) (30, 31).

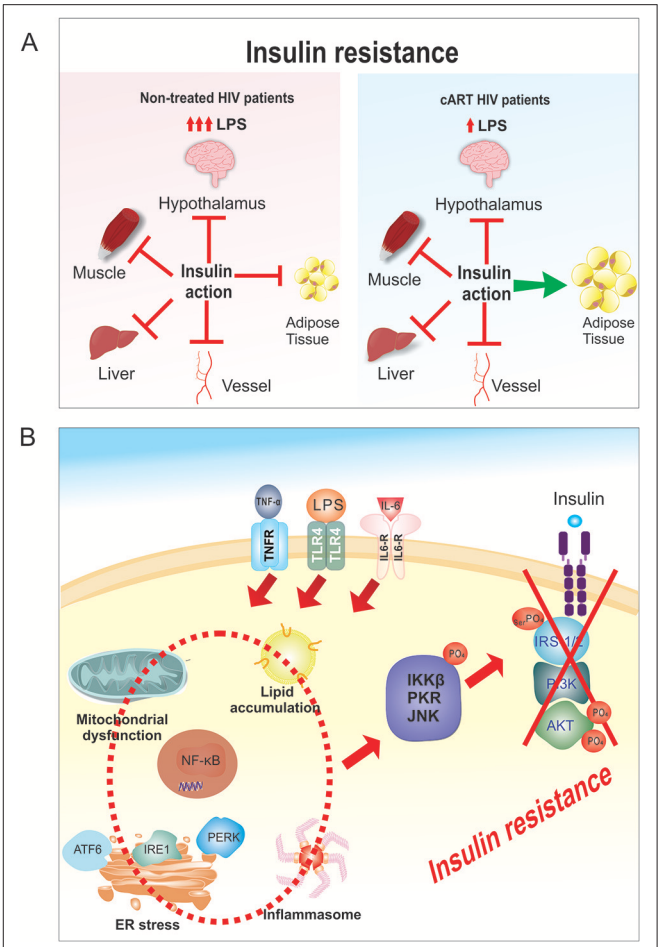

FIGURE 1 | (A) Tissue specific insulin resistance. In HIV untreated patients there is severe insulin resistance with increased LPS and cytokines that involves liver, hypothalamus, muscle, vessels and adipose tissue. After cART treatment the insulin resistance is mild/moderate, with reduced LPS and cytokines that probably spares adipose tissue. **(B)** Molecular mechanism of LPS-induced insulin resistance. The increase in LPS circulating levels in HIV patients will induce an increase in circulating inflammatory cytokines, and these increases will activate TLR4, IL-6, and TNFalpha receptors, which will induce ER stress, mitochondrial dysfunction, activation of inflammasome and an increase in intracellular lipid accumulation. Then, there will be activation of PKR, JNK, and IKKβ/NF-κB pathways in liver, muscle, adipose tissue, macrophages and also in other tissues. The activation of these serine kinases (PKR, JNK, and IKKβ) will induce serine phosphorylation of the IRS1/2 and consequently a down regulation in insulin signaling.

It is important to mention that bacterial lipopolysaccharide (LPS) from the Gram negative intestinal bacteria is continuously produced in the gut (secondary to death of Gram negative bacteria) and translocated to the circulation (32). This translocation depends on many factors including immune system, integrity of epithelia barrier, diet, and many other environmental factors. The increase in circulating LPS, through its own receptor -TLR4- induce the release of inflammatory cytokines that can contribute to insulin resistance (33, 34).

Previous data showed that there is an increase in LPS circulating levels in HIV patients, whether on treatment or not (35), which can induce at the same time TLR4 activation and endoplasmic reticulum (ER) stress (19, 36, 37). Then, there will be activation of PKR, JNK, and IKKβ/NF-κB pathways in liver, muscle, adipose tissue, macrophages, and also in other tissues. The activation of these serine kinases (PKR, JNK, and IKKβ) will induce serine phosphorylation of the insulin receptor substrate 1 and 2, and consequently a down regulation in insulin signaling (38, 39). The activation of NF-κB pathways in liver, adipose tissue, and macrophages will induce the production of proinflammatory cytokines (i.e., TNF-α, IL-1β, and IL-6), creating an inflammatory vicious cycle, which is even worst with the increased adiposity (40–43). Certainly, this aggravates inflammation and insulin resistance.

In addition to increase in circulating LPS and in proinflammatory cytokine TNF-α, IL-1β, and IL-6, the JNK and NF-κB pathways can also be activated by intracellular mechanisms that involve oxidative and endoplasmic reticulum (ER) stresses, activation of inflammasome and an increase in intracellular lipid accumulation (39, 44, 45) (**Figure 1B**). Additionally, augmented iNOS activity and the nitrosylation of insulin pathway proteins have been shown to promote insulin resistance (46, 47). In summary, an increase in LPS and proinflammatory cytokines and in intracellular mechanisms will activate serine kinases, resulting in insulin receptor substrate-1 (IRS-1) serine phosphorylation and insulin signal transduction inhibition (30, 31, 48).

Effect of Viral Suppression on Insulin Resistance

Protease inhibitors (PI) or nucleoside analog reverse transcriptase inhibitors (NRTI) have been shown to induce insulin resistance, dyslipidemia, and lipodystrophy, and consequently increase cardiovascular risk (17, 49–51). These drugs increase the nuclear localization of SREBP-1 (sterol regulatory element-binding protein 1), which is a transcription factor that regulates the expression of genes associated with lipid synthesis (52). In the liver, these antiviral drugs can increase the levels of free intracellular cholesterol and lipids (53), which can affect aging and the immune system response. In the muscle and adipose tissue, these drugs can induce ER stress and reduce glucose transporter 4 (GLUT4) translocation to the plasma membrane (54, 55). The NRTIs also inhibit mitochondrial DNA-polymerase, respiratory chain function, and ATP production, ultimately leading to adipocyte death (56–60).

HIV patients undergoing cART exhibit a partial reversal of immune activation and inflammation. Additionally, cART reduces opportunistic infections and cardiovascular risk factors, which is likely a result of some reduction in inflammation (61), although residual markers of inflammation and coagulation remains elevated in ART-treated HIV-infected patients (62). In treated patients the dyslipidemia correlates better with C-reactive protein and IL-6 levels, rather than with CD4 count or HIV viral load, suggesting that immune activation has a central role in the development of dyslipidemia (63). While cART improves some of the observed alterations, it does not reverse the immune activation or chronic inflammation completely. In fact, patients undergoing cART still present a proinflammatory and prothrombotic state, accompanied by changes in the number and size of low-density lipoprotein (LDL) and high-density lipoprotein (HDL) particles, which increases the risk of these patients developing cardiovascular complications (62, 64–67).

Effect of Microbiota Modulation on Insulin Resistance

While the progression from HIV infection to AIDS is primarily modulated by T cell activation and systemic inflammation, there is evidence that the gastrointestinal mucosa immune system also participates in this process (68). The human gut microbiota is mainly composed of four phyla: Firmicutes, Bacteroidetes, Actinobacteria, and Proteobacteria. The general population predominantly harbors Bacteroidetes, followed by Firmicutes; however, the composition of the gut microbiota is influenced by diet, age, geography, drugs, and cultural behaviors (69–72). Over the past 10 years, it is becoming clear that microbiota populations are modulated and may have a causal effect in more prevalent chronic conditions such as: obesity, diabetes, hypertension, and CVD (73).

Interestingly, HIV infection can also modulate the levels of bacteria of the gut microbiota. In fact, there is a decrease in the levels of the phylum *Bacteroidetes*, but some genders of this phylum, as *Prevotella*, increases when analyzed in treated and untreated patients (74–76). Such a change in the gut microbiota could result in increased tryptophan catabolism, chronic inflammation, and increased cardiovascular risk (77, 78). Additionally, an increase in *Prevotella* could augment circulating trimethylamine (TMA) levels, which is transformed into trimethylamine oxide (TMAO), and can have a role in the development of atherosclerosis (79).

Previous data showed that increased levels of choline and TMAO are associated with cardiovascular diseases (80). It is well known that ingested choline is transformed by gut microbiota in TMA, which enters portal circulation and in liver is converted in TMAO (80). It is interesting that fasting TMAO levels are independent predictor of atherosclerotic disease and high-risk mortality in coronary artery disease patients (81, 82). The mechanisms by which TMAO induces or accelerates atherosclerosis is not completely understood, it may involve macrophage activation and increase in foam cells and also modulation of platelet aggregation and adhesion (83). Moreover, besides promoting atherosclerosis lesion development, TMAO also aggravate pressure-overload heart failure in mice (84).

Recently, our group demonstrated that, in HIV patients, a close correlation exists between increased circulating LPS levels, a marker for intestinal permeability, and insulin resistance (35). The increased translocation of LPS and elevated serum levels induce the activation of the innate and adaptive immune systems (35, 85, 86). As discussed previously, in macrophages and most tissues, LPS binds to and activates TLR4, which initiates a complex cascade of signaling events, resulting in the downstream activation of the JNK and NF-kB pathways, and consequently

insulin resistance and systemic inflammation. Additionally, LPS has also been shown to increase adipose tissue, which augments body weight gain (35, 87, 88). Moreover, in HIV-infected patients, elevated levels of LPS have been linked to endothelial dysfunction and adverse metabolic outcomes (35, 88–91).

It is important to mention that the effect of cART introduction in the modulation of gut microbiota is not completely understood. However, very recently Ji et al. showed that this modulation after cART was differentially correlated with the immune status, especially in patients with CD4 + T cell counts>300/mm^3 (92). In these patients it was shown that the alpha diversity was correlated with CD4 + T cell counts, but the specific role of cART in increasing microbial diversity is still controversial (78, 92, 93). This correlation may explain the conflicting results in previous studies investigating alpha diversity in intestinal microbiota in HIV patients (93–96), indicating that this diversity is consequence of the immune status of the subjects. The immunological profile and cART seem to contribute together to alter the gut microbiota.

CONSEQUENCES OF IMMUNE ACTIVATION AND INSULIN RESISTANCE IN HIV-INFECTED PATIENTS

Chronic immune activation and insulin resistance can contribute to obesity, dyslipidemia, CVDs, and non-alcoholic fat liver disease (NAFLD) as well as neurocognitive disorders, metabolic disorders, bone abnormalities, and non-HIV associated cancers (12, 97–99). While the evolution of these complications depends on genetic and environmental factors, each condition has the potential of aggravating another (**Figure 2**).

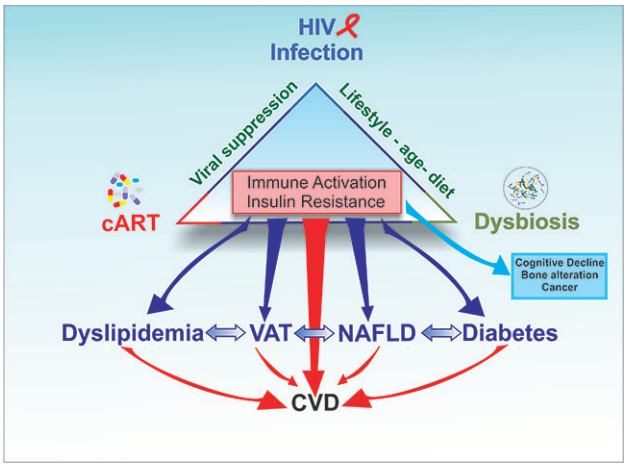

FIGURE 2 | The triad HIV infection/inflammation, antiretroviral therapy (cART), and gut microbiota contribute to induce immune activation and insulin resistance. The clinical consequences of chronic immune activation and insulin resistance can contribute to increase Visceral Adipose Tissue (VAT), dyslipidemia, CVDs and non-alcoholic fat liver disease (NAFLD) as well as neurocognitive disorders, metabolic disorders, bone abnormalities and non-HIV associated cancers While the evolution of these complications depends on genetic and environmental factors, each condition has the potential of aggravating another, increasing the risk of CVD in HIV patients.

Obesity and Lipodystrophy

Before the new generation of antiretroviral therapies, HIV was often associated with lipodystrophy, which is a marker for metabolic alterations and includes a broad spectrum of clinical alterations (100, 101). Previous studies showed that HIV infection severity was associated with an increased prevalence of lipodystrophy, which is secondary to HIV-infected macrophages infiltration and enhanced local inflammation in the adipose tissue (102, 103). In the past, the development of lipodystrophy was partially related to drugs (i.e., stavudine and zidovudine) included in the treatment regimen, but it is also influenced by age, CD4 levels, viral load, therapy duration, and race (especially caucasians). Remarkably, the new classes of cART and inhibitors (fusion, integrase, and entry) do not alter the metabolic parameters of fat distribution (1, 50).

Obesity and visceral adiposity are commonly observed in HIV-treated patients and are the result of factors associated with both traditional treatments and cART. As with most obese people, the increase in adipose tissue is associated with inflammatory and metabolic responses. Since many HIV patients have low muscle mass, excess adipose tissue may be present, even when the BMI is within the normal range. In fact, a recent study showed that when considering BMI, 60–70% of HIV-infected patients are considered overweight or obese (104–108). In most patients, there is an increase in visceral adipose tissue (VAT), which is usually indicative of a more deleterious metabolic profile (109–111).

In obese populations, metabolically healthy obesity is characterized by less VAT and reduced inflammation (112–115). These same more benign metabolic conditions have also been documented in some HIV infected patients considered overweight or obese. The reasons why some obese individuals, with or without HIV, have a more aggressive metabolic profile and associated risk factors are not completely understood, but it might involve adipocyte size and/or number, recruited inflammatory cells, hypoxia, and/or adiponectin levels (116–118).

The extrapolation of data from the obese population without HIV to those with HIV must be interpreted with care, since a large portion of the data related to adipose tissue dysfunction includes HIV patients with lipodystrophy. Although this alteration in fat distribution still occurs in treated HIV-infected patients, the prevalence of obesity is increasing, and in some patients, an association between obesity and lipodystrophy has been observed (119).

Dyslipidemia

During the 80's and early 90's, before the introduction of antiretroviral therapy, dyslipidemia was evident in more severe HIV cases, and was characterized by high triglyceride (TG) levels and low levels of HDL-cholesterol (HDL-C) and LDL-cholesterol (LDL-C). Although the exact mechanisms that account for the development of this kind of dyslipidemia are not fully understood, there is data suggesting that it may be

induced by insulin resistance resulting from HIV infection and inflammation (120–122). This observed pattern of dyslipidemia is not only observed in HIV patients, but is also detected in other infections and inflammations, and can become atherogenic if it persists (123, 124). In this regard, an increase in TNF-α level can impair the clearance of TGs and reduce the antilipolytic effect of insulin, thus stimulating lipolysis in HIV-patients with lipodystrophy.

Besides activation of the innate immune system and insulin resistance, which contributes to glucose metabolism dysregulation and dyslipidemia, other mechanisms may also contribute to explain this pattern of dyslipidemia. One such mechanism involves the adenosine-triphosphate binding cassette transporter A1 (ABCA1), a transmembrane transporter present in macrophages, which interacts with the HIV-produced accessory protein Nef. Under physiological conditions, ABCA1 shuttles cholesterol from macrophages (in peripheral tissues) to HDL, which was previously shown to be to reduce cardiovascular risk (87, 125). However, in HIV-infected patients, Nef downregulates ABCA1 expression and reduces the efflux of cholesterol to HDL. As a result, lipid accumulates inside the macrophage, and is transformed into foam cells, which is associated with atherosclerosis (125).

Another mechanism, that can contribute to the understanding of why this pattern of dyslipidemia is commonly observed in HIV-patients, is through the inhibition of an intracellular peroxisome protein, proliferator-activated receptor gamma (PPAR-γ) (126). This protein is critical for adipocyte differentiation, and is inhibited by the HIV viral protein, vpr. The inhibition of PPAR-γ blocks adipocyte differentiation, and leads to fatty acid accumulation and lipotoxicity. Moreover, HIV replication is also associated with an increase in fatty acid synthase (FAS) activity, which impacts fatty acid synthesis (127). These data suggest that in HIV-infected patients, not undergoing cART, there is an increase in fatty acid production that can contribute to the appearance of dyslipidemia and insulin resistance.

On the other side, it has been shown that cART not only suppresses HIV infection and reduces inflammation, but it also changes the dyslipidemia pattern, which is characterized by an increase in TGs and LDL-C, a reduction in HDL-C and maintenance of insulin resistance (128, 129). In fact, a recent meta-analysis study showed that cART patients have a higher risk of developing hypercholesterolemia and display higher TG levels than non-treated HIV patients (27). The previously described modulation of ABCA1 by Nef, which reduces the efflux of HDL, is also reversed by cART (130–132).

Cardiovascular Diseases and NAFLD

As previously mentioned, there is still an increased risk of CVD in the HIV-infected population, despite cART and the control of risk factors (1, 51). Even with the development of new antiretroviral drugs, the chronic immune activation and insulin resistance remain and contribute to this greater risk (12, 51). Also, recent data has shown that HIV-infected patients can present left ventricular systolic and diastolic dysfunction and myocardial fibrosis (133, 134).

Abnormal liver enzymes are also common in HIV-infected patients, despite the absence of alcohol consumption or viral hepatitis. These abnormalities have been associated with an increased prevalence of NAFLD and non-alcoholic steatohepatitis (NASH) (135). The actual prevalence of NAFLD and NASH in HIV-infected patients is not known because the methods used to define these alterations vary among studies (136). Recent data has shown that in HIV-infected patients, treated with cART, the prevalence of NAFLD is around 40%, and that these patients have a higher risk of developing NASH or cirrhosis than obese patients without HIV (137–141). These hepatic alterations are secondary to multiple factors, and immune activation, insulin resistance, cART, and aging are certainly involved in the process. It is also important to mention that NAFLD is a risk factor for diabetes and CVDs (142).

Neurocognitive Disorders, Metabolic Disorders, Bone Abnormalities, and Non-HIV Associated Cancers

The HIV-infected population can develop behavioral abnormalities, motor dysfunction, and dementia (12). The clinical presentation can vary from mild neurocognitive disorders to severe HIV-associated dementia (143, 144). The prevalence of these abnormalities is ∼50% (145), however, since the introduction of modern cART, the prevalence of severe forms of neurocognitive disorders has been dramatically reduced (146).

With regards to glucose metabolism, it is clear that current cART is much less metabolically toxic than previous therapies. However, HIV and cART are independently associated with glucose intolerance and diabetes (49). Again, while these abnormalities are secondary to multiple factors, glucose intolerance and diabetes are known to exacerbate the risk of these patients developing CVD.

Recent data has shown that HIV-infected patients have fracture rates three times higher than the control population (147, 148). In fact, decreased bone mineral density, osteopenia, and osteoporosis have been observed in these patients, and are probably related to immune activation and systemic inflammation, cART, low vitamin D, and/or aging.

The risk of some non HIV-associated cancers is 50% higher in HIV-infected patients than in non-infected patients (149, 150). For example, HIV infection is associated with a higher incidence of virus-related cancers such as: Kaposi sarcoma, lymphomas, and anal and liver cancer, which is most likely secondary to the poor immunological control of oncogenic viruses (12).

Overall, recent data showed that the mortality of HIV-infected people decreased in those below 65 years old, but increased after this age (112, 115), which is likely due to the increased risk of developing CVDs and dying from acute coronary syndrome. Furthermore, there is also an increase in the occurrence of coronary artery disease in young HIV-infected patients, when compared with the uninfected control population (113, 114, 151).

CONCLUSION

The introduction of antiretroviral drugs has changed the clinical prognosis of HIV-infected patients and the deaths of these individuals are now related to atherosclerotic CVDs, rather than from the viral infection itself. However, HIV infection, cART, and intestinal microbiota are associated with immune activation and insulin resistance, which can lead to the development of a variety of diseases and disorders, especially with regards to CVDs. While lifestyle modifications and pharmaceutical interventions can be employed to treat these altered metabolic functions, the mechanisms involved in the development of these chronic complications remain largely unresolved. The elucidation and understanding of these mechanisms will give rise to new classes of drugs that will further improve the quality of life of HIV-infected patients, over the age of 50.

AUTHOR CONTRIBUTIONS

MP and GR contributed to discussions and wrote, edited, and reviewed the article. DG, DM, HA, AO, and RP edited and reviewed the article. AS prepared to figures of the article, edited, and reviewed the article. MS contributed to discussions and wrote and reviewed the article. All authors approved the final version.

FUNDING

We also acknowledge the financial support CEPID/Fapesp 201307607-8, OCRC (Obesity and Comorbidities Research Center), INCT (National Institute of Science and Technology for Diabetes and Obesity), 465693/2014-8 and CAPES/CNPq (Conselho Nacional de Desenvolvimento Científico e Tecnológico).

REFERENCES

1. Ghosn J, Taiwo B, Seedat S, Autran B, Katlama C. HIV. *Lancet* (2018) 392:685–97. doi: 10.1016/S0140-6736(18)31311-4
2. Walensky RP, Paltiel AD, Losina E, Mercincavage LM, Schackman BR, Sax PE, et al. The survival benefits of AIDS treatment in the United States. *J Infect Dis.* (2006) 194:11–9. doi: 10.1086/505147
3. Lewden C, Bouteloup V, De Wit S, Sabin C, Mocroft A, Wasmuth JC, et al. All-cause mortality in treated HIV-infected adults with CD4 >/=500/mm3 compared with the general population: evidence from a large European observational cohort collaboration. *Int J Epidemiol.* (2012) 41:433–45. doi: 10.1093/ije/dyr164
4. Lohse N, Hansen AB, Pedersen G, Kronborg G, Gerstoft J, Sørensen HT, et al. Survival of persons with and without HIV infection in Denmark, 1995-2005. *Ann Intern Med.* (2007) 146:87–95. doi: 10.7326/0003-4819-146-2-200701160-00003
5. Sackoff JE, Hanna DB, Pfeiffer MR, Torian LV. Causes of death among persons with AIDS in the era of highly active antiretroviral therapy: New York City. *Ann Intern Med.* (2006) 145:397–406. doi: 10.7326/0003-4819-145-6-200609190-00003
6. Kim JH, Psevdos G, Gonzalez E, Singh S, Kilayko MC, Sharp V. All-cause mortality in hospitalized HIV-infected patients at an acute tertiary care hospital with a comprehensive outpatient HIV care program in New York City in the era of highly active antiretroviral therapy (HAART). *Infection* (2013) 41:545–51. doi: 10.1007/s15010-012-0386-7
7. Cerrato E, Calcagno A, D'Ascenzo F, Biondi-Zoccai G, Mancone M, Grosso Marra W, et al. Cardiovascular disease in HIV patients: from bench to bedside and backwards. *Open Heart* (2015) 2:e000174. doi: 10.1136/openhrt-2014-000174
8. Grunfeld C, Pang M, Doerrler W, Shigenaga JK, Jensen P, Feingold KR. Lipids, lipoproteins, triglyceride clearance, and cytokines in human immunodeficiency virus infection and the acquired immunodeficiency syndrome. *J Clin Endocrinol Metab.* (1992) 74:1045–52.
9. Anuurad E, Semrad A, Berglund L. Human immunodeficiency virus and highly active antiretroviral therapy-associated metabolic disorders and risk factors for cardiovascular disease. *Metab Syndr Relat Disord.* (2009) 7:401–10. doi: 10.1089/met.2008.0096
10. Lake JE, Currier JS. Metabolic disease in HIV infection. *Lancet Infect Dis.* (2013) 13:964–75. doi: 10.1016/S1473-3099(13)70271-8
11. Grunfeld C. Dyslipidemia and its treatment in HIV infection. *Top HIV Med.* (2010) 18:112–8.
12. Nasi M, De Biasi S, Gibellini L, Bianchini E, Pecorini S, Bacca V, et al. Ageing and inflammation in patients with HIV infection. *Clin Exp Immunol.* (2017) 187:44–52. doi: 10.1111/cei.12814
13. Justice AC. HIV and aging: time for a new paradigm. *Curr HIV/AIDS Rep.* (2010) 7:69–76. doi: 10.1007/s11904-010-0041-9
14. Guaraldi G, Prakash M, Moecklinghoff C, Stellbrink HJ. Morbidity in older HIV-infected patients: impact of long-term antiretroviral use. *AIDS Rev.* (2014) 16:75–89.
15. Collaboration ATC. Life expectancy of individuals on combination antiretroviral therapy in high-income countries: A collaborative analysis of 14 cohort studies. *Lancet* (2008) 372:293–9. doi: 10.1016/S0140-6736(08)61113-7
16. Kiage JN, Heimburger DC, Nyirenda CK, Wellons MF, Bagchi S, Chi BH, et al. Cardiometabolic risk factors among HIV patients on antiretroviral therapy. *Lipids Health Dis.* (2013) 12:50. doi: 10.1186/1476-511X-12-50
17. Non LR, Escota GV, Powderly WG. HIV and its relationship to insulin resistance and lipid abnormalities. *Transl Res.* (2017) 183:41–56. doi: 10.1016/j.trsl.2016.12.007
18. Blüher M, Kahn BB, Kahn CR. Extended longevity in mice lacking the insulin receptor in adipose tissue. *Science* (2003) 299:572–4. doi: 10.1126/science.1078223
19. Blüher M, Michael MD, Peroni OD, Ueki K, Carter N, Kahn BB, et al. Adipose tissue selective insulin receptor knockout protects against obesity and obesity-related glucose intolerance. *Dev Cell* (2002) 3:25–38. doi: 10.1016/S1534-5807(02)00199-5
20. Blüher M, Wilson-Fritch L, Leszyk J, Laustsen PG, Corvera S, Kahn CR. Role of insulin action and cell size on protein expression patterns in adipocytes. *J Biol Chem.* (2004) 279:31902–9. doi: 10.1074/jbc.M404570200
21. Neuhaus J, Jacobs DR, Baker JV, Calmy A, Duprez D, La Rosa A, et al. Markers of inflammation, coagulation, and renal function are elevated in adults with HIV infection. *J Infect Dis.* (2010) 201:1788–95. doi: 10.1086/652749
22. Naeger DM, Martin JN, Sinclair E, Hunt PW, Bangsberg DR, Hecht F, et al. Cytomegalovirus-specific T cells persist at very high levels during long-term antiretroviral treatment of HIV disease. *PLoS ONE* (2010) 5:e8886. doi: 10.1371/journal.pone.0008886
23. Schacker TW, Nguyen PL, Beilman GJ, Wolinsky S, Larson M, Reilly C, et al. Collagen deposition in HIV-1 infected lymphatic tissues and T cell homeostasis. *J Clin Invest.* (2002) 110:1133–9. doi: 10.1172/JCI0216413
24. Prada PO, Zecchin HG, Gasparetti AL, Torsoni MA, Ueno M, Hirata AE, et al. Western diet modulates insulin signaling, c-Jun N-terminal kinase activity, and insulin receptor substrate-1ser307 phosphorylation in a tissue-specific fashion. *Endocrinology* (2005) 146:1576–87. doi: 10.1210/en.2004-0767
25. Thirone AC, Carvalheira JB, Hirata AE, Velloso LA, Saad MJ. Regulation of Cbl-associated protein/Cbl pathway in muscle and adipose tissues of two animal models of insulin resistance. *Endocrinology* (2004) 145:281–93. doi: 10.1210/en.2003-0575
26. Srinivasa S, Fitch KV, Wong K, Torriani M, Mayhew C, Stanley T, et al. RAAS activation is associated with visceral adiposity and insulin resistance

among HIV-infected patients. *J Clin Endocrinol Metab.* (2015) 100:2873–82. doi: 10.1210/jc.2015-1461
27. Calza L, Manfredi R, Chiodo F. Insulin resistance and diabetes mellitus in HIV-infected patients receiving antiretroviral therapy. *Metab Syndr Relat Disord.* (2004) 2:241–50. doi: 10.1089/met.2004.2.241
28. Duncan AD, Goff LM, Peters BS: Type 2 diabetes prevalence and its risk factors in HIV: A cross-sectional study. *PLoS ONE* (2018) 13:e0194199. doi: 10.1371/journal.pone.0194199
29. Monroe AK, Glesby MJ, Brown TT. Diagnosing and managing diabetes in HIV-infected patients: current concepts. *Clin Infect Dis.* (2015) 60:453–62. doi: 10.1093/cid/ciu779
30. Carvalho BM, Oliveira AG, Ueno M, Araújo TG, Guadagnini D, Carvalho-Filho MA, et al. Modulation of double-stranded RNA-activated protein kinase in insulin sensitive tissues of obese humans. *Obesity* (2013) 21:2452–7. doi: 10.1002/oby.20410
31. Carvalho-Filho MA, Carvalho BM, Oliveira AG, Guadagnini D, Ueno M, Dias MM, et al. Double-stranded RNA-activated protein kinase is a key modulator of insulin sensitivity in physiological conditions and in obesity in mice. *Endocrinology* (2012) 153:5261–74. doi: 10.1210/en.2012-1400
32. Neal MD, Leaphart C, Levy R, Prince J, Billiar TR, Watkins S, et al. Enterocyte TLR4 mediates phagocytosis and translocation of bacteria across the intestinal barrier. *J Immunol.* (2006) 176:3070–9. doi: 10.4049/jimmunol.176.5.3070
33. Suganami T, Mieda T, Itoh M, Shimoda Y, Kamei Y, Ogawa Y. Attenuation of obesity-induced adipose tissue inflammation in C3H/HeJ mice carrying a Toll-like receptor 4 mutation. *Biochem Biophys Res Commun.* (2007) 354:45–9. doi: 10.1016/j.bbrc.2006.12.190
34. Cani PD, Amar J, Iglesias MA, Poggi M, Knauf C, Bastelica D, et al. Metabolic endotoxemia initiates obesity and insulin resistance. *Diabetes* (2007) 56:1761–72. doi: 10.2337/db06-1491
35. Pedro MN, Magro DO, da Silva E, Guadagnini D, Santos A, Pedro RD, et al. Plasma levels of lipopolysaccharide correlate with insulin resistance in HIV patients. *Diabetol Metab Syndr.* (2018) 10:7. doi: 10.1186/s13098-018-0308-7
36. Tarancon-Diez L, De Pablo-Bernal RS, Jiménez JL, Álvarez-Ríos AI, Genebat M, et al. Role of toll-like receptor 4 Asp299Gly polymorphism in the development of cardiovascular diseases in HIV-infected patients. *AIDS* (2018) 32:1035–41. doi: 10.1097/QAD.0000000000001797
37. Bandera A, Masetti M, Fabbiani M, Biasin M, Muscatello A, Squillace N, et al. The NLRP3 inflammasome is upregulated in HIV-infected antiretroviral therapy-treated individuals with defective immune recovery. *Front Immunol.* (2018) 9:214. doi: 10.3389/fimmu.2018.00214
38. Saad MJ, Folli F, Araki E, Hashimoto N, Csermely P, Kahn CR. Regulation of insulin receptor, insulin receptor substrate-1 and phosphatidylinositol 3-kinase in 3T3-F442A adipocytes. Effects of differentiation, insulin, and dexamethasone. *Mol Endocrinol.* (1994) 8:545–57.
39. Zanotto TM, Quaresma PGF, Guadagnini D, Weissmann L, Santos AC, Vecina JF, et al. Blocking iNOS and endoplasmic reticulum stress synergistically improves insulin resistance in mice. *Mol Metab.* (2017) 6:206–218. doi: 10.1016/j.molmet.2016.12.005
40. Hirosumi J, Tuncman G, Chang L, Gorgun CZ, Uysal KT, Maeda K, et al. A central role for JNK in obesity and insulin resistance. *Nature* (2002) 420:333–6. doi: 10.1038/nature01137
41. Yuan M, Konstantopoulos N, Lee J, Hansen L, Li ZW, Karin M, et al. Reversal of obesity- and diet-induced insulin resistance with salicylates or targeted disruption of Ikkbeta. *Science* (2001) 293:1673–7. doi: 10.1126/science.1061620
42. Aguirre V, Uchida T, Yenush L, Davis R, White MF. The c-Jun NH-terminal kinase promotes insulin resistance during association with insulin receptor substrate-1 and phosphorylation of Ser(307). *J Biol Chem.* (2000) 275:9047–54. doi: 10.1074/jbc.275.12.9047
43. Cai D, Yuan M, Frantz DF, Melendez PA, Hansen L, Lee J, et al. Local and systemic insulin resistance resulting from hepatic activation of IKK-beta and NF-kappaB. *Nat Med.* (2005) 11:183–90. doi: 10.1038/nm1166
44. da Silva KLC, Camacho AP, Mittestainer FC, Carvalho BM, Santos A, Guadagnini D, et al. Atorvastatin and diacerein reduce insulin resistance and increase disease tolerance in rats with sepsis. *J Inflamm.* (2018) 15:8. doi: 10.1186/s12950-018-0184-9
45. Castro G, CAreias MF, Weissmann L, Quaresma PG, Katashima CK, Saad MJ, et al. Diet-induced obesity induces endoplasmic reticulum stress and insulin resistance in the amygdala of rats. *FEBS Open Biol.* (2013) 3:443–9. doi: 10.1016/j.fob.2013.09.002
46. Carvalho-Filho MA, Ueno M, Carvalheira JB, Velloso LA, Saad MJ. Targeted disruption of iNOS prevents LPS-induced S-nitrosation of IRbeta/IRS-1 and Akt and insulin resistance in muscle of mice. *Am J Physiol Endocrinol Metab.* (2006) 291:E476–82. doi: 10.1152/ajpendo.00422.2005
47. Carvalho-Filho MA, Ueno M, Hirabara SM, Seabra AB, Carvalheira JB, de Oliveira MGet al. S-nitrosation of the insulin receptor, insulin receptor substrate 1, and protein kinase B/Akt: a novel mechanism of insulin resistance. *Diabetes* (2005) 54:959–67. doi: 10.2337/diabetes.54.4.959
48. Ozcan L, Ergin AS, Lu A, Chung J, Sarkar S, Nie D et al. Endoplasmic reticulum stress plays a central role in development of leptin resistance. *Cell Metab.* (2009) 9:35–51. doi: 10.1016/j.cmet.2008.12.004
49. Willig AL, Overton ET. Metabolic complications and glucose metabolism in HIV infection: a review of the evidence. *Curr HIV/AIDS Rep.* (2016) 13:289–96. doi: 10.1007/s11904-016-0330-z
50. Lake JE. The fat of the matter: obesity and visceral adiposity in treated HIV infection. *Curr HIV/AIDS Rep.* (2017) 14:211–9. doi: 10.1007/s11904-017-0368-6
51. Lambert CT, Sandesara PB, Hirsh B, Shaw LJ, Lewis W, Quyyumi AA, et al. HIV, highly active antiretroviral therapy and the heart: a cellular to epidemiological review. *HIV Med.* (2016) 17:411–24. doi: 10.1111/hiv.12346
52. Miserez AR, Muller PY, Spaniol V. Indinavir inhibits sterol-regulatory element-binding protein-1c-dependent lipoprotein lipase and fatty acid synthase gene activations. *AIDS* (2002) 16:1587–94. doi: 10.1097/00002030-200208160-00003
53. Zhou H, Gurley EC, Jarujaron S, Ding H, Fang Y, Xu Z, et al. HIV protease inhibitors activate the unfolded protein response and disrupt lipid metabolism in primary hepatocytes. *Am J Physiol Gastrointest Liver Physiol.* (2006) 291:G1071–80. doi: 10.1152/ajpgi.00182.2006
54. Murata H, Hruz PW, Mueckler M. Indinavir inhibits the glucose transporter isoform Glut4 at physiologic concentrations. *AIDS* (2002) 16:859–63. doi: 10.1097/00002030-200204120-00005
55. Murata H, Hruz PW, Mueckler M. The mechanism of insulin resistance caused by HIV protease inhibitor therapy. *J Biol Chem.* (2000) 275:20251–4. doi: 10.1074/jbc.C000228200
56. Carr A, Cooper DA. Adverse effects of antiretroviral therapy. *Lancet* (2000) 356:1423–30. doi: 10.1016/S0140-6736(00)02854-3
57. Nasi M, Pinti M, Chiesa E, Fiore S, Manzini S, Del Giovane C, et al. Decreased mitochondrial DNA content in subcutaneous fat from HIV-infected women taking antiretroviral therapy as measured at delivery. *Antivir Ther.* (2011) 16:365–72. doi: 10.3851/IMP1764
58. Maggiolo F, Roat E, Pinti M, Nasi M, Gibellini L, De Biasi S, et al. Mitochondrial changes during D-drug-containing once-daily therapy in HIV-positive treatment-naive patients. *Antivir Ther.* (2010) 15:51–9. doi: 10.3851/IMP1483
59. Galluzzi L, Pinti M, Troiano L, Prada N, Nasi M, Ferraresi R, et al. Changes in mitochondrial RNA production in cells treated with nucleoside analogues. *Antivir Ther.* (2005) 10:191–5.
60. Shiramizu B, Shikuma KM, Kamemoto L, Gerschenson M, Erdem G, Pinti M, et al. Placenta and cord blood mitochondrial DNA toxicity in HIV-infected women receiving nucleoside reverse transcriptase inhibitors during pregnancy. *J Acquir Immune Defic Syndr.* (2003) 32:370–4. doi: 10.1097/00126334-200304010-00004
61. Emery S, Neuhaus JA, Phillips AN, Babiker A, Cohen CJ, Gatell JM, et al. Major clinical outcomes in antiretroviral therapy (ART)-naive participants and in those not receiving ART at baseline in the SMART study. *J Infect Dis.* (2008) 197:1133–44. doi: 10.1086/586713
62. Funderburg NT. Markers of coagulation and inflammation often remain elevated in ART-treated HIV-infected patients. *Curr Opin HIV AIDS* (2014) 9:80–6. doi: 10.1097/COH.0000000000000019
63. Niv Y. Mucin genes expression in the intestine of Crohn's disease patients: A systematic review and meta-analysis. *J Gastrointestin Liver Dis.* (2016) 25:351–7. doi: 10.15403/jgld.2014.1121.253.niv
64. Angelovich TA, Hearps AC, Maisa A, Martin GE, Lichtfuss GF, Cheng WJ, et al. Viremic and virologically suppressed HIV infection increases

age-related changes to monocyte activation equivalent to 12 and 4 years of aging, respectively. *J Acquir Immune Defic Syndr.* (2015) 69:11–7. doi: 10.1097/QAI.0000000000000559
65. Munger AM, Chow DC, Playford MP, Parikh NI, Gangcuangco LM, Nakamoto BKet al. Characterization of lipid composition and high-density lipoprotein function in HIV-infected individuals on stable antiretroviral regimens. *AIDS Res Hum Retroviruses* (2015) 31:221–8. doi: 10.1089/aid.2014.0239
66. Lederman MM, Funderburg NT, Sekaly RP, Klatt NR, Hunt PW. Residual immune dysregulation syndrome in treated HIV infection. *Adv Immunol.* (2013) 119:51–83. doi: 10.1016/B978-0-12-407707-2.00002-3
67. van Wijk JP, Cabezas MC. Hypertriglyceridemia, metabolic syndrome, and cardiovascular disease in HIV-infected patients: effects of antiretroviral therapy and adipose tissue distribution. *Int J Vasc Med.* (2012) 2012:201027. doi: 10.1155/2012/201027
68. Brenchley JM, Douek DC. HIV infection and the gastrointestinal immune system. *Mucosal Immunol.* (2008) 1:23–30. doi: 10.1038/mi.2007.1
69. Gupta VK, Paul S, Dutta C: Geography, ethnicity or subsistence-specific variations in human microbiome composition and diversity. *Front Microbiol.* (2017) 8:1162. doi: 10.3389/fmicb.2017.01162
70. Rodríguez JM, Murphy K, Stanton C, Ross RP, Kober OI, Juge N, et al. The composition of the gut microbiota throughout life, with an emphasis on early life. *Microb Ecol Health Dis.* (2015) 26:26050. doi: 10.3402/mehd.v26.26050
71. Conlon MA, Bird AR. The impact of diet and lifestyle on gut microbiota and human health. *Nutrients* (2014) 7:17–44. doi: 10.3390/nu7010017
72. Monteiro NES, Roquetto AR, de Pace F, Moura CS, Santos AD, Yamada AT, et al. Dietary whey proteins shield murine cecal microbiota from extensive disarray caused by a high-fat diet. *Food Res Int*. (2016) 85:121–30. doi: 10.1016/j.foodres.2016.04.036
73. Saad MJ, Santos A, Prada PO. Linking gut microbiota and inflammation to obesity and insulin resistance. *Physiology* (2016) 31:283–93. doi: 10.1152/physiol.00041.2015
74. Marchetti G, Bellistrì GM, Borghi E, Tincati C, Ferramosca S, La Francesca M, et al. Microbial translocation is associated with sustained failure in CD4+ T-cell reconstitution in HIV-infected patients on long-term highly active antiretroviral therapy. *AIDS* (2008) 22:2035–8. doi: 10.1097/QAD.0b013e3283112d29
75. Tincati C, Douek DC, Marchetti G. Gut barrier structure, mucosal immunity and intestinal microbiota in the pathogenesis and treatment of HIV infection. *AIDS Res Ther.* (2016) 13:19. doi: 10.1186/s12981-016-0103-1
76. Liu J, Williams B, Frank D, Dillon SM, Wilson CC, Landay AL. Inside out: HIV, the gut microbiome, and the mucosal immune system. *J Immunol.* (2017) 198:605–14. doi: 10.4049/jimmunol.1601355
77. Caspari G, Beyer J, Schunter F, Knüver-Hopf J, Schmitt H. HIV-specific antibody among voluntary blood donors in Lower Saxony (FRG). *Blut* (1987) 55:181–7. doi: 10.1007/BF00320575
78. Vujkovic-Cvijin I, Dunham RM, Iwai S, Maher MC, Albright RG, Broadhurst MJ, et al. Dysbiosis of the gut microbiota is associated with HIV disease progression and tryptophan catabolism. *Sci Transl Med.* (2013) 5:193ra191. doi: 10.1126/scitranslmed.3006438
79. Srinivasa S, Fitch KV, Lo J, Kadar H, Knight R, Wong K, et al. Plaque burden in HIV-infected patients is associated with serum intestinal microbiota-generated trimethylamine. *AIDS* (2015) 29:443–52. doi: 10.1097/QAD.0000000000000565
80. Wang Z, Klipfell E, Bennett BJ, Koeth R, Levison BS, Dugar B, et al. Gut flora metabolism of phosphatidylcholine promotes cardiovascular disease. *Nature* (2011) 472:57–63. doi: 10.1038/nature09922
81. Senthong V, Wang Z, Fan Y, Wu Y, Hazen SL, Tang WH. Trimethylamine N-oxide and mortality risk in patients with peripheral artery disease. *J Am Heart Assoc.* (2016) 5:e004237. doi: 10.1161/JAHA.116.004237
82. Senthong V, Li XS, Hudec T, Coughlin J, Wu Y, Levison B, et al. Plasma Trimethylamine N-Oxide, a gut microbe-generated phosphatidylcholine metabolite, is associated with atherosclerotic burden. *J Am Coll Cardiol.* (2016) 67:2620–8. doi: 10.1016/j.jacc.2016.03.546
83. Zhu W, Gregory JC, Org E, Buffa JA, Gupta N, Wang Z, et al. Gut microbial metabolite TMAO enhances platelet hyperreactivity and thrombosis risk. *Cell* (2016) 165:111–24. doi: 10.1016/j.cell.2016.02.011
84. Organ CL, Otsuka H, Bhushan S, Wang Z, Bradley J, Trivedi R, et al. Choline diet and its gut microbe-derived metabolite, Trimethylamine N-Oxide, exacerbate pressure overload-induced heart failure. *Circ Heart Fail.* (2016) 9:e002314. doi: 10.1161/CIRCHEARTFAILURE.115.002314
85. Walli R, Herfort O, Michl GM, Demant T, Jäger H, Dieterle C, et al. Treatment with protease inhibitors associated with peripheral insulin resistance and impaired oral glucose tolerance in HIV-1-infected patients. *AIDS* (1998) 12:F167–73. doi: 10.1097/00002030-199815000-00001
86. Hommes MJ, Romijn JA, Endert E, Eeftinck Schattenkerk JK, Sauerwein HP. Insulin sensitivity and insulin clearance in human immunodeficiency virus-infected men. *Metabolism* (1991) 40:651–6. doi: 10.1016/0026-0495(91)90059-6
87. Khera AV, Cuchel M, de la Llera-Moya M, Rodrigues A, Burke MF, Jafri K, et al. Cholesterol efflux capacity, high-density lipoprotein function, and atherosclerosis. *N Engl J Med.* (2011) 364:127–35. doi: 10.1056/NEJMoa1001689
88. Riddler SA, Smit E, Cole SR, Li R, Chmiel JS, Dobs A, et al. Impact of HIV infection and HAART on serum lipids in men. *JAMA* (2003) 289:2978–82. doi: 10.1001/jama.289.22.2978
89. Jin C, Ji S, Xie T, Höxtermann S, Fuchs W, Lu X, et al. Severe dyslipidemia and immune activation in HIV patients with dysglycemia. HIV *Clin Trials* (2016) 17:189–96. doi: 10.1080/15284336.2016.1207297
90. (NCD-RisC) NRFC. Worldwide trends in diabetes since 1980: A pooled analysis of 751 population-based studies with 4.4 million participants. *Lancet* (2016) 387:1513–30. doi: 10.1016/S0140-6736(16)00618-8
91. Mujawar Z, Rose H, Morrow MP, Pushkarsky T, Dubrovsky L, Mukhamedova N, et al. Human immunodeficiency virus impairs reverse cholesterol transport from macrophages. *PLoS Biol.* (2006) 4:e365. doi: 10.1371/journal.pbio.0040365
92. Ji Y, Zhang F, Zhang R, Shen Y, Liu L, Wang J, et al. Changes in intestinal microbiota in HIV-1-infected subjects following cART initiation: influence of CD4+ T cell count. *Emerg Microbes Infect*. (2018) 7:113. doi: 10.1038/s41426-018-0117-y
93. Mutlu EA, Keshavarzian A, Losurdo J, Swanson G, Siewe B, Forsyth C, et al. A compositional look at the human gastrointestinal microbiome and immune activation parameters in HIV infected subjects. *PLoS Pathog.* (2014) 10:e1003829. doi: 10.1371/journal.ppat.1003829
94. Nowak P, Troseid M, Avershina E, Barqasho B, Neogi U, Holm K, et al. Gut microbiota diversity predicts immune status in HIV-1 infection. *AIDS* (2015) 29:2409–18. doi: 10.1097/QAD.0000000000000869
95. Lozupone CA, Li M, Campbell TB, Flores SC, Linderman D, Gebert MJ, et al. Alterations in the gut microbiota associated with HIV-1 infection. *Cell Host Microbe* (2013) 14:329–39. doi: 10.1016/j.chom.2013.08.006
96. Li SX, Armstrong A, Neff CP, Shaffer M, Lozupone CA, Palmer BE. Complexities of gut microbiome dysbiosis in the context of HIV infection and antiretroviral therapy. *Clin Pharmacol Ther.* (2016) 99:600–11. doi: 10.1002/cpt.363
97. Nasi M, Pinti M, Mussini C, Cossarizza A. Persistent inflammation in HIV infection: established concepts, new perspectives. *Immunol Lett*. (2014) 161:184–8. doi: 10.1016/j.imlet.2014.01.008
98. Psomas C, Younas M, Reynes C, Cezar R, Portalès P, Tuaillon E, et al. One of the immune activation profiles observed in HIV-1-infected adults with suppressed viremia is linked to metabolic syndrome: the ACTIVIH study. *EBioMedicine* (2016) 8:265–76. doi: 10.1016/j.ebiom.2016.05.008
99. Dirajlal-Fargo S, Moser C, Brown TT, Kelesidis T, Dube MP, Stein JH, et al. Changes in insulin resistance after initiation of raltegravir or protease inhibitors with tenofovir-emtricitabine: AIDS clinical trials group A5260s. *Open Forum Infect Dis.* (2016) 3:ofw174. doi: 10.1093/ofid/ofw174
100. Carr A, Samaras K, Burton S, Law M, Freund J, Chisholm DJ, et al. A syndrome of peripheral lipodystrophy, hyperlipidaemia and insulin resistance in patients receiving HIV protease inhibitors. *AIDS* (1998) 12:F51–8. doi: 10.1097/00002030-199807000-00003
101. Carr A, Samaras K, Thorisdottir A, Kaufmann GR, Chisholm DJ, Cooper DA. Diagnosis, prediction, and natural course of HIV-1 protease-inhibitor-associated lipodystrophy, hyperlipidaemia, and diabetes mellitus: A cohort study. *Lancet* (1999) 353:2093–9. doi: 10.1016/S0140-6736(98)08468-2
102. Jacobson DL, Knox T, Spiegelman D, Skinner S, Gorbach S, Wanke C. Prevalence of, evolution of, and risk factors for fat

atrophy and fat deposition in a cohort of HIV-infected men and women. *Clin Infect Dis.* (2005) 40:1837–45. doi: 10.1086/430379
103. Grinspoon S, Carr A. Cardiovascular risk and body-fat abnormalities in HIV-infected adults. *N Engl J Med.* (2005) 352:48–62. doi: 10.1056/NEJMra041811
104. Hernandez D, Kalichman S, Cherry C, Kalichman M, Washington C, Grebler T. Dietary intake and overweight and obesity among persons living with HIV in Atlanta Georgia. *AIDS Care* (2017) 29:767–71. doi: 10.1080/09540121.2016.1238441
105. Levy ME, Greenberg AE, Hart R, Powers Happ L, Hadigan C, Castel A, et al. High burden of metabolic comorbidities in a citywide cohort of HIV outpatients: evolving health care needs of people aging with HIV in Washington, DC. *HIV Med.* (2017) 18:724–35. doi: 10.1111/hiv.12516
106. Erlandson KM, Taejaroenkul S, Smeaton L, Gupta A, Singini IL, Lama JR, et al. A randomized comparison of anthropomorphic changes with preferred and alternative efavirenz-based antiretroviral regimens in diverse multinational settings. *Open Forum Infect Dis.* (2015) 2:ofv095. doi: 10.1093/ofid/ofv095
107. Buchacz K, Baker RK, Palella FJ, Shaw L, Patel P, Lichtenstein KA, et al. Disparities in prevalence of key chronic diseases by gender and race/ethnicity among antiretroviral-treated HIV-infected adults in the US. *Antivir Ther.* (2013) 18:65–75. doi: 10.3851/IMP2450
108. Achhra AC, Mocroft A, Reiss P, Sabin C, Ryom L, de Wit S, et al. Short-term weight gain after antiretroviral therapy initiation and subsequent risk of cardiovascular disease and diabetes: the D:A:D study. *HIV Med.* (2016) 17:255–68. doi: 10.1111/hiv.12294
109. Bhagwat P, Ofotokun I, McComsey GA, Brown TT, Moser C, Sugar CA, et al. Changes in abdominal fat following antiretroviral therapy initiation in HIV-infected individuals correlate with waist circumference and self-reported changes. *Antivir Ther.* (2017) 22:577–86. doi: 10.3851/IMP3148
110. Shah RV, Murthy VL, Abbasi SA, Blankstein R, Kwong RY, Goldfine AB, et al. Visceral adiposity and the risk of metabolic syndrome across body mass index: the MESA Study. *JACC Cardiovasc Imaging* (2014) 7:1221–35. doi: 10.1016/j.jcmg.2014.07.017
111. McComsey GA, Moser C, Currier J, Ribaudo HJ, Paczuski P, Dubé MP, et al. Body composition changes after initiation of raltegravir or protease inhibitors: ACTG A5260s. *Clin Infect Dis.* (2016) 62:853–62. doi: 10.1093/cid/ciw017
112. Centers for Disease Control and Prevention. Available online at: http://www.cdc.gov/hiv/library/reports/surveillance
113. Paisible AL, Chang CC, So-Armah KA, Butt AA, Leaf DA, Budoff M, et al. HIV infection, cardiovascular disease risk factor profile, and risk for acute myocardial infarction. *J Acquir Immune Defic Syndr.* (2015) 68:209–16. doi: 10.1097/QAI.0000000000000419
114. Womack JA, Chang CC, So-Armah KA, Alcorn C, Baker JV, Brown ST, et al. HIV infection and cardiovascular disease in women. *J Am Heart Assoc.* (2014) 3:e001035. doi: 10.1161/JAHA.114.001035
115. Friedman EE, Duffus WA. Chronic health conditions in Medicare beneficiaries 65 years old, and older with HIV infection. *AIDS* (2016) 30:2529–6. doi: 10.1097/QAD.0000000000001215
116. Haase J, Weyer U, Immig K, Klöting N, Blüher M, Eilers J, et al. Local proliferation of macrophages in adipose tissue during obesity-induced inflammation. *Diabetologia* (2014) 57:562–71. doi: 10.1007/s00125-013-3139-y
117. Bourlier V, Sengenès C, Zakaroff-Girard A, Decaunes P, Wdziekonski B, Galitzky J, et al. TGFbeta family members are key mediators in the induction of myofibroblast phenotype of human adipose tissue progenitor cells by macrophages. *PLoS ONE* (2012) 7:e31274. doi: 10.1371/journal.pone.0031274
118. Vandanmagsar B, Youm YH, Ravussin A, Galgani JE, Stadler K, Mynatt RL, et al. The NLRP3 inflammasome instigates obesity-induced inflammation and insulin resistance. *Nat Med.* (2011) 17:179–88. doi: 10.1038/nm.2279
119. Freitas P, Carvalho D, Santos AC, Matos MJ, Madureira AJ, Marques R, et al. Prevalence of obesity and its relationship to clinical lipodystrophy in HIV-infected adults on anti-retroviral therapy. *J Endocrinol Invest.* (2012) 35:964–70. doi: 10.3275/8187
120. Rose H, Woolley I, Hoy J, Dart A, Bryant B, Mijch A, et al. HIV infection and high-density lipoprotein: the effect of the disease vs. the effect of treatment. *Metabolism* (2006) 55:90–5. doi: 10.1016/j.metabol.2005.07.012
121. Zangerle R, Sarcletti M, Gallati H, Reibnegger G, Wachter H, Fuchs D. Decreased plasma concentrations of HDL cholesterol in HIV-infected individuals are associated with immune activation. *J Acquir Immune Defic Syndr.* (1994) 7:1149–56.
122. Constans J, Pellegrin JL, Peuchant E, Dumon MF, Pellegrin I, Sergeant C, et al. Plasma lipids in HIV-infected patients: A prospective study in 95 patients. *Eur J Clin Invest.* (1994) 24:416–20. doi: 10.1111/j.1365-2362.1994.tb02185.x
123. Huang CY, Lu CW, Liu YL, Chiang CH, Lee LT, Huang KC: Relationship between chronic hepatitis B and metabolic syndrome: A structural equation modeling approach. *Obesity* (2016) 24:483–9. doi: 10.1002/oby.21333
124. Nagano T, Seki N, Tomita Y, Sugita T, Aida Y, Itagaki M, et al. Impact of chronic *Hepatitis C Virus* genotype 1b infection on triglyceride concentration in serum lipoprotein fractions. *Int J Mol Sci.* (2015) 16:20576–94. doi: 10.3390/ijms160920576
125. Fitzgerald ML, Mujawar Z, Tamehiro N. ABC transporters, atherosclerosis and inflammation. *Atherosclerosis* (2010) 211:361–70. doi: 10.1016/j.atherosclerosis.2010.01.011
126. McHugh J, McHugh W. How to assess deep tendon reflexes. *Nursing* (1990) 20:62–4. doi: 10.1097/00152193-199008000-00024
127. Rasheed S, Yan JS, Lau A, Chan AS. HIV replication enhances production of free fatty acids, low density lipoproteins and many key proteins involved in lipid metabolism: A proteomics study. *PLoS ONE* (2008) 3:e3003. doi: 10.1371/journal.pone.0003003
128. Haugaard SB, Andersen O, Pedersen SB, Dela F, Fenger M, Richelsen B, et al. Tumor necrosis factor alpha is associated with insulin-mediated suppression of free fatty acids and net lipid oxidation in HIV-infected patients with lipodystrophy. *Metabolism* (2006) 55:175–82. doi: 10.1016/j.metabol.2005.08.018
129. Shinohara E, Yamashita S, Kihara S, Hirano K, Ishigami M, Arai T, et al. Interferon alpha induces disorder of lipid metabolism by lowering postheparin lipases and cholesteryl ester transfer protein activities in patients with chronic hepatitis C. *Hepatology* (1997) 25:1502–6. doi: 10.1002/hep.510250632
130. Zanni MV, Schouten J, Grinspoon SK, Reiss P. Risk of coronary heart disease in patients with HIV infection. *Nat Rev Cardiol.* (2014) 11:728–41. doi: 10.1038/nrcardio.2014.167
131. Lo J, Rosenberg ES, Fitzgerald ML, Bazner SB, Ihenachor EJ, Hawxhurst V, et al. High-density lipoprotein-mediated cholesterol efflux capacity is improved by treatment with antiretroviral therapy in acute human immunodeficiency virus infection. *Open Forum Infect Dis.* (2014) 1:ofu108. doi: 10.1093/ofid/ofu108
132. El Khoury P, Ghislain M, Villard EF, Le Goff W, Lascoux-Combe C, Yeni P, et al. Plasma cholesterol efflux capacity from human THP-1 macrophages is reduced in HIV-infected patients: impact of HAART. *J Lipid Res.* (2015) 56:692–702. doi: 10.1194/jlr.M054510
133. Kaplan RC, Hanna DB, Kizer JR. Recent insights into cardiovascular disease (CVD) risk among HIV-infected adults. *Curr HIV/AIDS Rep.* (2016) 13:44–52. doi: 10.1007/s11904-016-0301-4
134. Triant VA, Lee H, Hadigan C, Grinspoon SK. Increased acute myocardial infarction rates and cardiovascular risk factors among patients with human immunodeficiency virus disease. *J Clin Endocrinol Metab.* (2007) 92:2506–12. doi: 10.1210/jc.2006-2190
135. Rockstroh JK. Non-Alcoholic Fatty Liver Disease (NAFLD) and Non-Alcoholic Steatohepatitis (NASH) in HIV. *Curr HIV/AIDS Rep.* (2017) 14:47–53. doi: 10.1007/s11904-017-0351-2
136. Guaraldi G, Lonardo A, Maia L, Palella FJ. Metabolic concerns in aging HIV-infected persons: from serum lipid phenotype to fatty liver. *AIDS* (2017) 31 (Suppl. 2):S147–56. doi: 10.1097/QAD.0000000000001483
137. Morse CG, McLaughlin M, Matthews L, Proschan M, Thomas F, Gharib AM, et al. Nonalcoholic steatohepatitis and hepatic fibrosis in HIV-1-monoinfected adults with elevated aminotransferase levels on antiretroviral therapy. *Clin Infect Dis.* (2015) 60:1569–78. doi: 10.1093/cid/civ101
138. Macias J, Rivero-Juarez A, Neukam K, Tellez F, Merino D, Frias M, et al. Impact of genetic polymorphisms associated with nonalcoholic

fatty liver disease on HIV-infected individuals. *AIDS* (2015) 29:1927–35. doi: 10.1097/QAD.0000000000000799
139. Price JC, Seaberg EC, Latanich R, Budoff MJ, Kingsley LA, Palella FJ, et al. Risk factors for fatty liver in the multicenter AIDS cohort study. *Am J Gastroenterol.* (2014) 109:695–704. doi: 10.1038/ajg.2014.32
140. Crum-Cianflone N, Dilay A, Collins G, Asher D, Campin R, Medina S, et al. Nonalcoholic fatty liver disease among HIV-infected persons. *J Acquir Immune Defic Syndr.* (2009) 50:464–73. doi: 10.1097/QAI.0b013e318198a88a
141. Sterling RK, Smith PG, Brunt EM. Hepatic steatosis in human immunodeficiency virus: A prospective study in patients without viral hepatitis, diabetes, or alcohol abuse. *J Clin Gastroenterol.* (2013) 47:182–7. doi: 10.1097/MCG.0b013e318264181d
142. Younossi Z, Anstee QM, Marietti M, Hardy T, Henry L, Eslam M, et al. Global burden of NAFLD and NASH: trends, predictions, risk factors and prevention. *Nat Rev Gastroenterol Hepatol.* (2018) 15:11–20. doi: 10.1038/nrgastro.2017.109
143. Antinori A, Arendt G, Becker JT, Brew BJ, Byrd DA, Cherner M, et al. Updated research nosology for HIV-associated neurocognitive disorders. *Neurology* (2007) 69:1789–99. doi: 10.1212/01.WNL.0000287431.88658.8b
144. Ghafouri M, Amini S, Khalili K, Sawaya BE. HIV-1 associated dementia: symptoms and causes. *Retrovirology* (2006) 3:28. doi: 10.1186/1742-4690-3-28
145. Sacktor N, McDermott MP, Marder K, Schifitto G, Selnes OA, McArthur JC, et al. HIV-associated cognitive impairment before and after the advent of combination therapy. *J Neurovirol.* (2002) 8:136–42. doi: 10.1080/13550280290049615
146. Chan P, Brew BJ. HIV associated neurocognitive disorders in the modern antiviral treatment era: prevalence, characteristics, biomarkers, and effects of treatment. *Curr HIV/AIDS Rep.* (2014) 11:317–24. doi: 10.1007/s11904-014-0221-0
147. Triant VA, Brown TT, Lee H, Grinspoon SK. Fracture prevalence among human immunodeficiency virus (HIV)-infected versus non-HIV-infected patients in a large U.S. healthcare system. *J Clin Endocrinol Metab.* (2008) 93:3499–504. doi: 10.1210/jc.2008-0828
148. Collin F, Duval X, Le Moing V, Piroth L, Al Kaied F, Massip Pet al. Ten-year incidence and risk factors of bone fractures in a cohort of treated HIV1-infected adults. *AIDS* (2009) 23:1021–4. doi: 10.1097/QAD.0b013e3283292195
149. Shiels MS, Cole SR, Kirk GD, Poole C. A meta-analysis of the incidence of non-AIDS cancers in HIV-infected individuals. *J Acquir Immune Defic Syndr.* (2009) 52:611–22. doi: 10.1097/QAI.0b013e3181b327ca
150. Yanik EL, Katki HA, Engels EA. Cancer risk among the HIV-infected elderly in the United States. *AIDS* (2016) 30:1663–8. doi: 10.1097/QAD.0000000000001077
151. Currier JS, Taylor A, Boyd F, Dezii CM, Kawabata H, Burtcel B, et al. Coronary heart disease in HIV-infected individuals. *J Acquir Immune Defic Syndr.* (2003) 33:506–12. doi: 10.1097/00126334-200308010-00012

Conflict of Interest Statement: The authors declare that the research was conducted in the absence of any commercial or financial relationships that could be construed as a potential conflict of interest.

frontiers in Endocrinology

REVIEW
published: 30 August 2018
doi: 10.3389/fendo.2018.00503

The Role of Hepatocyte Growth Factor (HGF) in Insulin Resistance and Diabetes

Alexandre G. Oliveira[1,2†], Tiago G. Araújo[1,3†], Bruno de Melo Carvalho[1,4], Guilherme Z. Rocha[1], Andrey Santos[1] and Mario J. A. Saad[1*]*

[1] Department of Internal Medicine, State University of Campinas, Campinas, Brazil, [2] Department of Physical Education, Institute of Biosciences, São Paulo State University (UNESP), Rio Claro, Brazil, [3] Department of Physiology and Pharmacology, Federal University of Pernambuco, Recife, Brazil, [4] Institute of Biological Sciences, University of Pernambuco, Recife, Brazil

In obesity, insulin resistance (IR) and diabetes, there are proteins and hormones that may lead to the discovery of promising biomarkers and treatments for these metabolic disorders. For example, these molecules may impair the insulin signaling pathway or provide protection against IR. Thus, identifying proteins that are upregulated in IR states is relevant to the diagnosis and treatment of the associated disorders. It is becoming clear that hepatocyte growth factor (HGF) is an important component of the pathophysiology of IR, with increased levels in most common IR conditions, including obesity. HGF has a role in the metabolic flux of glucose in different insulin sensitive cell types; plays a key role in β-cell homeostasis; and is capable of modulating the inflammatory response. In this review, we discuss how, and to what extent HGF contributes to IR and diabetes pathophysiology, as well as its role in cancer which is more prevalent in obesity and diabetes. Based on the current literature and knowledge, it is clear that HGF plays a central role in these metabolic disorders. Thus, HGF levels could be employed as a biomarker for disease status/progression, and HGF/c-Met signaling pathway modulators could effectively regulate IR and treat diabetes.

Keywords: hepatocyte growth factor, HGF, obesity, insulin resistance, diabetes, inflammation, beta cells

OPEN ACCESS

Edited by:
Andrew J. McAinch,
Victoria University, Australia

Reviewed by:
Negar Naderpoor,
Monash University, Australia
Kerry Loomes,
University of Auckland, New Zealand

***Correspondence:**
Alexandre G. Oliveira
alexandre.gabarra@unesp.br
Mario J. A. Saad
msaad@fcm.unicamp.br

†These authors have contributed equally to this work

Specialty section:
This article was submitted to Obesity, a section of the journal Frontiers in Endocrinology

Received: *05 March 2018*
Accepted: *10 August 2018*
Published: *30 August 2018*

Citation:
Oliveira AG, Araújo TG, Carvalho BM, Rocha GZ, Santos A and Saad MJA (2018) The Role of Hepatocyte Growth Factor (HGF) in Insulin Resistance and Diabetes. Front. Endocrinol. 9:503. doi: 10.3389/fendo.2018.00503

INTRODUCTION

Obesity is a rapidly growing worldwide epidemic. It is estimated that more than 1 billion adults worldwide are obese (BMI $\geq$ 30 Kg/m^2) or overweight (BMI between 25 and 30 kg/m^2) (1–3). It is projected that by 2025, 40% of the population in the US, 30% in England and 20% in Brazil will be affected by obesity (1–3). The WHO has declared that obesity is a key factor in the development of type 2 diabetes (1). Along these lines, there are a plethora of studies that have investigated the roles of and relationships among nutrition, physical activity and genetic susceptibility as determinants of the current prevalence of obesity. Additionally, it is well established that there is a direct relationship between obesity, the onset of insulin resistance (IR) and diabetes.

Insulin resistance is manifested by reducing the ability of insulin to activate the insulin signaling pathway (4, 5). At the molecular level, IR is characterized by diverse alterations in various intracellular signaling pathways. In fact, it has been shown that insulin signaling is impaired in the liver, muscle, adipose tissue, hypothalamus, and others tissues, in IR states (6, 7). While there are several biological events that can lead to the impairment of the insulin signaling pathway, chronic

inflammation is perhaps the best described. Inflammation promotes serine phosphorylation of insulin receptor substrate (IRS), through the action of serine kinases such as c-Jun N-terminal kinase (JNK) and inhibitor of kappa B kinase (IKKβ) (6, 8, 9).

Diabetes is another major global health problem, from which the social and economic consequences are devastating. For example, this disease is directly or indirectly responsible for approximately 4 million deaths per year, which corresponds to 9% of the total world mortality (10). In 2013, the International Diabetes Federation (IDF) reported that diabetes affected 382 million people worldwide, and this number is expected to grow to 592 million, by 2035 (10, 11).

Obesity, IR and type 2 diabetes are closely related to sub-clinical and chronic inflammation, which is characterized by abnormal cytokine production, including an increase in acute phase molecules and other mediators, as well as inflammatory signaling pathway activation (6, 12, 13).

Within this inflammatory context, the liver may have an important contribution, because during overeating, which is common in obesity, it expresses and secretes several inflammatory proteins (14, 15). The liver may also play an important role in IR (16). Likewise, in obesity-induced IR, the suppression of hepatic glucose production becomes impaired, contributing to the development of hyperglycemia. Furthermore, the liver participates in metabolic regulation, through the expression and secretion of organokines, which are also referred to as hepatokines. Interestingly, these proteins influence metabolic processes through paracrine and endocrine signaling, rather than by autocrine signaling (17). Hepatokines include several growth factors such as fibroblast growth factor 21 (18), insulin-like growth factors, angiopoietin-related growth factor, and HGF. The characteristics and roles of the latter will be the focus of this review.

HGF synthesis and secretion are up-regulated in IR states, and is thought to be an important component of the pathophysiology of IR (19–30). Interestingly, the receptor of HGF, c-Met, is structurally related to the insulin receptor (INSR) (31). Furthermore, HGF signaling participates in the modulation of the metabolic flux of glucose in different insulin sensitive cell types such as β-cells, enterocytes, adipocytes, hepatocytes and myocytes (25, 31–36). HGF signaling also plays a key role in β-cell homeostasis (33, 37–47). Lastly, HGF has been shown to participate in the modulation of the inflammatory response (48–51). This review discusses the significance of each of these five HGF features in the pathophysiology of IR and diabetes and presents evidence for HGF in the etiology of cancer.

STRUCTURE AND MOLECULAR BIOLOGY OF HGF AND ITS RECEPTOR (C-MET)

Originally, HGF was identified as a liver-regenerative circulating factor, since levels of this protein increased following liver injury or hepatectomy (47, 52, 53). Currently, HGF is recognized as a molecule with diverse activities, and has been demonstrated to have mitogenic, morphogenic, and motogenic effects in different tissues (**Figure 1**) (54).

The HGF locus is harbored on chromosome 7q21.1, covering approximately 70 kb and consists of 18 exons and 17 introns (55). The translation of a single 6 kb transcript results in a pre-pro-polypeptide of 728 amino acids (56). In the liver, HGF is synthesized and secreted as an inactive single chain precursor (proHGF, 92 kDa). The active form of HGF is produced by proteolytic cleavage of proHGF, between Arg^{494} and Val^{495}. Active HGF consists of a heavy chain (62 kDa) and a light chain (32–36 kDa), which are covalently linked by a disulfide bridge (57, 58). *In vitro* studies have shown that blood coagulation factor XIIa, urokinase, plasminogen activator and HGF activator can all activate HGF. Among these proteases, HGF activator (34 kDa) is the most efficient at converting proHGF into mature HGF (59). Both the liver and, to a lesser extent, gastrointestinal tissue synthesize HGF activator (60, 61). Following translation, this protease circulates as an inactive precursor, activator proHGF (96 kDa), and is activated upon thrombin cleavage (62). These studies highlight the important role HGF activator plays in regulating HGF activity. Moreover, a HGF activator inhibitor (HAI-1) was recently isolated, and acts as a physiological HGF activator inhibitor at the cell surface (53, 63). However, its role needs to be better elucidated.

Biological activities (i.e., proliferation/survival/motogenesis) mediated by HGF binding to the c-Met receptor require the active form of HGF. This receptor is encoded for by the c-met protooncogene ($p190^{MET}$) (33). Additionally, the c-Met receptor is a dimer composed of an alpha-chain (50 kDa), and a beta-chain (145 kDa), which are linked together by a disulfide bond. The alpha chain is highly glycosylated and exposed on the cell surface, while the beta-chain is a transmembrane protein containing the kinase domain, the tyrosine autophosphorylation site and the

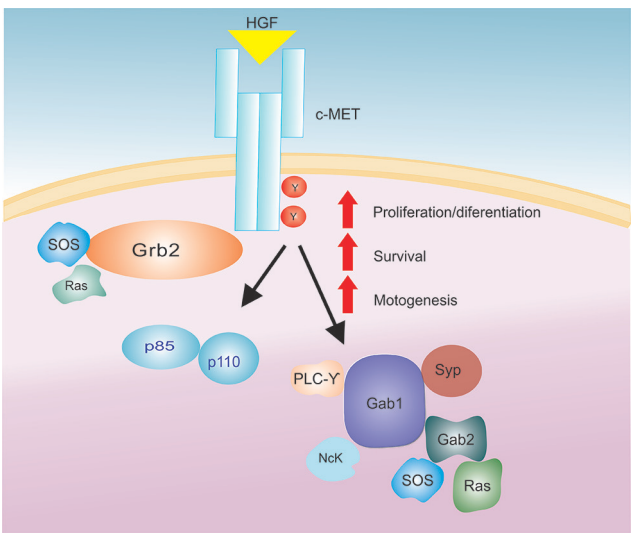

FIGURE 1 | The HGF/c-Met signaling axis. After HGF binding to the c-Met receptor there is an activation of a signaling cascade that increases several biological actions (proliferation/differentiation, survival and motogenesis).

multifunctional binding site (53, 64). The c-Met receptor is more closely related to the INSR, in terms of the overall structure of the protein and the sequence of the kinase domain, than any other member of the receptor tyrosine kinase (RTK) subclasses (65).

Upon HGF binding, c-Met activation and subsequent signal transduction rely on the presence of adenosine triphosphate (ATP) and Mg^{2+} ions, which promote receptor dimerization and trans-phosphorylation of the catalytic domain. Additionally, HGF binding to c-Met and subsequent phosphorylation of intracellular transducers such as: PI3K (p85 subunit), Gap, Ras, PLC-gamma, Src related tyrosine kinase, Grb-2, Gab-1, IRS-1, IRS-2 (**Figure 1**) (33, 53, 56, 66) has been shown to promote HGF functions in the cell.

For example, Fafalios et al. (31) demonstrated that c-Met activation in the liver induces the formation of a c-Met-INSR complex, which stimulates the recruitment of insulin receptor substrates (IRS-1 and IRS-2) and thereby amplifies insulin signaling (**Figure 2**). Furthermore, this study showed that activation of this complex improves hepatic glucose metabolism, by increasing glucose uptake and decreasing hepatic glucose production (31). These findings reinforce the notion that HGF-induced signaling, at least in the liver, imparts protection against IR. These effects need to be further elucidated in both the liver and other metabolic tissues in an IR state.

THE ROLE OF HGF IN THE MODULATION OF GLUCOSE FLUX IN DIFFERENT INSULIN SENSITIVE CELL TYPES

Several studies have demonstrated that HGF has regulatory effects on glucose transport and metabolism. One such study showed that HGF overexpression, in murine β-cells, increases the transcription of GLUT-2 and glucokinase, leading to increased glucose uptake and metabolism in these cells (32). On the other hand, the ablation of HGF/c-Met signaling, in adult murine β-cells, led to a decrease in GLUT-2 expression, followed by glucose intolerance and an impairment in glucose-stimulated insulin secretion (33). Additionally, HGF was shown to interfere with the function of the Na^{+}/glucose cotransporter and GLUT-5, in rat intestinal cells (34). Furthermore, HGF promotes the translocation of GLUT4 to the cell membrane and increases glucose uptake through the activation of PI3K, in 3T3-L1 adipocytes (25). With regards to regulating glucose transport and metabolism in the liver, it has been demonstrated that HGF is able to stimulate hepatic glucose uptake and suppress hepatic glucose output (31). In fact, an *in vitro* study demonstrated that HGF substantially increases glucose transport and metabolism in myotubes, through a mechanism mediated by the PI3K/Akt pathway, resulting in increased GLUT-1 and GLUT-4 plasma membrane expression (35). More recently, the same group presented further evidence of HGF participation in skeletal muscle glucose homeostasis (36). In this study, a transgenic model, capable of increasing skeletal muscle HGF levels by three-fold, without altering plasma HGF levels was employed. When these transgenic mice were fed a high-fat diet there was an observed improvement in glucose tolerance, and an increase in Akt phosphorylation levels in the gastrocnemius muscles (36). Thus, reinforcing the notion that HGF plays an important role in obesity-mediated IR in muscle.

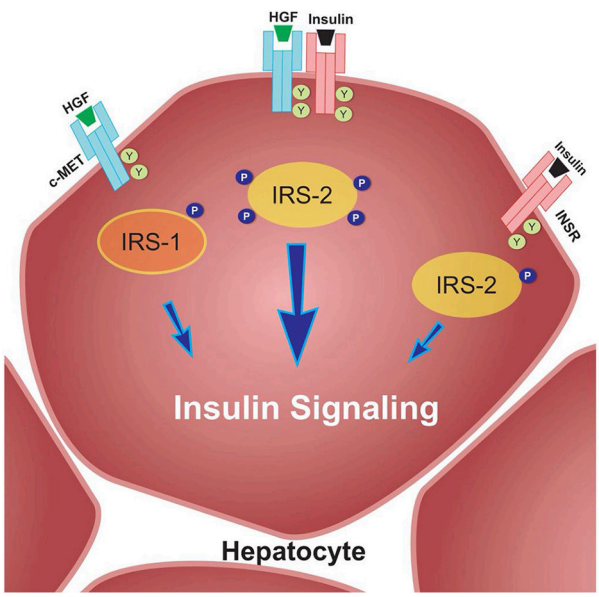

FIGURE 2 | c-Met/INSR crosstalk in hepatocytes. The c-Met/INSR complex increases the recruitment of IRS-1 and 2 and thereby amplifies the insulin signaling pathway in hepatocytes. Adapted from Fafalios et al. (31).

REGULATION OF PANCREATIC ISLET β-CELL HOMEOSTASIS BY HGF

There is a great interest in identifying endogenous regulatory factors that control both β-cell mass expansion and insulin secretion. In β-cell cultures, Otonkoski et al. (40) investigated the mitogenic and morphogenic activity of various growth factors, and were the first to observe the insulinotropic activity of HGF. Later, Hayek et al. (42) showed that adding HGF to culture medium induced β-cell proliferation. Furthermore, it was observed that mRNAs, encoding for HGF and c-Met receptor, are highly expressed in pancreatic β-cells during early development, and remain at low levels during puberty and throughout adult life (41). These studies have raised interest in identifying HGF as a potential element in the development of hyperplasia in β-cells, and subsequent hyperinsulinemia.

In 2000, Garcia-Ocana et al. developed transgenic mice that overexpressed HGF, with the intention of studying the role of this protein on the pancreatic islets, *in vivo*. The authors concluded that *in vivo* HGF overexpression increased β-cell proliferation, the number of islets, β-cell mass, as well as insulin production (47). Together these effects resulted in animals that displayed moderate hypoglycemia and hyperinsulinemia (**Figure 3A** summarizes main results of this study). In 2005, two studies used a c-Met receptor knockout mouse model to investigate the physiological consequence of HGF inhibition in pancreatic β-cells, and the results were discordant in some

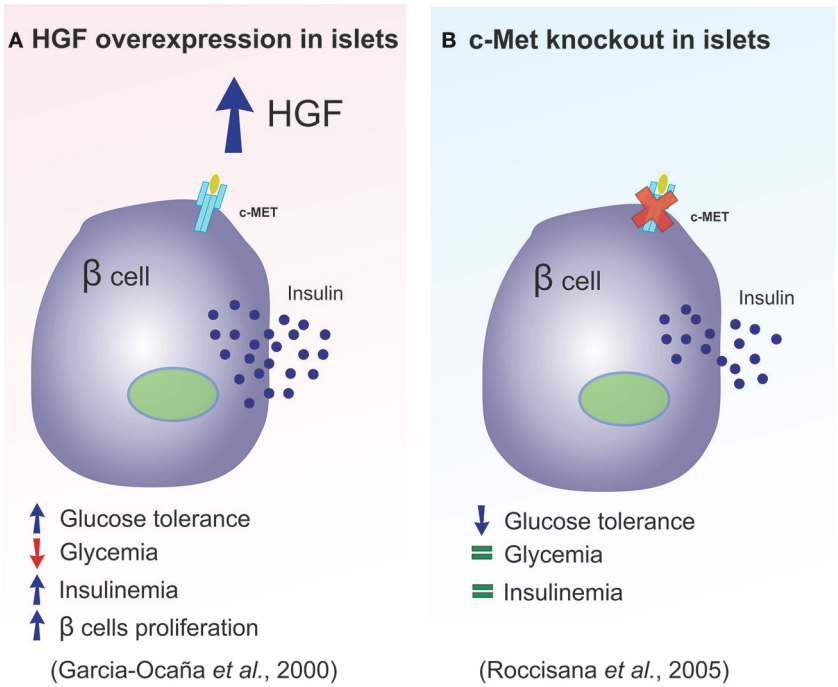

FIGURE 3 | HGF plays a key role in pancreatic β-cell homeostasis. **(A,B)** Diagram illustrating the main differences observed between the overexpression of HGF and the absence of the c-Met receptor in pancreatic β-cells.

aspects (33, 43). For example, Roccisana et al. (33) showed that c-Met receptor knockout animals presented a reduction in insulin secretion and a decrease in glucose tolerance, which was accompanied by a reduction in GLUT-2 expression in the β-cells. However, there were no observed changes in total β-cell mass, proliferation or islet morphology (33). The main findings of this research is illustrated in **Figure 3B**. On the other hand, Dai et al. (43) demonstrated that the size of the islets in this animal model was decreased, which was accompanied by reduced insulin content in the pancreas, lower insulin levels in the serum and mild hyperglycemia.

Furthermore, another study in mice demonstrated that the absence of c-Met, in the pancreas, led to a substantial increase in pancreatic β-cell death and a reduction in cell mass, which resulted in the manifestation of hypoinsulinemia. Consequently, these mice had a tendency to develop hyperglycemia in response to diabetogenic stimuli (46). Thus, these data indicate that HGF/c-Met-induced β-cell survival could be employed as a potential therapy for diabetes.

Another study from the Garcia-Ocaña group, demonstrated that HGF signaling is required for β-cell regeneration, following β-cell ablation (45). In this study, mice that underwent partial pancreatectomy (Ppx) and received a daily dose of HGF showed an increase in the rate of β-cell proliferation, when compared to animals that did not receive exogenous HGF. Conversely, c-Met knockout mice subjected to Ppx, had reduced β-cell mass, glucose intolerance, and decreased insulin secretion, when compared to wild type post-Ppx mice (45). More recently, a different mouse model was used to study the HGF-mediated regenerative effect (44). IRS2 KO mice are known to have an increased incidence of β-cell failure, increased apoptosis and reduced proliferation, which contributes to the development of diabetes in these mice (44, 67, 68). In order to investigate the effect of HGF on the observed β-cell failure, the IRS2 KO mice were cross-bred with transgenic mice overexpressing HGF in the β-cells. HGF overexpression was able to compensate for the negative effects related to the absence of IRS2, by normalizing β-cell mass and improving glucose homeostasis in the context of IR (44). Taken together, these findings indicate that HGF could be employed as a regenerative factor in the treatment of diabetes.

As mentioned above, the expression of c-Met in the β-cells results in enhanced HGF sensitivity, which can influence cell growth, survival and insulin secretion. Furthermore, HGF has both paracrine and endocrine properties, which are constantly regulating pathways involved in β-cell homeostasis. Following this line of reasoning, it was shown in hyperglycemia/diabetes, induced by stressful situations, that HGF has a protective role in physiological status of β-cells (37–39). Hence, HGF appears to be involved in the compensatory response of β-cells in two common conditions characterized by IR and associated with the pathophysiology of diabetes: (1) obesity, (2) pregnancy (37, 39). The latter has been shown to be directly associated with the development of gestational diabetes mellitus (GDM) (38).

In obesity, the most common insulin resistant condition, there is a compensatory pancreatic β-cell response against this hormonal resistance, which increases insulin secretion and maintains homeostatic glucose metabolism for a certain period of time. This compensatory β-cell response induces

hyperinsulinemia, and is the first step in the development of diabetes (39). Since HGF stimulates insulin secretion and increases β-cell mass, both *in vitro* and *in vivo*, and due to the fact that increased circulating levels of this hormone are associated with obesity, HGF might link insulin resistance and β-cell hyperplasia. In fact, our group demonstrated through a dose-dependent, longitudinal approach that: (a) circulating HGF levels strongly correlate with β-cell mass increase in the IR state; (b) the β-cell mass increases in a HGF dose-dependent manner; (c) pharmacological blockage of the HGF signaling pathway abolishes the β-cell mass compensatory response; and (d) circulating HGF levels increase before the onset of the IR-induced β-cell compensatory response, thus suggesting a causal role in this specific event. Moreover, c-Met inhibition negatively affects the already impaired insulin signaling in the liver of diet-induced obese rats (37, 39). These HGF-mediated effects on β-cell proliferation and expansion indicate that this hormone has a crucial role in increased metabolic demand, which is commonly observed in obesity-induced IR.

Another adaptive β-cell mechanism, in which HGF participates, occurs during pregnancy. In this situation, the β-cell adapts to an increased demand for insulin and undergoes structural and functional changes, such as β-cell expansion and enhanced insulin secretion. However, any perturbations or disturbances in this adaptive process can lead to the development of GDM (69). Interestingly, while searching for potential therapeutic targets, for the treatment of GDM, it was found that HGF expression is upregulated in rat islet endothelium at gestational day 15 (70), which also happens to be when maximal β-cell proliferation is detected (38). Based on this evidence and the other roles of HGF in β-cell homeostasis, it was hypothesized that maternal β-cell adaptation is mediated by HGF. In fact, it was recently demonstrated that in the absence of c-Met, during pregnancy, there was a substantial impairment in β-cell proliferation and survival, resulting in β-cell mass reduction. In pregnant mice, this sequence of events culminates with hypoinsulinemia, consequent hyperglycemia and glucose intolerance, all of which are features of GDM (38). These observations implicate the HGF/c-Met signaling pathway in the pathogenesis of GDM, since ablation and inhibition of HGF or c-Met results in the disease. In this regard, targeting the HGF/cMet signaling pathway might represent a potential strategy for the treatment of GDM.

ROLE OF ADIPOSE TISSUE DERIVED HGF

Obesity is associated with numerous metabolic changes, such as hyperinsulinemia and IR (71). The IR that occurs in adipose tissue may contribute to systemic IR and a variety of hepatic alterations (72, 73). Furthermore, secretion of adipokines, hormones, cytokines, chemokines, growth factors, acute phase proteins and HGF from the white adipose tissue (WAT) further complicates this condition (74). It is important to mention that even though HGF is considered a hepatokine, the synthesis and secretion of HGF has been demonstrated in murine 3T3-L1 adipocytes (20) and human adipose tissue (21, 22). Thus, it is quite plausible that the HGF synthesized in human adipose tissue plays an important role in obesity (23). Furthermore, due the importance of adipose tissue in IR, adipose-derived HGF expression might also have an influence on the obesity associated IR etiology. In fact, a recent study examined HGF secretion in different types of adipose tissue and observed that the HGF secretion pattern of the perivascular adipose tissue differs from the subcutaneous and visceral adipocytes (26). Surprisingly, this research also showed that, in both *in vitro* and *in vivo* models, perivascular fat cells have a much higher capacity for secreting adipokines, especially HGF, than other fat cell types. Additionally, it was shown that subjects with greater perivascular fat mass secreted more HGF (26), bringing to light the pathophysiological relevance of this hormone.

In humans, it has been demonstrated that levels of circulating HGF are elevated in obesity (27), metabolic syndrome (23), and diabetes mellitus (75). In obese individuals, circulating HGF levels were increased by more than 3-fold, when compared to lean individuals (27). HGF levels have also been correlated with anthropometric measures of obesity such as waist circumference, body mass index and body fat mass (24, 30). Furthermore, an association between weight loss induced by bariatric surgery and reduced HGF levels was previously observed, in obese patients (22, 28).

In patients with IR, a significant association between HGF and plasma insulin was observed suggesting a pathological link between them (23). A more thorough, 10-year prospective study proposed that elevated circulating levels of HGF were significantly associated with the development of IR (19). Furthermore, another prospective study, with over 12 years of follow-up, which included multi-ethnical individuals, also demonstrated that higher levels of serum HGF were positively associated with IR (76). Based on these data and the similarities between HGF and insulin, it is tempting to speculate that "HGF resistance" exists, which may contribute to glucose metabolism dysregulation. Finally, another study demonstrated that there is a significant correlation between circulating HGF levels and the Visceral Adiposity Index (VAI), which is a gender-specific mathematical index based on simple anthropometric and metabolic parameters as a presumed surrogate marker of adipose tissue function and distribution (29).

In summary, adipose tissue may be an important source of HGF, which may comprise an important component in adipose tissue dynamics. Thus, further emphasizing the role of HGF in the pathophysiological processes of obesity/IR/diabetes.

THE INVOLVEMENT OF HGF IN THE MODULATION OF THE INFLAMMATORY RESPONSE

Over the past 10 years, evidence has indicated that there is a correlation between IR and inflammation (6, 8, 77–79). In fact, subclinical chronic inflammation has been shown to be a major mechanism for the development of IR in peripheral tissues. This mechanism results in a chronic upregulation of pro-inflammatory cytokines (i.e., TNF-α and IL-6), which are known

to exert deleterious effects on the insulin signaling pathway in adipocytes, hepatocytes, and myocytes (6, 8, 80). Furthermore, the actions of macrophages have been studied extensively, since they have been shown to accumulate in the liver and WAT, and promote IR and liver disease (81–83).

Studies have shown that HGF is involved in the modulation of the inflammatory response. Notably, Coudriet et al. demonstrated that HGF could decrease the acute phase of the inflammatory response by attenuating the production of IL-6, and increasing IL-10 levels, in lipopolysaccharide (LPS) stimulated bone marrow derived macrophages (48). Similarly, Flaquer et al., using *db/db* mice to study diabetic nephropathy, demonstrated that when the HGF gene was delivered to these animals, there was a reduction in the circulating levels of IL-6 and MCP-1, an increase in the number of M2 macrophages and an improvement in glomeruli inflammation (49).

Two studies from the Morishita group (50, 51), demonstrated novel HGF-induced anti-inflammatory mechanisms. The first study utilized a transgenic mouse-model that overexpressed HGF (HGF-Tg), which inhibited LPS-induced oxidative stress and vascular tissue inflammation. These HGF-mediated protective effects against the LPS-induced reactive oxygen species (ROS) production and inflammation were achieved via epidermal growth factor receptor (EGFR) degradation and angiotensin II (Ang II) signaling inhibition (50). The second study was divided into two stages: an *in vitro* study and an *in vivo* study. The *in vitro* stage of the study demonstrated that HGF disrupts NF-κB signaling in RAW264 macrophages, as well as in co-culture with 3T3-L1 adipocytes, leading to an overall reduction in the expression of MCP-1, TNF-α, and IL-6 (51). The second stage employed ApoE KO mice, which exhibit a chronic inflammation phenotype, including adipose tissue macrophage infiltration, adipocyte hypertrophy and fatty liver. After crossing the ApoE KO mice with HGF-Tg, the chronic inflammation, presented by the ApoE KO mice, was significantly reduced. The authors also detected an increase in serum adiponectin levels in the ApoE KO/HGF-Tg mice (51). Taken together, these data suggest that HGF suppresses the production of pro-inflammatory cytokines and, conversely, increases the secretion of adiponectin, thus breaking the macrophage-adipocyte inflammatory cycle (**Figure 4**). Furthermore, it has been recently shown that administering an antibody against HGF to wild type mice fed a high-fat diet, resulted in a more pronounced IR (84). A similar result was previously observed with pharmacological blockage of HGF signaling (37). Together, these results reinforce the already presented protective role of HGF on glucose metabolism in obesity. The observed results from HGF-Tg mice fed a high fat diet (HFD) also highlight the different anti-inflammatory effects of HGF in adipose tissue including the reduction in the levels of chemoattractants (MCP-1 and CXCL2), inflammatory cytokines (TNF-α and iNOS), as well as, pan macrophage marker (F4/80) (84). Thus, HGF represents a potential therapeutic target for inhibiting the inflammatory response in adipose tissue and improving IR.

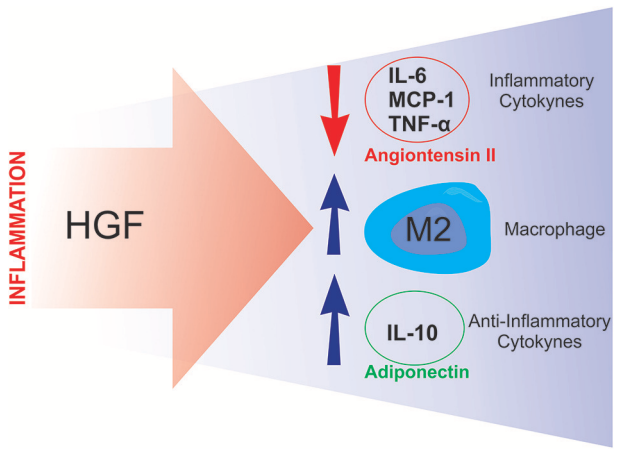

FIGURE 4 | Putative compensatory role of HGF. During the inflammatory process, HGF seems to attenuate inflammation by inducing anti-inflammatory responses such as: downregulating angiotensin II activity and inflammatory cytokine synthesis, and stimulating M2 macrophage polarization and anti-inflammatory cytokine production.

HGF SIGNALING IN CANCER

Activation of the HGF/c-Met signaling pathway is a hallmark of cancer cells and both HGF and c-Met have emerged as therapeutic targets. HGF, produced by some cancer cells, stimulates c-Met, through activation of the autocrine signaling system. Alternatively, HGF present in the tumor microenvironment activates c-Met receptors displayed on the surface of cancer cells, through the activation of the paracrine signaling system. The origin of HGF present in the tumor microenvironment is unknown and HGF could be synthesized by a variety of tissues throughout the body, such as the liver itself or by the adipose tissue. Recently, adipose tissue has been shown to be related to the increased prevalence and aggressiveness of some types of cancers (85–87). HGF is known to promote proliferation, migration, invasion and survival of cancer cells, and to confer resistance to therapy. Thus HGF is a possible link between obesity and cancer.

While researchers are currently investigating the relationship between HGF and cancer, some properties of HGF in the tumor microenvironment should be considered. Tumor stromal cells (macrophages, inflammatory cells, endothelial cells, and cancer-associated fibroblasts) secrete a variety of growth factors, chemokines and cytokines promoting a pro-inflammatory microenvironment for wound healing (88, 89). In fact, tumors could be considered wounds that do not heal (90). HGF is an important component of the fibroblast secretome (91), and has been shown to stimulate cancer cell invasiveness (88, 89), and promote the epithelial-mesenchymal transition (EMT), cell scattering and migration (52, 92–94).

As evidenced by the embryonic lethality in mice deficient in HGF or c-Met, it is thought that HGF/c-Met signaling stimulates the EMT, and plays a major role in embryogenesis, organogenesis,

tissue repair and wound healing. As a growth factor, HGF promotes the growth and survival of cancer cells, increases tumor aggressiveness, stimulates metastasis and is associated with resistance to therapy (95, 96).

Recently, established colon cancer cell lines and primary colon tumors have been shown to produce large amounts of HGF (97). High levels of HGF were also observed in the serum and tumor tissue of stage II and III colon cancer patients, and especially in patients with lymph node and liver metastasis (98, 99). Moreover, increased HGF levels have been correlated with lymph node metastasis and relapse in individuals with breast cancer (100, 101), multiple myeloma (102), and myeloid leukemia (103).

Sensitivity to anticancer treatment is largely influenced by stromal cells, and HGF derived from these cells is a notable factor that provides resistance to target drugs (104). In general, cancer cells do not produce HGF, themselves. Rather, cancer-associated fibroblasts are primarily responsible for HGF production, and as a result activate c-Met paracrinally. Thus, HGF might be an important stromal cell component of the tumor microenvironment (105–108).

Unfortunately, conventional cancer treatment (radiotherapy or chemotherapy), is not able to distinguish a malignant cell from a normal one. Targeted therapies have the ability to circumvent this apparent lack of specificity. In fact, drugs that can block specific cancer cell dependent pathways such as: EGFR, BRAF, HER2, and HGF/c-Met signaling are being developed, and are predicted to have fewer side effects. Previous studies have shown that cells that undergo EMT are more resistant to cell death (109, 110), thus it is possible that the HGF-induced EMT is responsible for the increased resistance to therapy. In fact, in lung cancer cells with c-Met amplification, HGF has been shown to be responsible for the observed resistance to anti-MET treatment (111, 112). Thus, HGF production by the stromal cells inhibits the response to MET kinase inhibitors, as well as other signaling pathways (111). Additionally, EMT is also responsible for the acquisition of a stem cell phenotype, which is metabolically altered and markedly resistant to therapies. Moreover, HGF induces Wnt signaling in colon cancer cells, resulting in a cancer stem cell phenotype *in vitro* and *in vivo* (113). Lastly, activation of HGF/c-Met signaling also contributes to the cancer stem cell phenotype in other types of cancer such as: gliomas (114, 115), colon cancer (107), head and neck cancer (116), prostate cancer (117) and pancreatic cancer (118).

The data related to the HGF/c-Met signaling pathway and cancer suggests that the pathway inhibition may stunt the growth and progression of cancers. Thus, inhibition of HGF synthesis or activity in stromal cells may be an effective approach for future targeted cancer therapy.

CONCLUSION AND PROSPECTS

It has been nearly three decades since human HGF cDNA was successfully cloned (52). Since that time to the present day, the biological functions of the HGF/c-Met axis have been extensively investigated. The results presented from the concerted efforts of numerous laboratories have provided compelling evidence for the essential physiologically relevant functions of HGF, as well as its therapeutic potential.

The liver-originated hormone, HGF, considered a hepatokine, can potentially interfere with energy metabolism (37, 39). Similar to what was observed with adipokines and myokines, HGF has uncertain mixed functions, which can improve the metabolic profile of type 2 diabetes or induce IR (14, 119). Future investigations into the physiological role of liver-derived factors will likely yield potential biomarkers and/or lead to the discovery of novel therapies against type 2 diabetes and other metabolic complications.

Although the great amount of evidence has suggested that increased levels of HGF are associated with the manifestation of IR, this review has highlighted some of the beneficial effects stemming from HGF activity observed in obesity. Additionally, due to the fact that HGF markedly increases glucose metabolism and transport in myocytes and adipocytes, future research needs to focus on elucidating the details of how HGF contributes to the protective mechanism against the development of IR, in the liver, and possibly other tissues, such as skeletal muscle and WAT. Further support, for HGF being utilized as a therapeutic target in the treatment of IR, comes from its role in β-cell hyperplasia, and subsequent hyperinsulinemia.

Beyond emphasizing the proposed utility of HGF as potential therapeutic target in IR, this review also discussed how maternal β-cell adaptation, during pregnancy, depends on the HGF/c-Met signaling pathway, and that impairment of this pathway can lead to the onset of GDM. Regarding obesity-induced IR, which is strongly associated with an inflammatory state, HGF also emerges as a positive factor. This is because HGF has the ability to blunt inflammation in adipose tissue, by increasing M2 macrophage polarization, and consequently augmenting the expression of IL-10, both of which are positively associated with insulin sensitivity (see **Figure 4**). Additionally, the HGF/c-Met pathway plays a key role in the onset and progression of human cancers, and pathway activation is associated with a poor prognosis. While HGF may serve as the link between obesity and cancer, it should be noted that given the association of HGF levels with tumor progression, metastasis and less favorable response to cancer treatment, employing HGF for the modulation of IR or treating diabetes may be significantly limited by its cancer-promoting properties.

Future research in the area should focus on understanding the regulatory mechanisms, and developing inhibitors and activators for the modulation of endogenous HGF levels. In fact, innovative mechanisms for controlling HGF expression and/or activity could generate unique therapies for the treatment of IR and diabetes.

AUTHOR CONTRIBUTIONS

All authors listed have made a substantial, direct and intellectual contribution to the work, and approved it for publication.

FUNDING

This work was supported by grants from Fundação de Amparo à Pesquisa do Estado de São Paulo (FAPESP), Coordenação de Aperfeiçoamento de Pessoal de Nível Superior/PNPD (CAPES/PNPD), and Conselho Nacional de Pesquisa (CNPq) (Instituto Nacional de Ciência e Tecnologia-Obesidade e Diabetes).

REFERENCES

1. WHO. *Obesity and Overweight* (2012), p. 311. Available online at: http://www.who.int/mediacentre/factsheets/fs311/en/
2. Sieck G. Physiology in perspective: the burden of obesity. *Physiology (Bethesda)* (2014) 29:86–7. doi: 10.1152/physiol.00004.2014
3. Cox AJ, West NP, Cripps AW. Obesity, inflammation, and the gut microbiota. *Lancet Diabet. Endocrinol.* (2015) 3:207–15. doi: 10.1016/S2213-8587(14)70134-2
4. Saad MJ, Araki E, Miralpeix M, Rothenberg PL, White MF, Kahn CR. Regulation of insulin receptor substrate-1 in liver and muscle of animal models of insulin resistance. *J Clin Invest*. (1992) 90:1839–49. doi: 10.1172/JCI116060
5. Pessin JE, Saltiel AR. Signaling pathways in insulin action: molecular targets of insulin resistance. *J Clin Invest*. (2000) 106:165–9. doi: 10.1172/JCI10582
6. Gregor MF, Hotamisligil GS. Inflammatory mechanisms in obesity. *Ann Rev Immunol*. (2011) 29:415–45. doi: 10.1146/annurev-immunol-031210-101322
7. Boura-Halfon S, Zick Y. Phosphorylation of IRS proteins, insulin action, and insulin resistance. *Am J Physiol Endocrinol Metab*. (2009) 296:E581–91. doi: 10.1152/ajpendo.90437.2008
8. Donath MY, Shoelson SE. Type 2 diabetes as an inflammatory disease. *Nat Rev Immunol*. (2011) 11:98–107. doi: 10.1038/nri2925
9. Solinas G, Karin M. JNK1 and IKKbeta: molecular links between obesity and metabolic dysfunction. *FASEB J*. (2010) 24:2596–611. doi: 10.1096/fj.09-151340
10. Seuring T, Archangelidi O, Suhrcke M. The economic costs of type 2 diabetes: a global systematic review. *Pharm Econ*. (2015) 33:811–31. doi: 10.1007/s40273-015-0268-9
11. Economic costs of diabetes in the U.S. in 2012. *Diabetes Care* (2013) 36:1033–46. doi: 10.2337/dc12-2625
12. Kahn SE, Hull RL, Utzschneider KM. Mechanisms linking obesity to insulin resistance and type 2 diabetes. *Nature* (2006) 444, 840–6. doi: 10.1038/nature05482
13. Shoelson SE, Lee J, Goldfine AB. Inflammation and insulin resistance. *J Clin Invest*. (2006) 116:1793–801. doi: 10.1172/JCI29069
14. Stefan N, Haring HU. The role of hepatokines in metabolism. *Nat Rev Endocrinol*. (2013) 9:144–52. doi: 10.1038/nrendo.2012.258
15. Cohen JC, Horton JD, Hobbs HH. Human fatty liver disease: old questions and new insights. *Science* (2011) 332:1519–23. doi: 10.1126/science.1204265
16. Nordlie RC, Foster JD, Lange AJ. Regulation of glucose production by the liver. *Ann Rev Nutr*. (1999) 19:379–406. doi: 10.1146/annurev.nutr.19.1.379
17. Meex RCR, Watt MJ. Hepatokines: linking nonalcoholic fatty liver disease and insulin resistance. *Nat. Rev. Endocrinol.* (2017) 13:509–20. doi: 10.1038/nrendo.2017.56
18. Li Q, Zhang Y, Ding D, Yang Y, Chen Q, Su D, et al. Association between serum fibroblast growth factor 21 and mortality among patients with coronary artery disease. *J Clin Endocrinol Metab*. (2016) 101:4886–94. doi: 10.1210/jc.2016-2308
19. Tsukagawa E, Adachi H, Hirai Y, Enomoto M, Fukami A, Ogata K, et al. Independent association of elevated serum hepatocyte growth factor levels with development of insulin resistance in a 10-year prospective study. *Clin Endocrinol. (Oxf.)* (2013) 79:43–8. doi: 10.1111/j.1365-2265.2012.04496.x
20. Rahimi N, Saulnier R, Nakamura T, Park M, Elliott B. Role of hepatocyte growth factor in breast cancer: a novel mitogenic factor secreted by adipocytes. *DNA Cell Biol*. (1994) 13:1189–97.
21. Fain JN, Madan AK, Hiler ML, Cheema P, Bahouth SW. Comparison of the release of adipokines by adipose tissue, adipose tissue matrix, and adipocytes from visceral and subcutaneous abdominal adipose tissues of obese humans. *Endocrinology* (2004) 145:2273–82. doi: 10.1210/en.2003-1336
22. Bell LN, Ward JL, Degawa-Yamauchi M, Bovenkerk JE, Jones R, Cacucci BM, et al. Adipose tissue production of hepatocyte growth factor contributes to elevated serum HGF in obesity. *Am J Physiol Endocrinol Metab*. (2006) 291:E843–8. doi: 10.1152/ajpendo.00174.2006
23. Hiratsuka A, Adachi H, Fujiura Y, Yamagishi S, Hirai Y, Enomoto M, et al. Strong association between serum hepatocyte growth factor and metabolic syndrome. *J Clin Endocrinol Metab*. (2005) 90:2927–31. doi: 10.1210/jc.2004-1588
24. Vistoropsky Y, Trofimov S, Malkin I, Kobyliansky E, Livshits G. Genetic and environmental determinants of hepatocyte growth factor levels and their association with obesity and blood pressure. *Ann Hum Biol*. (2008) 35:93–103. doi: 10.1080/03014460701822003
25. Bertola A, Bonnafous S, Cormont M, Anty R, Tanti JF, Tran A, et al. Hepatocyte growth factor induces glucose uptake in 3T3-L1 adipocytes through A Gab1/phosphatidylinositol 3-kinase/Glut4 pathway. *J Biol Chem*. (2007) 282:10325–32. doi: 10.1074/jbc.M611770200
26. Rittig K, Dolderer JH, Balletshofer B, Machann J, Schick F, Meile T, et al. The secretion pattern of perivascular fat cells is different from that of subcutaneous and visceral fat cells. *Diabetologia* (2012) 55:1514–25. doi: 10.1007/s00125-012-2481-9
27. Rehman J, Considine RV, Bovenkerk JE, Li J, Slavens CA, Jones RM, et al. Obesity is associated with increased levels of circulating hepatocyte growth factor. *J Am Coll Cardiol*. (2003) 41:1408–13. doi: 10.1016/S0735-1097(03)00231-6
28. Swierczynski J, Korczynska J, Goyke E, Adrych K, Raczynska S, Sledzinski Z. Serum hepatocyte growth factor concentration in obese women decreases after vertical banded gastroplasty. *Obes Surg*. (2005) 15:803–8. doi: 10.1381/0960892054222678
29. Amato MC, Pizzolanti G, Torregrossa V, Misiano G, Milano S, Giordano C. Visceral adiposity index (VAI) is predictive of an altered adipokine profile in patients with type 2 diabetes. *PLoS ONE* (2014) 9:e91969. doi: 10.1371/journal.pone.0091969
30. de Courten B, de Courten MP, Dougherty S, Forbes JM, Potts JR, Considine RV. Insulin infusion reduces hepatocyte growth factor in lean humans. *Metabolism* (2013) 62:647–50. doi: 10.1016/j.metabol.2012.10.013
31. Fafalios A, Ma J, Tan X, Stoops J, Luo J, Defrances MC, et al. A hepatocyte growth factor receptor (Met)-insulin receptor hybrid governs hepatic glucose metabolism. *Nat Med*. (2011) 17:1577–84. doi: 10.1038/nm.2531
32. Garcia-Ocana A, Vasavada RC, Cebrian A, Reddy V, Takane KK, Lopez-Talavera JC, et al. Transgenic overexpression of hepatocyte growth factor in the β-cell markedly improves islet function and islet transplant outcomes in mice. *Diabetes* (2001) 50:2752–62. doi: 10.2337/diabetes.50.12.2752
33. Roccisana J, Reddy V, Vasavada RC, Gonzalez-Pertusa JA, Magnuson MA, Garcia-Ocana A. Targeted inactivation of hepatocyte growth factor receptor c-met in beta-cells leads to defective insulin secretion and GLUT-2 downregulation without alteration of β-cell mass. *Diabetes* (2005) 54:2090–102. doi: 10.2337/diabetes.54.7.2090
34. Kato Y, Yu D, Schwartz MZ. Hepatocyte growth factor up-regulates SGLT1 and GLUT5 gene expression after massive small bowel resection. *J Pediatr Surg*. (1998) 33:13–5.
35. Perdomo G, Martinez-Brocca MA, Bhatt BA, Brown NF, O'Doherty RM, Garcia-Ocana A. Hepatocyte growth factor is a novel stimulator of glucose uptake and metabolism in skeletal muscle cells. *J Biol Chem*. (2008) 283:13700–6. doi: 10.1074/jbc.M707551200
36. Sanchez-Encinales V, Cozar-Castellano I, Garcia-Ocana A, Perdomo G. Targeted delivery of HGF to the skeletal muscle improves glucose homeostasis in diet-induced obese mice. *J Physiol Biochem*. (2015) 71:795–805. doi: 10.1007/s13105-015-0444-6
37. Araujo TG, Oliveira AG, Carvalho BM, Guadagnini D, Protzek AO, Carvalheira JB, et al. Hepatocyte growth factor plays a key role in insulin resistance-associated compensatory mechanisms. *Endocrinology* (2012) 153:5760–9. doi: 10.1210/en.2012-1496
38. Demirci C, Ernst S, Alvarez-Perez JC, Rosa T, Valle S, Shridhar V, et al. Loss of HGF/c-Met signaling in pancreatic beta-cells leads to incomplete

maternal beta-cell adaptation and gestational diabetes mellitus. *Diabetes* (2012) 61:1143–52. doi: 10.2337/db11-1154
39. Araujo TG, Oliveira AG, Saad MJ. Insulin-resistance-associated compensatory mechanisms of pancreatic Beta cells: a current opinion. *Front Endocrinol.* (2013) 4:146. doi: 10.3389/fendo.2013.00146
40. Otonkoski T, Beattie GM, Rubin JS, Lopez AD, Baird A, Hayek A. Hepatocyte growth factor/scatter factor has insulinotropic activity in human fetal pancreatic cells. *Diabetes* (1994) 43:947–53.
41. Otonkoski T, Cirulli V, Beattie M, Mally MI, Soto G, Rubin JS, et al. A role for hepatocyte growth factor/scatter factor in fetal mesenchyme-induced pancreatic beta-cell growth. *Endocrinology* (1996) 137:3131–9.
42. Hayek A, Beattie GM, Cirulli V, Lopez AD, Ricordi C, Rubin JS. Growth factor/matrix-induced proliferation of human adult beta-cells. *Diabetes* (1995) 44:1458–60.
43. Dai C, Huh CG, Thorgeirsson SS, Liu Y. Beta-cell-specific ablation of the hepatocyte growth factor receptor results in reduced islet size, impaired insulin secretion, and glucose intolerance. *Am J Pathol.* (2005) 167:429–36. doi: 10.1016/S0002-9440(10)62987-2
44. Alvarez-Perez JC, Rosa TC, Casinelli GP, Valle SR, Lakshmipathi J, Rosselot C, et al. Hepatocyte growth factor ameliorates hyperglycemia and corrects beta-cell mass in IRS2-deficient mice. *Mol Endocrinol.* (2014) 28:2038–48. doi: 10.1210/me.2014-1207
45. Alvarez-Perez JC, Ernst S, Demirci C, Casinelli GP, Mellado-Gil JM, Rausell-Palamos F, et al. Hepatocyte growth factor/c-Met signaling is required for beta-cell regeneration. *Diabetes* (2014) 63:216–23. doi: 10.2337/db13-0333
46. Mellado-Gil J, Rosa TC, Demirci C, Gonzalez-Pertusa JA, Velazquez-Garcia S, Ernst S, et al. Disruption of hepatocyte growth factor/c-Met signaling enhances pancreatic beta-cell death and accelerates the onset of diabetes. *Diabetes* (2011) 60:525–36. doi: 10.2337/db09-1305
47. Garcia-Ocana A, Takane KK, Syed MA, Philbrick WM, Vasavada RC, Stewart AF. Hepatocyte growth factor overexpression in the islet of transgenic mice increases beta cell proliferation, enhances islet mass, and induces mild hypoglycemia. *J Biol Chem*. (2000) 275:1226–32. doi: 10.1074/jbc.275.2.1226
48. Coudriet GM, He J, Trucco M, Mars WM, Piganelli JD. Hepatocyte growth factor modulates interleukin-6 production in bone marrow derived macrophages: implications for inflammatory mediated diseases. *PLoS ONE* (2010) 5:e15384. doi: 10.1371/journal.pone.0015384
49. Flaquer M, Franquesa M, Vidal A, Bolanos N, Torras J, Lloberas N, et al. Hepatocyte growth factor gene therapy enhances infiltration of macrophages and may induce kidney repair in db/db mice as a model of diabetes. *Diabetologia* (2012). doi: 10.1007/s00125-012-2535-z
50. Shimizu K, Taniyama Y, Sanada F, Azuma J, Iwabayashi M, Iekushi K, et al. Hepatocyte growth factor inhibits lipopolysaccharide-induced oxidative stress via epithelial growth factor receptor degradation. *Arterioscler Thromb Vasc Biol.* (2012) 32:2687–93. doi: 10.1161/ATVBAHA.112.300041
51. Kusunoki H, Taniyama Y, Otsu R, Rakugi H, Morishita R. Anti-inflammatory effects of hepatocyte growth factor on the vicious cycle of macrophages and adipocytes. *Hypertens Res*. (2014) 37:500–6. doi: 10.1038/hr.2014.41
52. Nakamura T, Nishizawa T, Hagiya M, Seki T, Shimonishi M, Sugimura A, et al. Molecular cloning and expression of human hepatocyte growth factor. *Nature* (1989) 342:440–3. doi: 10.1038/342440a0
53. Nakamura T, Sakai K, Matsumoto K. Hepatocyte growth factor twenty years on: Much more than a growth factor. *J Gastroenterol Hepatol*. (2011) 26(Suppl. 1):188–202. doi: 10.1111/j.1440-1746.2010.06549.x
54. Fiaschi-Taesch NM, Berman DM, Sicari BM, Takane KK, Garcia-Ocana A, Ricordi C, et al. Hepatocyte growth factor (HGF) enhances engraftment and function of non-human primate islets. *Diabetes* (2008) 57: 2745–54. doi: 10.2337/db07-1085
55. Seki T, Hagiya M, Shimonishi M, Nakamura T, Shimizu S. Organization of the human hepatocyte growth factor-encoding gene. *Gene* (1991) 102:213–9.
56. Stella MC, Comoglio PM. HGF: a multifunctional growth factor controlling cell scattering. *Int J Biochem Cell Biol.* (1999) 31:1357–62.
57. Naka D, Ishii T, Yoshiyama Y, Miyazawa K, Hara H, Hishida T, et al. Activation of hepatocyte growth factor by proteolytic conversion of a single chain form to a heterodimer. *J Biol Chem*. (1992) 267:20114–9.
58. Miyazawa K, Shimomura T, Naka D, Kitamura N. Proteolytic activation of hepatocyte growth factor in response to tissue injury. *J Biol Chem*. (1994) 269:8966–70.
59. Shimomura T, Miyazawa K, Komiyama Y, Hiraoka H, Naka D, Morimoto Y, et al. Activation of hepatocyte growth factor by two homologous proteases, blood-coagulation factor XIIa and hepatocyte growth factor activator. *Eur J Biochem*. (1995) 229:257–61.
60. Itoh H, Hamasuna R, Kataoka H, Yamauchi M, Miyazawa K, Kitamura N, et al. Mouse hepatocyte growth factor activator gene: its expression not only in the liver but also in the gastrointestinal tract. *Biochim Biophys Acta* (2000) 1491:295–302. doi: 10.1016/S0167-4781(00)00029-4
61. Yanagida H, Kaibori M, Hijikawa T, Kwon AH, Kamiyama Y, Okumura T. Administration of rhHGF-activator via portal vein stimulates the regeneration of cirrhotic liver after partial hepatectomy in rats. *J Surg Res*. (2006) 130:38–44. doi: 10.1016/j.jss.2005.08.002
62. Shimomura T, Kondo J, Ochiai M, Naka D, Miyazawa K, Morimoto Y, et al. Activation of the zymogen of hepatocyte growth factor activator by thrombin. *J Biol Chem*. (1993) 268:22927–32.
63. Hayashi T, Nishioka J, Nakagawa N, Kamada H, Gabazza EC, Kobayashi T, et al. Protein C inhibitor directly and potently inhibits activated hepatocyte growth factor activator. *J Thromb Haemost.* (2007) 5:1477–85. doi: 10.1111/j.1538-7836.2007.02594.x
64. Hartmann G, Naldini L, Weidner KM, Sachs M, Vigna E, Comoglio PM, et al. A functional domain in the heavy chain of scatter factor/hepatocyte growth factor binds the c-Met receptor and induces cell dissociation but not mitogenesis. *Proc Natl Acad Sci USA* (1992) 89:11574–8.
65. De Meyts P. Insulin and its receptor: structure, function and evolution. *Bioessays* (2004) 26:1351–62. doi: 10.1002/bies.20151
66. Rosario M, Birchmeier W. How to make tubes: signaling by the Met receptor tyrosine kinase. *Trends Cell Biol*. (2003) 13:328–35. doi: 10.1016/S0962-8924(03)00104-1
67. Withers DJ, Gutierrez JS, Towery H, Burks DJ, Ren JM, Previs S, et al. Disruption of IRS-2 causes type 2 diabetes in mice. *Nature* (1998) 391:900–4.
68. Kushner JA, Ye J, Schubert M, Burks DJ, Dow MA, Flint CL, et al. Pdx1 restores beta cell function in Irs2 knockout mice. *J Clin Invest*. (2002) 109:1193–201. doi: 10.1172/JCI14439
69. Ernst S, Demirci C, Valle S, Velazquez-Garcia S, Garcia-Ocana A. Mechanisms in the adaptation of maternal beta-cells during pregnancy. *Diabetes Manag. (Lond.).* (2011) 1:239–48. doi: 10.2217/dmt.10.24
70. Johansson M, Mattsson G, Andersson A, Jansson L, Carlsson PO. Islet endothelial cells and pancreatic beta-cell proliferation: studies *in vitro* and during pregnancy in adult rats. *Endocrinology* (2006) 147:2315–24. doi: 10.1210/en.2005-0997
71. Selig PM. Metabolic syndrome in the acute care setting. *AACN Clin Issues* (2006) 17:79–85.
72. Shiota G, Umeki K, Okano J, Kawasaki H. Hepatocyte growth factor and acute phase proteins in patients with chronic liver diseases. *J Med*. (1995) 26:295–308.
73. Marchesini G, Bugianesi E, Forlani G, Cerrelli F, Lenzi M, Manini R, et al. Nonalcoholic fatty liver, steatohepatitis, and the metabolic syndrome. *Hepatology* (2003) 37:917–23. doi: 10.1053/jhep.2003.50161
74. Trayhurn P, Beattie JH. Physiological role of adipose tissue: white adipose tissue as an endocrine and secretory organ. *Proc Nutr Soc*. (2001) 60:329–39.
75. Rajpathak SN, Wassertheil-Smoller S, Crandall J, Liu S, Ho GY. Hepatocyte growth factor and clinical diabetes in postmenopausal women. *Diabetes Care* (2010) 33:2013–5. doi: 10.2337/dc10-0710
76. Bancks MP, Bielinski SJ, Decker PA, Hanson NQ, Larson NB, Sicotte H, et al. Circulating level of hepatocyte growth factor predicts incidence of type 2 diabetes mellitus: the Multi-Ethnic Study of Atherosclerosis (MESA). *Metabolism* (2016) 65:64–72. doi: 10.1016/j.metabol.2015.10.023
77. Wellen KE, Hotamisligil GS. Inflammation, stress, and diabetes. *J Clin Invest*. (2005) 115:1111–9. doi: 10.1172/JCI25102
78. Xu H, Barnes GT, Yang Q, Tan G, Yang D, Chou CJ, et al. Chronic inflammation in fat plays a crucial role in the development of obesity-related insulin resistance. *J Clin Invest*. (2003) 112:1821–30. doi: 10.1172/JCI19451
79. Kahn BB, Flier JS. Obesity and insulin resistance. *J Clin Invest*. (2000) 106:473–81. doi: 10.1172/JCI10842
80. Pickup JC. Inflammation and activated innate immunity in the pathogenesis of type 2 diabetes. *Diabetes Care* (2004) 27:813–23. doi: 10.2337/diacare.27.3.813

81. Kanda H, Tateya S, Tamori Y, Kotani K, Hiasa K, Kitazawa R, et al. MCP-1 contributes to macrophage infiltration into adipose tissue, insulin resistance, and hepatic steatosis in obesity. *J Clin Invest*. (2006) 116:1494–505. doi: 10.1172/JCI26498
82. Kamei N, Tobe K, Suzuki R, Ohsugi M, Watanabe T, Kubota N, et al. Overexpression of monocyte chemoattractant protein-1 in adipose tissues causes macrophage recruitment and insulin resistance. *J Biol Chem*. (2006) 281:26602–14. doi: 10.1074/jbc.M601284200
83. Odegaard JI, Ricardo-Gonzalez RR, Red Eagle A, Vats D, Morel CR, Goforth MH, et al. Alternative M2 activation of Kupffer cells by PPARdelta ameliorates obesity-induced insulin resistance. *Cell Metab* (2008) 7:496–507. doi: 10.1016/j.cmet.2008.04.003
84. Muratsu J, Iwabayashi M, Sanada F, Taniyama Y, Otsu R, Rakugi H, et al. Hepatocyte growth factor prevented high-fat diet-induced obesity and improved insulin resistance in mice. *Sci Rep*. (2017) 7:130. doi: 10.1038/s41598-017-00199-4
85. Calle EE, Rodriguez C, Walker-Thurmond K, Thun MJ. Overweight, obesity, and mortality from cancer in a prospectively studied cohort of U.S. adults. *N Engl J Med*. (2003) 348:1625–38. doi: 10.1056/NEJMoa021423
86. Roberts DL, Dive C, Renehan AG. Biological mechanisms linking obesity and cancer risk: new perspectives. *Ann Rev Med*. (2010) 61:301–16. doi: 10.1146/annurev.med.080708.082713
87. Osorio-Costa F, Rocha GZ, Dias MM, Carvalheira JB. Epidemiological and molecular mechanisms aspects linking obesity and cancer. *Arq Bras Endocrinol Metabol*. (2009) 53:213–26. doi: 10.1590/S0004-27302009000200013
88. Joyce JA, Pollard JW. Microenvironmental regulation of metastasis. *Nat Rev Cancer* (2009) 9:239–52. doi: 10.1038/nrc2618
89. Cirri P, Chiarugi P. Cancer-associated-fibroblasts and tumour cells: a diabolic liaison driving cancer progression. *Cancer Metast Rev*. (2012) 31:195–208. doi: 10.1007/s10555-011-9340-x
90. Dvorak HF. Tumors: wounds that do not heal. Similarities between tumor stroma generation and wound healing. *N Engl J Med*. (1986) 315:1650–9. doi: 10.1056/NEJM198612253152606
91. Kalluri R. The biology and function of fibroblasts in cancer. *Nat Rev Cancer* (2016) 16:582–98. doi: 10.1038/nrc.2016.73
92. Weidner KM, Arakaki N, Hartmann G, Vandekerckhove J, Weingart S, Rieder H, et al. Evidence for the identity of human scatter factor and human hepatocyte growth factor. *Proc Natl Acad Sci USA* (1991) 88:7001–5.
93. Naldini L, Weidner KM, Vigna E, Gaudino G, Bardelli A, Ponzetto C, et al. Scatter factor and hepatocyte growth factor are indistinguishable ligands for the MET receptor. *EMBO J*. (1991) 10:2867–78.
94. Stoker M, Gherardi E, Perryman M, Gray J. Scatter factor is a fibroblast-derived modulator of epithelial cell mobility. *Nature* (1987) 327:239–42. doi: 10.1038/327239a0
95. Sierra JR, Tsao MS. c-MET as a potential therapeutic target and biomarker in cancer. *Therap Adv Med Oncol*. (2011) 3(1 Suppl):S21–35. doi: 10.1177/1758834011422557
96. Comoglio PM, Giordano S, Trusolino L. Drug development of MET inhibitors: targeting oncogene addiction and expedience. *Nat Rev Drug Discov*. (2008) 7:504–16. doi: 10.1038/nrd2530
97. Seneviratne D, Ma J, Tan X, Kwon YK, Muhammad E, Melhem M, et al. Genomic instability causes HGF gene activation in colon cancer cells, promoting their resistance to necroptosis. *Gastroenterology* (2015) 148:181–91 e17. doi: 10.1053/j.gastro.2014.09.019
98. Fukuura T, Miki C, Inoue T, Matsumoto K, Suzuki H. Serum hepatocyte growth factor as an index of disease status of patients with colorectal carcinoma. *Br J Cancer* (1998) 78:454–9.
99. Toiyama Y, Miki C, Inoue Y, Okugawa Y, Tanaka K, Kusunoki M. Serum hepatocyte growth factor as a prognostic marker for stage II or III colorectal cancer patients. *Int J Cancer* (2009) 125:1657–62. doi: 10.1002/ijc.24554
100. Toi M, Taniguchi T, Ueno T, Asano M, Funata N, Sekiguchi K, et al. Significance of circulating hepatocyte growth factor level as a prognostic indicator in primary breast cancer. *Clin Cancer Res*. (1998) 4:659–64.
101. Taniguchi T, Toi M, Inada K, Imazawa T, Yamamoto Y, Tominaga T. Serum concentrations of hepatocyte growth factor in breast cancer patients. *Clin Cancer Res*. (1995) 1:1031–4.
102. Seidel C, Borset M, Turesson I, Abildgaard N, Sundan A, Waage A. Elevated serum concentrations of hepatocyte growth factor in patients with multiple myeloma. The Nordic Myeloma Study Group. *Blood* (1998) 91:806–12.
103. Verstovsek S, Kantarjian H, Estey E, Aguayo A, Giles FJ, Manshouri T, et al. Plasma hepatocyte growth factor is a prognostic factor in patients with acute myeloid leukemia but not in patients with myelodysplastic syndrome. *Leukemia* (2001) 15:1165–70.
104. Straussman R, Morikawa T, Shee K, Barzily-Rokni M, Qian ZR, Du J, et al. Tumour micro-environment elicits innate resistance to RAF inhibitors through HGF secretion. *Nature* (2012) 487:500–4. doi: 10.1038/nature11183
105. Owusu BY, Bansal N, Venukadasula PK, Ross LJ, Messick TE, Goel S, et al. Inhibition of pro-HGF activation by SRI31215, a novel approach to block oncogenic HGF/MET signaling. *Oncotarget* (2016) 7:29492–506. doi: 10.18632/oncotarget.8785
106. Pallangyo CK, Ziegler PK, Greten FR. IKKbeta acts as a tumor suppressor in cancer-associated fibroblasts during intestinal tumorigenesis. *J Exp Med*. (2015) 212:2253–66. doi: 10.1084/jem.20150576
107. Luraghi P, Reato G, Cipriano E, Sassi F, Orzan F, Bigatto V, et al. MET signaling in colon cancer stem-like cells blunts the therapeutic response to EGFR inhibitors. *Cancer Res*. (2014) 74:1857–69. doi: 10.1158/0008-5472.CAN-13-2340-T
108. Jia CC, Wang TT, Liu W, Fu BS, Hua X, Wang GY, et al. Cancer-associated fibroblasts from hepatocellular carcinoma promote malignant cell proliferation by HGF secretion. *PLoS ONE* (2013) 8:e63243. doi: 10.1371/journal.pone.0063243
109. Smith BN, Bhowmick NA. Role of EMT in metastasis and therapy resistance. *J Clin Med*. (2016) 5:17. doi: 10.3390/jcm5020017
110. Huang J, Li H, Ren G. Epithelial-mesenchymal transition and drug resistance in breast cancer (Review). *Int J Oncol*. (2015) 47:840–8. doi: 10.3892/ijo.2015.3084
111. Owusu BY, Thomas S, Venukadasula P, Han Z, Janetka JW, Galemmo RA Jr., et al. Targeting the tumor-promoting microenvironment in MET-amplified NSCLC cells with a novel inhibitor of pro-HGF activation. *Oncotarget* (2017) 8:63014–25. doi: 10.18632/oncotarget.18260
112. Kandoth C, McLellan MD, Vandin F, Ye K, Niu B, Lu C, et al. Mutational landscape and significance across 12 major cancer types. *Nature* (2013) 502:333–9. doi: 10.1038/nature12634
113. Vermeulen L, De Sousa EMF, van der Heijden M, Cameron K, de Jong JH, Borovski T, et al. Wnt activity defines colon cancer stem cells and is regulated by the microenvironment. *Nat Cell Biol*. (2010) 12:468–76. doi: 10.1038/ncb2048
114. De Bacco F, D'Ambrosio A, Casanova E, Orzan F, Neggia R, Albano R, et al. MET inhibition overcomes radiation resistance of glioblastoma stem-like cells. *EMBO Mol Med*. (2016) 8:550–68. doi: 10.15252/emmm.201505890
115. Boccaccio C, Comoglio PM. The MET oncogene in glioblastoma stem cells: implications as a diagnostic marker and a therapeutic target. *Cancer Res*. (2013) 73:3193–9. doi: 10.1158/0008-5472.CAN-12-4039
116. Sun S, Liu S, Duan SZ, Zhang L, Zhou H, Hu Y, et al. Targeting the c-Met/FZD8 signaling axis eliminates patient-derived cancer stem-like cells in head and neck squamous carcinomas. *Cancer Res*. (2014) 74:7546–59. doi: 10.1158/0008-5472.CAN-14-0826
117. van Leenders GJ, Sookhlall R, Teubel WJ, de Ridder CM, Reneman S, Sacchetti A, et al. Activation of c-MET induces a stem-like phenotype in human prostate cancer. *PLoS ONE* (2011) 6:e26753. doi: 10.1371/journal.pone.0026753
118. Li C, Wu JJ, Hynes M, Dosch J, Sarkar B, Welling TH, et al. c-Met is a marker of pancreatic cancer stem cells and therapeutic target. *Gastroenterology* (2011) 141:2218–27 e5. doi: 10.1053/j.gastro.2011.08.009
119. Iroz A, Couty JP, Postic C. Hepatokines: unlocking the multi-organ network in metabolic diseases. *Diabetologia* (2015) 58:1699–703. doi: 10.1007/s00125-015-3634-4

Conflict of Interest Statement: The authors declare that the research was conducted in the absence of any commercial or financial relationships that could be construed as a potential conflict of interest.

frontiers in Endocrinology

ORIGINAL RESEARCH
published: 30 May 2018
doi: 10.3389/fendo.2018.00249

Rosiglitazone and a β_3-Adrenoceptor Agonist Are Both Required for Functional Browning of White Adipocytes in Culture

*Jon Merlin[1], Masaaki Sato[1], Ling Yeong Chia[1], Richard Fahey[1], Mohsen Pakzad[2], Cameron J. Nowell[1], Roger J. Summers[1], Tore Bengtsson[3], Bronwyn A. Evans[1] and Dana S. Hutchinson[1,4]**

[1] Drug Discovery Biology, Monash Institute of Pharmaceutical Sciences, Monash University, Parkville, VIC, Australia, [2] Department of Toxicology and Pharmacology, Faculty of Pharmacy, Pharmaceutical Sciences Research Center, Tehran University of Medical Sciences, Tehran, Iran, [3] Department of Molecular Biosciences, The Wenner-Gren Institute, Stockholm University, Stockholm, Sweden, [4] Department of Pharmacology, Monash University, Clayton, VIC, Australia

The recruitment of brite (or beige) adipocytes has been advocated as a means to combat obesity, due to their ability to phenotypically resemble brown adipocytes (BA). Lineage studies indicate that brite adipocytes are formed by differentiation of precursor cells or by direct conversion of existing white adipocytes, depending on the adipose depot examined. We have systematically compared the gene expression profile and a functional output (oxygen consumption) in mouse adipocytes cultured from two contrasting depots, namely interscapular brown adipose tissue, and inguinal white adipose tissue (iWAT), following treatment with a known browning agent, the peroxisome proliferator-activated receptor (PPARγ) activator rosiglitazone. Prototypical BA readily express uncoupling protein (UCP)1, and upstream regulators including the β_3-adrenoceptor and transcription factors involved in energy homeostasis. Adipocytes from inguinal WAT display maximal UCP1 expression and mitochondrial uncoupling only when treated with a combination of the PPARγ activator rosiglitazone and a β_3-adrenoceptor agonist. In conclusion, brite adipocytes are fully activated only when a browning agent (rosiglitazone) and a thermogenic agent (β_3-adrenoceptor agonist) are added in combination. The presence of rosiglitazone throughout the 7-day culture period partially masks the effects of β_3-adrenoceptor signaling in inguinal white adipocyte cultures, whereas including rosiglitazone only for the first 3 days promotes robust β_3-adrenoceptor expression and provides an improved window for detection of β_3-adrenoceptor responses.

Keywords: adipocyte, beta adrenergic receptors, uncoupling protein 1, adrenoceptor, seahorse xf96 analysis, rosiglitazone, CL316243

OPEN ACCESS

Edited by:
Sudip Bajpeyi, The University of Texas at El Paso, United States

Reviewed by:
Daniel John Fazakerley, University of Sydney, Australia
Sarah M. Turpin-Nolan, Max-Planck-Institut für Stoffwechselforschung, Germany

***Correspondence:**
Dana S. Hutchinson
dana.hutchinson@monash.edu

Specialty section:
This article was submitted to Obesity, a section of the journal Frontiers in Endocrinology

Received: *31 January 2018*
Accepted: *02 May 2018*
Published: *30 May 2018*

Citation:
Merlin J, Sato M, Chia LY, Fahey R, Pakzad M, Nowell CJ, Summers RJ, Bengtsson T, Evans BA and Hutchinson DS (2018) Rosiglitazone and a β_3-Adrenoceptor Agonist Are Both Required for Functional Browning of White Adipocytes in Culture. Front. Endocrinol. 9:249. doi: 10.3389/fendo.2018.00249

INTRODUCTION

The remarkable prevalence of obesity worldwide has sparked considerable interest in therapeutic strategies that are effective and safe in promoting weight loss. In conjunction with lifestyle modification, such strategies range from surgical intervention to reduce stomach capacity, through to pharmaceutical interventions aimed primarily at modulating neural pathways that affect food/

caloric intake. There are no pharmacological interventions that primarily act on adipose tissue, despite its obvious role in obesity. There are two types of adipose tissue with distinct functions: white adipose tissue (WAT) that stores chemical energy in the form of triacylglycerol, and brown adipose tissue (BAT) that releases chemical energy in the form of heat (thermogenesis).

Classical BAT depots have been studied extensively in adult rodents. They are highly innervated and are activated by centers in the brain responsive to cold exposure, leading to the release of norepinephrine (NE) from sympathetic nerves. Upon binding of NE to BAT β_3-adrenoceptors (β_3-ARs), increased levels of intracellular cyclic AMP (cAMP) promote lipolysis, and this breakdown of triglycerides leads to release of free fatty acids that upregulate and activate uncoupling protein 1 (UCP1). Activated UCP1 uncouples mitochondrial respiration leading to heat generation, thus β_3-AR signaling increases respiration and non-shivering thermogenesis, with prototypical BAT adipocytes being remarkably rich in mitochondria (1).

β_3-AR signaling in response to NE or synthetic receptor agonists occurs almost exclusively in peripheral tissues, including adipose tissue/adipocytes, bladder, and gastrointestinal tract. While there is detectable expression in the rodent brain (2), and central administration of β_3-AR agonists directly into hypothalamic/third ventricle regions can reduce food intake and weight (3, 4) and increase c-fos immunoreactivity (5), it is unlikely that peripheral administration of β_3-AR agonists such as CL316243 and mirabegron would have direct central effects, since they do not readily cross the blood–brain barrier (6, 7). Any effects that peripheral administration of β_3-AR agonists has centrally are thought to occur indirectly through fatty acids liberated from lipolysis in peripheral adipose tissues.

In addition to prototypical white or brown adipocytes (BA), beige or brite adipocytes have been described (8, 9). These cells reside in WAT depots but can be "browned" by various stimuli, most notably cold exposure or activation of β-AR signaling, and by the peroxisome proliferator-activated receptor (PPARγ) agonist rosiglitazone. Activation of brite/beige adipocytes leads to an increase in mitochondrial uncoupling similar to that occurring in BAT. Two studies indicate that brite or beige adipocytes contribute significantly to whole body energy expenditure: mouse models that have increased beige/brite adipocytes in WAT are protected from diet-induced obesity (10), and browning of WAT contributes to non-shivering adaptive thermogenesis in the absence of classical BA (11). Adult humans possess both brown and beige/brite adipose tissue. Humans were thought to lose BAT after infancy, but phenotypically beige/brite adipocytes have been isolated from human supraclavicular fat depots and neck biopsies (9, 12, 13).

There is considerable interest in identifying additional agents that promote browning of adipose tissue, as increased expenditure of energy as heat would be of therapeutic utility in obesity and type 2 diabetes. To date, agents and processes with browning potential fall into a number of classes, namely (i) cold exposure, activation of the sympathetic nervous system (SNS), and β_3-AR agonists; (ii) G protein-coupled receptor (GPCR), ion channel, and signaling pathway modulators; (iii) exercise and associated factors; (iv) growth factors and cytokines; (v) nutritional and dietary factors; and (vi) PPAR agonists. The evidence for these as browning agents has been reviewed elsewhere (14).

Many studies of browning agents have employed a combination of cultured adipocytes and whole animal experiments. Clearly *in vivo* experiments have the advantage that test compounds are acting on cell populations as they exist in whole animals, thereby providing valid information on predicted clinical efficacy. It is important to understand the mechanism of action, however, particularly in relation to the precise cells targeted by browning agents. In the whole animal, such agents could be acting directly on adipocytes, but it is equally possible that they are targeting the central nervous system (15), or indirectly the sympathetic nervous system (16).

Cultured adipocytes thus offer a system for characterizing the direct effect of browning agents, and also have advantages in facilitating high-throughput screening of compounds. The ideal model system would be cultured human adipocytes with the potential to undergo browning, however, there have been difficulties in using human cultures or cell lines—(i) even in human subjects with highly inducible BAT (17), beige/brite adipocytes are localized to the neck and supraclavicular regions, and presumably arise from specialized cells within these adipose depots, and (ii) human primary cultures or immortalized lines such as SGBS cells require strongly adipogenic media in order to differentiate, including, for example, rosiglitazone, dexamethasone, 3-isobutyl-1-methylxanthine (IBMX), cortisol, transferrin, triiodothyronine, and insulin (9, 18). In particular, the inclusion of rosiglitazone and IBMX (to increase cAMP), is highly likely to promote browning in conjunction with differentiation.

The primary cultured adipocytes most often utilized to study browning are differentiated from the stromal vascular fraction (SVF) of mouse inguinal WAT (iWAT) depots. Again these cultures generally include rosiglitazone at least for the first 2–4 days of culture (19–23), thus the mature adipocytes are likely to have undergone browning as well as differentiation. The aim of our study was to systematically clarify the effect of rosiglitazone on cultured adipocytes in the presence or absence of recognized browning agents targeting the β_3-AR. We have examined adipocytes isolated from FVB/N mouse interscapular brown and inguinal white depots and cultured in a minimal medium consisting of DMEM supplemented with 10% newborn calf serum, 4.5 g/l glucose, and 2.4 nM insulin (8). We tested the effect of 1 μM rosiglitazone added to the culture medium for the entire 7 days or for the first 3 days only. The adipocyte cultures were treated for a further 24 h with CL316243 (in the absence of rosiglitazone), as a recognized browning agent. We find that BA cultures differentiate well even in the absence of rosiglitazone, whereas inguinal white adipocytes (iWA) require rosiglitazone for at least the first 3 days of culture. Substantial browning occurs only after 7-day rosiglitazone treatment in iWA, though induction of UCP1 and the thermogenic gene Cpt1b can be induced by CL316243 after 3 days of rosiglitazone. The highest levels of UCP1 mRNA occur following 7-day rosiglitazone combined with CL316243 treatment, and the vast majority of BA and iWA cells become positive for UCP1 immunostaining under these conditions.

MATERIALS AND METHODS

Ethical Statement

All experiments were conducted with ethical permission from the Monash University Animal Ethics Committee, ethics approval numbers MIPS.2015.14 and VCP.2009.22, which complied with the National Health and Medical Research Council of Australia (NHMRC) guidelines for use of animals in scientific research.

Adipocyte Culture

Adipocyte isolation and culturing was performed as described previously (24). Inbred FVB/N mice (3–4 weeks of age, either sex) were bred at the Monash University Parkville animal facility. Mice were killed by CO_2 inhalation and BAT isolated from the interscapular, cervical, and axillary depots, while WAT was isolated from the subcutaneous depots. Pooled tissue pieces were finely minced in DMEM and transferred to a digestion solution [0.2% (wt/vol) collagenase type II, 0.1 M HEPES (pH 7.4), 123 mM NaCl, 5 mM KCl, 1 mM $CaCl_2$, 4.5 mM glucose, 1.5% (wt/vol) BSA]. Tissues were digested for 30 min at 37°C with continuous mixing. Cells were filtered through a 250 μm nylon mesh filter into sterile tubes and kept on ice for 15 min whereupon the mature adipocytes float to the top. The top layer of the suspension was removed and the remaining cell suspension filtered through a 25-μm nylon mesh filter and centrifuged (700 × *g*, 10 min). The pellet containing preadipocytes was resuspended in DMEM and centrifuged (700 × *g*, 10 min). The pellet was suspended in culture medium (6 ml/animal for WAT, 4.8 ml/animal for BAT) and plated in either Seahorse cell culture plates (100 μl/well), 8-well chamber slides (200 μl/well), or 6-well plates (2 ml/well). The culture medium consisted of DMEM containing 4.5 g/l glucose, 10% (vol/vol) newborn calf serum, 2.4 nM insulin, 25 μg/ml sodium ascorbate, 10 mM HEPES, 4 mM L-glutamine, 50 U/ml penicillin, and 50 μg/ml streptomycin, and supplemented where indicated with 1 μM rosiglitazone. Adipocytes were grown at 37°C in 8% CO_2. Cells were washed in pre-warmed DMEM and medium renewed on day 1, then every second day. All experiments were conducted on day 7. For experiments treated for 7 days with 1 μM rosiglitazone (7-day Rosi), rosiglitazone was included in control media from day 1 to 7 (the day of experiment). In some experiments as indicated, 1 μM rosiglitazone was only included in the culture media from day 1 to 3, whereupon the cells were cultured in the absence of rosiglitazone until use on day 7.

Reverse Transcription-qPCR

Cells were serum starved on day 6 in DMEM/Nutrient Mix F-12 (1:1) with 4 mM L-glutamine, 0.5% BSA, 2.4 nM insulin, 10 mM Hepes, 50 IU/ml penicillin, 50 μg/ml streptomycin, and 50 μg/ml sodium ascorbate, with rosiglitazone (1 μM) as indicated. Media was replaced with DMEM containing 4.5 g/l glucose, 0.5% BSA, 25 μg/ml sodium ascorbate, 10 mM HEPES, 4 mM L-glutamine, 50 U/ml penicillin, and 50 μg/ml streptomycin, and supplemented with norepinephrine (1 μM), or CL316243 (1 μM) as indicated. Media was aspirated, the cells washed in warmed PBS, and plates rapidly frozen at −80°C until use. Total RNA was extracted using RNeasy Plus Mini Kits (QIAGEN), as per the manufacturer's instructions (samples in **Figure 5** were extracted using TriReagent (Sigma-Aldrich), according to the manufacturer's instructions). RNA samples were DNAse treated using DNA-*free* DNA Removal Kit (Invitrogen), according to manufacturer's instructions. Where tissues were used, interscapular BAT or inguinal WAT were excised from similarly aged (3- to 4-week-old FVB/N mice of either sex) and housed mice (room temperature 22°C), and tissues rapidly frozen (−80°C). RNA from tissues was extracted using TriReagent according to manufacturer's instructions (Sigma-Aldrich).

For preparation of cDNA, 0.5 μg of RNA was reverse-transcribed using iScript Reverse Transcription Supermix for RT-qPCR (Bio-Rad), in a total volume of 10 μl. For each independent sample, qPCR was performed in duplicate using TaqMan Gene Expression assays (Life Technologies) for Prdm16, Hoxc9, Ppara, Ppargc1a, Pparg, Ppargc1b, Fabp4, Adipoq, Slc27a1, Fasn, Pck1, Acaca, Fabp3, Acox1, Sirt3, Cpt1b, Cox4i1, Prdx3 Acadl, Vdac1, Pdk4, Slc2a1, Slc2a4, Hk2, Pfkm, Gapdh, Pgk1, Ucp1, Adrb3, and the reference gene Actb. The cDNA was diluted to the equivalent of 2.5 ng/μl of starting RNA and 4 μl added to 6 μl reaction mix comprising 1× TaqMan Gene Expression Assay and 1× TaqMan Fast Advanced Master Mix dispensed in 96-well plate, as per manufacturer's instructions. After initial denaturation at 95°C for 30 s, fluorescence was detected over 40 cycles (95°C for 5 s, 60°C for 30 s). C_q values were automatically calculated by the Realplex analysis module. qPCR presented in **Figure 5** was performed on a CFX Connect™ real-time PCR detection system (BioRad) and samples were initially denatured at 50°C for 2 min, 95°C for 10 min, and fluorescence detected over 40 cycles (95°C for 15 s, 60°C for 1 min), and C_q values automatically calculated by the BioRad analysis module. All data are expressed as expression of the gene of interest relative to Actb, calculated as $(2^{-\Delta C_q}) * 1{,}000$. Multiplication of all values by 1,000 does not change the relative expression levels and was done for two reasons; (i) it facilitates viewing of the data because even values for poorly expressed genes are greater than 1.0, and (ii) it positions expression values in the same range as RPKM or FPKM values obtained in RNA-Seq studies, as the average value for Actb in numerous cell and tissue types is 1,000. All statistics for gene expression were performed on ΔC_q values, as these data are normally distributed. For the purpose of statistics, where genes were not detected within 40 cycles (and were, therefore, not detectably expressed), an over-assumption C_q value of 40 was used.

Custom PCR Array

We designed a custom mouse qPCR array in 384-well plates that comprised 2 sets of 192 genes, including Actb as a reference gene, a genomic DNA control (Lonza) and 190 genes representing a broad cross-section of targets downstream of 25 different transcription factors (**Table 1**). Each array plate was used to analyze expression in a control and rosiglitazone-treated adipocyte culture from BA or iWA. cDNA was prepared as described above, then 4 μl equivalent to 10 ng of starting RNA was added to each well containing 1× SYBR Green PCR Master Mix (Applied Biosystems) and Lonza-dispensed primer sets in a total volume of 10 μl. qPCR reactions were carried out at the Australian Genome Research Facility (Parkville, VIC, USA) on a 7900HT Real-Time PCR System (Applied Biosystems).

TABLE 1 | Categorization of genes assessed by the StellARray custom array system.

Gene-associated category	Genes
Signaling	
Kinases	*Akt1*, *Camkk1*, *Map2k2*, *Map3k7*, *Pak2*, *Pyk2*, *Trib3*
Phosphatases	*Dusp1*, *Dusp9*, *Ppm1d*, *Ppp1r15a*, *Ppp3ca*, *Pten*
G Protein-related	*Arhgef2*, *Rgs2*
Regulatory binding proteins	*Pmepa1*, *Rcan1*
Apoptosis, stress response	*Bax*, *Bbc3*, *Bcl10*, *Bcl2*, *Bcl2l1*, *Bcl2l11*, *Birc3*, *Birc5*, *Bnip3*, *Bnip3l*, *Casp1*, *Casp3*, *Casp9*, *Cflar*, *Fas*, *Gadd45a*, *Gadd45b*, *Hspa1a*, *Hspa1b*, *Hspa5*, *Hspb1*, *Hspb2*, *Prdx3*, *Sp1*, *Xiap*
Cell cycle regulation	*Ccna2*, *Ccnd1*, *Ccnd2*, *Ccnd3*, *Ccne1*, *Ccne2*, *Cdk2*, *Cdk4*, *Cdkn1a*, *Cdkn1b*, *Cdkn1c*, *Cdkn2a*, *Cdkn2b*, *Lats2*, *Rb1*, *Sik1*, *Trp53*
Cytoskeletal constituents and reorganization	*Acta1*, *Acta2*, *Actb*, *Cap1*, *Grasp*, *Hsp90b1*, *Rac1*, *Vcl*
Proteolysis, ubiquitination	*Fbxo32*, *Mdm2*, *Socs1*, *Socs3*
Transcription factors, transcriptional regulators	*Atf3*, *Bcl6*, *Calr*, *Cebpb*, *Ddit3*, *Ddit4*, *Egr1*, *Esrra*, *Fos*, *Hdac1*, *Hdac9*, *Hes1*, *Jun*, *Junb*, *Klf10*, *Mef2a*, *Mef2c*, *Myc*, *Nfkb1*, *Nfkbia*, *Notch1*, *Nr4a3*, *Per2*, *Pparg*, *Ppargc1a*, *Ppargc1b*, *Srebf1*, *Srf*, *Stat1*, *Stat3*, *Stat6*
Enzymes	*Acaca*, *Acadl*, *Acox1*, *Cox4i1*, *Cpt1a*, *Cpt1b*, *Gamt, Gapdh*, *Gck*, *Gls2*, *Gsk3b*, *Hk2*, *Hmox1*, *Ldha*, *Lpl*, *Mest*, *Nos2*, *Pck2*, *Pcx*, *Pfkm*, *Ptgs2*, *Sod1*, *Sod2*, *Sod3*
Hormones, growth factors, cytokines	*Adipoq*, *Angpt1*, *Angpt2*, *Angptl4*, *Bmp4*, *Ccl2*, *Ctgf*, *Igf2*, *Il6*, *Inhba*, *Nppb*, *Ptn*, *Rspo1*, *Smad7*, *Spp1*, *Tgfb1*, *Tnf*, *Vegfa*
Mitochondrial function	*Fasn*, *Lonp1*, *Sirt3*, *Tfam*, *Tomm20*, *Ucp2*, *Ucp3*, *Vdac1*
Ion channels, transmembrane transporters	*Fabp3*, *Slc2a1*, *Slc2a4*
Extracellular matrix, cell adhesion	*Col1a1*, *Icam1, Mmp9, Mmp13, Serpine1, Vcam1*
Additional genes in array with negligible adipocyte expression	*Alox5*, *Bmp2*, *Cap2*, *Ccl26*, *Ccna1*, *Ccnb1*, *Cdk1*, *Dapk2*, *Foxa2*, *Gata4*, *Hey2*, *Ins1*, *Ins2*, *Isl1*, *Kcnj11*, *Mafa*, *Mmp7*, *Mstn*, *Myocd*, *Myog*, *Neurod1*, *Nkx2-2*, *Nkx2-5*, *Nkx6-1*, *Nr4a1*, *Nr4a2*, *Pdx1*, *Ppp1r3a*, *Slc2a2*, *Xirp2*

Ingenuity Pathway Analysis (IPA)

Patterns of gene expression were examined using IPA software. For each of the adipocyte datasets, we uploaded fold-change between rosiglitazone treated and control cultures, along with the final expression value in rosiglitazone-treated cultures and *P* values for significant differential expression. The datasets were filtered for fold-changes of at least 2 in either direction, expression values normalized to Actb (as described above) of at least 1.0 in at least one culture condition, and *P*-values <0.05 (Student's *t*-test), leaving 171 genes. IPA core analysis was used to determine enrichment of molecular and cellular functions or upstream regulators predicted from observed patterns of up or down-regulation among the expressed genes. IPA uses Fisher's Exact Test to test the hypothesis that patterns of gene expression related to functions or to upstream regulators are not due to chance. This analysis provides *P* values that signify the degree of enrichment of differentially expressed genes, and activation *z*-scores that take into account the direction of change compared to effects predicted from the IPA knowledge base (25). A *z*-score of at least 2.0 is considered significant.

External Data

We reanalyzed publically available RNA sequencing data obtained from Hao et al. (26) (upstream analysis shown in **Figure 6**). In this published study 8-week-old male C57BL/6J mice were housed at thermoneutrality (28–30°C) on a 12:12 h light–dark cycle and fed standard chow diet *ad libitum*. After 8 days, mice were either retained at thermoneutrality or transferred to 4°C for 2 or 4 days. Mice were killed by cervical dislocation for isolation of total RNA from interscapular BAT and inguinal WAT. Data consisting of tag counts per million were generated by digital gene expression profiling, mapped to NCBI RefSeq mRNAs, and deposited in Gene Expression Omnibus (accession number GSE63031). We uploaded the 0- and 2-day cold exposure datasets to IPA to compare upstream regulators between BAT and iWAT, as described in the legend to **Figure 6**. The mouse experiments described by Hao et al. (26) were approved by the Norwegian or Danish Animal Research Authority.

Immunocytochemistry for Detection of UCP-1

Cells were seeded in 8-well culture chamber slides (BD Biosciences, Franklin Lakes, BJ). On day 7, cells were fixed with 4% formaldehyde in PBS for 15 min, and quenched with 150 mM Tris pH 8.0 for 10 min. Cells were permeablized with 0.1% Triton X-100 for 10 min, blocked for 1 h at room temperature (5% BSA in PBS), and incubated with UCP1 (Abcam) primary antibody solution (diluted 1:1,000 in 1% BSA in PBS) overnight at 4°C. Alexa Fluor 488-conjugated goat anti-rabbit IgG (1:1,000 dilution in 1% BSA in PBS) was added and incubated at room temperature for 2 h. Images were observed on a Leica DMLB epifluorescence microscope. Images were acquired using a DC350F camera with IM500 software (Leica Microsystems AB; Kista, Sweden). Quantification was performed using Fiji (ImageJ version 1.50 g) (27), using a script developed by C.J. Nowell. Cells identified by DAPI staining in images were judged to be negative/positive for the protein of interest (UCP-1) in a blinded manner and counted using ImageJ software, performed by J. Merlin. No distinction was made in the relative intensities of staining within images.

Measurement of Oxygen Consumption Rates

Oxygen consumption rates (OCR) were measured using the Seahorse xF96 (Seahorse Bioscience). On day 7, adipocytes were washed twice in XF assay media (Seahorse Bioscience) supplemented with 25 mM glucose, 0.5 mM sodium pyruvate,

2 mM L-glutamine and 1% fatty free BSA, and 160 µl added/well. OCR was measured as described in detail (28) with some modifications. 6 baseline rate measurements were made using a 2 min mix, 5 min measure cycle. After 6 basal measurements, oligomycin A (5 µM) was added for 6 measurements, followed by a combination of antimycin A (1 µM) and rotenone (0.1 µM) for 6 measurements. OCR rates immediately prior to oligomycin A injection at measurement number 6 were used as the basal rates and defined as 100%.

Statistical Analysis

All data are expressed as mean ± SEM of *n*. Statistical significance was determined by Student's *t*-test, multiple comparisons one-way ANOVA with Tukey's test, or multiple comparisons Kruskal–Wallis test (for non-parametric analyses), as indicated in Figure legends. $P < 0.05$ was considered significant.

RESULTS

Rosiglitazone Treatment of Cultures From Inguinal WAT Increases Differentiation and the Expression of Genes Related to Thermogenesis

7-day rosiglitazone treatment (1 µM) promoted expression of genes associated with both maturation of white adipocytes, and thermogenic re-programming (**Figure 1**; **Table 2**). While BA cultures differentiate in the absence of rosiglitazone, displaying robust expression of the mature adipocyte marker Fabp4 (**Figure 1B**), iWA cultures express lower levels of Fabp4 (36% relative to BA), indicating that a much lower proportion of cells undergo differentiation under control conditions (in DMEM containing 4.5 g/l glucose, 10% (vol/vol) newborn calf serum, and 2.4 nM insulin). However, following 7d of rosiglitazone treatment, Fabp4 mRNA levels are similar to that in iWAT tissues, and also to BA tissue and cultures (**Figure 1**; **Table 2**). Likewise, the genes Acaca (acetyl CoA carboxylase), Fasn (fatty acid synthase), Slc27a1 (FATP1), Pck1 (phosphoenolpyruvate carboxykinase), and Adipoq (adiponectin), all characteristic of mature adipocytes, are expressed in control and treated BAs, whereas all of these genes are low in control iWA, and significantly increased by rosiglitazone (**Figure 1B**). Conversely, the white adipocyte marker Hoxc9 is expressed to some extent in both control and rosiglitazone-treated iWA cultures but is negligible in BA under any conditions (**Figure 1**).

The BA transcriptional regulator Prdm16 is expressed in both control and rosiglitazone-treated BA cultures, and is substantially increased in iWA cultures treated with rosiglitazone (**Figure 1A**), suggesting browning of iWA under 7-day rosiglitazone treatment as we have shown previously (29). Pparg, encoding the rosiglitazone-targeted nuclear receptor PPARγ, a major regulator of adipocyte differentiation, is expressed in control white adipocyte cultures but also significantly increased by rosiglitazone in treated iWA. These findings indicate that control iWA cultures contain few fully differentiated adipocytes, but a significant population of Hoxc9-positive preadipocytes (**Figure 1A**). Upon rosiglitazone treatment, levels of Fabp4, Adipoq, Fasn, Slc27a1, and Acaca expression in iWA equal or exceed those found in treated BA cultures, indicating a high degree of differentiation.

Figure 1D shows genes involved in fatty acid metabolism and mitochondrial function. In particular, Cpt1b (carnitine palmitoyltransferase 1B) is the rate-limiting step for fatty acid oxidation and consequent stimulation of mitochondrial respiration, while Fabp3 is also required for efficient fatty acid oxidation (30). Cpt1b mRNA is 65 times higher in control BA than in iWA cultures, and in BA, undergoes 6.4-fold induction in the presence of rosiglitazone. iWA display a striking 455-fold induction, reaching levels similar to those in BA. Similarly, Fabp3 is induced by 630-fold in iWA cultures following rosiglitazone treatment. Additional genes related to thermogenesis (Acadl, Vdac1, Acox1, Sirt3, Pdk4, Prdx3, Cox4i1) display significantly higher expression in rosiglitazone-treated iWA than in control cultures. Ppara (PPARα), which promotes expression of genes essential for many aspects of fatty acid metabolism, and Ppargc1a (PGC-1α), a master regulator of adipocyte browning and mitochondrial biogenesis, are induced by 77- and 83-fold, respectively, in adipocytes from iWAT following rosiglitazone treatment (**Figure 1A**).

Analysis of genes related to glucose handling (**Figure 1C**) showed significant increases in the insulin responsive GLUT transporter Slc2a4 (GLUT4), and glucose metabolism enzymes Hk2, Pfkm, and Gapdh, in iWA cultures treated with rosiglitazone, further indicating the differentiation of iWA cultures toward an insulin-sensitive mature adipocyte population. Rosiglitazone treatment also increased the expression of Slc2a4, Gapdh, and Pgk1 in BAs, likewise suggesting changes in insulin-mediated glucose handling, but also a significant increase in Slc2a1 (GLUT1), which has been shown to be the major GLUT involved in β_3-AR-mediated glucose uptake in BA (31).

In parallel with individual qPCR assays, we obtained a comprehensive view of rosiglitazone-induced changes in cultured mouse adipocytes by analyzing mRNA levels of 160 expressed genes quantified using a custom qPCR array (categorized in **Table 1**). Products of these genes participate in a broad cross-section of molecular and cellular functions, and represent targets of diverse upstream transcriptional regulators. We assessed the expression of 4 genes from both the qPCR array and TaqMan assays (Cpt1b, Fabp3, Ppargc1a, and Sirt3). Because expression is normalized to the reference gene Actb, the two methods give closely corresponding values for a given sample, showing less inter-assay variation than the inter-sample differences seen using either method. Genes displaying greater than twofold change of expression in either direction ($P < 0.05$) were subject to enrichment analysis using IPA software (Qiagen). The significantly enriched molecular and cellular functions are similar between BA and iWA (**Figure 2A**). The top score is for molecular transport (which encompasses a wide array of cellular processes), but the remaining significant functions are related largely to energy homeostasis, fatty acid metabolism, and ATP generation. **Figure 2B** shows the upregulated genes expected to contribute to these functions in rosiglitazone-treated iWAs.

As shown in **Figure 2A**, there are four functions that show an apparent difference between BA and iWA. Increases in the "transport of lipid," "metabolism of nucleic acid component," and "transport of carbohydrate" functions are significant in only one of iWA or BA, but in each of these three cases the number of genes showing a direction

of expression change consistent with increased function is small. For example, significantly increased transport of carbohydrate is predicted in BA, based on enhanced expression of 10 genes positively linked to this function (Hk2, Ppargc1a, Ppargc1b, Ptgs2, Slc2a1, Slc2a4, Sod1, Tnf, Trib3, and UCP1). In iWA, only seven of these genes display increased expression, so in these cells transport of carbohydrate is no longer predicted to be significantly affected. This finding is not borne out by the functional phenotype of iWA, as rosiglitazone treatment

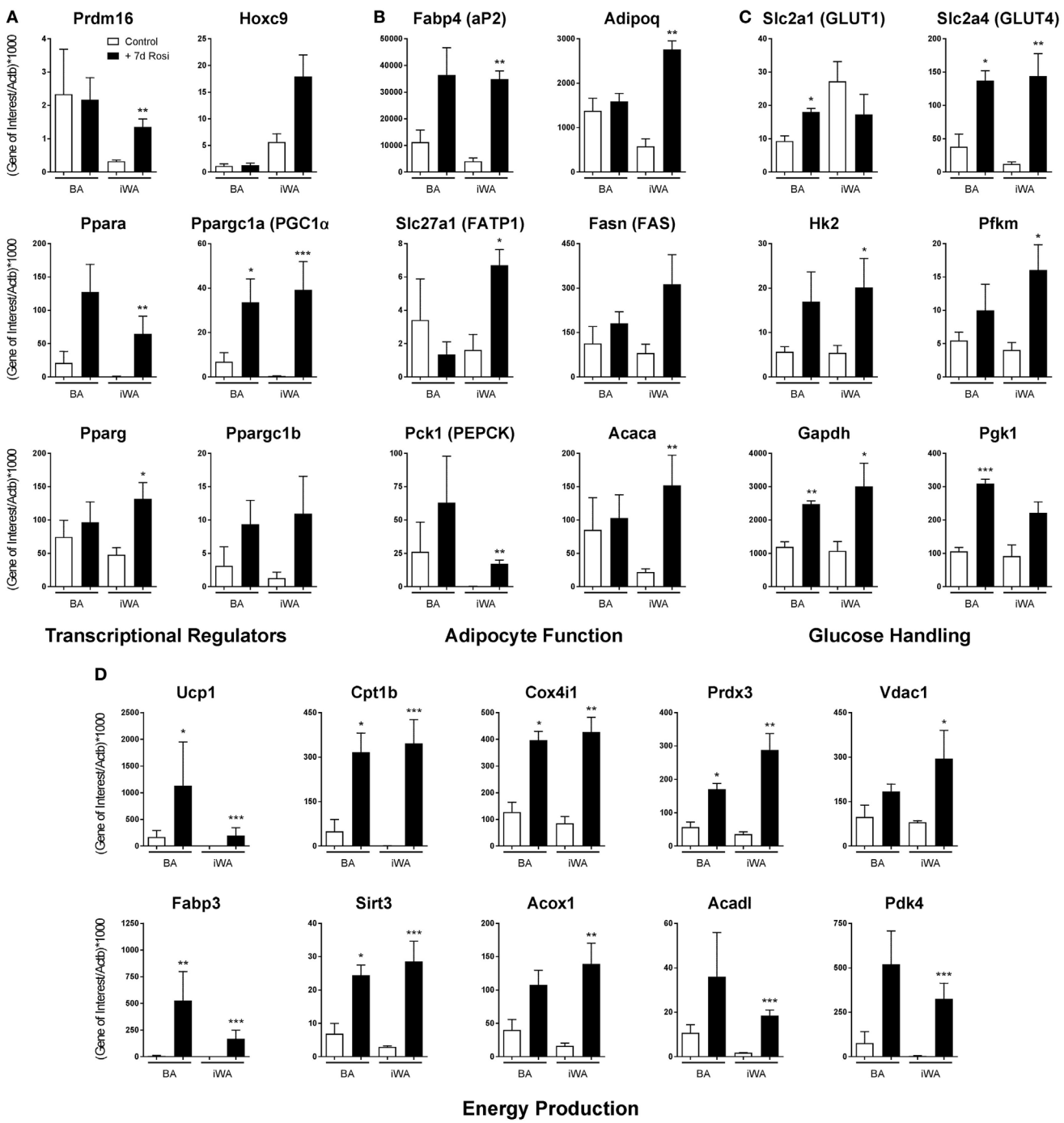

FIGURE 1 | Rosiglitazone treatment increases expression of genes associated with thermogenesis in white adipocyte cultures. 7-day 1 μM rosiglitazone treatment (7-day Rosi) of brown (BA), or inguinal white adipocyte (iWA) cultures derived from the stromal vascular fraction, increased the expression of a range of transcriptional regulators **(A)**, adipocyte function genes **(B)**, genes involved in the uptake and handling of glucose **(C)**, and genes involved in adipocyte energy production **(D)**. Data represent mean ± SEM of three independent experiments, performed in duplicate, relative to β-actin expression. $^{*}P < 0.05$, $^{**}P < 0.01$, $^{***}P < 0.001$ indicate statistical significance (unpaired Student's *t*-test) between rosiglitazone-treated and control cultures.

TABLE 2 | Comparison of gene expression in interscapular brown (BA) and inguinal white adipocytes (iWA) cultured for 7 days in the presence or absence of rosiglitazone (Rosi, 1 μM, 7 days), and in freshly isolated brown adipose tissue (BAT) and iWAT from mice housed at 22°C.

Gene	Cultured BA (control)	Cultured BA (+Rosiglitazone)	Interscapular BAT
Acot11	1.58 ± 0.34	2.58 ± 1.24	396 ± 65.6
Cpt1b	49.7 ± 39.9	317 ± 64.5	607 ± 97.3
Fabp3	6.94 ± 6.12	527 ± 272	123 ± 32.7
Fabp4	11,223 ± 4,563	36,435 ± 10,226	10,179 ± 2,555
Sirt3	17.1 ± 9.85	59.1 ± 13.4	79.3 ± 17.2
Ucp1[a]	2.62 ± 0.57	982 ± 375	10,344 ± 3,271
Prdm16	2.34 ± 1.35	2.17 ± 0.66	11.3 ± 1.49
Ppargc1a	6.87 ± 4.09	33.6 ± 10.6	22.3 ± 1.25
Pck1	26.2 ± 22.3	63.1 ± 34.8	1,115 ± 168
Pdk4	96.3 ± 84.9	521 ± 284	819 ± 157
Sirt1	8.42 ± 3.83	8.29 ± 1.15	9.06 ± 1.02
Adrb3[a]	3.38 ± 1.49	4.23 ± 0.99	4.19 ± 1.24
Gene	**Cultured iWA (control)**	**Cultured iWA (+Rosiglitazone)**	**Inguinal WAT**
Acot11	0.21 ± 0.06	0.91 ± 0.08	12.8 ± 0.78
Cpt1b	0.76 ± 0.21	346 ± 80.9	104 ± 13.9
Fabp3	0.19 ± 0.03	169 ± 79.7	63 ± 14
Fabp4	4070 ± 1211	34890 ± 3021	12,144 ± 2,412
Sirt3	2.99 ± 0.71	47.3 ± 12	18.1 ± 2.36
Ucp1[a]	0.04 ± 0.03	45.9 ± 13.4	1,775 ± 361
Prdm16	0.33 ± 0.04	1.35 ± 0.24	2.63 ± 0.41
Ppargc1a	0.47 ± 0.06	39.2 ± 12.8	7.74 ± 2.3
Pck1	0.26 ± 0.12	17.3 ± 2.71	419 ± 43.2
Pdk4	5.52 ± 0.59	326 ± 88	139 ± 23.8
Sirt1	4.69 ± 0.15	8.04 ± 1.16	4.65 ± 0.59
Adrb3[a]	0.49 ± 0.26	3.32 ± 1.01	3.04 ± 0.17

[a]*Data for Ucp1 and Adrb3 expression in control and rosiglitazone-treated adipocytes obtained from Merlin et al. (29). All data are expressed relative to Actb expression*1,000 ± SEM of three independent experiments (as per **Figure 1**).*

significantly increases glucose uptake in response to norepinephrine and CL316243 (29). This reflects our observation that the limiting step in agonist-stimulated glucose uptake is the abundance of the β_3-AR, which is markedly enhanced when iWAs are cultured in the presence of rosiglitazone [**Table 2**; (29)]. Interestingly, the function "synthesis of reactive oxygen species" is predicted to be decreased in iWA (*z*-score of −2.2, based on 23 differentially expressed genes), while this function is not significantly affected by rosiglitazone treatment in BA (*z*-score of +0.27, 16 genes). Genes displaying changes in expression expected to enhance or inhibit synthesis of reactive oxygen species (ROS) are shown in **Figure 2C** (iWA) and **Figure 2D** (BA). The overlapping genes all display the same direction of change in expression in iWA and BA, but in iWA cultures there are 15 genes for which up- or down-regulation is expected to reduce ROS. The induction of genes encoding anti-oxidant enzymes, including superoxide dismutase SOD1 and SOD2 in iWAT also occurs *in vivo* following rosiglitazone treatment (32).

Brite Adipocytes Display Increased UCP1 Protein and Uncoupling Capacity in Response to 24 h Treatment With the β_3-AR Agonist CL316243

As chronic β-AR treatment of BA upregulates UCP-1 mRNA and protein levels (1), we treated BA and iWA cultures in the presence/absence of 7-d rosiglitazone (1 μM) with norepinephrine (1 μM, 24 h) or CL316243 (1 μM, 24 h). Norepinephrine and CL316243 caused a small increase in UCP1 mRNA expression (**Figure 3B**) and immunoreactivity (**Figures 3A,C**) in control BA, but this response was significantly amplified in rosiglitazone-treated BA cultures. The effect of combined rosiglitazone and β-AR agonist treatment was even more evident in iWA cultures. These data are consistent with the presence or absence of β_3-ARs in these cultures (29). There were significant changes in the proportion of UCP1-positive cells between all control cultures and those treated with rosiglitazone alone (**Figures 3A,C**). Following an additional 24 h in the presence of CL316243, there were also significant differences in UCP1-positive cells between control and rosiglitazone-treated iWA cultures (**Figure 3C**).

In order to investigate whether the increase in UCP1 mRNA/protein levels following rosiglitazone, norepinephrine, or CL316243 treatment affected mitochondrial uncoupling in white adipocytes, we measured OCR in the presence of the ATP synthase inhibitor oligomycin (5 μM), and in the presence of rotenone (0.1 μM) and antimycin A (1 μM), that define non-mitochondrial sources of OCR. In control iWA cells, oligomycin inhibited OCR by ~50% (**Figure 4**). In iWA cells treated 7-day with rosiglitazone (1 μM), oligomycin inhibited OCR by only 34%. The insensitivity to oligomycin was enhanced when rosiglitazone treated cells were also treated with either NE (1 μM, 2 and 24 h) or CL316243 (1 μM, 2 and 24 h). This suggests an increase in uncoupled respiration. This was further assessed by treating the cells with a combination of rotenone (0.1 μM) and antimycin A (1 μM), that define non-mitochondrial sources of OCR (~36% of OCR was due to non-mitochondrial sources; **Figure 4**). After correction for non-mitochondrial OCR (indicated in dotted arrows in **Figures 4C,D**, and illustrated as % OCR due to proton leak in **Figures 4E,F**), we can see that mitochondrial uncoupling (proton leak) accounts for 14% of OCR in control iWA cells, 27% in rosiglitazone-treated cells, and this level rises to 40–50% in rosiglitazone-treated iWA cells further treated with NE or CL316243. These results suggest that rosiglitazone-induced brite adipocytes possess a greater mitochondrial uncoupling capacity, and that β_3-AR treatment of brite adipocytes significantly increases this capacity.

The Effects of Rosiglitazone on Adipocyte Differentiation, and the Thermogenic Potential of iWA, Are Separable Following 3-Day Treatment

Our studies indicate that 7-d rosiglitazone treatment promotes both differentiation and browning of iWA cultures. It is common practice to induce adipocyte differentiation using an adipogenic cocktail, generally containing IBMX, dexamethasone, insulin, high glucose, and often 1 μM rosiglitazone, particularly in studies involving human adipocytes. However, the presence of rosiglitazone, and perhaps IBMX that increases cellular cAMP and thus mimics the effect of β-AR agonists, are confounding factors in any attempt to attribute browning capacity to agents being tested using cultures derived from the stromal vascular fraction (14). Several published studies have included rosiglitazone in mouse adipocyte cultures only for the first 2–4 days before removing rosiglitazone

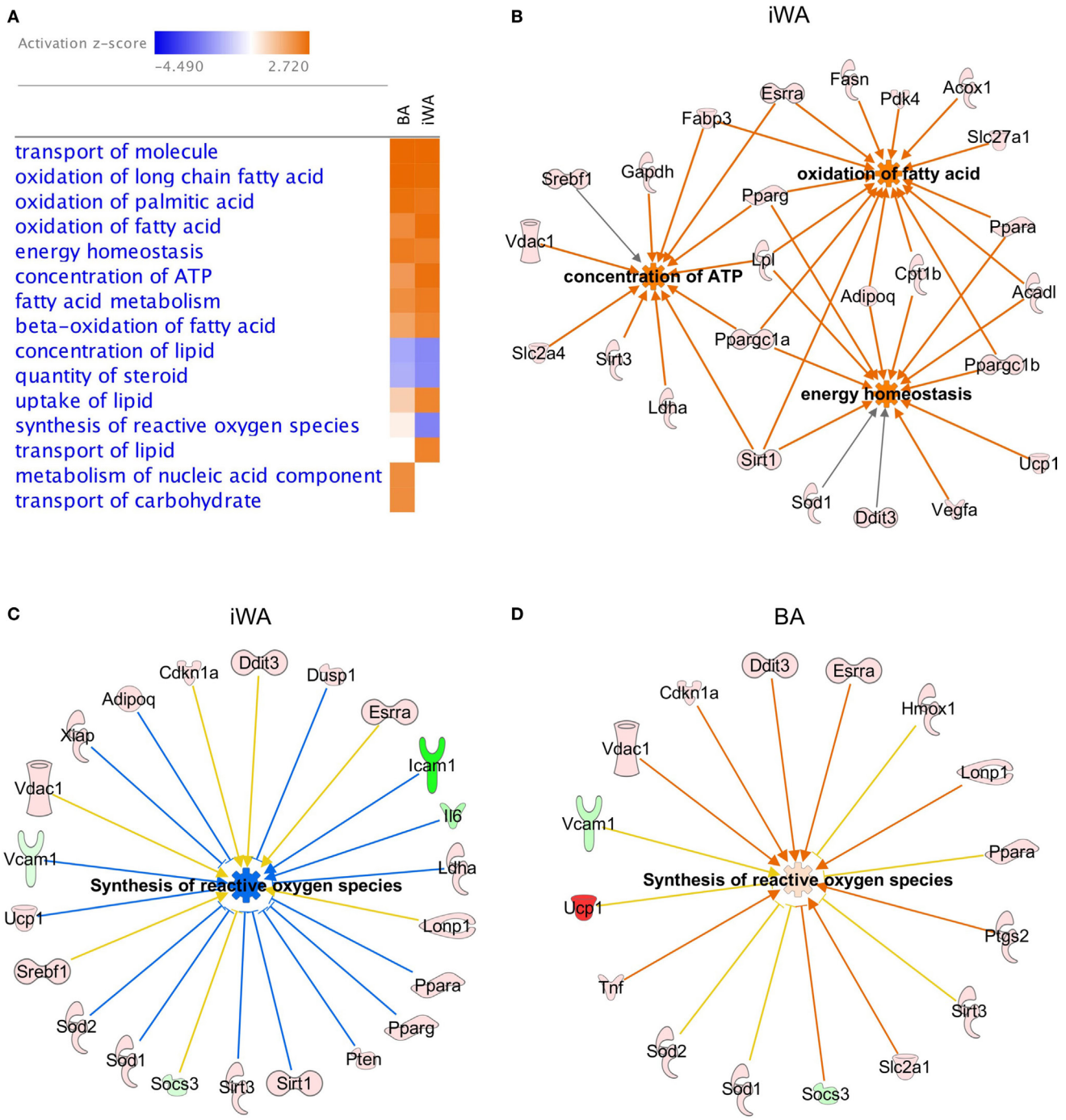

FIGURE 2 | Molecular and cellular functions of genes differentially expressed in control or rosiglitazone-treated adipocytes. Ingenuity Pathway Analysis (IPA) software was used to compare downstream functions consistent with observed patterns of target gene up- or down-regulation in adipocyte cultures treated with rosiglitazone relative to vehicle **(A)**. Functions are ranked according to the sum of activation *z*-scores across brown adipocyte (BA) and inguinal white adipocytes (iWA) cultures, irrespective of positive or negative direction. *Z*-scores ≥|2| describe statistically significant matches between known functions and observed patterns of gene regulation, and also whether functions are predicted to be up- or down-regulated downstream of the observed changes (activated shown in orange, inhibited shown in blue) (25). Network of genes upregulated in iWAT that contribute to key non-redundant cellular functions (oxidation of fatty acid, concentration of ATP and energy homeostasis) **(B)**. Differentially expressed genes identified by IPA that contribute to synthesis of reactive oxygen species (ROS) in iWA **(C)** and BA **(D)**. In both panels, coloring of genes red or pink denotes upregulation and green denotes downregulation. In panel **(C)**, blue lines signify genes showing a change in expression consistent with reduced ROS synthesis, while yellow lines signify genes that are not consistent with this function. The *z*-score for iWA is −2.2, below the significance threshold of |2|, whereas that for BA is +0.27 and not significant. iWA cultures treated with rosiglitazone display fourfold increases in expression of the key anti-oxidant genes Sod1 and Sod2 relative to control cultures.

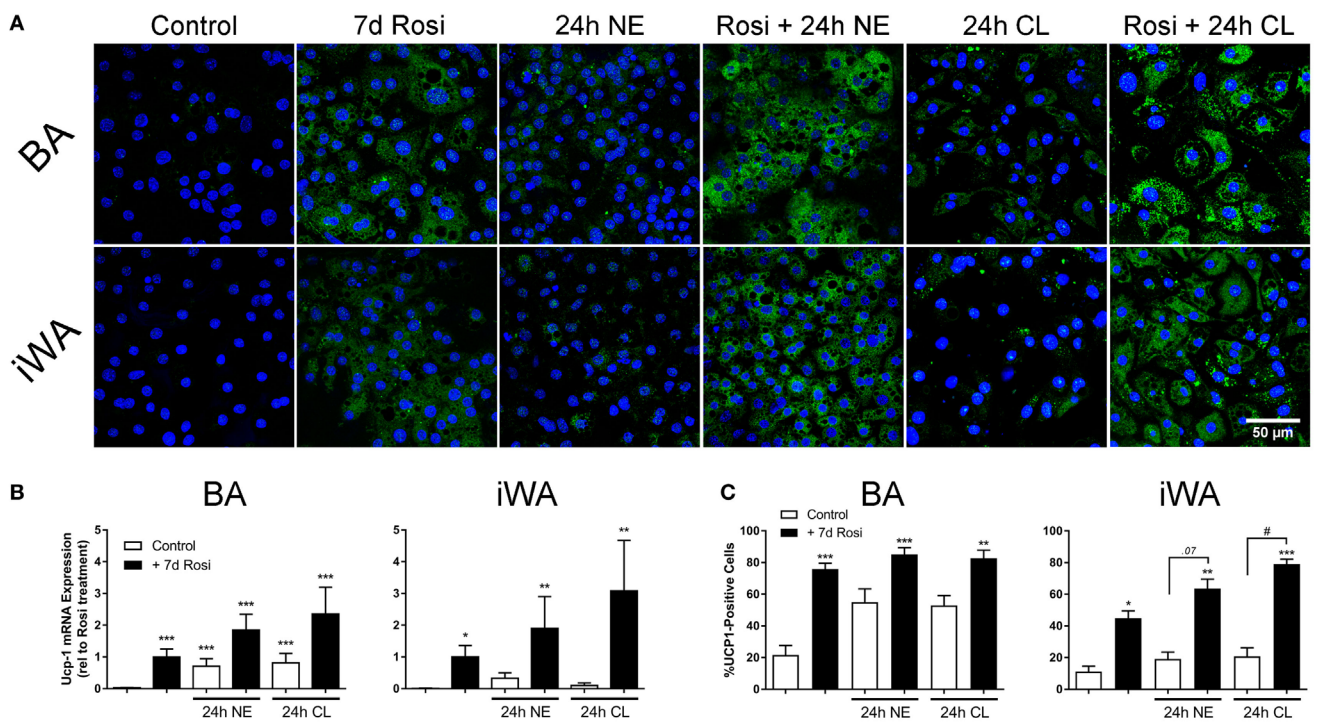

FIGURE 3 | Effect of combined rosiglitazone and β-adrenoceptor agonist treatment on uncoupling protein 1 (UCP1) mRNA and protein content. **(A)** Representative images obtained using a UCP-1 antibody (green) in brown (BA) and inguinal white adipocytes (iWA) following rosiglitazone (1 µM, 7 days) treatment in the presence/absence of norepinephrine (NE, 1 µM, 24 h) or CL316243 (CL, 1 µM, 24 h). Nuclei are stained blue by DAPI staining. **(B)** Expression of UCP1 mRNA in BA and iWA following rosiglitazone (1 µM, 7 days) treatment in the presence/absence of norepinephrine (NE, 1 µM, 24 h) or CL316243 (CL, 1 µM, 24 h). Values from each rosiglitazone-treated BA experiment were expressed relative to their normalized value, and levels in all other cells/treatments expressed relative to this value, expressed as mean ± SEM from 3 to 5 independent experiments performed in duplicate. $^{*}P < 0.05$, $^{**}P < 0.01$, $^{***}P < 0.001$ indicate statistical significance from control (unpaired one-way ANOVA, Tukey's multiple comparisons post-test). **(C)** Quantification of proportion of UCP-1-positive cells in **(A)**. Data represent mean ± SEM of 5–6 independent experiments. Data are confined between 0 and 100% and are, therefore, non-parametrically distributed. $^{*}P < 0.05$, $^{**}P < 0.01$, $^{***}P < 0.001$ indicate statistical significance from control cells, $^{\#}P < 0.05$, $^{\#\#}P < 0.01$ indicate statistical significance from respective adrenergic control (multiple comparisons Kruskal–Wallis test, one-way ANOVA).

from the media for the remainder of the differentiation protocol, instead of including rosiglitazone for the entire differentiation period [e.g., Ref. (19, 21–23, 33)]. We therefore examined changes in gene expression in both BA and iWA cultures treated with rosiglitazone for the entire 7 days compared to the first 3 days only (**Figure 5**). In iWA cultures, 3-d rosiglitazone promoted increases in Adrb3 mRNA that were 50% of those seen after the full 7-d treatment. 1–3 day rosiglitazone did not significantly alter expression of UCP1, Fabp3, Fabp4, or Cpt1b, in contrast to the substantial increases seen in 7d-treated cultures. We also tested the effect of CL316243 (1 µM, 24 h) on cultures differentiated with rosiglitazone for 3 or 7 days. CL316243 increased the expression of Ucp1 in 1–3 day cultures, whereas it had no effect on control cultures, indicating that 3 days does provide a suitable window to test for browning capacity. After 7 days in the presence of rosiglitazone, CL316243 treatment for 24 h did increase UCP1 mRNA further (although not significant in this cohort of adipocytes due to high variation observed), and also seen in **Figure 3**, however, there was no increase in Fabp3 or Cpt1b expression associated with 24 h CL316243. Thus longer exposure to rosiglitazone essentially masks some of the effects of CL316243.

Modulation of Gene Expression in BA and iWA Cultured From the SVF Compared to *In Vivo* Adipose Depots

Our gene expression data and previous functional studies (29) indicate that although BA and iWA cultures are derived from adipocyte precursors in the SVF, the mature adipocytes retain distinct properties according to their site of origin. It has been shown recently that *in vivo* treatment of mice with rosiglitazone induces a population of mature UCP1-positive inguinal adipocytes that have a distinct profile compared to populations induced by *in vivo* treatment with CL316243 (34). This differs from our findings based on adipocytes derived from the SVF, as in our cultures prior differentiation with rosiglitazone was required in order for cells to induce expression of the β_3-AR and thereby become responsive to CL316243. This suggests that the mature adipocytes residing in iWAT depots differ from those derived from differentiation of the SVF. We compared the regulation of gene expression by rosiglitazone in our cultures with that demonstrated by transcriptome sequencing of RNA from BAT and iWAT subjected to sympathetic stimulation due to cold exposure

of mice for 2 days (26). We also compared the expression of key adipocyte and thermogenic genes in our cultures with that in freshly isolated BAT and iWAT (**Table 2**). These tissues were isolated from mice subject to mild thermal stress by housing at 22°C, rather than at thermoneutrality (35, 36).

We used IPA to compare upstream regulators associated with all BA and iWA genes differentially expressed in the presence of rosiglitazone (twofold change in either direction, $P < 0.05$). As would be expected for cells treated with rosiglitazone, high-scoring upstream regulators across all cultures were closely associated with the PPARγ/PGC-1α network previously implicated in activating thermogenesis (**Figure 6A**). We also performed IPA upstream regulator analysis on the data from RNA sequencing of adipose depots from cold-exposed mice

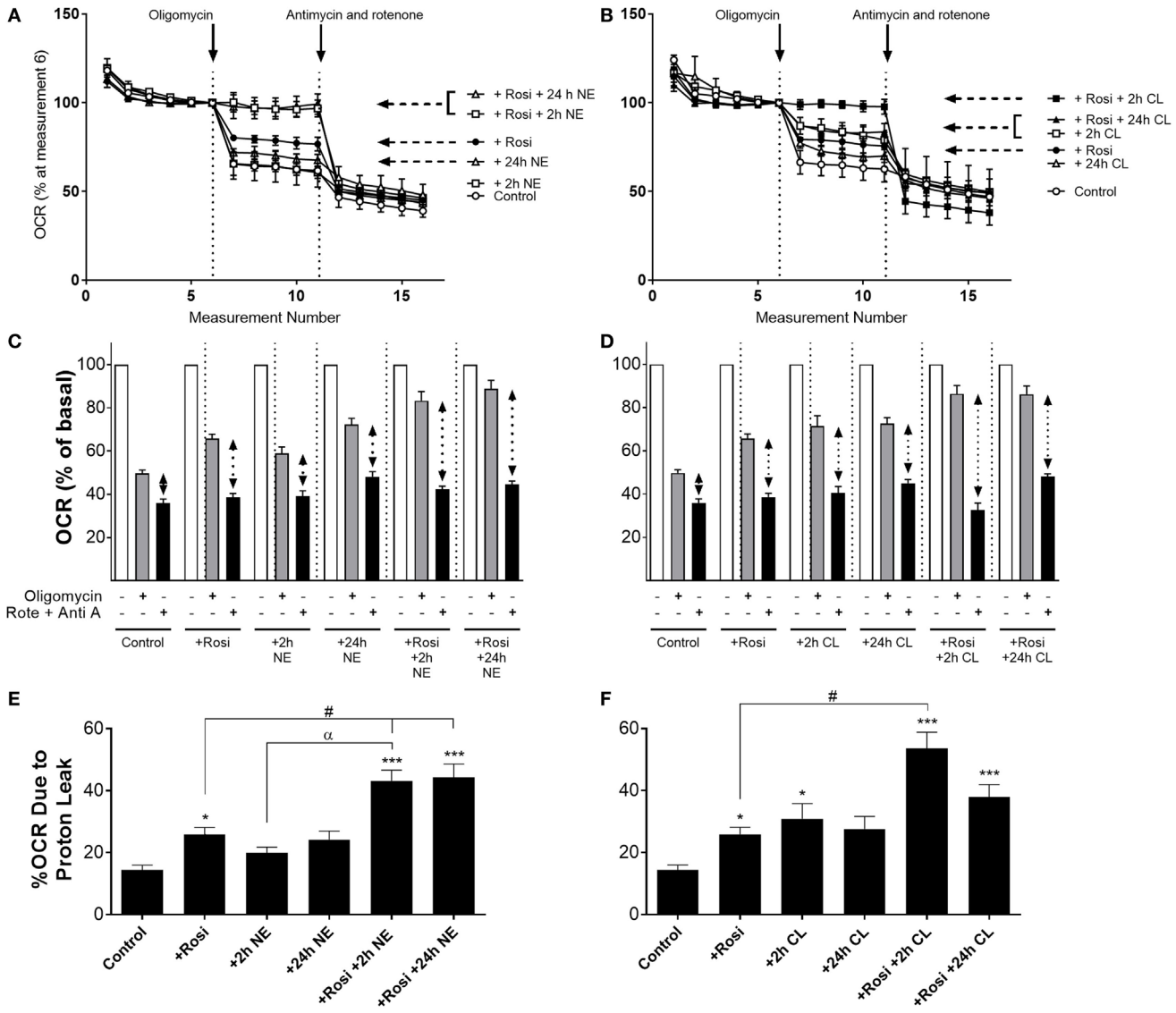

FIGURE 4 | Effect of combined rosiglitazone and β-adrenoceptor agonist treatment on oligomycin-insensitive oxygen consumption in inguinal white adipocytes (iWA). Control or rosiglitazone (1 μM, 7 days) treated iWA were treated with **(A,C)** 1 μM norepinephrine (NE; 2 or 24 h) or **(B,D)** 1 μM CL316243 (CL; 2 or 24 h) prior to measurement of oxygen consumption rates (OCR). Cells were treated in the Seahorse XF96 with the ATP-synthase inhibitor oligomycin (5 μM) or a combination of the mitochondrial inhibitors 0.1 μM rotenone (Rote) and 1 μM antimycin A (Anti A). Data are mean ± SEM of 12–38 independent experiments performed in duplicate. Data in **(A,B)** are representative traces of two experiments performed in duplicate. Arrows indicate the addition of oligomycin (5 μM) or the combination of rotenone (0.1 μM) and antimycin A (1 μM), with basal OCR set to 100% before the addition of oligomycin at rate 6 to account for variations in the raw data between adipocyte cultures made on different days. **(E,F)** The relative changes in OCR between oligomycin (defining OCR due to ATP synthase) and rotenone/antimycin A (defining OCR due to non-mitochondrial sources) are expressed as % OCR due to proton leak [calculated from the results presented in **(C,D)** indicated with the dotted arrows]. Data are non-parametrically distributed and, therefore, statistically analyzed by non-parametrically analysis. $^{*}P < 0.05$, $^{**}P < 0.01$, $^{***}P < 0.001$ indicate statistical significance from control cells, $^{\#}P < 0.05$ indicates statistical significance from rosiglitazone-treated cells, $^{\alpha}P < 0.05$ indicates statistical significance from adrenergic treatment alone (multiple comparisons Kruskal–Wallis test, one-way ANOVA).

[(26), **Figure 6B**]. In BAT and iWAT, seven of the highest scoring upstream regulators from the *in vivo* study corresponded to those seen in our rosiglitazone-treated cultures. This highlights the previously characterized thermogenic pathway involving activation of PPARγ by endogenous fatty acids released due to sympathetic stimulation of lipolysis (37). When we compared expression of key adipocyte and thermogenic genes in control and rosiglitazone-treated cultures with that in native AT depots, many showed similar levels in rosiglitazone-treated cultures and in BAT or iWAT. There are, however, striking differences in levels of UCP1, Acot11, and Pck1 mRNA, which each display over 10-fold higher expression in native BAT and iWAT than in the corresponding rosiglitazone-treated cultures (**Table 2**; **Figure 6**).

DISCUSSION

The presence of active BAT in humans (38–41) has reignited research into ways to promote increased thermogenesis in humans as a strategy to combat obesity and its related disorders such as type 2 diabetes. This is in part due to the overwhelming

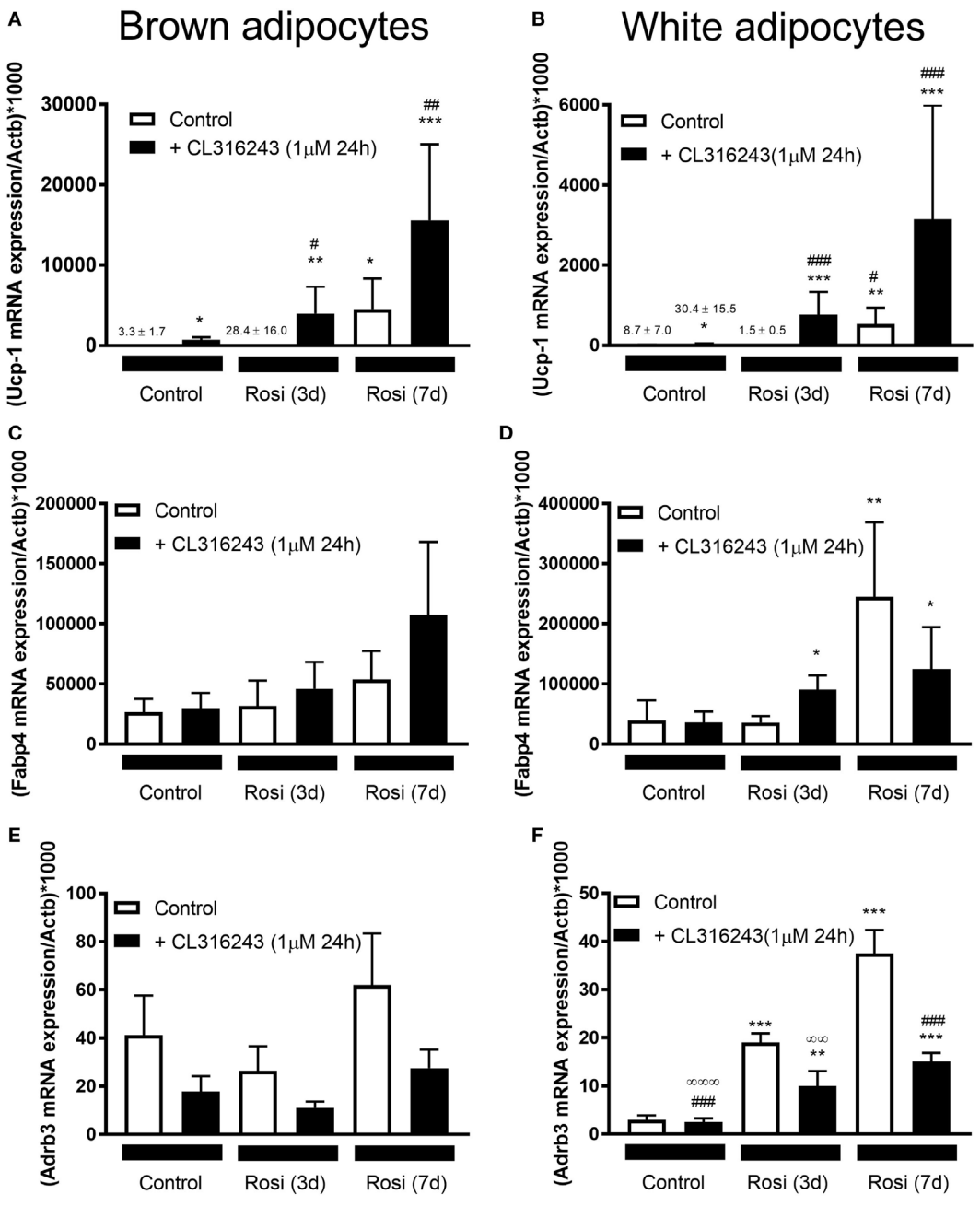

FIGURE 5 | Continued

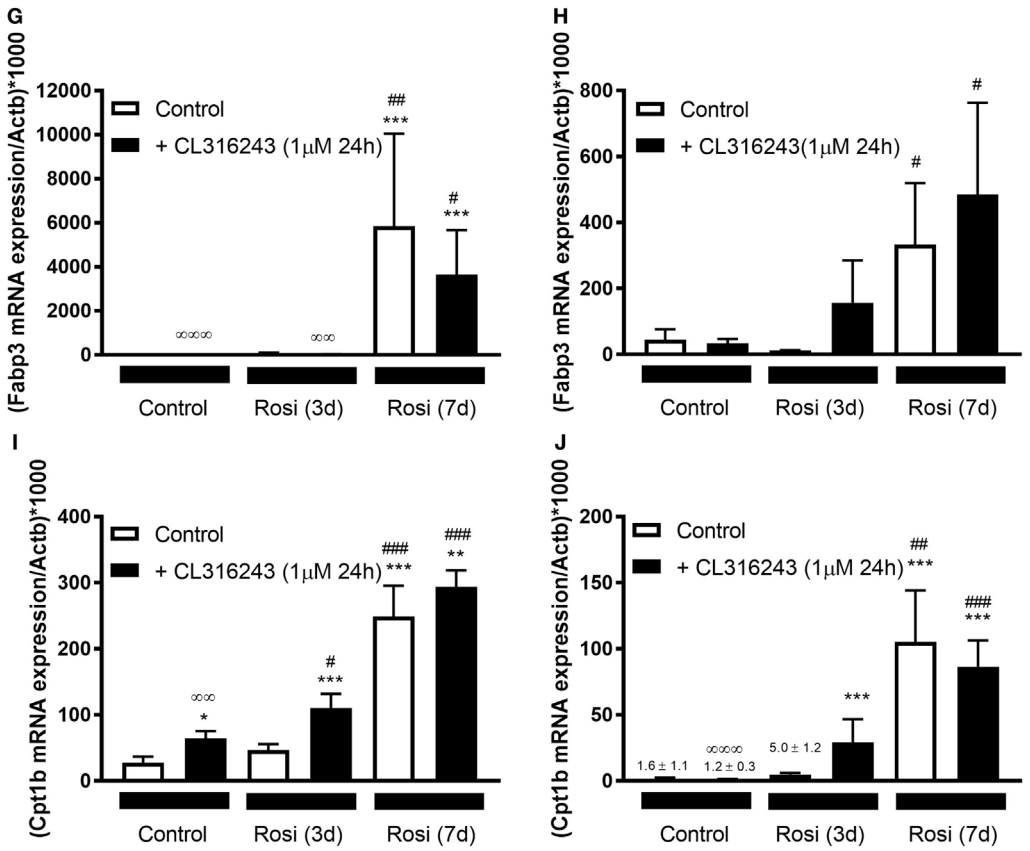

FIGURE 5 | Effect of different lengths of time of rosiglitazone on gene expression in white and brown adipocytes (BA). Control or rosiglitazone [1 μM, 3 days (3d), or 7 days (7d)] treated brown or inguinal white adipocytes (iWA) were treated with 1 μM CL316243 (24 h) prior to measurement of several genes, including Ucp1 **(A,B)**, Fabp4 **(C,D)**, Adrb3 **(E,F)**, Fabp3 **(G,H)**, or Cpt1b **(I,J)**. Data represent mean ± SEM of 6 (BA) or 7–8 (iWA) independent experiments, performed in duplicate, relative to β-actin (Actb) expression. $^{*}P < 0.05$, $^{**}P < 0.01$, $^{***}P < 0.001$ indicate statistical significance between all treatments and the control cultures. $^{\#}P < 0.05$, $^{\#\#}P < 0.01$, $^{\#\#\#}P < 0.001$ indicate statistical significance between all treatments and the Rosi (3d) treated cultures. $^{\infty}P < 0.05$, $^{\infty\infty}P < 0.01$, $^{\infty\infty\infty}P < 0.001$ between all treatments and the Rosi (7 days) treated cultures. Data analyzed by Tukey's multiple comparisons of one-way ANOVA performed on the ΔC_t values, which are normally distributed. One sample (iWA treated with rosiglitazone for 3 days) was excluded from all analysis due to poor integrity of its RNA. A single measurement of *Adrb3* for iWA treated with CL316243, and of Fabp4 for BA treated with Rosi 7 days, was excluded from the analysis due to failure of the qPCR reaction.

evidence that activation of β_3-ARs leading to increased UCP1 expression and function in BAT can reverse obesity, and prevent the development of insulin resistance and diabetes in rodents (42–45). However, translation of these responses observed in rodents has not led to effective treatments in humans (46, 47). This may in part be due to human tissue comprising adipocytes that are more akin to mouse beige or brite adipocytes rather than classical BAs, based on gene expression profiling (9, 48). Thus research into beige/brite adipocytes, and how they can be induced by different stimuli [reviewed in Ref. (14)] may offer greater therapeutic potential. It is critical to this research that model systems comprising cultured adipocytes respond in the same way to browning agents as endogenous cells *in vivo*.

We have characterized FVB/N mouse adipocytes induced by rosiglitazone in culture, utilizing a method for *in vitro* differentiation (8) that in control cultures lacks potential brite-inducing agents commonly used in adipocyte differentiation cocktails (such as triiodothyronine, IBMX, and rosiglitazone itself). We show that BA undergo differentiation in control cultures, but still display increased expression of UCP1 mRNA and protein in the presence of rosiglitazone. iWA cultures undergo both differentiation and browning due to inclusion of rosiglitazone. In BA cultures treated with rosiglitazone, 80% of cells become UCP1-positive, while this figure is 45% in iWA cultures (**Figure 3B**). These findings align with our observation that the key transcriptional regulators Prdm16 and PPARα are expressed at somewhat lower levels in iWA. Importantly, PPARγ and PGC-1α show comparable robust expression in rosiglitazone-treated BA and iWA (**Figure 1**).

Cultured Adipocytes From iWAT Depots Require Priming by Rosiglitazone for Induction of UCP1 and Thermogenic Genes by the β_3-AR Agonist CL316243

We showed previously that the majority of BA cells express β_3-AR protein in control and rosiglitazone-treated cultures, whereas in iWA cultures the proportion of β_3-AR-positive cells increase markedly in the presence of rosiglitazone (29), concomitant with

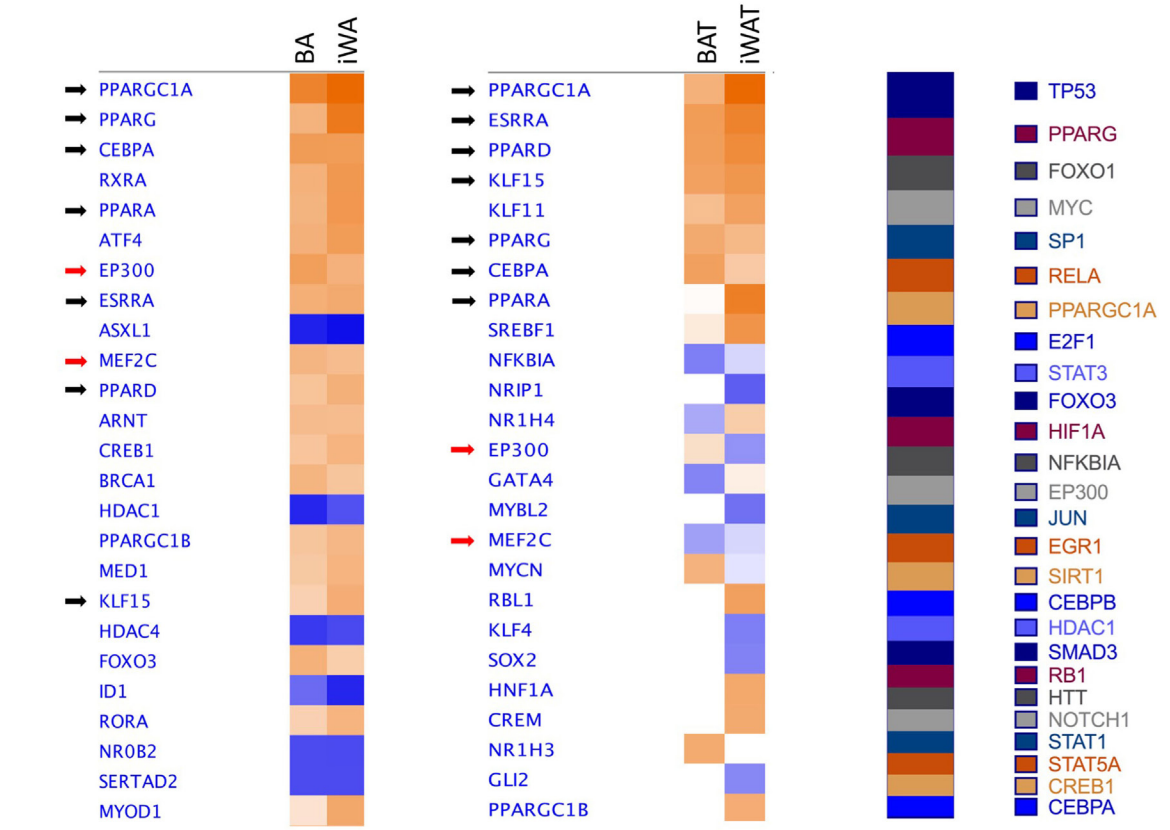

FIGURE 6 | Comparison analysis [ingenuity pathway analysis (IPA)] of transcriptional regulators governing gene expression in rosiglitazone-treated adipocytes and 2-day cold-exposed mice. IPA software was used to determine upstream regulators consistent with observed patterns of target gene up- or down-regulation in adipocyte cultures treated with rosiglitazone relative to vehicle-treated control cultures **(A)**. Transcriptional regulators are ranked according to the sum of activation *z*-scores across brown adipocyte and inguinal white adipocytes (iWA) cultures, irrespective of positive or negative direction. *Z*-scores ≥|2| describe statistically significant matches between known regulators and observed patterns of up- and down-regulated genes, and also predict the activation state of each putative regulator (activated shown in orange, inhibited shown in blue) (25). As an example, the top transcriptional regulators in rosiglitazone-treated iWAs are PGC-1α ($z = +4.88$, *P* value = 1.83E-46), PPARγ ($z = +4.35$, *P* value = 5.89E-44), and PPARα ($z = +3.38$, *P* value = 1.19E-32). These are predicted to be activated based on *z*-score, and are themselves upregulated in the treated cultures (83-, 3-, and 77-fold, respectively). *P* values (Fisher's Exact Test) describe the significance of overlap between the observed differentially expressed genes and all genes associated with a particular upstream regulator in the Ingenuity database, curated from published literature. As an additional comparison, we re-analyzed literature-derived RNA sequencing data for adipose depots from cold-exposed mice (26) **(B)**. 8-week-old mice were housed at 28–30°C for 8 days, then one group maintained at thermoneutrality and a second group housed at 4°C for 2 days. Fold-change values were calculated for all genes expressed in iWAT and brown adipose tissue (BAT) of mice at 4°C compared to control mice at 28–30°C. These fold changes were analyzed using IPA and upstream regulators compared by *z*-score between BAT and iWAT. **(C)** Shows the predicted upstream regulators across the entire set of 171 genes found to be expressed in adipocyte cultures, ranked by log(*P*-value of overlap), demonstrating that the dataset is not biased toward the regulators predicted to govern differential expression in adipocyte cultures.

increased levels of β_3-AR mRNA (**Figure 5**). This in turn facilitates the response to β_3-AR agonists (29). This may represent a special case, however, it is equally likely that receptors targeted by other agents are similarly induced during adipocyte differentiation and/or browning. In mice, the β_3-AR is expressed in native BAT and iWAT at levels similar to those in rosiglitazone-treated cultures (**Table 2**), consistent with widespread findings that *in vivo* treatment with CL316243 can induce browning in iWAT depots (9, 35, 49). The utility of cultured adipocytes as a screening platform is clearly dependent on the presence of the target receptors.

Wu et al. (9) suggested that the inherent capacity for brite adipogenesis *in vivo* is independent of external factors, such as innervation, blood flow, oxygen supply, and nutrients. While differentiation of cultured adipocytes from the SVF does occur in a cell-autonomous manner, properties of the precursor cells appear to be specified by the environment from which they were derived, with a significant contribution from SNS innervation. *In vivo*, BAs possess a well-established ability to adapt to chronic β-AR activation; prolonged exposure to cold increases UCP1 expression in BAT (50, 51), which is inhibited by sympathetic denervation of BAT

(37, 52). This upregulation in UCP1 occurs *via* β_3-ARs and can be inhibited by β_3-AR selective antagonists (53, 54). The requirement for intact sympathetic innervation has also been demonstrated in iWAT. For example, 3-week-old mice have high levels of UCP1 expression in iWAT, but this is markedly reduced by 8 weeks of age (35). At 8 weeks, mature adipocytes within iWAT re-express UCP1 in response to CL316243 stimulation, but this effect is abolished in mice undergoing prior surgical denervation of iWAT depots at 3 weeks. Thus sympathetic tone due to the mild cold-stress associated with housing mice at room temperature (55) maintains browning capacity in iWAT. We observed high UCP1 expression in native iWAT from animals housed at 22°C, reflecting this thermal stress (**Table 2**). Conversely, UCP1 mRNA is undetectable in the iWAT of mice housed at thermoneutrality [28–30°C (56)].

Importantly, reports of CL316243-induced browning have used mice housed at room temperature rather than at thermoneutrality (9, 35, 49). Previous studies have demonstrated an *in vitro* effect of CL316243 on UCP1 expression and function only in white adipocytes cultured in the presence of rosiglitazone or adipogenic cocktails (9, 49). Likewise, we found that while 24 h β_3-AR stimulation (NE or CL316243) increased the proportion of UCP1-expressing cells in both control and treated BA cultures, neither agent alone induced significant browning of iWA cultures (**Figure 3**). These findings may recapitulate the requirement for intact SNS innervation of WAT seen *in vivo*, as sympathetic tone and consequent β-AR activation would be expected to drive lipolysis and subsequent activation of PPARγ by endogenous fatty acids. From our overall profiling of gene expression using the custom qPCR array, we examined predicted upstream regulators (IPA) based on genes differentially expressed following 7d rosiglitazone in cultured adipocytes, and these regulators were compared to those predicted in BAT and iWAT of mice subject to cold exposure for 2 days (26). In both cases, the top upstream regulators included PGC-1α, PPARγ, PPARα, PPARδ, CEBPα, ERRα (estrogen-related receptor α), and KLF15 (**Figure 6**), consistent with a common mechanism of induction that is dependent on PPARγ.

Functional Demonstration of iWA Browning

The therapeutic potential of adipocyte browning is contingent upon the dissipation of energy through mitochondrial uncoupling becoming dominant over energy storage as triglycerides. We previously have shown that increased UCP1 function in brite adipocytes (defined as the percentage of OCR due to proton leak) is increased in brite adipocytes as compared to white adipocytes (29), which correlates with an increase in the expression of several genes involved in energy production (**Figure 1**). To assess whether combined treatment of iWA cells with rosiglitazone and a β-AR agonist (2 or 24 h treatment with either NE or CL316243) could further increase UCP1 function, we analyzed our OCR data, as described by Collins and colleagues (57), by defining the mitochondrial capacity that is not coupled to ATP synthesis. Rosiglitazone treatment of iWA induces a significant increase in this non-coupled spare capacity at the level of mitochondria, which is further increased in iWA also treated with either NE or CL316243 (**Figure 4**). These results indicate that the combination of both a browning agent (rosiglitazone) and a β_3-AR agonist are required for maximal effects on mitochondrial function in brite adipocytes. This demonstrates that inguinal-derived brite adipocytes are geared toward mitochondrial uncoupling (and energy expenditure), consistent with a previous report that brite adipocytes are thermogenically competent, in that their mitochondria are functional and able to uncouple *via* UCP1 (58).

UCP1 is activated upon release of fatty acids generated following adrenergic stimulation of lipolysis, however, a recent study has also demonstrated that UCP1 activity is sensitized in the presence of ROS due to sulfenylation at Cys253 (59). *In vivo*, increased ROS due to deletion of Sod2 (encoding Mn-superoxide dismutase) leads to enhanced expression of key fatty acid oxidation genes in iWAT, and elevated mitochondrial oxygen consumption (60). Furthermore, UCP1 plays a central role in protecting adipocytes from mitochondrial dysfunction in the presence of high ROS and calcium overload (61). Thus, UCP1 is both activated by and protects against the effects of increased mitochondrial ROS. Our gene expression profiling and IPA indicates that rosiglitazone treatment may have dual protective actions in iWA, by increasing expression of UCP1 and at the same time inducing Sod1, Sod2, and other genes implicated in reduced ROS synthesis (**Figure 2C**).

Culture Conditions That Promote Adipogenesis but Not Browning

Another issue raised by our study is whether it is possible to separate the effects of rosiglitazone on adipocyte differentiation from those on thermogenic programming in iWA. Certainly 7d rosiglitazone treatment promotes induction of UCP1, with further substantial increases following an additional 24 h in the presence of CL316243 (**Figures 3** and **5**). In contrast, Fabp3 and Cpt1b are increased by 7d rosiglitazone but there is no potentiation of expression by CL316243, indicating that responses to the β_3-AR agonist are in part masked by prolonged rosiglitazone treatment. The magnitude of responses was smaller when rosiglitazone was included in the cultures only for the first 3 days of the 7-day culture period, however, this protocol did provide an improved window for observing the browning effect of 24 h CL316243 over and above rosiglitazone alone, with significant increases in expression of UCP1 (96-fold). The capacity to respond to CL316243 in these 3d cultures may be dictated solely by rosiglitazone-induced expression of the β_3-AR, or it may reflect other aspects of the differentiation process. We cannot say at this time whether the 3d iWA most closely resemble the brite adipocytes seen *in vivo* (34), though profiling both 3d and 7d cultures would be worthwhile as it would facilitate a better understanding of the relationship between these adipocytes and those induced by PPARγ activation in mice.

CONCLUSION

While there is a wealth of data on the gene expression of brite adipocytes (8, 9, 56, 62–66), these studies have generally aimed to identify differential genetic markers between brown, white, and brite adipocytes. We have instead sought to determine the similarities of brite adipocytes to conventional BAs in metabolic responses and profiles of thermogenic gene expression. We have demonstrated that the induction of brite adipocytes involves the upregulation of metabolic genes associated with thermogenesis,

along with expression of β_3-ARs, and this allows for adrenergically mediated activation of UCP1. Furthermore, brite adipocytes display the adaptive capacity observed in BAs, capable of responding to sustained adrenergic stimuli. Our findings indicate that cultured white adipocytes derived from regions such as iWAT with adequate sympathetic innervation respond efficiently to agonists, but only in combination with an additional priming stimulus such as rosiglitazone. This contrasts with *in vivo* iWAT depots in which chronic sympathetic tone is sufficient to maintain the capacity for brite activation. Our results emphasize the importance of activating both browning and thermogenic programs in cultured white adipocytes in order to reach maximum browning capacity. This understanding will translate into better model systems for the screening of beige or brite capacity to combat obesity and type 2 diabetes.

ETHICS STATEMENT

All experiments were conducted with ethical permission from the Monash University Animal Ethics Committee, ethics approval numbers MIPS.2015.14 and VCP.2009.22, which complied with the National Health and Medical Research Council of Australia (NHMRC) guidelines for use of animals in scientific research.

AUTHOR CONTRIBUTIONS

JM designed and performed most of the experiments with assistance from MS and CN (confocal microscopy). RF, MP, and LC (qPCR), DH (adipocyte cultures, Seahorse studies), and BE (IPA analysis). JM, BE, and DH wrote the manuscript with help and suggestions from RS and TB. DH, BE, and TB conceived the research. All authors discussed the results and commented on the manuscript.

FUNDING

DH was supported by a National Health and Medical Research Council of Australia (NHMRC) Career Development Fellowship (545952), a Monash University Research Accelerator Program, and supported by a Bioplatforms Australia/NHMRC grant. RS is supported by a NHMRC Program Grant (519461, 1055134). MS was supported by a NHMRC International Training Fellowship (606763). JM was supported by an Australian Postgraduate Award. MP was supported by an Iranian Ministry of Health Fellowship. TB is supported by Diabetesfonden, Vinnova, and Vetenskapsrådet (Sweden).

REFERENCES

1. Cannon B, Nedergaard J. Brown adipose tissue: function and physiological significance. *Physiol Rev* (2004) 84:277–359. doi:10.1152/physrev.00015.2003
2. Summers RJ, Papaioannou M, Harris S, Evans BA. Expression of β_3-adrenoceptor mRNA in rat brain. *Br J Pharmacol* (1995) 116:2547–8. doi:10.1111/j.1476-5381.1995.tb17205.x
3. Tsujii S, Bray GA. Food intake of lean and obese Zucker rats following ventricular infusions of adrenergic agonists. *Brain Res* (1992) 587:226–32. doi:10.1016/0006-8993(92)91001-U
4. Richard JE, Lopez-Ferreras L, Chanclon B, Eerola K, Micallef P, Skibicka KP, et al. CNS beta3-adrenergic receptor activation regulates feeding behavior, white fat browning, and body weight. *Am J Physiol Endocrinol Metab* (2017) 313(3):E344–58. doi:10.1152/ajpendo.00418.2016
5. Castillo-Melendez M, McKinley MJ, Summers RJ. Intracerebroventricular administration of the beta(3)-adrenoceptor agonist CL 316243 causes Fos immunoreactivity in discrete regions of rat hypothalamus. *Neurosci Lett* (2000) 290(3):161–4. doi:10.1016/S0304-3940(00)01359-8
6. DiCioccio AT. *The Pharmacokinetics and Biodistribution of a Novel Beta3 Agonist in the Rat Utilizing Microdialysis*. Jamaica, NY: PhD, St. John's University (1997).
7. Department of Health Therapeutic Goods Adminstration. Australian public assessment report for mirabegron. (2014). Available from: https://www.tga.gov.au/auspar/auspar-mirabegron (accessed June 12, 2017).
8. Petrovic N, Walden TB, Shabalina IG, Timmons JA, Cannon B, Nedergaard J. Chronic peroxisome proliferator-activated receptor γ (PPARγ) activation of epididymally derived white adipocyte cultures reveals a population of thermogenically competent, UCP1-containing adipocytes molecularly distinct from classic brown adipocytes. *J Biol Chem* (2010) 285(10):7153–64. doi:10.1074/jbc.M109.053942
9. Wu J, Bostrom P, Sparks LM, Ye L, Choi JH, Giang AH, et al. Beige adipocytes are a distinct type of thermogenic fat cell in mouse and human. *Cell* (2012) 150(2):366–76. doi:10.1016/j.cell.2012.05.016
10. Seale P, Conroe HM, Estall J, Kajimura S, Frontini A, Ishibashi J, et al. Prdm16 determines the thermogenic program of subcutaneous white adipose tissue in mice. *J Clin Invest* (2011) 121(1):96–105. doi:10.1172/JCI44271
11. Schulz TJ, Huang P, Huang TL, Xue R, McDougall LE, Townsend KL, et al. Brown-fat paucity due to impaired BMP signalling induces compensatory browning of white fat. *Nature* (2013) 495(7441):379–83. doi:10.1038/nature11943
12. Cypess AM, White AP, Vernochet C, Schulz TJ, Xue R, Sass CA, et al. Anatomical localization, gene expression profiling and functional characterization of adult human neck brown fat. *Nat Med* (2013) 19(5):635–9. doi:10.1038/nm.3112
13. Lidell ME, Betz MJ, Dahlqvist Leinhard O, Heglind M, Elander L, Slawik M, et al. Evidence for two types of brown adipose tissue in humans. *Nat Med* (2013) 19(5):631–4. doi:10.1038/nm.3017
14. Merlin J, Evans BA, Dehvari N, Sato M, Bengtsson T, Hutchinson DS. Could burning fat start with a brite spark? Pharmacological and nutritional ways to promote thermogenesis. *Mol Nutr Food Res* (2016) 60(1):18–42. doi:10.1002/mnfr.201500251
15. Dodd GT, Decherf S, Loh K, Simonds SE, Wiede F, Balland E, et al. Leptin and insulin act on POMC neurons to promote the browning of white fat. *Cell* (2015) 160(1–2):88–104. doi:10.1016/j.cell.2014.12.022
16. Enriori PJ, Sinnayah P, Simonds SE, Garcia Rudaz C, Cowley MA. Leptin action in the dorsomedial hypothalamus increases sympathetic tone to brown adipose tissue in spite of systemic leptin resistance. *J Neurosci* (2011) 31(34):12189–97. doi:10.1523/JNEUROSCI.2336-11.2011
17. Cypess AM, Weiner LS, Roberts-Toler C, Elia EF, Kessler SH, Kahn PA, et al. Activation of human brown adipose tissue by a β_3-adrenergic receptor agonist. *Cell Metab* (2015) 21(1):33–8. doi:10.1016/j.cmet.2014.12.009
18. Fischer-Posovszky P, Newell FS, Wabitsch M, Tornqvist HE. Human SGBS cells – a unique tool for studies of human fat cell biology. *Obes Facts* (2008) 1(4):184–9. doi:10.1159/000145784
19. Schulz TJ, Huang TL, Tran TT, Zhang H, Townsend KL, Shadrach JL, et al. Identification of inducible brown adipocyte progenitors residing in skeletal muscle and white fat. *Proc Natl Acad Sci U S A* (2011) 108(1):143–8. doi:10.1073/pnas.1010929108
20. Bostrom P, Wu J, Jedrychowski MP, Korde A, Ye L, Lo JC, et al. A PGC1-α-dependent myokine that drives brown-fat-like development of white fat and thermogenesis. *Nature* (2012) 481(7382):463–8. doi:10.1038/nature10777
21. Gnad T, Scheibler S, von Kugelgen I, Scheele C, Kilic A, Glode A, et al. Adenosine activates brown adipose tissue and recruits beige adipocytes via A2A receptors. *Nature* (2014) 516(7531):395–9. doi:10.1038/nature13816
22. Roberts LD, Bostrom P, O'Sullivan JF, Schinzel RT, Lewis GD, Dejam A, et al. β-Aminoisobutyric acid induces browning of white fat and hepatic β-oxidation and is inversely correlated with cardiometabolic risk factors. *Cell Metab* (2014) 19(1):96–108. doi:10.1016/j.cmet.2013.12.003

23. Li YL, Li X, Jiang TT, Fan JM, Zheng XL, Shi XE, et al. An additive effect of promoting thermogenic gene expression in mice adipose-derived stromal vascular cells by combination of rosiglitazone and CL316,243. *Int J Mol Sci* (2017) 18(5):1002. doi:10.3390/ijms18051002
24. Nechad M, Kuusela P, Carneheim C, Bjorntorp P, Nedergaard J, Cannon B. Development of brown fat cells in monolayer culture. I. Morphological and biochemical distinction from white fat cells in culture. *Exp Cell Res* (1983) 149(1):105–18.
25. Kramer A, Green J, Pollard J Jr, Tugendreich S. Causal analysis approaches in Ingenuity Pathway Analysis. *Bioinformatics* (2014) 30(4):523–30. doi:10.1093/bioinformatics/btt703
26. Hao Q, Yadav R, Basse AL, Petersen S, Sonne SB, Rasmussen S, et al. Transcriptome profiling of brown adipose tissue during cold exposure reveals extensive regulation of glucose metabolism. *Am J Physiol Endocrinol Metab* (2015) 308(5):E380–92. doi:10.1152/ajpendo.00277.2014
27. Schindelin J, Arganda-Carreras I, Frise E, Kaynig V, Longair M, Pietzsch T, et al. Fiji: an open-source platform for biological-image analysis. *Nat Methods* (2012) 9(7):676–82. doi:10.1038/nmeth.2019
28. Nadanaciva S, Rana P, Beeson GC, Chen D, Ferrick DA, Beeson CC, et al. Assessment of drug-induced mitochondrial dysfunction via altered cellular respiration and acidification measured in a 96-well platform. *J Bioenerg Biomembr* (2012) 44(4):421–37. doi:10.1007/s10863-012-9446-z
29. Merlin J, Sato M, Nowell C, Pakzad M, Fahey R, Gao J, et al. The PPARγ agonist rosiglitazone promotes the induction of brite adipocytes, increasing β-adrenoceptor-mediated mitochondrial function and glucose uptake. *Cell Signal* (2018) 42:54–66. doi:10.1016/j.cellsig.2017.09.023
30. Vergnes L, Chin R, Young SG, Reue K. Heart-type fatty acid-binding protein is essential for efficient brown adipose tissue fatty acid oxidation and cold tolerance. *J Biol Chem* (2011) 286(1):380–90. doi:10.1074/jbc.M110.184754
31. Olsen JM, Sato M, Dallner OS, Sandstrom AL, Pisani DF, Chambard JC, et al. Glucose uptake in brown fat cells is dependent on mTOR complex 2-promoted GLUT1 translocation. *J Cell Biol* (2014) 207(3):365–74. doi:10.1083/jcb.201403080
32. Rong JX, Qiu Y, Hansen MK, Zhu L, Zhang V, Xie M, et al. Adipose mitochondrial biogenesis is suppressed in db/db and high-fat diet-fed mice and improved by rosiglitazone. *Diabetes* (2007) 56(7):1751–60. doi:10.2337/db06-1135
33. Fisher FM, Kleiner S, Douris N, Fox EC, Mepani RJ, Verdeguer F, et al. FGF21 regulates PGC-1α and browning of white adipose tissues in adaptive thermogenesis. *Genes Dev* (2012) 26(3):271–81. doi:10.1101/gad.177857.111
34. Wang H, Liu L, Lin JZ, Aprahamian TR, Farmer SR. Browning of white adipose tissue with roscovitine induces a distinct population of UCP1(+) adipocytes. *Cell Metab* (2016) 24(6):835–47. doi:10.1016/j.cmet.2016.10.005
35. Contreras GA, Lee YH, Mottillo EP, Granneman JG. Inducible brown adipocytes in subcutaneous inguinal white fat: the role of continuous sympathetic stimulation. *Am J Physiol Endocrinol Metab* (2014) 307(9):E793–9. doi:10.1152/ajpendo.00033.2014
36. Abreu-Vieira G, Fischer AW, Mattsson C, de Jong JM, Shabalina IG, Ryden M, et al. Cidea improves the metabolic profile through expansion of adipose tissue. *Nat Commun* (2015) 6:7433. doi:10.1038/ncomms8433
37. Festuccia WT, Blanchard PG, Richard D, Deshaies Y. Basal adrenergic tone is required for maximal stimulation of rat brown adipose tissue UCP1 expression by chronic PPARγ activation. *Am J Physiol Regul Integr Comp Physiol* (2010) 299(1):R159–67. doi:10.1152/ajpregu.00821.2009
38. Nedergaard J, Bengtsson T, Cannon B. Unexpected evidence for active brown adipose tissue in adult humans. *Am J Physiol Endocrinol Metab* (2007) 293(2):E444–52. doi:10.1152/ajpendo.00691.2006
39. Cypess AM, Lehman S, Williams G, Tal I, Rodman D, Goldfine AB, et al. Identification and importance of brown adipose tissue in adult humans. *N Engl J Med* (2009) 360(15):1509–17. doi:10.1056/NEJMoa0810780
40. van Marken Lichtenbelt WD, Vanhommerig JW, Smulders NM, Drossaerts JM, Kemerink GJ, Bouvy ND, et al. Cold-activated brown adipose tissue in healthy men. *N Engl J Med* (2009) 360(15):1500–8. doi:10.1056/NEJMoa0808718
41. Virtanen KA, Lidell ME, Orava J, Heglind M, Westergren R, Niemi T, et al. Functional brown adipose tissue in healthy adults. *N Engl J Med* (2009) 360(15):1518–25. doi:10.1056/NEJMoa0808949
42. Nagase I, Yoshida T, Kumamoto K, Umekawa T, Sakane N, Nikami H, et al. Expression of uncoupling protein in skeletal muscle and white fat of obese mice treated with thermogenic β_3-adrenergic agonist. *J Clin Invest* (1996) 97(12):2898–904. doi:10.1172/JCI118748
43. Collins S, Daniel KW, Petro AE, Surwit RS. Strain-specific response to β_3-adrenergic receptor agonist treatment of diet-induced obesity in mice. *Endocrinology* (1997) 138(1):405–13. doi:10.1210/endo.138.1.4829
44. Inokuma K, Okamatsu-Ogura Y, Omachi A, Matsushita Y, Kimura K, Yamashita H, et al. Indispensable role of mitochondrial UCP1 for antiobesity effect of β_3-adrenergic stimulation. *Am J Physiol Endocrinol Metab* (2006) 290(5):E1014–21. doi:10.1152/ajpendo.00105.2005
45. Kim H, Pennisi PA, Gavrilova O, Pack S, Jou W, Setser-Portas J, et al. Effect of adipocyte β_3-adrenergic receptor activation on the type 2 diabetic MKR mice. *Am J Physiol Endocrinol Metab* (2006) 290(6):E1227–36. doi:10.1152/ajpendo.00344.2005
46. Arch JR. Challenges in β_3-adrenoceptor agonist drug development. *Ther Adv Endocrinol Metab* (2011) 2(2):59–64. doi:10.1177/2042018811398517
47. Arch JR. Thermogenesis and related metabolic targets in anti-diabetic therapy. *Handb Exp Pharmacol* (2011) 203:201–55. doi:10.1007/978-3-642-17214-4_10
48. Scheele C, Larsen TJ, Nielsen S. Novel nuances of human brown fat. *Adipocyte* (2014) 3(1):54–7. doi:10.4161/adip.26520
49. Sharp LZ, Shinoda K, Ohno H, Scheel DW, Tomoda E, Ruiz L, et al. Human BAT possesses molecular signatures that resemble beige/brite cells. *PLoS One* (2012) 7(11):e49452. doi:10.1371/journal.pone.0049452
50. Bouillaud F, Ricquier D, Mory G, Thibault J. Increased level of mRNA for the uncoupling protein in brown adipose tissue of rats during thermogenesis induced by cold exposure or norepinephrine infusion. *J Biol Chem* (1984) 259(18):11583–6.
51. Nedergaard J, Cannon B. [^{3}H]GDP binding and thermogenin amount in brown adipose tissue mitochondria from cold-exposed rats. *Am J Physiol* (1985) 248(3 Pt 1):C365–71. doi:10.1152/ajpcell.1985.248.3.C365
52. Desautels M, Dulos RA, Mozaffari B. Selective loss of uncoupling protein from mitochondria of surgically denervated brown adipose tissue of cold-acclimated mice. *Biochem Cell Biol* (1986) 64(11):1125–34. doi:10.1139/o86-148
53. Nisoli E, Tonello C, Landi M, Carruba MO. Functional studies of the first selective β_3-adrenergic receptor antagonist SR 59230A in rat brown adipocytes. *Mol Pharmacol* (1996) 49(1):7–14.
54. Tonello C, Dioni L, Briscini L, Nisoli E, Carruba MO. SR59230A blocks β_3-adrenoceptor-linked modulation of uncoupling protein-1 and leptin in rat brown adipocytes. *Eur J Pharmacol* (1998) 352(1):125–9. doi:10.1016/S0014-2999(98)00404-X
55. Feldmann HM, Golozoubova V, Cannon B, Nedergaard J. UCP1 ablation induces obesity and abolishes diet-induced thermogenesis in mice exempt from thermal stress by living at thermoneutrality. *Cell Metab* (2009) 9(2):203–9. doi:10.1016/j.cmet.2008.12.014
56. Walden TB, Hansen IR, Timmons JA, Cannon B, Nedergaard J. Recruited vs. nonrecruited molecular signatures of brown, "brite," and white adipose tissues. *Am J Physiol Endocrinol Metab* (2012) 302(1):E19–31. doi:10.1152/ajpendo.00249.2011
57. Yehuda-Shnaidman E, Buehrer B, Pi J, Kumar N, Collins S. Acute stimulation of white adipocyte respiration by PKA-induced lipolysis. *Diabetes* (2010) 59(10):2474–83. doi:10.2337/db10-0245
58. Shabalina IG, Petrovic N, de Jong JM, Kalinovich AV, Cannon B, Nedergaard J. UCP1 in brite/beige adipose tissue mitochondria is functionally thermogenic. *Cell Rep* (2013) 5:1196–203. doi:10.1016/j.celrep.2013.10.044
59. Chouchani ET, Kazak L, Jedrychowski MP, Lu GZ, Erickson BK, Szpyt J, et al. Mitochondrial ROS regulate thermogenic energy expenditure and sulfenylation of UCP1. *Nature* (2016) 532(7597):112–6. doi:10.1038/nature17399
60. Han YH, Buffolo M, Pires KM, Pei S, Scherer PE, Boudina S. Adipocyte-specific deletion of manganese superoxide dismutase protects from diet-induced obesity through increased mitochondrial uncoupling and biogenesis. *Diabetes* (2016) 65(9):2639–51. doi:10.2337/db16-0283
61. Kazak L, Chouchani ET, Stavrovskaya IG, Lu GZ, Jedrychowski MP, Egan DF, et al. UCP1 deficiency causes brown fat respiratory chain depletion and sensitizes mitochondria to calcium overload-induced dysfunction. *Proc Natl Acad Sci U S A* (2017) 114(30):7981–6. doi:10.1073/pnas.1705406114
62. Timmons JA, Wennmalm K, Larsson O, Walden TB, Lassmann T, Petrovic N, et al. Myogenic gene expression signature establishes that brown and white adipocytes originate from distinct cell lineages. *Proc Natl Acad Sci U S A* (2007) 104(11):4401–6. doi:10.1073/pnas.0610615104
63. Jespersen NZ, Larsen TJ, Peijs L, Daugaard S, Homoe P, Loft A, et al. A classical brown adipose tissue mRNA signature partly overlaps with brite in

the supraclavicular region of adult humans. *Cell Metab* (2013) 17(5):798–805. doi:10.1016/j.cmet.2013.04.011

64. Rosenwald M, Perdikari A, Rulicke T, Wolfrum C. Bi-directional interconversion of brite and white adipocytes. *Nat Cell Biol* (2013) 15(6):659–67. doi:10.1038/ncb2740
65. Rosell M, Kaforou M, Frontini A, Okolo A, Chan YW, Nikolopoulou E, et al. Brown and white adipose tissues: intrinsic differences in gene expression and response to cold exposure in mice. *Am J Physiol Endocrinol Metab* (2014) 306(8):E945–64. doi:10.1152/ajpendo.00473.2013
66. de Jong JM, Larsson O, Cannon B, Nedergaard J. A stringent validation of mouse adipose tissue identity markers. *Am J Physiol Endocrinol Metab* (2015) 308(12):E1085–105. doi:10.1152/ajpendo.00023.2015

Conflict of Interest Statement: TB owns stocks in the following pharmaceutical companies: Sigrid Therapeutics AB, Atrogi AB, and Glucox Biotechnology AB. DH owns stocks in Glucox Biotechnology AB. DH and RS are consultants for Atrogi AB.

frontiers in Endocrinology

ORIGINAL RESEARCH
published: 10 October 2018
doi: 10.3389/fendo.2018.00549

Association Between Different Indicators of Obesity and Depression in Adults in Qingdao, China: A Cross-Sectional Study

Jing Cui[1,2†], Xiufen Sun[3†], Xiaojing Li[1,2†], Ma Ke[4], Jianping Sun[1,2], Nafeesa Yasmeen[5], Jamal Muhammad Khan[6], Hualei Xin[1,2], Shouyong Xue[7] and Zulqarnain Baloch[8*]*

[1] Qingdao Municipal Center for Disease Control and Prevention, Qingdao, China, [2] Qingdao Institute of Preventive Medicine, Qingdao, China, [3] Qingdao Shi'nan Municipal Center for Disease Control and Prevention, Qingdao, China, [4] College of Traditional Chinese Medicine, Shandong University of Traditional Chinese Medicine, Jinan, China, [5] Institute of Microbiology, Agriculture University Faisalabad Pakistan, Bahawalpur, Pakistan, [6] Department of Patho-biology, The Islamia University of Bahawalpur, University College of Veterinary and Animal Sciences, Bahawalpur, Pakistan, [7] Qingdao Shi'bei Municipal Center for Disease Control and Prevention, Qingdao, China, [8] College of Veterinary Medicine, South China Agricultural University, Guangzhou, China

OPEN ACCESS

Edited by:
Andrew J. McAinch,
Victoria University, Australia

Reviewed by:
Scott B. Teasdale,
University of New South Wales, Australia
Guoqin Xu,
Guangzhou Sport University, China

***Correspondence:**
Shouyong Xue
sbjkxue@163.com
Zulqarnain Baloch
znbalooch@yahoo.com

[†]These authors have contributed equally to this work

Specialty section:
This article was submitted to Obesity, a section of the journal Frontiers in Endocrinology

Received: 26 May 2018
Accepted: 29 August 2018
Published: 10 October 2018

Citation:
Cui J, Sun X, Li X, Ke M, Sun J, Yasmeen N, Khan JM, Xin H, Xue S and Baloch Z (2018) Association Between Different Indicators of Obesity and Depression in Adults in Qingdao, China: A Cross-Sectional Study. Front. Endocrinol. 9:549. doi: 10.3389/fendo.2018.00549

Background: This study was designed to investigate the perceived relationship between body weight and depression risk in a Chinese population in Qingdao, China.

Methods: A population-based cross-sectional survey was performed with 4,573 participants (between 35 and 74 years) from the year 2009 to 2012 in Qingdao, China. We applied the Zung self-rating depression scale to ascertain the level of depression in participants. The associations between different indicators of obesity [body mass index (BMI), waist circumference (WC), and waist-to-hip ratio (WHR)] and depression were assessed by logistic regression based on the Chinese criteria of obesity. Sensitivity analysis was done based on the Asian and WHO criteria of obesity.

Results: The Zung scores for the 243 participants (5.2%) were over 45 and they were entitled as depression. Furthermore, multivariable logistic analyses revealed that being overweight [odds ratios (OR): 1.48, 95% confidence intervals [95% CI]: 1.08–2.03] and having abdominal obesity (WC category in Chinese criteria) (OR: 1.47, 95% CI: 1.08-2.00) were often associated with a higher risk for depression compared to normal weight subjects. Sensitivity analysis revealed that abdominal obesity (Asian criterion) (OR: 1.41, 95% CI: 1.03-1.91) was a significant risk factor for depression. Similarly, being overweight (WHO criterion) (OR: 1.39, 95% CI: 1.03-1.87) was an obvious risk factor for depression.

Conclusion: Being overweight and having abdominal obesity (WC category) were found to be linked with a higher risk of depression. However, abdominal obesity (WHR category) was not associated with depression.

Keywords: depression, body mass index, waist circumference, waist-to-hip ratio, cross-sectional study

Abbreviations: BMI, Body mass index; CI, Confidence intervalsl; OR, Odds ratio; WC, waist circumference; WHO, World Health Organisation.

INTRODUCTION

Significant progress has indeed been made in improving public health in the world; however, many serious health issues still need to be resolved such as depression and obesity. The global prevalence of being overweight and obese was estimated to be 39% and 13% in adults aged 18 years and over in 2017, respectively (1). In 2018, the World Health Organization (WHO) estimates that depression is seen to affect approximately 300 million people worldwide (2). In China, the prevalence of obesity has been continuously increasing during the last few decades (3–5). Additionally, depression is also frequently diagnosed at public and private clinics. According to health officials, approximately 26 million people are struggling with symptoms of mild depression annually in China (6).

Several population-based studies conducted in Western countries demonstrated that the risk for depression was positively associated with being overweight and obesity (7–12). In another study, a U-shaped association between BMI and depression has been reported (10). However, estimates obtained from the Chinese population are found to be controversial (13–15). Several research activities have reported a negative correlation between the risk for depression and obesity among middle-aged and the elderly Chinese (13, 14). In contrast, Li et al. observed a significant positive association between obesity and increased depression scores in the Chinese elderly (aged ≥ 65 years) (15). Nonetheless, mechanisms underlying the association between obesity and depression are still unclear. Some studies have shown that the brain–reward regions for depression and obesity, such as the dopaminergic pathways, can enhance positive mood. Yet, they also cause increased intake of "comfort" food, which may lead to obesity (16, 17). As a matter of fact, the perceptions regarding obesity are different between the Western world and the Chinese. While obesity is a stigma in Western countries (18), it is considered as a symbol of wealth in China (13–15). Regardless of these differences, it may be due to population diversity, different body weight criteria, and depression standards in China.

The association between obesity and depression has been normally studied in adolescents and the elderly population in China (19–21); yet there is a need to explore various indicators of obesity in detail. Hence, this large population-based cross-sectional survey was carried out to assess the potential relationship between depression and different body weight levels among the general population of Qingdao, China.

METHODS

Ethical Considerations

All the participants voluntarily signed the consent prior to their participation. The security, anonymity, and the privacy of participants were strictly respected. This study was approved by the Ethics Committee of the Qingdao Municipal Center for Disease Control and Prevention.

Study Population

This cross-sectional population-based survey was conducted in the eastern city of Qingdao, Mainland China during 2009 to 2012. Inclusion and exclusion criteria have already been described in our previous study (22). Briefly, a total of 6,100 Chinese adults (between 35-74 years old) were selected with a stratified, random cluster sampling procedure and invited to participate in the survey. A total of 5,110 individuals agreed to take part in our survey, with a response rate of 83.8%. From the 5,110 individuals, 454 participants were excluded due to an insufficient Zung score or body mass index (BMI) or waist circumference (WC) or waist-to-hip ratio (WHR) baseline information. Therefore, results from the current study were based on data from 4,656 participants, accounting for 76.3% of the initially invited individuals.

Questionnaires

A standard questionnaire was designed to collect basic information which included age, gender, marital status, educational background, occupation, smoking, and alcohol consumption. The marital status was divided into married/cohabiting and unmarried (single, divorced, or widowed). Educational attainment was categorized into three groups: illiterate/ elementary school, junior high school, and senior high school or higher. Occupational physical activity (PA) was categorized into light (housewife, retired, or unemployed), moderate (teacher, doctor, or nurse), and heavy (worker, farmer, or fisherman), according to occupation. Smoking was classified into current smokers (smoking every day and occasional smoking in the past years) and noncurrent smokers (including ex-smokers and nonsmokers). Alcohol consumption was categorized into regular drinkers (drinking every day in the past years) and noncurrent drinkers (including ex-drinkers, rare drinkers, and nondrinkers). Personal monthly income was categorized into ≤999 Chinese Yuan (CNY), 1,000–2,999 CNY, and ≥3,000 CNY.

The plasma glucose level was determined by the glucose oxidase method. All subjects (without prediagnosed diabetes) underwent a standard 2-h 75-g oral glucose tolerance test. Diabetes was diagnosed on the basis of the WHO/International Diabetes Federation criteria (23). Subjects with fasting plasma glucose (FPG) level of ≥7.0 mmol/l and/or 2-h postload plasma glucose (2-hPG) level of ≥11.0 mmol/l were diagnosed with diabetes. The individual was taken as nondiabetic if FPG was <7.0 mmol/l and/or 2-hPG <11.1 mmol/l.

Blood pressure was measured using a mercury sphygmomanometer. Measurements were taken three times in 5-min intervals. The mean of the three readings was used for data analysis. Hypertension was defined by a mean systolic blood pressure of ≥140 mmHg and/or a mean diastolic blood pressure of ≥90 mmHg and/or an established diagnosis of hypertension at the baseline (24).

Anthropometric Measurement

We measured the participant's height and weight while wearing light clothes and no shoes. The BMI was calculated as the weight in kilograms divided by the height in squared meters (kg/m^2). Waist circumference (WC) was measured at the midpoint between the lower rib margin and the iliac crest. Hip circumference (HC) was measured at the maximal horizontal

girth between the waist and the thigh. The WHR was calculated by dividing WC (in cm) by HC (cm).

Assessment of Depression

Depression was assessed using the Zung Depression Rating Scale (ZDRS) (25, 26). The ZDRS questionnaire contains 20 questions divided into 10 positively and 10 negatively phrased questions. Each question was scored as 1 through 4, and the total scores ranged from 20 to 80 based on the participant's feelings (sadness, indifference, or happiness) toward family, work, and living conditions, respectively. Participants were divided into two major groups: normal (20–44) and depressed (≥45) (25).

Criteria for Obesity

Overweight and obesity were defined in accordance with the published criteria (26, 27). According to the Chinese criteria, subjects were divided into four BMI categorical groups as: underweight (BMI <18.5 kg/m^2), normal weight (18.5–23.9 kg/m^2), overweight (24.0–27.9 kg/m^2), and obese (≥28.0 kg/m^2). According to Asian criteria, subjects were subdivided as: underweight (BMI <18.5 kg/m^2), normal weight (18.5–22.9 kg/m^2), overweight (23.0–24.9 kg/m^2), and obese (≥25.0 kg/m^2) (27) and according to the WHO criteria as: underweight (BMI < 18.5 kg/m^2), normal weight (18.5–24.9 kg/m^2), overweight (25.0–29.9 kg/m^2), and obese (≥30.0 kg/m^2) (28).

Based on the value of WC, subjects were further subdivided into two groups as follows: normal (<85.0 cm for males and <80.0 cm for females); abdominal obesity, (≥85.0 cm for males and ≥80.0 cm for females) according to Chinese criteria (26). Alternatively, subjects were subdivided into: normal (<90.0 cm for males and <80.0 cm for females) and abdominal obesity, (≥90.0 cm for males and ≥ 80.0 cm for females) according to the Asian guidelines (27). Finally, according to the WHO guidelines, subjects were divided into normal (<94.0 cm for males and < 80.0 cm for females) and abdominal obesity (≥94.0 cm for males and ≥80.0 cm for females) (28).

Subjects were divided into two categories based on their WHR cutoffs points (Chinese guidelines): normal (<0.9 for males and <0.85 for females) and abdominal obesity (≥0.90 for males and ≥ 0.85 for females) (26); or the Asian WHR cutoff points: normal (<0.95 for males and <0.80 for females) and abdominal obesity (≥0.95 for males and ≥0.80 for females) (29) or the WHO WHR cutoff points: normal (<1.00 for males and <0.85 for females) and abdominal obesity (≥1.00 for males and ≥0.85 for females) (28).

Statistical Analysis

Statistical analyses were performed using IBM SPSS Statistics 17.0. Continuous variables and categorical variables were presented as the mean ± standard deviation and the number (percentages), respectively. Using data from the 2010 census in Qingdao, the age-standardized prevalence of depression was calculated according to different obesity criterion for the age group of 35–74 years. Logistic regression was used to determine the possible link between the risk for depression and different indicators of obesity (BMI, WC, and WHR). Odds ratios (ORs) and 95% confidence intervals (CIs) were estimated by logistic regression to obtain the association between depression and each variable. Sensitivity analysis was done based on the Asian and WHO criteria of obesity. A *P*-value <0.05 was considered to be statistically significant.

RESULTS

The demographic information, social-economic status, lifestyle information, and anthropometric measurement have been shown in **Table 1**. In this study, a total of 4,656 participants were enrolled; among them, 1,804 were males (38.6%) and 2,852 were females (61.4%). The mean age was 52.3 ± 10.7 years (rang 35–74 years).

TABLE 1 | Characteristics of the population included in the study.

Characteristic	Total *N* = 4,656
Sex, female, *n* (%)	2852 (61.3)
Age, years (mean ± SD)	52.3 ± 10.7
Zung score (mean ± SD)	29.8 ± 7.9
Depression, *n* (%)	243 (5.2)
BMI (kg/m2, mean ± SD)?	25.0 ± 3.7
Normal, *n* (%)	1871 (40.2)
Underweight, *n* (%)	83 (1.8)
Overweight, *n* (%)	1815 (39.0)
Obese, *n* (%)	887 (19.1)
WC (cm, mean ± SD)?	83.8 ± 10.6
Normal, *n* (%)	1982 (42.6)
Abdominal obesity, *n* (%)	2674 (57.4)
WHR (mean ± SD) ?	0.87 ± 0.07
Normal, *n* (%)	2306 (49.5)
Abdominal obesity, *n* (%)	2350 (50.5)
Hypertension, *n* (%)	2159 (46.5)
Diabetes, *n* (%)	741 (15.9)
Urban living, *n* (%)	1384 (29.7)
Married, *n* (%)	4361 (93.7)
EDUCATIONAL ATTAINMENT, *n* (%)	
Illiterate /elementary school	1904 (41.0)
Junior high school	1723 (37.1)
Senior high school or higher	1022 (22.0)
OCCUPATIONAL PA, *n* (%)	
Light	483 (10.5)
Moderate	346 (7.5)
Heavy	3796 (82.1)
Current smoker, *n* (%)	1137 (24.8)
Current drinker, *n* (%)	751 (16.1)
INCOME (CNY/MONTH), *n* (%)	
≤599	2372 (52.4)
600–1999	1820 (40.2)
≥2000	332 (7.4)

BMI, body mass index; WC, waist circumference; HC, hip circumference; WHR, waist-to-hip ratio; PA, physical activity; CNY, Chinese Yuan. ? obesity and abdominal obesity is defined according to Chinese criteria. n, number.

According to the BMI category, the age-standardized prevalence of depression was higher in underweight (10.5%) and overweight participants (6.0%) compared with the normal weight (4.3%); however, the difference was not statistically significant. Based on the WC category, a slightly higher age-standardized prevalence of depression was observed in the abdominal obesity participants (5.7%) compared with the normal WC participants (4.3%), and the difference was statistically significant. The corresponding age-standardized prevalence of depression was 5.5% in normal WHR participants and 4.7% in the abdominal obesity participants, respectively, and the difference was nonsignificant. The age-standardized prevalence of depression according to BMI, WC, and WHR has shown in **Figure 1**.

In this study, we determined the role of potential risk factors in depression using multivariable regression analysis according to the Chinese criterion (**Table 2**). Overweight indicated higher risk of depression (OR: 1.49, 95%CI: 1.08-2.05) compared with normal weight. We observed a significant relationship between abdominal obesity and depression risk according to WC.

Next, we performed a sensitivity analysis according to the Asian and WHO criteria (model 1 and model 2, respectively; **Table 3**). In model 1, sensitivity analysis based on Asian criterion revealed that overweight and obesity (BMI category) were not significantly associated with depression, while abdominal obesity (according to WC) was significantly associated with depression similar to that of Chinese criterion. In model 2, based on the WHO criterion, abdominal obesity (according to WC) was not significantly associated with depression, while overweight participants in the BMI category were significantly associated with depression.

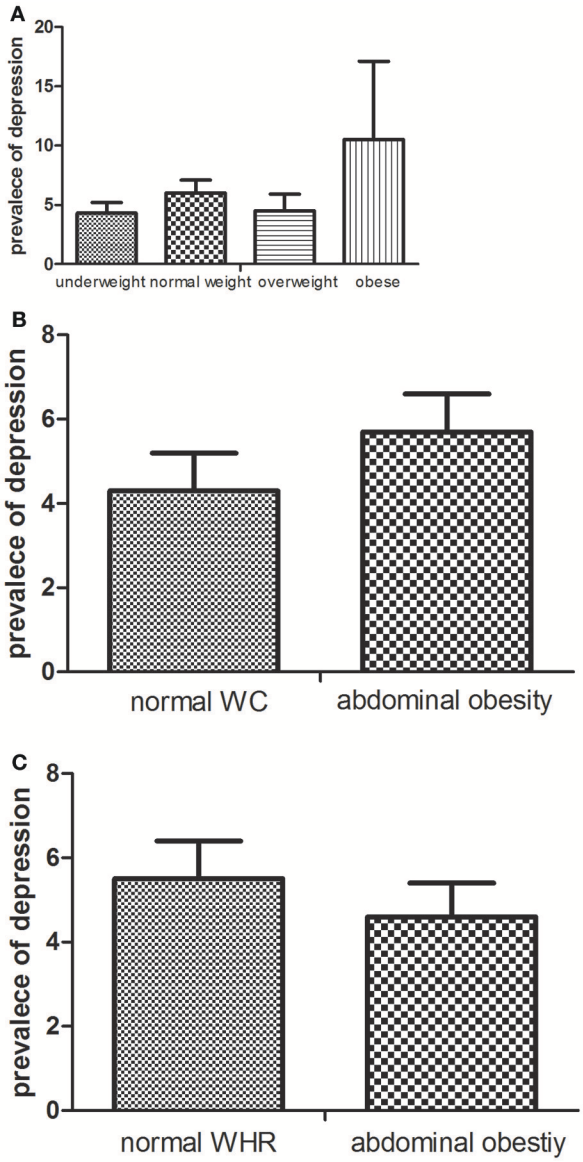

FIGURE 1 | The age-standardized prevalence (%) of depression according to BMI **(A)**, WC **(B)**, and WHR **(C)**.

DISCUSSION

In this study, we investigated the association between depression and body weight among adult people in Qingdao, China. Our results showed that the prevalence of depression was higher among the overweight participants (according to BMI category in China) and abdominal obesity participants (according to WC category in China) compared with other groups. Additionally, we defined prevalence of depression by using a Zung score equal to or greater than 45. In Qingdao, the overall prevalence of depression rate of 5.2% (5.5% in males and 5.0% in females) was lower than the documented rates in South Korea (overall 5.7%, 3.9% in males and 7.0% in females) (30). Additionally, a cross-sectional study of 512 891 Chinese adults, aged 30–79 years, had also revealed a lower pooled prevalence of depression compared with the current study (2.4%) (31). This difference might be due to social and family factors. Residents of the eastern coastal areas could not convincingly adapt to rapid industrialization and urbanization; thus it lead to depression. Secondly, accompanied with China entering the aging society, the "empty nest" phenomenon is the leading cause of unaccompanied, unattended, and psychosocial problems (such as depression) in middle-aged and elderly adults (32, 33). Depression, in turn, affects the middle-aged and the elderly population's social and physical activities, which strongly influenced the wellbeing of elderly adults (34).

The prevalence of depression is higher in underweight than normal individuals. However, there was an insignificant positive association between underweight and depression in general adults in Mainland China. Our results are inconsistent with the estimates reported in Japan, Korea, and Taiwan (13, 30, 35, 36). These trends can be observed in different age populations, and underweight elderly adults are far more likely to be depressed (13, 30, 35, 36). Yet, the common population tends to have a distortion of body weight, which entitles thinness as a beauty symbol owing to social standard (37). Our observations also support this fact.

TABLE 2 | Risk factors associated with depression determined by multivariable logistic regression according to the Chinese criterion.

	Model 1	Model 2	Model 3
Female	1.09 (0.72–1.62)	1.05 (0.70–1.56)	1.09 (0.73–1.62)
age	1.01 (1.00–1.03)	1.01 (1.00–1.03)	1.01 (1.00–1.03)
BMI CATEGORY			
Normal	1.00		
Underweight	1.24 (0.44–3.50)		
Overweight	**1.48 (1.08–2.03)***		
Obese	1.16 (0.76–1.78)		
WC CATEGORY			
Abdominal obesity		**1.47 (1.08–2.00)***	
WHR CATEGORY			
Abdominal obesity			0.86 (0.64–1.17)
Hypertension	0.81 (0.60–1.10)	0.78 (0.58–1.06)	0.86 (0.64–1.17)
Diabetes	0.81 (0.55–1.21)	0.80 (0.54–1.19)	0.84 (0.56–1.24)
Urban living	1.45 (0.95–2.22)	1.44 (0.95–2.20)	1.49 (0.98–2.28)
Unmarried	**1.96 (1.26–3.06)***	**1.93 (1.24–3.01)***	**1.93 (1.24–3.01)***
EDUCATIONAL ATTAINMENT			
Illiterate /elementary school	1.00	1.00	1.00
Junior high school	0.81 (0.55–1.19)	0.79 (0.54–1.16)	0.79 (0.54–1.17)
Senior high school or higher	0.69 (0.41–1.14)	0.68 (0.41–1.13)	0.66 (0.40–1.11)
OCCUPATIONAL PHYSICAL ACTIVITY			
Light	1.00	1.00	1.00
Moderate	0.88 (0.48–1.61)	0.86 (0.47–1.56)	0.90 (0.49–1.64)
Heavy	0.71 (0.46–1.11)	0.72 (0.46–1.12)	0.72 (0.46–1.12)
Current smoker	0.76 (0.51–1.15)	0.77 (0.51–1.16)	0.79 (0.52–1.19)
Current drinker	0.85 (0.55–1.31)	0.84 (0.55–1.30)	0.86 (0.56–1.32)
INCOME (CHINESE YUAN/MONTH)			
≤599	1.00	1.00	1.00
600–1999	0.91 (0.49–1.71)	0.92 (0.49–1.71)	0.91 (0.48–1.70)
≥2000	1.14 (0.65–2.00)	1.14 (0.65–2.00)	1.12 (0.64–1.98)

*Model 1, model 2 and Model 3, the risk factors listed in the table were entered at the same time.*P < 0.05 for factors associated with depression.*

TABLE 3 | Sensitivity analyses for depression according to the Asian and WHO criteria.

	Model 1	Model 2
BMI CATEGORY		
Normal	1.00	1.00
Underweight	1.20 (0.42–3.42)	1.14 (0.41–3.21)
Overweight	1.14 (0.75–1.71)	**1.39 (1.03–1.87)***
Obese	1.33 (0.95–1.88)	0.56 (0.28–1.13)
WC CATEGORY		
Abdominal obesity	**1.41 (1.03–1.91)***	1.32 (0.96–1.82)
WHR CATEGORY		
Abdominal obesity	1.19 (0.83–1.70)	1.02 (0.72–1.46)

*Model 1 is according to Asia criterion. Model 2 is according to WHO criterion. All models were adjusted for gender, age, hypertension, diabetes, resident districts, marital status, educational attainment, occupational physical activity, smoking status, alcohol drinking status, personal monthly income. BMI category, WC category, and WHR category entered models separately. *P < 0.05 for factors associated with depression.*

The prevalence of depression was higher in overweight and abdominal obesity (WC category) participants compared with the normal participants. In contrast, we did not observe a similar association in obese and abdominal obesity (WHR category) participants. This trend can be explained by the Chinese cultural heritage that usually associates overweight with a higher economic status, since those who can afford to eat more could attain more body weight and vice versa. In China, prevalence of obesity was substantially higher in rich people (38, 39). The overweight carries a social stigma, such as body image, self-esteem, and social life, which can help a bit for depression (40).

In this study, our analysis revealed a significant positive association between being overweight and depression, while a nonsignificant association between being obese and depression. However, the association of BMI with depression is still controversial. A nonsignificant positive relationship between being overweight and depression has been reported in developed countries such as Canada (41). Additionally, Palinkas et al. observed a nonsignificant inverse association between being overweight and depression in women (42). Moreover, a nonsignificant negative association between depression and obesity has also been reported previously (12, 43). In contrast, several studies reported a significant positive association between depression and obesity (11, 12, 20, 21, 44, 45). Young people regarded thinness as a beauty symbol. However, middle-aged and elderly people are still more likely to view obesity as a symbol of wealth and happiness in the traditional Chinese culture. Meanwhile, in this study, participants are mainly middle-aged and the elderly people aged 35 years or over, which is the possible reason for the current observations.

Next, we examined the effect of abdominal obesity on depression. We observed a significant positive association between abdominal obesity and depression. These results are in agreement with those of Takeuchi et al. (46) and Vogelzangs et al. (47). In contrast, Herva et al. (48), Gil et al. (49), and Zavala GA (12) reported a nonsignificant positive association between depression and abdominal obesity. The absence of significant associations between abdominal obesity (WHR category) and depression were inconsistent with the results reported by Ahlberg et al. (50).

Here, for the first time, we reported a significant association between being overweight, abdominal obesity (WC category), and depression in the general population of Qingdao China, but not in obese or abdominal obesity (WHR category) participants, which might be due to the following reasons. First, cultural factors are known to influence the association between depression and body weight. A higher socioeconomic status is generally associated with more concern for body image and abnormal body weight, which can possibly be a stress factor that leads to depression (51, 52). Second, diet is an important factor in the association between depression and body weight status. Emotions of individuals can also affect food

intake. Depression was associated with emotional eating such as negative emotional overeaters (53). Moreover, a negative emotion, such as depression, is further inclined to uncontrolled eating and/or overeating (54). However, this will ultimately lead to a high body weight gain. Finally, we cannot underestimate the roles of neurological mechanisms (16, 17, 55) and/or genetic susceptibility (56), which may also lead to depression and an abnormal weight status.

Previous studies had reported conflicting results in China, partly because different studies had used different criteria to define obesity. Therefore, in this study, we performed sensitivity analyses according to the Asian and WHO criteria of obesity. Sensitivity analyses showed a significant positive association between depression and abdominal obesity (WC category in Asian criteria), and being overweight (BMI category in WHO criteria) after adjustment for gender, age, hypertension, diabetes, resident districts, marital status, educational attainment, occupational PA, smoking status, alcohol-drinking status, and personal monthly income. These results were slightly different from the results produced using the Chinese criteria. Taken together, we suggest that the association between depression and weight status is influenced by the criteria adopted. Additionally, the reciprocal and complex associations of being overweight, abdominal obesity, and depression are strongly intertwined, and these phenomena are likely to be true for the earlier-mentioned results. Hence, further large-scale research is needed to reveal the association between obesity and depression among the whole Chinese population.

This study suffered from a few limitations. First, the present study was a cross-sectional study that does not reflect the underlying mechanisms between depression and weight status. Therefore, a follow-up study is imperative. Second, this study was performed on a relatively small sample size of the adult community in Qingdao, China.

CONCLUSION

We observed that overweight and abdominal obesity (WC category) participants were at a higher risk of depression according to Chinese criterion. However, abdominal obesity according to WHR was not associated with depression. Furthermore, Asian and WHO criteria of obesity might influence the association between depression and body weight status. On all accounts, controlling being overweight and having abdominal obesity had a protective impact on depression. Future research will involve a larger multicenter study in China to further investigate the relationship between body weight and depression.

ETHICS AND CONSENT TO PARTICIPATE

All the participants voluntarily signed the informed consent before their participation and the consent of ethics, including three urban districts (Shinan, Shibei, and Sifang) and three rural districts (Huangdao, Jiaonan, and Jimo), was obtained from the ethics committee in Qingdao Municipal Center for Disease Control and Prevention. This study was approved by the local ethics committee at Qingdao Municipal Health and Family planning commission.

AVAILABILITY OF DATA AND MATERIALS

The aggregate data supporting findings contained within this manuscript will be shared upon request submitted by the corresponding author. Identifying patient data will not be shared.

AUTHOR CONTRIBUTIONS

ZB, JC, and JS were the primary authors and leading investigators. NY, JC, MK, ZB, and HX carried out the experiments, analyzed experimental results. ZB, JC, and JS wrote the manuscript. All authors read and approved the final manuscript.

FUNDING

This study was funded by the Bayer Healthcare in China and World Diabetes Foundation [WDF07-308].

ACKNOWLEDGMENTS

We are grateful to the participants, primary care doctors, and nurses who participated in this survey.

REFERENCES

1. Available online at: http://www.who.int/news-room/fact-sheets/detail/obesity-and-overweight
2. Available online at: http://www.who.int/news-room/fact-sheets/detail/depression
3. Xi B, Liang Y, He T, Reilly KH, Hu Y, Wang Q et al. Secular trends in the prevalence of general and abdominal obesity among Chinese adults, 1993-2009. *Obes Rev*. (2012) 13:287–96. doi: 10.1111/j.1467-789X.2011.00944.x
4. Hu L, Huang X, You C, Li J, Hong K, Li P, et al. Prevalence of overweight, obesity, abdominal obesity and obesity-related risk factors in southern China. *PLoS ONE* (2017) 12:e0183934. doi: 10.1371/journal.pone.0183934
5. Wu J, Xu H, He X, Yuan Y, Wang C, Sun J, et al. Six-year changes in the prevalence of obesity and obesity-related diseases in Northeastern China from 2007 to 2013. *Sci Rep*. (2017) 7:41518. doi: 10.1038/srep41518
6. Cesar C. *Depression Exacts a Heavy Toll on Chinese People's Health*. Counter punch (2018).
7. Eidsdottir ST, Kristjansson AL, Sigfusdottir ID, Garber CE, Allegrante JP. Association between higher BMI and depressive symptoms in Icelandic adolescents: the mediational function of body image. *Eur Public Health J*. (2014) 24:888–92. doi: 10.1093/eurpub/ckt180
8. de Wit LM, van Straten A, van Herten M, Penninx BW, Cuijpers P. Depression and body mass index, a u-shaped association. *BMC Public Health* (2009) 9:14. doi: 10.1186/1471-2458-9-14
9. Marijnissen RM, Bus BA, Holewijn S, Franke B, Purandare N, de Graaf J, et al. Depressive symptom clusters are differentially associated with general and visceral obesity. *J Am. Geriatr Soc*. (2011) 59:67–72. doi: 10.1111/j.1532-5415.2010.03228.x
10. Johnston E, Johnson S, McLeod P, Johnston M. The relation of body mass index to depressive symptoms. *Can J Public Health* (2004) 95:179–83.

11. Gibson-Smith D, Bot M, Snijder M, Nicolaou M, Derks EM, Stronks K, et al. The relation between obesity and depressed mood in a multi-ethnic population. The HELIUS study. *Soc Psychiatry Psychiatr Epidemiol.* (2018) 53:629–38. doi: 10.1007/s00127-018-1512-3
12. Zavala GA, Kolovos S, Chiarotto A, Bosmans JE, Campos-Ponce M, Rosado JL et al. Association between obesity and depressive symptoms in Mexican population. *Soc Psychiatry Psychiatr Epidemiol.* (2018) 53:639–46. doi: 10.1007/s00127-018-1517-y
13. Chang HH, Yen ST. Association between obesity and depression: evidence from a longitudinal sample of the elderly in Taiwan. *Aging Ment Health* (2012) 16:173–80. doi: 10.1080/13607863.2011.605053
14. Qian J, Li N, Ren X. Obesity and depressive symptoms among Chinese people aged 45 and over. *Sci Rep*. (2017) 7:45637. doi: 10.1038/srep45637
15. Li ZB, Ho SY, Chan WM, Ho KS, Li MP, Leung GM, et al. Obesity and depressive symptoms in Chinese elderly. *Int J Geriatr Psychiatry* (2004) 19:68–74. doi: 10.1002/gps.1040
16. Tindell AJ, Smith KS, Berridge KC, Aldridge JW. Dynamic computation of incentive salience: "wanting" what was never "liked". *J Neurosci.* (2009) 29:12220–8. doi: 10.1523/JNEUROSCI.2499-09.2009
17. Nestler EJ. Epigenetics: Stress makes its molecular mark. *Nature* (2012) 490:171–2. doi: 10.1038/490171a
18. Puhl R, Brownell KD. Ways of coping with obesity stigma: review and conceptual analysis. *Eat Behav*. (2003) 4:53–78. doi: 10.1016/S1471-0153(02)00096-X
19. Sun Y, Liu Y, Tao FB. Associations Between Active Commuting to School, Body Fat, and Mental Well-being: Population-Based, Cross-Sectional Study in China. *J Adolesc Health* (2015) 6:679–85. doi: 10.1016/j.jadohealth.2015.09.002.
20. Luo H, Li J, Zhang Q, Cao P, Ren X, Fang A, et al. Obesity and the onset of depressive symptoms among middle-aged and older adults in China: evidence from the CHARLS. *BMC Public Health* (2018) 18:909. doi: 10.1186/s12889-018-5834-6
21. Qin T, Liu W, Yin M, Shu C, Yan M, Zhang J, et al. Body mass index moderates the relationship between C-reactive protein and depressive symptoms: evidence from the China Health and Retirement Longitudinal Study. *Sci Rep*. (2017) 7:39940. doi: 10.1038/srep39940
22. Zhang Y, Sun J, Pang Z, Wang X, Gao W, Ning F, et al. The impact of new screen-detected and previously known type 2 diabetes on health-related quality of life: a population-based study in Qingdao, China. *Qual. Life Res.* (2014) 23:2319–26. doi: 10.1007/s11136-014-0674-z
23. M. I. O. C. *Definition and Diagnosis of Diabetes Mellitus and Intermediate Hyperglycemia*. Geneva World Health Organization (2006).
24. 1999 World Health Organization-International Society of Hypertension Guidelines for the Management of Hypertension. Guidelines Subcommittee. (1999) *J Hypertens*. 17:151–83.
25. Fountoulakis KN, Lacovides A, Samolis S, Kleanthous S, Kaprinis SG, St K, et al. Reliability, validity and psychometric properties of the Greek translation of the Zung Depression Rating Scale. *BMC Psychiatry* (2001) 1:6. doi: 10.1186/1471-244X-1-6
26. Disease Control CM. *Chinese Guidelines on Overweight and Obesity Prevention and Control in Adults*. Beijing: People' s Medical Publishing House (2006).
27. WE C. Appropriate body-mass index for Asian populations and its implications for policy and intervention strategies. *Lancet* (2004) 363:157–63. doi: 10.1016/S0140-6736(03)15268-3
28. WE C. *Waist Circumference and Waist-Hip Ratio: Report of a WHO Expert Consultation Geneva, 8-11 December 2008*. World Health Organization, (2008).
29. Lean ME, Han TS, Morrison CE. Waist circumference as a measure for indicating need for weight management. *BMJ* (1995) 311:158–61.
30. Oh J, Chae JH, Kim TS. Age-specific association between body mass index and depression: The Korea National Health and Nutrition Examination Survey 2014. *Int J Obes.* (2018) 42:327–33. doi: 10.1038/ijo.2017.234
31. Chen Y, Bennett D, Clarke R, Guo Y, Yu C, Bian Z, et al. Patterns and correlates of major depression in Chinese adults: a cross-sectional study of 0.5 million men and women. *Psychol Med*. (2017) 47:958–70. doi: 10.1017/S0033291716002889
32. Wang G, Hu M, Xiao SY, Zhou L. Loneliness and depression among rural empty-nest elderly adults in Liuyang, China: a cross-sectional study. *BMJ Open* (2017) 7:e016091. doi: 10.1136/bmjopen-2017-016091
33. Gao YL, Wei YB, Shen YD, Tang YY, Yang JR. China's empty nest elderly need better care. *J Am Geriatr Soc*. (2014) 62:1821–2. doi: 10.1111/jgs.12997
34. Xie LQ, Zhang JP, Peng F, Jiao NN. Prevalence and related influencing factors of depressive symptoms for empty-nest elderly living in the rural area of YongZhou, China. *Arch Gerontol Geriatr*. (2010) 50:24–9. doi: 10.1016/j.archger.2009.01.003
35. Kuo SY, Lin KM, Chen CY, Chuang YL, Chenv WJ. Depression trajectories and obesity among the elderly in Taiwan. *Psychol. Med*. (2011) 41:1665–76. doi: 10.1017/S0033291710002473
36. Hidese S, Asano S, Saito K, Sasayama D, Kunugi H. Association of depression with body mass index classification, metabolic disease, and lifestyle: A web-based survey involving 11,876 Japanese people. *J Psychiatr Res*. (2018) 102:23–8. doi: 10.1016/j.jpsychires.2018.02.009
37. Cash TF. Body image: past, present, and future. *BODY IMAGE* (2004) 1:1–5. doi: 10.1016/S1740-1445(03)00011-1
38. Xiao Y, Zhao N, Wang H, Zhang J, He Q, Su D, et al. Association between socioeconomic status and obesity in a Chinese adult population. *BMC Public Health* (2013) 13:355. doi: 10.1186/1471-2458-13-355
39. Zhao P, Gu X, Qian D, Yang F. Socioeconomic disparities in abdominal obesity over the life course in China. *Int J Equity Health* (2018) 17:96. doi: 10.1186/s12939-018-0809-x
40. Phelan SM. An update on research examining the implications of stigma for access to and utilization of bariatric surgery. *Curr Opin Endocrinol Diabetes Obes*. (2018) 25:321–5. doi: 10.1097/MED.0000000000000431
41. Chen Y, Jiang Y, Mao Y. Association between obesity and depression in Canadians. *J Womens Health* (2009) 18:1687–92. doi: 10.1089/jwh.2008.1175
42. Palinkas LA, Wingard DL, Barrett-Connor E. Depressive symptoms in overweight and obese older adults: a test of the "jolly fat" hypothesis. *J Psychosom Res*. (1996) 40:59–66.
43. Wade TW, Oberhelman SS, Angstman KB, Sawchuk CN, Meunier MR, Angstman GL, et al. Diabetes and obesity not associated with 6-month remission rates for primary care patients with depression. *Psychosomatics* (2015) 56:354–61. doi: 10.1016/j.psym.2014.05.012
44. de Wit L, Luppino F, van Straten A, Penninx B, Zitman F, Cuijpers P. Depression and obesity: a meta-analysis of community-based studies. *Psychiatry Res*. (2010) 178:230–5. doi: 10.1016/j.psychres.2009.04.015
45. Zhong W, Cruickshanks KJ, Schubert CR, Nieto FJ, Huang GH, Klein BE, et al. Obesity and depression symptoms in the Beaver Dam Offspring Study population. *Depress. Anxiety* (2010) 27:846–51. doi: 10.1002/da.20666
46. Takeuchi T, Nakao M, Nomura K, Yano E. Association of metabolic syndrome with depression and anxiety in Japanese men. *Diabetes Metab*. (2009) 35:32–6. doi: 10.1016/j.diabet.2008.06.006
47. Vogelzangs N, Beekman AT, Kritchevsky SB, Newman AB, Pahor M, Yaffe K, et al. Psychosocial risk factors and the metabolic syndrome in elderly persons: findings from the Health, Aging and Body Composition study. *J Gerontol A Biol Sci Med Sci*. (2007) 62:563–9.
48. Herva A, Rasanen P, Miettunen J, Timonen M, Laksy K, Veijola J, et al. Co-occurrence of metabolic syndrome with depression and anxiety in young adults: the Northern Finland 1966 Birth Cohort Study. *Psychosom Med*. (2006) 68:213–6. doi: 10.1097/01.psy.0000203172.02305.ea
49. Gil K, Radzillowicz P, Zdrojewski T, Pakalska-Korcala A, Chwojnicki K, Piwonski J, et al. Relationship between the prevalence of depressive symptoms and metabolic syndrome. Results of the SOPKARD Project. *Kardiol Pol*. (2006) 64:464–9.
50. Ahlberg AC, Ljung T, Rosmond R, McEwen B, Holm G, Akesson HO, et al. Depression and anxiety symptoms in relation to anthropometry and metabolism in men. *Psychiatry Res*. (2002) 112:101–10.
51. Wu YK, Berry DC. Impact of weight stigma on physiological and psychological health outcomes for overweight and obese adults: a systematic review. *J Adv Nurs*. (2018) 74:1030–42. doi: 10.1111/jan.13511
52. Stevens SD, Herbozo S, Morrell HE, Schaefer LM, Thompson JK. Adult and childhood weight influence body image and depression through weight stigmatization. *J Health Psychol*. (2017) 22:1084–93. doi: 10.1177/1359105315624749

53. Bourdier L, Morvan Y, Kotbagi G, Kern L, Romo L, Berthoz S. Examination of emotion-induced changes in eating: A latent profile analysis of the Emotional Appetite Questionnaire. *Appetite* (2018) 123:72–81. doi: 10.1016/j.appet.2017.11.108
54. Bongers P, de Graaff A, Jansen A. 'Emotional' does not even start to cover it: Generalization of overeating in emotional eaters. *Appetite* (2016) 96:611–6. doi: 10.1016/j.appet.2015.11.004
55. Kelley AE, Berridge KC. The neuroscience of natural rewards: relevance to addictive drugs. *J Neurosci*. (2002) 22:3306–11.
56. Stunkard AJ, Faith MS, Allison KC. Depression and obesity. *Biol Psychiatry* (2003) 54:330–7.

Conflict of Interest Statement: The authors declare that the research was conducted in the absence of any commercial or financial relationships that could be construed as a potential conflict of interest.

frontiers in Endocrinology

ORIGINAL RESEARCH
published: 02 July 2018
doi: 10.3389/fendo.2018.00315

Fat Mass Follows a U-Shaped Distribution Based on Estradiol Levels in Postmenopausal Women

*Georgia Colleluori[1,2,3], Rui Chen[1,2], Nicola Napoli[3], Lina E. Aguirre[4], Clifford Qualls[5], Dennis T. Villareal[1,2] and Reina Armamento-Villareal[1,2]**

[1] Division of Endocrinology and Metabolism, Department of Internal Medicine, Baylor College of Medicine, Houston, TX, United States, [2] Center for Translational Research on Inflammatory Diseases, Michael E. DeBakey VA Medical Center, Houston, TX, United States, [3] Division of Endocrinology, University Campus Biomedico of Rome, Rome, Italy, [4] Division of Endocrinology and Metabolism, Department of Internal Medicine, New Mexico VA Health Care System, Albuquerque, NM, United States, [5] Division of Mathematics and Statistics, University of New Mexico School of Medicine, Albuquerque, NM, United States*

Objective: Estradiol (E2) regulates adipose tissue resulting in increased fat mass (FM) with declining E2. However, increased visceral fat and hyperestrogenemia are features of obese individuals. It is possible that adipocytes in obese individuals are less sensitive to E2 resulting in higher FM. Our objective is to identify the range of serum E2 for which postmenopausal women have the lowest FM and best body composition.

Methods: Cross-sectional data from 252 community-dwelling postmenopausal women, 42–90 years old. Subjects were stratified into categories of E2 (pg/ml): (1) ≤10.5; (2) 10.6–13.9; (3) 14.0–17.4; and (4) ≥17.5. Body composition by dual-energy X-ray absorptiometry. Serum E2 by radioimmunoassay. Between-group comparisons by analysis of covariance.

Results: E2 linearly increased with increasing body weight and body mass index ($r = 0.15$ and $p = 0.01$ for both), but not with total FM (kg) or % FM ($r = 0.07$, $p = 0.34$ and $r = -0.04$, $p = 0.56$, respectively). However, total FM (kg) followed a U-shaped distribution and was significantly lower in group 3 (27.6 ± 10.6), compared with groups 1: (34.6 ± 12.5), 2: (34.0 ± 12.4), and 4: (37.0 ± 10.6), $p = 0.005$. % FM was also lowest in group 3. While fat-free mass (FFM, kg) increased with increasing E2 ($p < 0.001$), % FFM was highest in group 3.

Conclusion: In our population of postmenopausal women, FM followed a U-shaped distribution according to E2 levels. E2 between 14.0 and 17.4 pg/ml is associated with the best body composition, i.e., lowest total and % FM and highest % FFM. Given the role of E2 in regulating body fat, high FM at the high end of the E2 spectrum may suggest reduced E2 sensitivity in adipocytes among obese postmenopausal women.

Clinical Trials: ClinicalTrials.gov identifier: NCT00146107.

Keywords: estradiol, obesity, adipocyte, adipose tissue, body composition, estrogen receptor, estrogen receptor alpha, estrogen receptor beta

OPEN ACCESS

Edited by:
Andrew J. McAinch, Victoria University, Australia

Reviewed by:
David Scott, Monash University, Australia
Fernando Lizcano, Universidad de La Sabana, Colombia

****Correspondence:***
Reina Armamento-Villareal
reina.villareal@bcm.edu

Specialty section:
This article was submitted to Obesity, a section of the journal Frontiers in Endocrinology

Received: *15 January 2018*
Accepted: *25 May 2018*
Published: *02 July 2018*

Citation:
Colleluori G, Chen R, Napoli N, Aguirre LE, Qualls C, Villareal DT and Armamento-Villareal R (2018) Fat Mass Follows a U-Shaped Distribution Based on Estradiol Levels in Postmenopausal Women. Front. Endocrinol. 9:315. doi: 10.3389/fendo.2018.00315

INTRODUCTION

Over one-third of US adults are obese (1). Considering the 10-fold rise in the worldwide incidence of obesity among children and adolescents during the past four decades, the number of obese adults could increase further in the coming years (2). High visceral fat mass (FM), common in obese individuals, is a risk factor for the development of cardiovascular disease, type 2 diabetes, and certain types of cancer, reason for which obesity is considered a major public health burden of the twenty-first century (1, 3). Research on the mediators of body fat deposition and distribution is thus crucial. Estrogen has been recognized as a regulator of FM (4–7), and in sufficient amount favors a "pear-shaped" fat distribution among women through promotion of both visceral lipolysis and subcutaneous adipogenesis (4, 8). Thus, the decreased lipid utilization and visceral FM accumulation in postmenopausal women is attributed to a severe reduction in estrogen levels (4–7). In rat adipocytes, estrogen depletion resulted in increased lipoprotein lipase and lipid deposition, while estradiol (E2) treatment reversed this process (9).

Although high E2 levels could be theorized as protective against developing obesity, it is interesting to note that obesity is classically characterized by relative hyperestrogenemia. It is in fact expected that increased aromatase activity in the expanded adipose tissue volume in obese individuals would result in high E2 levels (10). However, because these individuals remain obese, this observation may suggest impaired regulation of FM by E2 or reduced E2 sensitivity.

We thus hypothesize that total body fat varies according to E2 levels with individuals in the lower and higher end of the E2 spectrum having higher body fat. To the best of our knowledge, there are no reports describing the optimum E2 levels associated, primarily, with the lowest body fat and, secondarily, with the best body composition profile in postmenopausal women. The aim of this study is to determine the association of body fat and fat-free mass (FFM) with circulating E2 and to identify the range of serum E2 levels associated with the lowest body fat and the best body composition profile in postmenopausal women.

MATERIALS AND METHODS

Study Population

This is a secondary analysis of cross-sectional data collected from otherwise healthy community-dwelling postmenopausal women participating in a study investigating the relationship between polymorphisms in the different CYP450 enzymes that metabolize estrogen and the effect on bone health (11, 12) or those undergoing a lifestyle intervention trial (13). These protocols were approved by the Washington University School of Medicine institutional review board. Both studies were conducted in accordance with the guidelines in the Declaration of Helsinki for the ethical treatment of human subjects. Participants were recruited using advertisement or direct mailing. All of the participants were provided written informed consent. Exclusion criteria include the use of medications that affect gonadal hormone levels such as estrogens and androgens, medications that affect bone metabolism such as glucocorticoids, anticonvulsants, bisphosphonates, selective estrogen receptor modulators (e.g., raloxifene and tamoxifen), aromatase inhibitors, as were medical conditions that affect bone metabolism such as hyperparathyroidism, chronic renal failure, Paget's diseases of the bone, chronic liver disease, and osteomalacia. All women in this study were at least 1 year from their last menstrual period or had a bilateral oophorectomy. Subjects were stratified into different groups based on serum E2 (pg/ml) as follows: (1) ≤10.5; (2) 10.6–13.9; (3) 14.0–17.4; and (4) ≥17.5.

Body Mass Index (BMI)

Subjects were requested to empty their pockets, remove shoes, heavy clothing, and heavy jewelries (e.g., watches, necklaces, and bracelets) to measure their body weight using a standard weighing scale. A stadiometer was used to measure height. BMI was calculated as body weight in kilograms divided by the square of the height in meters (kilograms/meters^2).

Body Composition

Because body composition was not part of the original protocol in one study and was added on after several women were enrolled in the study (11, 14), we only have the body composition data in 147 women. Total body mass, FFM, FM, and truncal fat were measured using whole body dual-energy X-ray absorptiometry (Hologic Delphi 4500/w; Hologic, Waltham, MA, USA; Enhanced Whole Body 11.2 software version, Hologic) as previously described (15). The coefficients of variation for these measurements in our laboratory are <2% (15). The percentages of total FM were obtained from the estimated readings given by the machine for the different regions of interest. % FFM was calculated as the FFM divided by the whole body mass multiplied by 100 [(FFM/whole body mass) × 100].

Biochemical Data

Serum E2 levels were measured by ultrasensitive radioimmunoassay (RIA, Diagnostic System Laboratory, Webster, TX, USA) (11, 14). The coefficient of variability for this assay in our laboratory is less than 10% (11, 12, 16).

Statistical Analysis

Between-group differences in body composition, BMI, age, and E2 were assessed by analysis of covariance. The main outcome investigated, total FM, was normally distributed in our population ($p = 0.41$) according to the Shapiro–Wilk test. We performed power calculation for the definition of the groups to optimize the trade-off between-group sample sizes versus variances; this resulted in 4 groups with a minimum of 32 participants per group with 80% power and 0.05 alpha to detect a difference of at least 8 kg of FM between the nadir (group 3) and the end groups (groups 1 and 4). Differences in body composition and BMI were analyzed adjusting for age. Least significant difference procedure to discriminate among the means was performed as *post hoc* analysis. Data were managed using Excel 2010 (Microsoft, Redmond, WA, USA) and analyzed using Statgraphics X64 (Statgraphics Technologies, The Plains, VA, USA). Results are expressed as the mean ± SD in the text and tables and mean ± SE in the figures. A $p < 0.05$ was considered statistically significant.

RESULTS

Data from 252 women were included in our analysis (**Table 1**): mean age (66.1 ± 7.6 years old), weight (79.3 ± 18.5 kg), BMI (29.8 ± 6.5 kg/m^2), and E2 (14.1 ± 5.6 pg/ml). Subjects' characteristics according to E2 categories are reported in **Table 1**.

Body mass index did not significantly differ between those with and without body composition measurement (29.3 ± 5.9 vs 27.8 ± 5.5 kg/m^2, respectively, $p = 0.07$). Similarly, E2 levels were not significantly different between the two groups (14.4 ± 6.0 vs 14.1 ± 5.5 pg/ml for those with and without body composition assessment, respectively). However, age and body weight were significantly higher in participants who had body composition (66.6 ± 6.5 vs 63.7 ± 8.6 years old, $p = 0.002$; 78.0 ± 18.0 vs 73.2 ± 16.8 kg, $p = 0.03$, respectively).

Body mass index and body weight were the highest in group 4 (E2 ≥ 17.5 pg/ml, **Table 1**) and were both positively correlated to circulating E2 ($r = 0.15$ and $p = 0.01$ for both variables). On the other hand, total FM (kg) and % FM did not follow a linear relationship with circulating E2 ($r = 0.07$, $p = 0.34$ and $r = -0.04$, $p = 0.56$, respectively). However, analysis according to the different categories of E2 levels showed that both FM (kg) (**Figure 1A**) and % FM (**Figure 1B**) follow a U-shaped trend according to E2 levels. FFM (kg) increased with increasing E2 ($r = 0.22$, $p = 0.007$, **Figure 2A**), while % FFM did not follow a linear relationship with E2 ($r = -0.001$, $p = 0.98$). % FFM in fact follows a bell-shaped curve (**Figure 2B**) with women in group 3 having the highest % FFM. Truncal FM (kg) was the lowest in group 3 (E2: 14.0–17.4 pg/ml), while % truncal FM and % truncal lean mass did not differ significantly among the groups (**Table 2**).

DISCUSSION

Our study showed that postmenopausal women with circulating E2 between 14.0 and 17.4 pg/ml measured by RIA have the best body composition profile with the lowest total and % FM, and the highest % FFM. Furthermore, FM in postmenopausal women followed a U-shaped distribution according to E2 levels, with individuals with E2 levels <14.0 and >17.4 pg/ml having higher body fat.

According to the US Centers for Disease Control and Prevention, obesity and its related disorders are a leading cause of mortality worldwide (1). Hormones play a key role in obesity etiology and progression, though obesity is known to be multifactorial in origin, with causes including genetic, lifestyle, and environmental factors. Gender-dependent adipose tissue distribution and body composition changes after menopause are among the clinical observations linking estrogen to adipocyte development (5). During menopausal transition, women experience a shift from a gynoid to an android fat distribution (5, 7), and become three times more likely to develop obesity and metabolic syndrome than premenopausal women (17). Consistently, visceral FM reduction and improved cardiometabolic profile were reported in a meta-analysis including over 100 clinical trials (18) of women undergoing postmenopausal hormone replacement. The role of E2 in regulating fat distribution is well illustrated in male-to-female transgender patients having a change from an android to a gynoid fat habitus after 12 months of E2 therapy (19).

Interestingly, obesity is often accompanied by a state of relative hyperestrogenemia because of the high aromatase expression/activity in the adipocytes of obese subjects (10). Considering the positive role exerted by estrogens on adipose mass and distribution, the coexistence of high-visceral fat content and elevated estrogen levels in obese individuals may appear inconsistent. This scenario raises the possibility that adipocytes in obese individuals, who have high E2 levels, are not as sensitive to the lipolytic effects of estrogens. This in turn may suggest a different mechanism for the increased body fat at both ends of the estrogen spectrum, from estrogen deficiency on one end to estrogen resistance on the other end. Another explanation for the association between higher body fat at higher end of estrogen level spectrum is the type of obesity developed from a multifactorial cause, independent of estrogen levels. Obesity, together with its associated high aromatase activity, then subsequently leads to the development of higher estrogen levels and possibly to E2 resistance.

To date, results from studies exploring the correlation between estrogens and body fat or BMI are contradictory (20–25). Despite numerous studies investigating the impact of estrogen adequacy or lack thereof on FM (4), to the best of our knowledge, there is no information on the optimum circulating E2 in relation to body fat and FFM in postmenopausal women. Our study showed the existence of a narrow range of serum E2 (14.0–17.4 pg/ml) for which postmenopausal women have the lowest total and % body fat, and highest % FFM. This identifies the E2 levels associated with the best body composition profile in this population.

TABLE 1 | Population characteristics according to circulating estradiol (E2).

Groups	1	2	3	4	*p* Value
E2 (pg/ml)	**<10.5**	**10.5–13.9**	**14.0–17.4**	**≥17.5**	
N (%)	53 (21)	87 (35)	56 (22)	56 (22)	
Age (years old)	67.5 ± 7.0	65.9 ± 8.5	65.6 ± 7.8	65.7 ± 7.6	0.52
Body mass index (kg/m^2)	29.9 ± 6.7*	29.0 ± 6.1*	28.1 ± 5.5*	32.8 ± 6.8	<0.0001
Body weight (kg)	78.4 ± 18.1*	76.0 ± 17.6*	75.8 ± 16.2*	88.9 ± 19.6	<0.001
E2 (pg/ml)	8.4 ± 1.5	12.1 ± 0.8	15.0 ± 0.9	22.0 ± 5.9	<0.001$^\gamma$

Data are reported as mean ± SD adjusted for age.

**p < 0.05 for comparison with group 4.*

$^\gamma$All groups differ significantly from each other (p < 0.05).

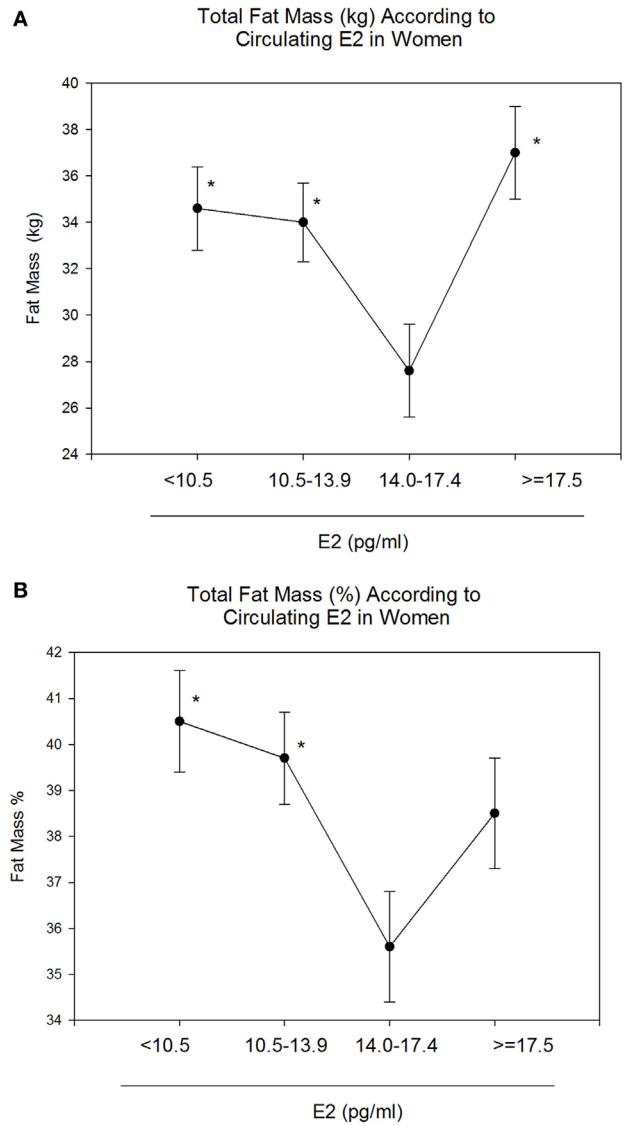

FIGURE 1 | Total fat mass (FM) (kg and %) according to estradiol (E2) categories. E2 levels between 14.0 and 17.4 pg/ml correspond to the lowest total FM [kg–%, **(A,B)**]. Data are reported as mean ±SE. *Comparison with group 3 (E2: 14.0–17.4), $p < 0.05$.

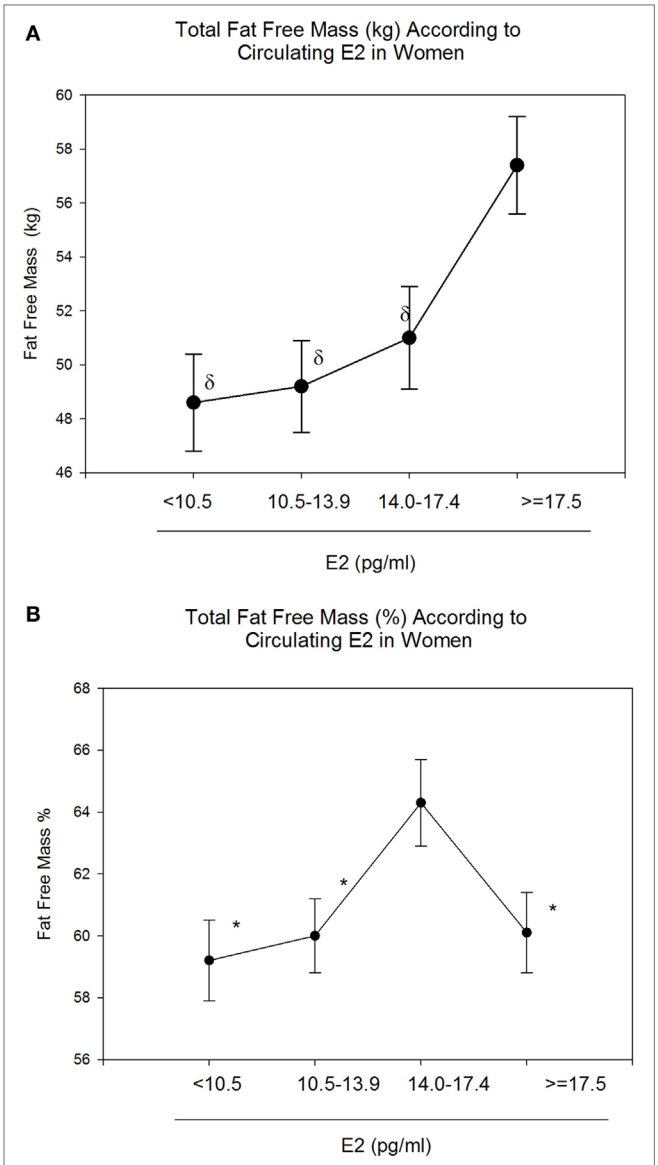

FIGURE 2 | Total fat-free mass (FFM) (kg and %) according to estradiol (E2) categories. E2 levels between 14.0 and 17.4 pg/ml correspond to the highest FFM (%) **(B)**. However, absolute FFM increases with increasing E2 **(A)**. Data are reported as mean ± SE. *Comparison with group 3 (E2: 14.0–17.4), $p < 0.05$; $^{\delta}$Comparison with group 4 (E2: 10.5–13.9), $p < 0.05$.

Furthermore, FM followed a U-shaped curve according to E2 levels, with those with E2 levels below 14.0 and above 17.4 pg/ml having higher FM. Considering our results, it is possible that the persistently high-body fat in obese women leads to down-regulation of ER-alpha (ERα) in adipocytes and reduced E2 sensitivity despite higher E2 levels.

Estrogen is also the main sex hormone regulating FM in men (26). In fact, estrogen resistance was first described in a man with an inactivating mutation of the ERα (23). Besides the peculiar skeletal profile, the subject was obese (23). Both ERα and ER-beta (ERβ) are expressed in adipose tissue; however, the former seems to be more relevant to its regulation (4). ERα knock-out male and female mice had higher adiposity compared with wild-type mice, while body fat in ERβKO mice was similar to wild-type mice (4). A study conducted on Swedish women reported lower ERα expression in the subcutaneous adipose tissue of obese ($N = 17$) when compared with non-obese ($N = 16$), suggesting a different sensitivity to estrogens depending on BMI (27). On the other hand, ERα expression in subcutaneous adipose tissue was found to increase after weight loss in 23 obese women (28). Since body composition and estrogen levels were not measured in these studies, one can only speculate, but not confirm, that increased body fat and higher estrogen levels were present in these patients. Given our data, it is possible that obese subjects in that study could have either high- or low-circulating E2.

TABLE 2 | Body composition of the trunk according to estradiol (E2) categories.

Groups	1	2	3	4	*p* Value
E2 (pg/ml)	**<10.5**	**10.5–13.9**	**14.0–17.4**	**≥17.5**	
N (%)	36 (24.5)	42 (28.5)	34 (23)	35 (24)	
Trunk fat mass (FM) (kg)	16.0 ± 6.1[δ]	17.1 ± 7.5*	13.8 ± 5.8[δ]	19.1 ± 6.5*	<0.01
Trunk FM (%)	32.1 ± 6.8	34.4 ± 8.9	32.5 ± 7.9	37.4 ± 7.2	0.16
Trunk lean mass (kg)	21.8 ± 2.3	22.3 ± 6.3	21.9 ± 2.7	24.7 ± 4.6	0.17

Data are reported as mean ± SD adjusted for age.
**p < 0.05 for comparison with group 3.*
[δ]p < 0.05 for comparison with group 4.

We speculate that a possible sequence of events following the drop in estrogen levels during menopause which include the physiologic increase in body fat, which in turn leads to increased adipose tissue production of estrogen in an effort to compensate for the expanded FM. However, the persistent hyperestrogenemia could lead to ER downregulation and thus reduced adipocyte response to estrogen.

After the age of 40, the prevalence of obesity significantly increases in American women (29) and E2 deficiency is postulated as a critical triggering factor (5). E2 deficiency promotes metabolic dysfunction predisposing to metabolic syndrome, type 2 diabetes, and cardiovascular events (7). Considering the regulation of adipose tissues by estrogen and its implications on the cardiometabolic health (7), the identification of optimum E2 values associated with the best body composition profile would be of clinical relevance. In our group of postmenopausal women, serum E2 values between 14.0 and 17.4 pg/ml corresponded to the best body composition profile; aside from the lowest absolute and percent FM, % FFM was also relatively higher in group 3. FFM increased with increasing E2 levels possibly because of the beneficial effect exerted by E2 on both bone mineral density (30) and muscle homeostasis as suggested by a very recent publication (31).

Our study has limitations. We used of RIA for E2 measurement. Liquid chromatography/mass spectrometry (LC/MS) is considered the gold standard for sex steroid assay because of its high sensitivity and ability to detect very low E2 concentrations (32). However, RIA has been used in prior studies with good reproducibility (30). Nevertheless, according to a study by Hsing et al. exploring the reproducibility of both techniques, steroid hormone levels measured by RIA and MS were highly correlated despite the consistently higher E2 assayed by RIA (32). More importantly, they concluded that the intra- and inter-assay variability of both techniques were equally reliable (32). It is thus possible that the E2 cutoffs we identified will be shifted downwards if our E2 assay was done by LC/MS instead of RIA. Other limitations include the small sample size and the lack of adjustment for confounders, such as additional hormones, diet, and exercise (data not available in our study), which could affect body composition. In addition, the cross-sectional study design does not allow us to establish a causal relationship between the outcomes investigated and E2 levels.

In conclusion, to the best of our knowledge, this is the first study investigating the optimum E2 levels associated with the lowest FM and the best body composition in postmenopausal women. Since FM is comparably high in people with low- and high-serum E2, our observation raises questions regarding E2 sensitivity and the ability of E2 to regulate FM and distribution in women with high E2 levels, i.e., E2 ≥ 17.5 pg/ml. Prospective investigation using LC/MS to measure E2 with a bigger sample size is needed to confirm our observation and to explore the possibility of E2 resistance among individuals with relative hyperestrogenemia.

ETHICS STATEMENT

This study was carried out in accordance with the recommendations of the Washington University School of Medicine institutional review board with written informed consent from all subjects. All subjects gave written informed consent in accordance with the Declaration of Helsinki. The protocol was approved by the Washington University School of Medicine institutional review board.

AUTHOR CONTRIBUTIONS

RA-V and DV designed the studies. GC, RC, NN, LA, DV, and RA-V conducted the study and collected the data. GC, CQ, and RA-V analyzed and interpreted the data. GC, RC, NN, LA, CQ, DV, and RV drafted the manuscript. Revising manuscript content and approving the final version: all take responsibility for the manuscript content, the integrity of the data analysis, and approval of the final version of the manuscript.

ACKNOWLEDGMENTS

This study was supported by the resources at the Washington University School of Medicine St Louise, MO, USA; the Michael E. DeBakey VA Medical Center, Houston, TX, USA; and the Center for Translational Research in Inflammatory Diseases (CTRID) at the Michael E. DeBakey VA Medical Center, Houston, TX, USA. The authors thank participants for their contribution.

FUNDING

This work was supported by National Institutes of Health grants R03 R049401 (to RA-V), K12 HD01459 (Building Interdisciplinary Research Careers in Women's Health), P30-DK020579, and grant RO1-AG025501.

REFERENCES

1. Centers for Disease Control and Prevention. *Overweight & Obesity*. 8-29-2017. Available from: https://www.cdc.gov/obesity/data/adult.html (Accessed: May 29, 2018).
2. NCD Risk Factor Collaboration (NCD-RisC). Worldwide trends in body-mass index, underweight, overweight, and obesity from 1975 to 2016: a pooled analysis of 2416 population-based measurement studies in 128.9 million children, adolescents, and adults. *Lancet* (2017) 390(10113):2627–42. doi:10.1016/S0140-6736(17)32129-3
3. World Health Organization. 10-10-2017. Available from: http://www.who.int/en/news-room/fact-sheets/detail/obesity-and-overweight (Accessed: May 29, 2018).
4. Barros RP, Gustafsson JA. Estrogen receptors and the metabolic network. *Cell Metab* (2011) 14(3):289–99. doi:10.1016/j.cmet.2011.08.005
5. Lizcano F, Guzman G. Estrogen deficiency and the origin of obesity during menopause. *Biomed Res Int* (2014) 2014:757461. doi:10.1155/2014/757461
6. Wohlers LM, Spangenburg EE. 17Beta-estradiol supplementation attenuates ovariectomy-induced increases in ATGL signaling and reduced perilipin expression in visceral adipose tissue. *J Cell Biochem* (2010) 110(2):420–7. doi:10.1002/jcb.22553
7. Clegg D, Hevener AL, Moreau KL, Morselli E, Criollo A, Van Pelt RE, et al. Sex hormones and cardiometabolic health: role of estrogen and estrogen receptors. *Endocrinology* (2017) 158(5):1095–105. doi:10.1210/en.2016-1677
8. Al-Qahtani SM, Bryzgalova G, Valladolid-Acebes I, Korach-André M, Dahlman-Wright K, Efendić S, et al. 17beta-estradiol suppresses visceral adipogenesis and activates brown adipose tissue-specific gene expression. *Horm Mol Biol Clin Investig* (2017) 29(1):13–26. doi:10.1515/hmbci-2016-0031
9. Hamosh M, Hamosh P. The effect of estrogen on the lipoprotein lipase activity of rat adipose tissue. *J Clin Invest* (1975) 55(5):1132–5. doi:10.1172/JCI108015
10. Schneider G, Kirschner MA, Berkowitz R, Ertel NH. Increased estrogen production in obese men. *J Clin Endocrinol Metab* (1979) 48(4):633–8. doi:10.1210/jcem-48-4-633
11. Napoli S, Faccio R, Shrestha V, Bucchieri S, Rini GB, Armamento-Villareal R. Estrogen metabolism modulates bone density in men. *Calcif Tissue Int* (2007) 80(4):227–32. doi:10.1007/s00223-007-9014-4
12. Napoli N, Villareal DT, Mumm S, Halstead L, Sheikh S, Cagaanan M, et al. Effect of CYP1A1 gene polymorphisms on estrogen metabolism and bone density. *J Bone Miner Res* (2005) 20(2):232–9. doi:10.1359/JBMR.041110
13. Villareal DT, Chode S, Parimi N, Sinacore DR, Hilton T, Armamento-Villareal R, et al. Weight loss, exercise, or both and physical function in obese older adults. *N Engl J Med* (2011) 364(13):1218–29. doi:10.1056/NEJMoa1008234
14. Napoli N, Vattikuti S, Yarramaneni J, Giri TK, Nekkalapu S, Qualls C, et al. Increased 2-hydroxylation of estrogen is associated with lower body fat and increased lean body mass in postmenopausal women. *Maturitas* (2012) 72(1):66–71. doi:10.1016/j.maturitas.2012.02.002
15. Shah K, Stufflebam A, Hilton TN, Sinacore DR, Klein S, Villareal DT. Diet and exercise interventions reduce intrahepatic fat content and improve insulin sensitivity in obese older adults. *Obesity (Silver Spring)* (2009) 17(12):2162–8. doi:10.1038/oby.2009.126
16. Shah K, Armamento-Villareal R, Parimi N, Chode S, Sinacore DR, Hilton TN, et al. Exercise training in obese older adults prevents increase in bone turnover and attenuates decrease in hip bone mineral density induced by weight loss despite decline in bone-active hormones. *J Bone Miner Res* (2011) 26(12):2851–9. doi:10.1002/jbmr.475
17. Eshtiaghi R, Esteghamati A, Nakhjavani M. Menopause is an independent predictor of metabolic syndrome in Iranian women. *Maturitas* (2010) 65(3):262–6. doi:10.1016/j.maturitas.2009.11.004
18. Salpeter SR, Walsh JM, Ormiston TM, Greyber E, Buckley NS, Salpeter EE. Meta-analysis: effect of hormone-replacement therapy on components of the metabolic syndrome in postmenopausal women. *Diabetes Obes Metab* (2006) 8(5):538–54. doi:10.1111/j.1463-1326.2005.00545.x
19. Elbers JM, Asscheman H, Seidell JC, Gooren LJ. Effects of sex steroid hormones on regional fat depots as assessed by magnetic resonance imaging in transsexuals. *Am J Physiol* (1999) 276(2 Pt 1):E317–25.
20. Olson MB, Shaw LJ, Kaizar EE, Kelsey SF, Bittner V, Reis SE, et al. Obesity distribution and reproductive hormone levels in women: a report from the NHLBI-sponsored WISE study. *J Womens Health (Larchmt)* (2006) 15(7):836–42. doi:10.1089/jwh.2006.15.836
21. Gallicchio L, Visvanathan K, Miller SR, Babus J, Lewis LM, Zacur H, et al. Body mass, estrogen levels, and hot flashes in midlife women. *Am J Obstet Gynecol* (2005) 193(4):1353–60. doi:10.1016/j.ajog.2005.04.001
22. Hetemaki N, Savolainen-Peltonen H, Tikkanen MJ, Wang F, Paatela H, Hämäläinen E, et al. Estrogen metabolism in abdominal subcutaneous and visceral adipose tissue in postmenopausal women. *J Clin Endocrinol Metab* (2017) 102(12):4588–95. doi:10.1210/jc.2017-01474
23. Smith EP, Boyd J, Frank GR, Takahashi H, Cohen RM, Specker B, et al. Estrogen resistance caused by a mutation in the estrogen-receptor gene in a man. *N Engl J Med* (1994) 331(16):1056–61. doi:10.1056/NEJM199410203311604
24. de Ridder CM, Bruning PF, Zonderland ML, Thijssen JH, Bonfrer JM, Blankenstein MA, et al. Body fat mass, body fat distribution, and plasma hormones in early puberty in females. *J Clin Endocrinol Metab* (1990) 70(4):888–93. doi:10.1210/jcem-70-4-888
25. Aguirre L, Napoli N, Waters D, Qualls C, Villareal DT, Armamento-Villareal R. Increasing adiposity is associated with higher adipokine levels and lower bone mineral density in obese older adults. *J Clin Endocrinol Metab* (2014) 99(9):3290–7. doi:10.1210/jc.2013-3200
26. Finkelstein JS, Lee H, Burnett-Bowie SA, Pallais JC, Yu EW, Borges LF, et al. Gonadal steroids and body composition, strength, and sexual function in men. *N Engl J Med* (2013) 369(11):1011–22. doi:10.1056/NEJMoa1206168
27. Nilsson M, Dahlman I, Rydén M, Nordström EA, Gustafsson JA, Arner P, et al. Oestrogen receptor alpha gene expression levels are reduced in obese compared to normal weight females. *Int J Obes (Lond)* (2007) 31(6):900–7. doi:10.1038/sj.ijo.0803528
28. Dahlman I, Linder K, Arvidsson Nordström E, Andersson I, Lidén J, Verdich C, et al. Changes in adipose tissue gene expression with energy-restricted diets in obese women. *Am J Clin Nutr* (2005) 81(6):1275–85. doi:10.1093/ajcn/81.6.1275
29. Flegal KM, Carroll MD, Ogden CL, Curtin LR. Prevalence and trends in obesity among US adults, 1999–2008. *JAMA* (2010) 303(3):235–41. doi:10.1001/jama.2009.2014
30. Khosla S, Atkinson EJ, Melton LJ III, Riggs BL. Effects of age and estrogen status on serum parathyroid hormone levels and biochemical markers of bone turnover in women: a population-based study. *J Clin Endocrinol Metab* (1997) 82(5):1522–7. doi:10.1210/jc.82.5.1522
31. Ribas V, Drew BG, Zhou Z, Phun J, Kalajian NY, Soleymani T, et al. Skeletal muscle action of estrogen receptor alpha is critical for the maintenance of mitochondrial function and metabolic homeostasis in females. *Sci Transl Med* (2016) 8(334):334ra54. doi:10.1126/scitranslmed.aad3815
32. Hsing AW, Stanczyk FZ, Bélanger A, Schroeder P, Chang L, Falk RT, et al. Reproducibility of serum sex steroid assays in men by RIA and mass spectrometry. *Cancer Epidemiol Biomarkers Prev* (2007) 16(5):1004–8. doi:10.1158/1055-9965.EPI-06-0792

Conflict of Interest Statement: The authors declare that the research was conducted in the absence of any commercial or financial relationships that could be construed as a potential conflict of interest.

frontiers in Endocrinology

ORIGINAL RESEARCH
published: 07 August 2018
doi: 10.3389/fendo.2018.00449

Inverse Association of Circulating SIRT1 and Adiposity: A Study on Underweight, Normal Weight, and Obese Patients

Stefania Mariani[1], Maria R. di Giorgio[1], Paolo Martini[2], Agnese Persichetti[3], Giuseppe Barbaro[1], Sabrina Basciani[1], Savina Contini[1], Eleonora Poggiogalle[1], Antonio Sarnicola[2], Alfredo Genco[4], Carla Lubrano[1], Aldo Rosano[5], Lorenzo M. Donini[1], Andrea Lenzi[1] and Lucio Gnessi[1]*

[1] Section of Medical Physiopathology, Food Science and Endocrinology, Department of Experimental Medicine, Sapienza University of Rome, Rome, Italy, [2] Italian Hospital Group, Center for the Treatment of Eating Disorders and Obesity "Villa Pia", Guidonia, Italy, [3] Department of Molecular Medicine, Sapienza University of Rome, Rome, Italy, [4] Department of Surgical Sciences, Policlinico Umberto I, Sapienza University of Rome, Rome, Italy, [5] Roman Academy of Public Health, Rome, Italy

OPEN ACCESS

Edited by:
Beverly Sara Muhlhausler, University of Adelaide, Australia

Reviewed by:
Frida Renstrom, Lund University, Sweden
Kathleen Grace Mountjoy, University of Auckland, New Zealand

***Correspondence:**
Stefania Mariani
stefaniamariani@yahoo.com

Specialty section:
This article was submitted to Obesity, a section of the journal Frontiers in Endocrinology

Received: *11 January 2018*
Accepted: *20 July 2018*
Published: *07 August 2018*

Citation:
Mariani S, di Giorgio MR, Martini P, Persichetti A, Barbaro G, Basciani S, Contini S, Poggiogalle E, Sarnicola A, Genco A, Lubrano C, Rosano A, Donini LM, Lenzi A and Gnessi L (2018) Inverse Association of Circulating SIRT1 and Adiposity: A Study on Underweight, Normal Weight, and Obese Patients. Front. Endocrinol. 9:449. doi: 10.3389/fendo.2018.00449

Context: Sirtuins (SIRTs) are NAD+-dependent deacetylases, cellular sensors to detect energy availability, and modulate metabolic processes. SIRT1, the most studied family member, influences a number of tissues including adipose tissue. Expression and activity of SIRT1 reduce with weight gain and increase in conditions of starvation.

Objective: To focus on SIRT1 plasma concentrations in different conditions of adiposity and to correlate SIRT1 with fat content and distribution, energy homeostasis and inflammation in under-weight, normal-weight, and obese individuals.

Materials and Methods: 21 patients with anorexia nervosa, 26 normal-weight and 75 patients with obesity were evaluated. Body fat composition by dual-energy X-ray absorptiometry, ultrasound liver adiposity, echocardiographic epicardial fat thickness (EFT), inflammatory (ESR, CRP, and fibrinogen), and metabolic (FPG, insulin, LDL- and HDL-cholesterol, triglycerides) parameters, calculated basal metabolic rate (BMR) and plasma SIRT1 (ELISA) were measured.

Results: SIRT1 was significantly higher in anorexic patients compared to normal-weight and obese patients (3.27 ± 2.98, 2.27 ± 1.13, and 1.36 ± 1.31 ng/ml, respectively). Linear regression models for each predictor variable adjusted for age and sex showed that SIRT1 concentration was inversely and significantly correlated with EFT, fat mass %, liver fat content, BMR, weight, BMI, WC, LDL-cholesterol, insulin, ESR. Stepwise multiple regression analysis revealed that age and EFT were the best independent correlates of SIRT1 ($\beta = -0.026 \pm 0.011$, $p = 0.025$, and $\beta = -0.516 \pm 0.083$, $p < 0.001$, respectively).

Conclusions: Plasma SIRT1 shows a continuous pattern that inversely follows the whole spectrum of adiposity. SIRT1 significantly associates with EFT, a strong index of visceral fat phenotype, better than other indexes of adiposity studied here.

Keywords: sirtuins, circulating SIRT1, adiposity, anorexia, obesity, body fat mass

INTRODUCTION

Sirtuins (SIRTs) are nutrient sensing, metabolic regulators, and chromatin silencers (1). SIRT1, the most-studied SIRT, is best known for mediating lifespan extension by consistently improving health during aging. Results mainly derived from animal studies show that SIRT1 protects against or delays the onset of metabolic diseases, neurodegeneration, cardiovascular diseases, and some types of cancers (1, 2). SIRT1 modifies the acetylation status of many different targets in cytoplasm, mitochondria, and nucleus, and it carries out its protective roles by activating key transcription factors, improving lipid metabolism, reducing inflammation, and acting as a tumor suppressor by preserving genomic integrity. SIRT1 plays also an essential role in adaptive metabolic and endocrine responses (3). Several metabolic disorders such as liver steatosis, diabetes, and obesity associate with defects in SIRT1 pathways. Obesity is associated with low NAD(+)/SIRT pathway expression in subcutaneous adipose tissue of BMI-discordant monozygotic twins, highlighting a strong relationship of reduced SIRTs expression with inflammation, insulin resistance, and impaired mitochondrial homeostasis (4). Visceral adiposity negatively correlates with SIRT1 expression (5, 6). Accordingly, we have previously shown an inverse association between plasma SIRT1 and ectopic fat distribution in patients affected by obesity (7, 8) in particular with epicardial and liver fat depots, both typical examples of visceral fat with particularly detrimental effect because of localized and systemic toxic effects (9, 10). Although the main source of circulating SIRT1 is not known (11–13), these results indicate that the negative metabolic effects of obesity could be related, at least in part, to the reduced levels of SIRT1 in the blood. Moreover, what regulates circulating SIRT1 vs. tissue SIRT1 is still unknown.

Conversely, SIRTs tissue enzymatic activity increases in conditions of nutrient depletion and starvation. SIRT1 expression rises in cultured cells, and in multiple tissues of mice after overnight or 24 h fasting (14, 15). An increased expression of SIRT1 is seen after long periods of calorie restriction (CR) in mice (16). Analogously, in man, 30 days and 7 weeks of CR cause a rise of tissue and plasma levels of SIRT1, respectively (17, 18). Indeed, SIRT1 has been identified as a novel factor responsible for some beneficial effects of CR, and previous studies showed that weight loss induces an increase in tissue and circulating SIRT1 levels in obese patients (19, 20).

Therefore, SIRT1 may act differently in states of nutritional excess compared with states of nutritional deprivation.

Circulating SIRT1 has not been studied yet in underweight individuals or in subjects who restrict eating. Thus, in relation to its opposite behavior in condition of hyper- or hypo-nutrition, we evaluated SIRT1 blood concentration, body fat composition, markers of energy homeostasis, inflammation and some metabolic parameters in underweight, normal-weight, and obese individuals, i.e., in subjects with defect or excess of body fat mass. The aim of the study was to investigate the plasma SIRT1 concentration across the whole spectrum of adiposity, and its relationship with fat distribution and metabolic, inflammatory and energy settings.

SUBJECTS AND METHODS

Study participants were recruited among subjects referring to the High Specialization Center for the Care of Obesity (CASCO), Department of Experimental Medicine, "Sapienza" University of Rome, and from the Italian Hospital Group, "Villa Pia," Guidonia, Italy, from January 2015 to February 2017. The study was approved by the ethical committee of the Sapienza University of Rome, Policlinico Umberto I, and was concordant with Helsinki Declaration. Each patient gave a written informed consent before admission to the study.

Over the 2 year recruitment period, a total of 50 patients with anorexia nervosa (AN), 400 obese individuals and 150 normal-weight consecutive subjects were screened. After screening, 122 patients were included. 21 underweight patients with AN based on the diagnostic criteria of the DSM-5 (3 males, 18 females, age range 16–68 year, BMI range 10.63–20.23 Kg/m^2); 26 normal-weight control individuals (7 males, 19 females, age range 20–59 year, BMI range 20.22–24.83 kg/m^2); 75 patients affected by obesity (19 males, 56 females, age range 18–65 year, BMI range 31.36–59.0 kg/m^2). The subjects were excluded either on the basis of the criteria reported below or declined to participate. A portion of the obese and normal-weight patients were included in two previous studies (7, 8).

The exclusion criteria were: uncontrolled hypertension, heart diseases, lung diseases, type 1 diabetes, uncontrolled type 2 diabetes, corticosteroids for systemic use, any medication potentially affecting body weight or body composition, cirrhosis and other chronic liver diseases, acromegaly, hypothyroidism, acute illness, current or past presence of hepatitis B surface antigen and antibody to hepatitis C virus, excessive alcohol intake ($\geq$140 g/week for men or 70 g/week for women).

All patients underwent complete medical examination and anthropometric measurements [body weight (kg), height (m), waist circumference (WC) at the level of umbilicus (cm)]. Body weight was measured by Tanita BWB-800A digital medical scale (Tanita Corporation, Arlington Heights, IL, USA). BMI was calculated by the formula weight (kg)/height(m)^2.

Fasting plasma glucose (FPG, mg/dl) and insulin (mU/L), total cholesterol (TC, mg/dl), high-density lipoprotein (HDL)-cholesterol (mg/dl), low-density lipoprotein (LDL)-cholesterol (mg/dl), triglycerides (TG, mg/dl), erythrocyte sedimentation rate (ESR, mm/h), C-reactive protein (CRP, μg/L), fibrinogen (g/L), and SIRT1 (ng/ml) were assessed after a 12-h overnight fast. Plasma samples for SIRT1 analyses were frozen at −80°C until measurement. Because intermittent fasting might influence the circulating levels of SIRT1, a special attention was paid to withdrawing the blood at the same 12 h time interval from the last meal for all patients. Dual energy X-ray absorptiometry (DXA) body composition, echocardiographic epicardial fat thickness measurements (mm) and liver adiposity by ultrasound were also recorded.

The estimated BMR value was calculated using the Harris & Benedict equation and expressed in kcal/day. Following the equations for men and women:

$$\text{Men} = 66.4 + 13.75\times(\text{Wt}) + 5\times(\text{Ht}) - 6.8\times(\text{Age})$$
$$\text{Women} = 655 + 9.6\times(\text{Wt}) + 1.85\times(\text{Ht}) - 4.7\times(\text{Age})$$

SIRT1 Assay

SIRT1 was determined by a monoclonal antibody-based ELISA method using a commercially available human SIRT1 ELISA kit (MyBioSource, Cod. GDMBS705558) with an inter- and intra-assay coefficient of variation of 10 and 8%, respectively, and a detection limit of 0.039 ng/mL.

Microtiter plates were coated with equal amount of primary mouse anti-human SIRT1 monoclonal IgG. 100 μL standard and plasma samples were pipetted in each well and the protocol was followed by using secondary avidin conjugated horseradish peroxidase. The formation of horseradish peroxidase was measured at 405 nm using ELISA reader (Quanta Biotech, UK). Seven different concentrations of purified SIRT1 (0.15, 0.312, 0.625, 1.25, 2.5, 5.0, and 10 ng/mL) were used to plot a standard curve. A calibration curve was added to each plate used.

Body Composition Evaluation by DXA Analysis

DXA was performed by one single experienced technician using a DXA scan (Hologic Inc., Bedford, MA, USA, QDR 4500 W). The coefficient of variation for fat mass (FM) was <1.5%. Body composition was measured in the whole body and, with the use of specific anatomic landmarks determined by a standard software (Hologic Inc., S/N 47168 VER. 11.2), in the trunk, which included neck, chest, abdominal, and pelvic areas. The upper perimeter was the inferior edge of the chin and the lower borders intersect the middle of the femoral necks without touching the brim of the pelvis. Scans were performed according to the manufacturer's instructions.

Determination of Liver Adiposity

The determination of liver fat content was based on liver-kidney contrast measured with ultrasonography by one single trained radiologist with extensive experience in abdominal ultrasound examinations. The analysis was carried out using a Esaote Medica apparatus equipped with a convex 3.5 MHz probe (Esaote MyLab40, Esaote Europe B.V., The Netherlands). The severity of liver adiposity was based according to the brightness of the liver estimated as a numerical value: 0 = absent; 1 = mild lipid accumulation; and 2 = moderate/severe lipid accumulation.

Echocardiographic Epicardial Fat Thickness Measurements

Epicardial Fat Thickness (EFT) was measured through a validated echocardiographic procedure (21). Participants underwent high-resolution M-B-mode transthoracic echocardiography using a 2.5-MHz probe, and spectral Doppler exam of the common carotid artery using a 7.5- MHz probe (Esaote MyLab40, Esaote Europe B.V., The Netherlands). The EFT was identified as the echo-free space between the outer wall of the myocardium and the visceral layer of the pericardium, and its thickness was measured perpendicularly on the free wall of the right ventricle (RV) at end-systole in three cardiac cycles. The average value of three cardiac cycles from each echocardiographic view was considered. All echocardiograms were recorded by the same experienced operator who was blinded to the other study data.

Statistical Analysis

Variables were expressed as mean ± SD. Differences between groups were analyzed using Student's *T*-test. A matrix correlation among variables was calculated. Each variable, in relation to SIRT1, was tested by the use of regression analyses, taking into account sex and age for their potential confounding effect. Violations of normality of the regression models were tested through the Shapiro-Wilk test. In the stepwise regression analysis, we included significant ($p < 0.05$) predictors from linear regression along with variables deemed important, a priori, on clinical grounds. To avoid colinearity, the correlation between variables was assessed and the more clinically relevant variable of a pair of highly correlated variables was included. To arrive to a parsimonious model, covariates were selected with a stepwise regression procedure using backward elimination. The parameters selected were age, sex, waist circumference, EFT, liver steatosis, HDL-cholesterol, ESR, and basal metabolic rate. All *p*-values presented were two-tailed, and values <0.05 were considered statistically significant. Data were analyzed with the use of STATISTICA software, version 6.1 (Stat Soft, Inc., Tulsa, Oklahoma).

RESULTS

The characteristics of the study population, stratified according to the patients BMI, are summarized in **Table 1**. Statistical significances presented for participant characteristics are all obtained from unadjusted analysis. The mean BMI was 16.22 ± 2.44 kg/m^2, 23.39 ± 1.24 kg/m^2, and 40.95 ± 6.83 kg/m^2 in anorexic patients, normal weight and obesity group, respectively. WC was constantly ≥80 cm in females and ≥94 cm in males affected by obesity. The differences in weight, BMI, WC, EFT, total-FM%, trunk-FM% were statistically significant ($p < 0.001$) across the groups. BMR was significantly higher in obese patients compared to underweight ($p < 0.0001$) and normal-weight ($p < 0.0001$) patients and between underweight and normal-weight patients as well ($p < 0.05$).

Circulating SIRT1 Levels

Underweight patients showed the highest values of SIRT1 followed by normal-weight and obese individuals. The differences in SIRT1 levels were statistically significant between obese subjects and both normal-weight ($p = 0.002$) and underweight patients ($p < 0.0001$).

Fat Amount and Distribution

The characteristics of the adiposity of the patients are summarized in **Table 1**. EFT, total FM % and truncal FM % were significantly reduced in underweight patients compared

to both normal-weight subjects and patients affected by obesity ($p < 0.001$).

Both underweight and obese patients had an abnormally high accumulation of liver fat evaluated by ultrasonography compared to normal-weight. However, the degree of liver steatosis was significantly lower in underweight patients (mild degree) compared to obese patients (moderate/severe degree) ($p < 0.0001$).

Metabolic and Inflammatory Parameters

There were important metabolic differences between the categories of patients (**Table 1**). FPG was lower in underweight patients compared to normal-weight and obese patients ($p < 0.0001$). As expected, the highest basal insulin was found in the obesity group. The differences in insulin levels between underweight and normal-weight subjects ($p = 0.013$), and between normal-weight and obese patients ($p = 0.002$) were statistically significant.

LDL-cholesterol levels were comparable in underweight and normal-weight patients, while obese individuals showed higher values of both total and LDL-C ($p < 0.05$). Indeed, HDL-C was higher in anorexic patients compared to normal-weight ($p < 0.0001$) and obese ($p < 0.0001$), while there were not differences between normal-weight and obese patients ($p = 0.534$).

Analogously, the triglycerides concentrations did not differ between underweight and normal-weight subjects ($p = 0.45$), but were significantly higher in patient affected by obesity compared to normal-weight individuals ($p = 0.03$). All the markers of inflammation followed a clear pattern with a statistical significant increase from underweight, to normal-weight, to obese patients.

Regression Analysis

Table 2 shows the regression analysis results for each predictor variable in relation to SIRT1 adjusted for age and sex. SIRT1 was inversely associated with EFT, total FM%, liver steatosis, body weight, BMI, and WC. Concerning the metabolic variables, SIRT1 was negatively associated with LDL-cholesterol, insulin, and BMR. Finally, SIRT1 was inversely correlated with ESR.

There was no significant association between SIRT1 and triglycerides, HDL-cholesterol, fasting glycaemia, trunk FM%, fibrinogen and CRP.

Given that metabolic and inflammatory markers are influenced by degree of adiposity, we ran an additional set of analyses that included adjustment for WC, beyond age and sex, to assess whether the associations observed for SIRT1 were independent from adiposity. We found that the association between SIRT1 and either inflammatory (ESR, CRP, fibrinogen) or metabolic (FPG, insulin, HDL-cholesterol, LDL-cholesterol, triglycerides) parameters was abolished once adjusted for WC, suggesting that the major drive for the variation of circulating SIRT1 levels is the adiposity *per se* (data not shown). WC was

TABLE 1 | Demographic, anthropometric and clinical characteristics of the patients.

Variables	Underweight ($n = 21$)	Normal weight ($n = 26$)	Obese subjects ($n = 75$)
Age (years)	32.42 ± 14.62	42.53 ± 10.97	40.88 ± 12.59
Sex (male/female)	3/18	7/19	19/56
SIRT1 (ng/ml)	3.27 ± 2.98	2.27 ± 1.13	1.36 ± 1.31
Weight (kg)	43.79 ± 10.47	65.44 ± 6.71	114.98 ± 22.56
BMI (kg/m^2)	16.22 ± 2.44	23.39 ± 1.24	40.95 ± 6.83
WC (cm)	66.76 ± 8.13	76.50 ± 8.61	125.86 ± 15.34
Fat Mass (%)	16.83 ± 6.21	25.90 ± 4.30	40.08 ± 5.34
Truncal Fat Mass (%)	12.04 ± 5.03	19.78 ± 3.06	38.39 ± 5.20
EFT (mm)	4.01 ± 0.62	6.86 ± 0.55	8.64 ± 0.86
Liver steatosis (degrees)*	Mild	Absent	Moderate/Severe
FPG (mg/dl)	74.23 ± 8.84	96.84 ± 13.73	102.12 ± 20.82
Insulin (μIU/ml)	5.98 ± 3.90	8.97 ± 3.34	17.25 ± 13.65
HDL-C (mg/dl)	72.71 ± 15.81	50.38 ± 17.23	48.67 ± 12.90
LDL-C (mg/dl)	90.80 ± 48.60	103.73 ± 25.96	122.65 ± 28.62
Triglycerides (mg/dl)	99.52 ± 65.85	111.61 ± 44.24	139.62 ± 63.23
ESR (mm/h)	12.70 ± 11.03	22.80 ± 7.84	31.58 ± 18.14
CRP (μg/L)	712.5 ± 788.7	5065 ± 2358.6	6662.6 ± 4221.9
Fibrinogen (g/L)	2.89 ± 0.57	3.50 ± 0.70	3.84 ± 0.77
BMR (kcal/day)	1245.1 ± 149.3	1389.0 ± 303.8	1964.5 ± 349.7

*SIRT1, sirtuin1; BMI, body mass index; WC, waist circumference; EFT, epicardial fat thickness; FPG, fasting plasma glucose; HDL-C, high-density lipoprotein-cholesterol; LDL-C, low-density lipoprotein-cholesterol; ESR, erythrocyte sedimentation rate; CRP, C-reactive protein; BMR, basal metabolic rate. Values are expressed as means ± SD. *The severity of liver adiposity was based according to the brightness of the liver estimated as a numerical value: 0 = absent; 1 = mild lipid accumulation; and 2 = moderate/severe lipid accumulation. For each variable, missing values were < 2%. Information on missing values is therefore not provided in the table.*

TABLE 2 | Age- and sex-adjusted linear regression analysis of SIRT1.

Variables	β Coeff.	SE	*p*
Weight (kg)	−0.02	0.00	< 0.001
BMI (kg/m^2)	−0.055	0.01	< 0.001
WC (cm)	−0.026	0.01	< 0.001
Fat Mass (%)	−0.060	0.02	< 0.001
Truncal Fat Mass (%)	0.04	0.04	0.34
EFT (mm)	−0.396	0.07	< 0.001
Liver steatosis (degrees)	−0.585	0.23	0.01
FPG (mg/dl)	−0.010	0.01	0.26
Insulin (μIU/ml)	−0.028	0.01	0.03
HDL-C (mg/dl)	0.019	0.01	0.07
LDL-C (mg/dl)	−0.011	0.00	0.03
Triglycerides (mg/dl)	0.00	0.00	0.36
ESR (mm/h)	−0.024	0.01	0.02
CRP (μg/L)	0.000	0.00	0.07
Fibrinogen (g/L)	−0.38	0.20	0.06
BMR (kcal/day)	−0.002	0.00	< 0.001

BMI, body mass index; WC, waist circumference; EFT, epicardial fat thickness; FPG, fasting plasma glucose; HDL-C, high-density lipoprotein-cholesterol; LDL-C, low-density lipoprotein-cholesterol; ESR, erythrocyte sedimentation rate; CRP, C-reactive protein; BMR, basal metabolic rate.

adjusted for because WC is a reliable representative of adiposity and SIRT1 expression parallels visceral fat.

Backward Stepwise Regression Analysis

Multivariate stepwise regression analysis was used to identify factors that influence circulating SIRT1 across AN, obese and normal-weight groups. We considered only a sub-set of the variables initially tested in linear regressions for the backward stepwise analysis (age, sex, WC, EFT, liver steatosis, HDL-cholesterol, ESR and BMR), depending on both preliminary statistics and clinical appraisal.

The results from the analysis provide the set of independent variables that best explain the variance in plasma SIRT1 levels in the current sample, although the results are limited by the small sample size. In the study population, age and EFT were the sole determinants of circulating SIRT1 with a β-coefficient of −0.026 ($p = 0.025$) and −0.516 ($p = < 0.001$), respectively, and a R^2 value of 0.3698 (**Table 3**).

DISCUSSION

In this study, we compared the circulating levels of SIRT1 in condition of deficiency, normal content or excess body fat in underweight, normal-weight, and obese patients. We found a significant negative correlation between plasma SIRT1 and adipose tissue, with the highest levels observed in participants with extremely reduced fat content (**Figure 1**). This observation is novel and opens new questions dealing with the regulation of SIRT1 production and its function in relation to adipose tissue.

Several studies have provided insights into the mechanisms underlying endocrine, metabolic, and adaptive changes in states of chronic starvation (22).

SIRT1 concentrations were negatively correlated with insulinemia and LDL-cholesterol. This is likely explained by the compelling evidence that SIRT1 overexpression offers substantial benefits on serum cholesterol and insulin levels and increased resistance to high-fat diet induced glucose intolerance and insulin resistance (23–25). No association was found between SIRT1 levels and triglycerides, although contradictory results have been obtained with resveratrol, a potent SIRT1 activator, that was found either to reduce (26) or to have no effects (27) on plasma triglycerides.

TABLE 3 | Stepwise multiple regression analysis results to identify predictor variables associated with circulating SIRT1 (ng/ml).

Variables	β Coeff.	SE	*p*
Age (yr)	−0.026	0.011	0.025
EFT (mm)	−0.516	0.083	<0.001

EFT, epicardial fat thickness. Variables included in the starting model for circulating SIRT1 were: age, sex, waist circumference, EFT, liver steatosis, high-density lipoprotein cholesterol, erythrocyte sedimentation rate and basal metabolic rate. We left in the model all variables that met the 0.15 significance level for entry into the stepwise model. R-squared value = 0.3698.

SIRT1 is an essential negative inflammatory regulator in high-fat diet or alcohol induced fatty liver diseases, mainly through deacetylating NF-κB and down-modulating NF-κB transcriptional activity, thereby reducing macrophage infiltration and pro-inflammatory cytokines production in the liver as well as in the adipose tissue (28). Indeed, in line with other studies (29, 30), we found that underweight patients were less inflamed compared to normal-weight and obese patients and ESR was inversely associated to the pattern of SIRT1 and proportional to fat mass. This coincides with the assumption that obese patients, generally, show a pro-inflammatory phenotype and express less SIRT1 than lean subjects.

It is worth to be mentioned that additional adjusted regression models for WC, a reliable predictor of visceral adiposity, abolished the association between SIRT1 and inflammatory and metabolic parameters, indicating that fat content is the most relevant determinant of SIRT1 circulating levels in this study.

In the stepwise regression analysis, epicardial fat, out of all the markers of adiposity included in the study whose expression is linearly associated with SIRT1, is the variable most strongly associated with SIRT1. The strict association between EFT and blood SIRT1 was not unexpected, being already seen previously (8). But, then again, human studies have shown that SIRT1 is expressed in visceral adipose tissue and reduced by obesity (31) and echocardiographic measurement

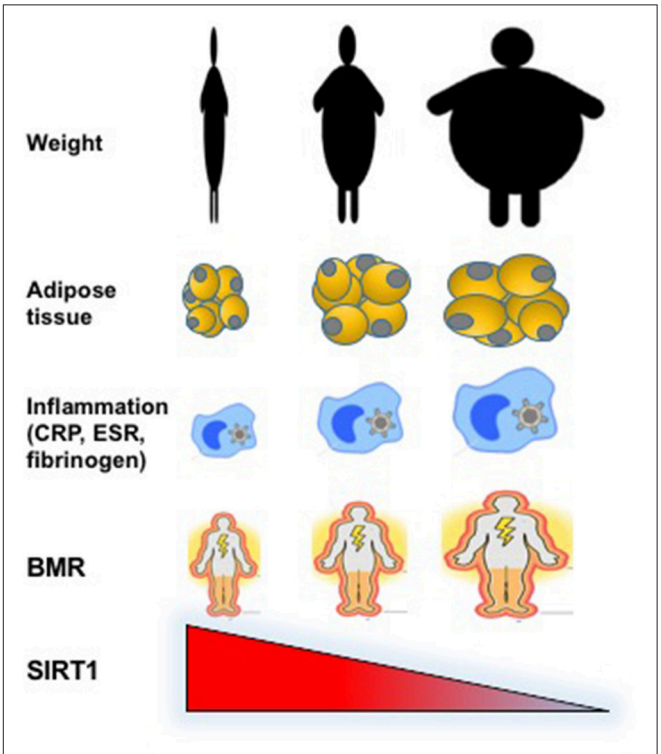

FIGURE 1 | Graphical representation of the inverse relationship between circulating levels of SIRT1 and weight, fat abundance and distribution, inflammatory, and metabolic parameters in underweight, normal weight, and obese individuals.

of epicardial fat can provide a more specific and sensitive measurement of intraabdominal visceral fat (32). Therefore, a possible explanation for the preferred association between EFT and SIRT1 might depend on the robust representativeness of epicardial fat as visceral fat as opposed to other measures of adiposity used and SIRT1. In line with previous studies (8), partly based on the same study sample, the inverse relationship between SIRT1 and EFT adds a new potential mechanism to the evidence supporting the role of epicardial adipose tissue in the development of atherosclerosis and its complications, inflammation, and metabolic syndrome in obese patients.

Furthermore, it is relevant the negative association seen between age and circulating SIRT1 levels. This observation confirms what previously reported in a comprehensive study aimed at identifying the pattern of serum SIRT1 activity according to age (33).

Individuals with AN have lower resting energy expenditure than normal-weight controls (34) and CR is a powerful stimulus for SIRT1 activation (18), likely an adaptive mechanism to preserve energy for vital functions. Accordingly, in SIRT1 gain-of-function transgenic mice, SIRT1 behaves as a "*thrifty gene*" that protects against metabolic diseases by instructing the organism to limit energy consumption and expenditure (23). Although our data are purely associative in nature, they seem to confirm the hypothesis that SIRT1 levels have the tendency to match with energy saving since the higher the SIRT1 values the lower the BMR values. Further studies to reveal the relationship between SIRT1 and BMR are warranted.

Although dysregulations of peripheral adipokines, gut-secreted peptides and central neurotransmitters involved in appetite modulation have been detected in patients with AN (35), the significance of these derangements for the development, course and prognosis of eating disorders is still not clear. Actually, there are no conclusive data as to whether alterations of feeding regulatory substances precede the appearance of an eating disorder or are the consequence of the nutritional aberrations occurring in the disorder. It has been suggested, although not definitively proved, that those alterations, even when secondary to malnutrition and/or to aberrant eating behaviors, might contribute to the genesis and the maintenance of some symptomatic aspects of AN, thus affecting the course and the prognosis of the disease. Whether the high levels of circulating SIRT1 in AN individuals is a consequence of the feeding behavior of these patients and whether they may modulate eating-related or non-eating-related psychopathological aspects of AN deserve to be deeply investigated. Interestingly, hypothalamic SIRT1 stimulates food intake and weight gain (36), raising the hypothesis that forms of AN might associate with SIRT resistance. These considerations may be an interesting starting point to study whether SIRT resistance might play a role in the pathogenesis of AN.

SIRT1 is found in a wide range of tissues and organs, highly expressed in liver and adipose tissue and regulated by nutritional status. In general CR stimulates SIRT expression (17, 18, 37) while high calorie diet reduces it. Thus, SIRT1 tissue expression and activity is influenced by the availability of energy suggesting that SIRT1 could have a role in the regulation of normal energy balance. Accordingly, plasma SIRT1 levels and fat mass are inversely regulated, with SIRT1 concentrations being increased in a catabolic condition and decreased in conditions of extreme BMIs.

Remarkably, CR dependent changes occur in a highly tissue-specific manner, as demonstrated by comparing circadian gene expression in the liver vs. epidermal and skeletal muscle stem cells (38). *De novo* oscillating genes under CR show an enrichment in SIRT1 targets in the liver due to enhanced SIRT1 activity (39). Therefore, we hypothesize that the increased circulating SIRT1 levels recorded in severely underweight patients may reflect the reorganization of metabolic pathway linked to SIRT1 in the liver of calorie restricted anorexic individuals.

The measurement of the circulating SIRT1 in severely underweight patients may provide new pathogenetic hypothesis for some of the features of AN.

Limitations of our study are the relatively small number of study subgroups and the use of calculated BMR values. Moreover, males and females were not analyzed separately because of the scarcity of males in our sample. We recognize that our results and conclusions are based on observational data and that the associations between SIRT1 levels and the variables measured do not establish causative roles. The strength of our study is the separation and comparison of different weight subgroups.

In conclusion, circulating SIRT1 inversely parallels the entire spectrum of fat phenotype, basal metabolic rate, inflammatory status, and eating behavior from anorexia to obesity through normal weight.

ETHICS STATEMENT

This study was carried out in accordance with the recommendations of the guidelines, Ethical Committee of the University of Rome La Sapienza with written informed consent from all subjects. All subjects gave written informed consent in accordance with the Declaration of Helsinki. The protocol was approved by the ethical committee of the Sapienza University of Rome, Policlinico Umberto I.

AUTHOR CONTRIBUTIONS

SM and LG conceived the project, developed the overall research plan, and wrote the manuscript. PM, AP, and AS selected the patients and collected the patients' data. MdG made the ultrasound determination of liver adiposity. GB made the echocardiographic epicardial fat thickness measurements. SB and SC made the circulating SIRT1 assay. SM, EP, and AR made the statistical analysis. SM, LG, AG, CL, LD, and AL interpreted the data and critically revised the manuscript for important intellectual content. All authors read and approved the final manuscript.

FUNDING

Sapienza University of Rome, Ricerca di Ateneo 2016.

REFERENCES

1. Buler M, Andersson U, Hakkola J. Who watches the watchmen? Regulation of the expression and activity of sirtuins. *FASEB J.* (2016) 30:3942–60. doi: 10.1096/fj.201600410RR
2. Nogueiras R, Habegger KM, Chaudhary N, Finan B, Banks AS, Dietrich MO, et al. Sirtuin 1 and sirtuin 3: physiological modulators of metabolism. *Physiol Rev.* (2012) 92:1479–514. doi: 10.1152/physrev.00022.2011
3. Chalkiadaki A, Guarente L. Sirtuins mediate mammalian metabolic responses to nutrient availability. *Nat Rev Endocrinol.* (2012) 8:287–96. doi: 10.1038/nrendo.2011.225
4. Jukarainen S, Heinonen S, Rämö JT, Rinnankoski-Tuikka R, Rappou E, Tummers M, et al. Obesity is associated with low NAD(+)/SIRT pathway expression in adipose tissue of BMI-discordant monozygotic twins. *J Clin Endocrinol Metab.* (2016) 101:275–83. doi: 10.1210/jc.2015-3095
5. Lee H, Chu SH, Park JY, Park HK, Im JA, Lee JW. Visceral adiposity is associated with SIRT1 expression in peripheral blood mononuclear cells: a pilot study. *Endocr J.* (2013) 60:1269–73. doi: 10.1507/endocrj.EJ13-0207
6. Costa Cdos S, Hammes TO, Rohden F, Margis R, Bortolotto JW, Padoin AV, et al. SIRT1 transcription is decreased in visceral adipose tissue of morbidly obese patients with severe hepatic steatosis. *Obes Surg.* (2010) 20:633–9. doi: 10.1007/s11695-009-0052-z
7. Mariani S, Fiore D, Basciani S, Persichetti A, Contini S, Lubrano C, et al. Plasma levels of SIRT1 associate with non-alcoholic fatty liver disease in obese patients. *Endocrine* (2015) 49:711–6. doi: 10.1007/s12020-014-0465-x
8. Mariani S, Costantini D, Lubrano C, Basciani S, Caldaroni C, Barbaro G, et al. Circulating SIRT1 inversely correlates with epicardial fat thickness in patients with obesity. *Nutr Metab Cardiovasc Dis.* (2016) 26:1033–8. doi: 10.1016/j.numecd.2016.06.001
9. Granér M, Nyman K, Siren R, Pentikäinen MO, Lundbom J, Hakkarainen A, et al. Ectopic fat depots and left ventricular function in nondiabetic men with nonalcoholic fatty liver disease. *Circ Cardiovasc Imaging* (2014) 8:e001979. doi: 10.1161/CIRCIMAGING.114.001979
10. Iozzo P. Myocardial, perivascular, and epicardial fat. *Diabetes Care* (2011) 34 (Suppl 2):S371–9. doi: 10.2337/dc11-s250
11. Boutant M, Cantó C. SIRT1 metabolic actions: Integrating recent advances from mouse models. *Mol Metab.* (2013) 3:5–18. doi: 10.1016/j.molmet.2013.10.006
12. Xu L, Xu S, Lin L, Gu X, Fu C, Fang Y, et al. High-fat diet mediates anxiolytic-like behaviors in a time-dependent manner through the regulation of SIRT1 in the brain. *Neuroscience* (2018) 372:237–45. doi: 10.1016/j.neuroscience.2018.01.001
13. Wang L, Quan N, Sun W, Chen X, Cates C, Rousselle T, et al. Cardiomyocyte specific deletion of Sirt1 gene sensitizes myocardium to ischemia and reperfusion injury. *Cardiovasc Res.* (2018) 114:805–21. doi: 10.1093/cvr/cvy033
14. Nemoto S, Fergusson MM, Finkel T. Nutrient availability regulates SIRT1 through a forkhead-dependent pathway. *Science* (2004) 306:2105–8. doi: 10.1126/science.1101731
15. Kanfi Y, Peshti V, Gozlan YM, Rathaus M, Gil R, Cohen HY. Regulation of SIRT1 protein levels by nutrient availability. *FEBS Lett.* (2008) 582:2417–23. doi: 10.1016/j.febslet.2008.06.005
16. Cohen HY, Miller C, Bitterman KJ, Wall NR, Hekking B, Kessler B, et al. Calorie restriction promotes mammalian cell survival by inducing the SIRT1 deacetylase. *Science* (2004) 305:390–2. doi: 10.1126/science.1099196
17. Mansur AP, Roggerio A, Goes MF, Avakian SD, Leal DP, Maranhão RC, et al. Serum concentrations and gene expression of sirtuin 1 in healthy and slightly overweight subjects after caloric restriction or resveratrol supplementation: a randomized trial. *Int J Cardiol.* (2017) 227:788–94. doi: 10.1016/j.ijcard.2016.10.058
18. Kitada M, Kume S, Takeda-Watanabe A, Tsuda S, Kanasaki K, Koya D. Calorie restriction in overweight males ameliorates obesity-related metabolic alterations and cellular adaptations through anti-aging effects, possibly including AMPK and SIRT1 activation. *Biochim Biophys Acta* (2013) 1830:4820–7. doi: 10.1016/j.bbagen.2013.06.014
19. Moschen AR, Wieser V, Gerner RR, Bichler A, Enrich B, Moser P, et al. Adipose tissue and liver expression of SIRT1, 3, and 6 increase after extensive weight loss in morbid obesity. *J Hepatol.* (2013) 59:1315–22. doi: 10.1016/j.jhep.2013.07.027
20. Mariani S, Fiore D, Persichetti A, Basciani S, Lubrano C, Poggiogalle E, et al. Circulating SIRT1 increases after intragastric balloon fat loss in obese patients. *Obes Surg.* (2016) 26:1215–20. doi: 10.1007/s11695-015-1859-4
21. Iacobellis G. Barbarini G, Letizia C, Barbaro G. Epicardial fat thickness and nonalcoholic fatty liver disease in obese subjects. *Obesity* (2014) 22:332–6. doi: 10.1002/oby.20624
22. Misra M, Klibanski A. Endocrine consequences of anorexia nervosa. *Lancet Diabetes Endocrinol.* (2014) 2:581–92. doi: 10.1016/S2213-8587(13)70180-3
23. Banks AS, Kon N, Knight C, Matsumoto M, Gutiérrez-Juárez R, Rossetti L, et al. SirT1 gain of function increases energy efficiency and prevents diabetes in mice. *Cell Metab.* (2008) 8:333–41. doi: 10.1016/j.cmet.2008.08.014
24. Bordone L, Cohen D, Robinson A, Motta MC, van Veen E, Czopik A, et al. SIRT1 transgenic mice show phenotypes resembling calorie restriction. *Aging Cell* (2007) 6:759–67. doi: 10.1111/j.1474-9726.2007.00335.x
25. Pfluger PT, Herranz D, Velasco-Miguel S, Serrano M, Tschop MH. Sirt1 protects against high-fat diet-induced metabolic damage. *Proc Natl Acad Sci USA.* (2008) 105:9793–8. doi: 10.1073/pnas.0802917105
26. Timmers S, Konings E, Bilet L, Houtkooper RH, van de Weijer T, Goossens GH, et al. Calorie restriction-like effects of 30 days of resveratrol supplementation on energy metabolism and metabolic profile in obese humans. *Cell Metab.* (2011) 14:612–22. doi: 10.1016/j.cmet.2011.10.002
27. Poulsen MM, Vestergaard PF, Clasen BF, Radko Y, Christensen LP, Stødkilde-Jørgensen H, et al. High-dose resveratrol supplementation in obese men: an investigator-initiated, randomized, placebo-controlled clinical trial of substrate metabolism, insulin sensitivity, and body composition. *Diabetes* (2013) 62:1186–95. doi: 10.2337/db12-0975
28. Ding RB, Bao J, Deng CX. Emerging roles of SIRT1 in fatty liver diseases. *Int J Biol Sci.* (2017) 13:852–67. doi: 10.7150/ijbs.19370
29. Omodei D, Pucino V, Labruna G, Procaccini C, Galgani M, Perna F, et al. Immune-metabolic profiling of anorexic patients reveals an anti-oxidant and anti-inflammatory phenotype. *Metabolism* (2015) 64:396–405. doi: 10.1016/j.metabol.2014.10.025
30. Haluzíková D, Dostálová I, Kaválková P, Roubícek T, Mráz M, Papezová H, et al. Serum concentrations of adipocyte fatty acid binding protein in patients with anorexia nervosa. *Physiol Res.* (2009) 58:577–81.
31. Jokinen R, Pirnes-Karhu S, Pietiläinen KH, Pirinen E. Adipose tissue NAD(+)-homeostasis, sirtuins and poly(ADP-ribose) polymerases -important players in mitochondrial metabolism and metabolic health. *Redox Biol.* (2017) 12:246–63. doi: 10.1016/j.redox.2017.02.011
32. Quez Martínez AL, Tepach Gutiérrez N, Vega García S, et al. Epicardial adipose tissue is associated with visceral fat, metabolic syndrome, and insulin resistance in menopausal women. *Rev Esp Cardiol.* (2014) 67:436–41. doi: 10.1016/j.rec.2013.10.011
33. Lee HJ, Yang SJ. Aging-Related correlation between serum Sirtuin 1 activities and basal metabolic rate in women, but not in men. *Clin Nutr Res.* (2017) 6:18–26. doi: 10.7762/cnr.2017.6.1.18
34. Misra M, Tsai P, Anderson EJ, Hubbard JL, Gallagher K, Soyka LA, et al. Nutrient intake in community-dwelling adolescent girls with anorexia nervosa and in healthy adolescents. *Am J Clin Nutr.* (2006) 84:698–706. doi: 10.1093/ajcn/84.4.698
35. Monteleone P, Castaldo E, Maj M. Neuroendocrine dysregulation of food intake in eating disorders. *Regul Pept.* (2008) 149:39–50. doi: 10.1016/j.regpep.2007.10.007

36. Cakir I, Perello M, Lansari O, Messier NJ, Vaslet CA, Nillni EA. Hypothalamic Sirt1 regulates food intake in a rodent model system. *PLoS ONE* (2009) 4:e8322. doi: 10.1371/journal.pone.0008322
37. Crujeiras AB, Parra D, Goyenechea E, Martínez JA. Sirtuin gene expression in human mononuclear cells is modulated by caloric restriction. *Eur J Clin Invest.* (2008) 38:672–8. doi: 10.1111/j.1365-2362.2008.01998.x
38. Solanas G, Peixoto FO, Perdiguero E, Jardí M, Ruiz-Bonilla V, Datta D, et al. Aged stem cells reprogram their daily rhythmic functions to adapt to stress. *Cell* (2017) 170:678–92.e20. doi: 10.1016/j.cell.2017.07.035
39. Sato S, Solanas G, Peixoto FO, Bee L, Symeonidi A, Schmidt MS, et al. Circadian reprogramming in the liver identifies metabolic pathways of aging. *Cell* (2017) 170:664–77.e11. doi: 10.1016/j.cell.2017.07.042

Conflict of Interest Statement: The authors declare that the research was conducted in the absence of any commercial or financial relationships that could be construed as a potential conflict of interest.

frontiers in Endocrinology

ORIGINAL RESEARCH
published: 19 July 2018
doi: 10.3389/fendo.2018.00406

Slim Body Weight Is Highly Associated With Enhanced Lipoprotein Functionality, Higher HDL-C, and Large HDL Particle Size in Young Women

Ki-Hoon Park[1,2,3†], *Dhananjay Yadav*[1,2,3†], *Suk-Jeong Kim*[1,2,3], *Jae-Ryong Kim*[4] *and Kyung-Hyun Cho*[1,2,3*]

[1] Department of Medical Biotechnology, Yeungnam University, Gyeongsan, South Korea, [2] Research Institute of Protein Sensor, Yeungnam University, Gyeongsan, South Korea, [3] LipoLab, Gyeongsan, South Korea, [4] Department of Biochemistry and Molecular Biology, Smart-Aging Convergence Research Center, College of Medicine, Yeungnam University, Daegu, South Korea

OPEN ACCESS

Edited by:
Sudip Bajpeyi,
The University of Texas at El Paso, United States

Reviewed by:
Andrew James Murphy,
Baker Heart and Diabetes Institute, Australia
Brie Sorrenson,
University of Auckland, New Zealand
Andras G. Lacko,
University of North Texas Health Science Center, United States
C. Roger White,
University of Alabama at Birmingham, United States

***Correspondence:**
Kyung-Hyun Cho
chok@yu.ac.kr

[†]Co-first authors.

Specialty section:
This article was submitted to Obesity, a section of the journal Frontiers in Endocrinology

Received: 09 March 2018
Accepted: 29 June 2018
Published: 19 July 2018

Citation:
Park K-H, Yadav D, Kim S-J, Kim J-R and Cho K-H (2018) Slim Body Weight Is Highly Associated With Enhanced Lipoprotein Functionality, Higher HDL-C, and Large HDL Particle Size in Young Women. Front. Endocrinol. 9:406. doi: 10.3389/fendo.2018.00406

There has been no information about the correlations between body weight distribution and lipoprotein metabolism in terms of high-density lipoproteins-cholesterol (HDL-C) and cholesteryl ester transfer protein (CETP). In this study, we analyzed the quantity and quality of HDL correlations in young women (21.5 ± 1.2-years-old) with a slim ($n = 21$, 46.2 ± 3.8 kg) or plump ($n = 30$, 54.6 ± 4.4 kg) body weight. Body weight was inversely correlated with the percentage of HDL-C in total cholesterol (TC). The plump group showed 40% higher body fat (26 ± 3 %) and 86% more visceral fat mass (VFM, 1.3 ± 0.3 kg) than the slim group, which showed 18 ± 2% body fat and 0.7 ± 0.2 kg of VFM. Additionally, the plump group showed 20% higher TC, 58% higher triglyceride (TG), and 12% lower HDL-C levels in serum. The slim group showed 34% higher apoA-I but 15% lower CETP content in serum compared to the plump group. The slim group showed a 13% increase in particle size and 1.9-fold increase in particle number with enhanced cholesterol efflux activity. Although the plump group was within a normal body mass index (BMI) range, its lipid profile and lipoprotein properties were distinctly different from those of the slim group in terms of CETP mass and activity, HDL functionality, and HDL particle size.

Keywords: body weight, blood pressure, lipoproteins, apoA-I, HDL-cholesterol

INTRODUCTION

Maintenance of a slim body shape is greatly desired for health and beauty purposes, especially in young women. However, there has been no information about the correlations between body weight distribution and lipoprotein metabolism. It is well known that serum high-density lipoprotein-cholesterol (HDL-C) level is inversely correlated with the incidence of coronary artery disease (1). HDL plays important roles in promoting anti-atherosclerotic, anti-diabetic, and anti-thrombotic activities (2) in serum and interacts with many antioxidant enzymes such as paraoxonase (3, 4). However, HDL can be altered under various health conditions (5), such as changed dietary patterns (6), pathogen infection (7), and environmental stress (8). Therefore, HDL-C may be a good biomarker for the diagnosis of many diseases and disease progression by

monitoring changes in its antioxidant and anti-inflammation abilities (9). However, it is well known that dysfunctional HDL is frequently found in patients with metabolic diseases such as obesity (10).

Although overweight status and obesity are associated with low HDL-C levels, there has been no report characterizing HDL particles from overweight subject. In the context of metabolic syndrome, obese persons (body mass index, BMI >30) with insulin resistance were shown to have low HDL-C levels, specifically 41% in women (<45 mg/dL), and 31% in men (<35 mg/dL) (11). Reduction of the HDL-C level is linked with increased very low-density lipoprotein (VLDL) production via elevation of cholesteryl ester transfer protein (CETP) activity. Further, obese subjects often show increased CETP activity (12, 13).

Apolipoprotein A-I (apoA-I), the major protein of HDL, exerts antioxidant and anti-inflammatory activities in lipid-free and lipid-bound states along with cholesterol efflux activity (14) in macrophages and insulin secretion activity in pancreatic beta cells. During the progression of obesity or insulin resistance in early metabolic syndrome, tumor necrosis factor-α (TNF-α) is up-regulated while apoA-I production is down-regulated. On the other hand, apoA-I gene expression can be down-regulated by increased production of adipokines and inflammatory cytokines (15, 16).

Progression of overweight status is associated with various complications such as hypertension, hyperglycemia, and coronary artery disease mediated via several mechanisms, including reduced HDL-C and elevated total cholesterol (TC), low-density lipoprotein cholesterol (LDL-C), and triglyceride (TG) levels (17). Although a high quantity of serum lipids has been well established as a cause of obesity and hypertension in adolescents, there has been no report on the quality of lipids and lipoproteins according to body weight. Furthermore, there has been no report comparing lipoprotein quality between two groups (slim and plump) showing a slight difference in body weight within a normal range, whereas lipid and lipoprotein properties of obese patients have been relatively well investigated.

In the current study, we compared lipoprotein biomarkers between slim (around 46 kg) and plump (around 55 kg) young women groups, although both are considered as having a normal body weight. Between the plump and slim type, lipid and lipoprotein qualities were compared to identify new biomarkers contributing to a slim body shape in young women.

MATERIALS AND METHODS

Subjects

We randomly recruited healthy female volunteers ($n = 51$) enrolled at Yeungnam University in 2015. Heavy alcohol consumers (>30 g EtOH/day) and those who had consumed any prescribed drugs to treat hyperlipidemia, diabetes mellitus, or hypertension were excluded. All subjects had unremarkable medical records without illicit drug use or past history of systemic diseases. The study was approved by the Institutional Review Board at Yeungnam University (Gyeongsan, South Korea) endorsed the protocol (IRB #7002016-A-2016-021) and the participants signed an informed consent form prior to research commencement.

Anthropometric Analysis

Blood pressure was measured each morning at 2-week intervals by an Omron HEM-1000 (Kyoto, Japan). Height, body weight, BMI, total body fat (%), total body fat mass (kg), and visceral fat mass (VFM) (kg) were measured individually at the same time of day at 2-week intervals using an X-scan plus II body composition analyzer (Jawon Medical, Gyeongsan, Korea).

Vascular Stiffness Analysis

Systolic and diastolic blood pressures were measured in triplicate using a semi-automated non-invasive oscillometric sphygmomanometer using the SphygmoCor system (Actor Medical, Sydney, Australia) following a 5 min rest period (18). Pulse wave was analyzed with SphygmoCor software. Augmentation pressure is the gain in aortic pressure above its first systolic push, which is thought to be determined by pressure wave reflection but may be influenced by ventricular ejection aspects. However, the augmentation index, the ratio of augmentation pressure to aortic or central pulse pressure, is widely used as a measure of pressure wave reflection (19, 20). Measurements were performed by a technician trained in the technique and blinded to the characteristics of each subject.

Plasma Analysis

Blood was obtained from all subjects following overnight fasting. Blood was collected using a vacutainer (BD Biosciences, Franklin Lakes, NJ, USA) containing EDTA (final concentration, 1 mM). Plasma was isolated by low-speed centrifugation (3,000 rpm) and stored at −80°C until analysis. To analyze plasma, TC, TG, HDL-C, glucose, aspartate aminotransferase (AST), and alanine aminotransferase (ALT) levels were measured using commercially available kits (Cleantech TS-S; Wako Pure Chemical, Osaka, Japan).

Characterization of Lipoproteins

Very low-density lipoprotein (VLDL, d <1.019 g/mL), LDL (1.019 <d <1.063), HDL_2 (1.063 < d <1.125), and HDL_3 (1.125 < d <1.225) were isolated from pooled plasma of each group via sequential ultracentrifugation (21), and the density was adjusted by addition of NaCl and NaBr in accordance with standard protocols. Samples were centrifuged for 22 h at 10°C at 100,000 g using a Himac CP-100NX (Hitachi, Tokyo, Japan) using P50AT4-0124 rotor in our laboratory. Protein concentrations of lipoproteins were determined via Lowry protein assay, as modified by Markwell et al. (22). Expression levels of apoA-I (28 kDa) and apo-B (550 kDa) were determined by SDS-PAGE.

To assess the degree of lipoprotein oxidation, the concentration of oxidized species in lipoproteins was determined by the thiobarbituric acid-reacting substance (TBARS) assay method using malondialdehyde as a standard (23). To compare the extent of glycation between groups, advanced glycation end products (AGEs) in lipoproteins were determined from reading fluorometric intensities at 370 nm (excitation) and 440 nm (emission), as our previous report (24), using a

spectrofluorometer LS55 (Perkin Elmer, Shelton, CT, USA) with the WinLab software package (version 4.0).

Cholesteryl Ester Transfer Protein Assay

A rHDL-containing apoA-I and cholesteryl oleate were synthesized in accordance with the method described by Cho (25) and Cho et al. (26) using trace amounts of [^{3}H]-cholesteryl oleate (TRK886, 3.5 μCi/mg of apoA-I; GE Healthcare). The rHDL was immobilized using CNBr-activated Sepharose 4B resin (Amersham Biosciences) for easy separation after the reaction in accordance with the manufacturer's instructions. CE transfer reaction was performed in 300-μL reaction mixtures containing human serum (20 μL) or HDL_3 (20 μL, 2 mg/mL) as a CETP source, [^{3}H]-rHDL-agarose (20 μL, 0.25 mg/mL) as a CE-donor, and human LDL (20 μL, 0.25 mg/mL) as a CE-acceptor. After incubation of 4 h at 37°C, the reaction was halted via brief centrifugation (10,000 g) for 3 min at 4°C. The supernatant containing CE-acceptor (150 μL) was then subjected to scintillation counting, and percentage transfer of [^{3}H]-CE from [^{3}H]-rHDL to LDL was calculated.

Ferric Reducing Ability of Plasma Assay and Paraoxonase Activity

The ferric reducing ability of plasma (FRAP) was determined using the method described by Benzie and Strain (27). The antioxidant activities of individual HDL fractions were estimated by measuring increases in absorbance produced by generated ferrous ions. Paraoxonase-1 (PON-1) activity was then determined by measuring the initial velocity of *p*-nitrophenol production at 37°C, as determined by measuring the absorbance at 405 nm (microplate reader, Bio-Rad model 680; Bio-Rad, Hercules, CA, USA), as described previously (28) with slight modifications (29). Prior to the measurement, HDL was extensively dialyzed against PBS to remove EDTA.

Phagocytosis of LDL Into Macrophages

THP-1 cells, a human monocytic cell line, were obtained from the American Type Culture Collection (ATCC, #TIB-202^{TM}, Manassas, VA, USA) and maintained in RPMI-1640 medium (Hyclone, Logan, UT) supplemented with 10% fetal bovine serum until needed. Cells that had undergone no more than 20 passages were incubated in medium containing phorbol 12-myristate 13-acetate (PMA, 150 nM) in 24-well plates for 48 h at 37°C in a humidified incubator (5% CO_2, 95% air) in order to induce differentiation into macrophages. Differentiated and adherent macrophages were then rinsed with warm PBS, followed by incubation with 450 μL of fresh RPMI-1640 medium containing 0.1% FBS and 50 μg of each LDL (1 mg of protein/mL in PBS) for 48 h at 37°C in a humidified incubator. After incubation, cells were washed with PBS three times and then fixed in 4% paraformaldehyde for 10 min. Next, fixed cells were stained with oil-red O staining solution (0.67%) and washed with distilled water. THP-1 macrophage-derived foam cells were then observed and photographed using a Nikon Eclipse TE2000 microscope (Tokyo, Japan) at 400× magnification. Cell media (0.2 mL) were then analyzed by TBARS assay to evaluate changes in levels of oxidized species using malondialdehyde (MDA) as a standard.

Anti-atherogenic Activity of HDL_3

Differentiated and adherent macrophages were then rinsed with warm PBS and incubated with 400 μL of fresh RPMI-1640 medium containing 0.1% fetal bovine serum, 50 μg of oxLDL (1 mg of protein/mL in PBS), and 30 μg of HDL_3 (2 mg of protein/mL in PBS) from each group for 48 h at 37°C in a humidified incubator. After incubation, cells were stained with oil-red O solution (0.67%) to visualize the amount of lipid species in cells. THP-1 macrophage-derived foam cells were then observed and photographed using a Nikon Eclipse TE2000 microscope (Tokyo, Japan) at 400× magnification. The stained area was quantified via computer-assisted morphometry using Image Proplus software (version 4.5.1.22, Media Cybernetics, Bethesda, MD).

Cholesterol Efflux

THP-1 cells were incubated in medium containing phorbol 12-myristate 13-acetate (PMA, 150 nM) in a plate for 48 h at 37°C in a humidified incubator in order to induce differentiation into macrophages. Macrophages were treated with radiolabeled cholesterol (0.1 μCi of [^{3}H]-cholesterol) in RPMI 1640 medium (Hyclone, Logan, UT) containing 1% fetal bovine serum (Hyclone, Logan, UT) per well (0.5 mL) for 48 h. Media containing the isotope was saved and replaced with fresh media containing 0.3 mM 8-(4-chlorophenylthio)-cyclic adenosine monophosphate (cAMP, Cat# C3912, Sigma-Aldrich, St. Louis, MO) to up-regulate the cellular cholesterol pump (ATP-binding cassette transporter 1, ABCA1) for 18 h. After removal of media containing cAMP, 28 μg of HDL_3 was added and the sample incubated with serum-free media (0.5 mL) for 24 h. Subsequently, cell media (0.5 mL) in individual wells were collected into a 1.7 mL tube. Cells were then rinsed with PBS three times and dissolved in 0.2 mL of RIPA buffer (50 mM Tris-HCl [pH 8.0], 150 mM NaCl, 5 mM EDTA [pH 8.0], 1% NP-40, 0.5% sodium deoxycholate, 0.1% sodium dodecyl sulfate) to lyse cells. An aliquot of the cell lysate (0.1 mL) was mixed with a scintillation cocktail (3 mL) to quantify the amount of isotope indicating uptake of cholesterol into cells. After scintillation counting of [^{3}H]-cholesterol in cells and media, the amount of effluxed cholesterol from cells was calculated using the following formula as previously reported (30):

$$\%\ \text{Cholesterol efflux} = \frac{(\text{media counts} \times \text{dilution factor})}{(\text{media count} \times \text{dilution factor}) + (\text{cell lysis count} \times \text{dilution factor})} \times 100$$

$$\%\ \text{Net efflux} = \%\ \text{cholesterol efflux}\ (\text{with HDL3}) - \%\ \text{blank efflux}\ (\text{without HDL3})$$

ELISA and Western Blotting

The quantity of apoA-I in serum was determined in each group by ELISA using a commercially available kit (Quantikine ELISA, DAPA10, R&D systems, Minneapolis, MN). In order to quantify serum CETP, each well of a polystyrene microplate (#3590; Corning Inc., Corning, NY, USA) was coated with anti-human CETP rabbit antibody (ab19012; Abcam, Cambridge, UK) at a concentration of 0.25 μg/mL, followed by incubation overnight at 4°C. Equally, diluted serum sample was incubated for 2 h at room temperature. After extensive washing, anti-human CETP mouse antibody (ab2726; Abcam, 1 μg/mL) was added and the sample incubated for 2 h at room temperature. To develop the color reaction, anti-mouse IgG antibody (ab6728; Abcam, 0.5 μg/mL) conjugated with horseradish peroxidase was added. For color development, 3,3′,5,5′-tetramethylbenzidine (TMB) substrate solution (Cat. No. 555214; BD Biosciences, Flanklin Lakes, NJ, USA) was added and quantified using a Victor X4 microplate reader (Perkin Elmer, Waltham, MA).

Apolipoprotein/lipoprotein compositions were compared via sodium dodecyl sulfate-polyacrylamide gel electrophoresis (SDS-PAGE) using identical protein loading quantities (3 μg of total protein per lane) from individual HDL_3, and expression levels of apolipoprotein were analyzed via immunodetection. Anti-human apoA-I antibody (ab7613), anti-paraoxonase antibody (ab24261), and anti-IL-6 antibody (ab6672) were purchased from Abcam (Cambridge, UK). Relative band intensity (BI) was compared via band scanning with Chemi-Doc® XRS + (Bio-Rad, Hercules, CA) using Image Lab software (Version 5.2).

Electron Microscopy

Transmitted electron microscopy (TEM) was performed with a Hitachi electron microscope (model H-7600; Ibaraki, Japan) operated at 80 kV as in our previous report (31). HDL_2 were negatively stained with 1% sodium phosphotungstate (pH 7.4) with a final apolipoprotein concentration of 0.3 mg/mL in TBS.

Zebrafish and Embryos

Wildtype zebrafish and embryos were maintained according to standard protocols. Zebrafish maintenance and experimental procedures were approved by the Committee of Animal Care and Use of Yeungnam University (Gyeongsan, Korea). Zebrafish and embryos were maintained in a system cage (3 L volume, acrylic tank) and 6-well plates, respectively, at 28°C during treatment under a 14:10 h light:dark cycle.

Microinjection of Zebrafish Embryos

To compare antioxidant and anti-inflammatory activities of HDL between slim and plump, HDL_3 from each group was injected into zebrafish embryos, as in our previous report (32). Embryos at 1-day post-fertilization (dpf) were individually microinjected using a pneumatic picopump (PV820; World Precision Instruments, Sarasota, FL, USA) equipped with a magnetic manipulator (MM33; Kantec, Bensenville, IL, USA) and a pulled microcapillary pipette-using device (PC-10; Narishigen, Tokyo, Japan). To minimize bias, injections were performed at the same position on each yolk. Filter-sterilized solution of each LDL or HDL_3 was injected into flasks of embryos. Following injection, live embryos were observed under a stereomicroscope (Motic SMZ 168; Hong Kong) and photographed using a Motic cam2300 CCD camera.

Imaging of Reactive Oxygen Species (ROS)

Injection of HDL_3 from slim and plump group into the zebrafish embryo in the presence of ox LDL was done and changes in reactive oxygen species (ROS) levels in larvae were imaged by dihydroethidium (DHE; cat # 37291, BioChemika) staining, as previously described (33). Images were obtained by fluorescence microscopy (Ex = 588 nm and Em = 605 nm) on a Nikon Eclipse TE2000 instrument (Tokyo, Japan). To avoid bias, red fluorescence was measured in the trunk area away from the injection site. Quantification of the stained area was carried out via computer-assisted morphometry using Image Proplus software (version 4.5.1.22, Media Cybernetics, Bethesda, MD).

Data Analysis

All data are expressed as the mean ± SD from at least three independent experiments with duplicate samples. Data comparisons were assessed by Student's *t*-test using the SPSS program (version 14.0; SPSS, Inc., Chicago, IL, USA). In the human study, data in the same group were evaluated via one-way analysis of variance (ANOVA) using SPSS (version 14.0; Chicago, IL, USA), and differences between the means were assessed using Duncan's multiple-range test. Statistical significance was defined as $p < 0.05$.

RESULTS

BMI and Serum HDL-C

All participants were very similar in age (21.5 ±1.2 years old) and height (161.5 ± 4.2 cm). Participants were of normal body weight and BMI but were divided into a plump group (around 55 kg of BW) and slim group (around 46 kg of BW).

The plump group showed a significantly higher BMI, body fat percentage, and VFM than the slim group, as shown in **Table 1**. The systolic blood pressure and diastolic blood pressure were not found to be significant between the slim and plump group.

Serum Lipid Level and Body Shape

The plump group showed 1.2- and 1.6-fold higher serum TC and TG levels, respectively, than the slim group, although all TC and TG levels were within their normal ranges (**Table 2**). However, the plump group showed 12% lower HDL-C and 1.7-fold higher TG/HDL-C than the slim group. The slim group showed 1.3-fold higher % HDL-C and serum apoA-I content than the plump group. Serum uric acid level of the plump group was slightly higher than that of the slim group. However, there was no significant difference in serum glucose, uric acid, or AST/ALT level between the groups.

CETP Mass and Activity

Interestingly, the plump group showed significantly higher CETP mass than the slim group (**Table 2**). Furthermore, there was a significant difference in serum CETP activity ($p = 0.0202$)

TABLE 1 | Anthropometric data.

	Total ($n = 51$)	Plump ($n = 30$)	Slim ($n = 21$)	p-value
Age (years)	21.5 ± 1.2	21.9 ± 1.7	21.1 ± 0.5	0.0712
Height (cm)	161.5 ± 4.2	161.5 ± 4.3	161.6 ± 4.4	0.4728
Weight (kg)	50.2 ± 5.8	54.6 ± 4.4	46.2 ± 3.8***	<0.001
BMI (kg/m^2)	19.2 ± 2.0	20.9 ± 1.3	17.7 ± 1.0***	<0.001
Body fat (%)	22.1 ± 4.4	25.9 ± 3.0	18.7 ± 2.1***	<0.001
Visceral fat mass (kg)	1.0 ± 0.4	1.3 ± 0.3	0.7 ± 0.2***	<0.001
Subcutaneous fat mass (kg)	10.3 ± 3.0	12.9 ± 2.1	8.0 ± 1.5***	<0.001
Systolic blood pressure (mmHg)	114.2 ± 9.6	117.0 ± 8.2	111.6 ± 10.3	0.1037
Diastolic blood pressure (mmHg)	68.5 ± 8.1	71.0 ± 8.6	66.2 ± 7.2	0.0896
Blood pulse (beats/min)	83.9 ± 10.3	82.8 ± 11.7	84.9 ± 9.3	0.3255
Augmentation Pressure (mmHg)	0.9 ± 2.7	3.0 ± 2.5	−0.2 ± 2.2	0.0137
Augmentation Index	3.3 ± 9.0	10.2 ± 5.6	−0.6 ± 8.4	0.0128
Reference age (years)	24.1 ± 9.1	30.0 ± 13.9	20.8 ± 2.3	0.0339

$^{***}p < 0.001$ vs. plump group.

TABLE 2 | Serum profile.

	Total ($n = 31$)	Plump ($n = 20$)	Slim ($n = 11$)	p-value
TC (mg/dL)	188.3 ± 35.9	206.1 ± 31.1	172.1 ± 33.1*	0.0129
TG(mg/dL)	63.3 ± 24.6	78.4 ± 27.3	49.7 ± 10.9**	0.0035
HDL-C (mg/dL)	70.5 ± 11.9	65.9 ± 8.2	74.7 ± 13.6*	0.0454
%HDL-C	38.4 ± 8.6	32.6 ± 6.2	43.8 ± 6.9***	0.0005
TG/HDL-C	0.9 ± 0.4	1.2 ± 0.5	0.7 ± 0.2**	0.0032
LDL-C (mg/dL)	106.8 ± 33.8	126.0 ± 32.4	89.5 ± 25.5**	0.0070
%LDL-C	54.7 ± 8.4	59.3 ± 7.4	50.5 ± 7.2**	0.0086
apoA-I (mg/mL)	2.7 ± 1.2	2.3 ± 1.1	3.1 ± 1.2*	0.0467
CETP mass	2.1 ± 0.3	2.3 ± 0.3	2.0 ± 0.3*	0.0477
%CE-transfer	28.9 ± 3.4	30.6 ± 3.9	27.4 ± 1.9*	0.0202
Glucose (mg/dL)	79.5 ± 5.7	80.5 ± 5.1	78.6 ± 6.2	0.2300
Uric acid (mg/dL)	5.8 ± 1.1	6.1 ± 1.1	5.6 ± 1.0	0.1380
AST (karmen/mL)	15.8 ± 1.5	15.5 ± 1.4	16.1 ± 1.6	0.1838
ALT (karmen/mL)	15.5 ± 2.2	14.9 ± 2.0	16.1 ± 2.3	0.1087

$^{*}p < 0.05$; $^{**}p < 0.01$; $^{***}p < 0.001$ vs. plump group.

between the slim and plump groups although around 10% of activity was different (**Table 2**).

Correlation of HDL-C and Body Shape

As shown in Supplementary Figure 1A, height generally increased with elevation of % HDL-C. Although there was no statistical difference, height and % HDL-C showed positive correlations. However, % HDL-C was inversely correlated with body weight, as shown in Supplementary Figure 1B. Correlations between BMI and % HDL-C (**Figure 1A**) and between % HDL-C and % body fat mass (**Figure 1B**) also showed clear inverse relationships. Visceral fat mass was inversely correlated with % HDL-C ($p < 0.0001$, Supplementary Figure 2A). However, visceral fat was positively correlated with CETP mass (Supplementary Figure 2B).

Correlation of HDL-C and Blood Pressure

Both systolic and diastolic blood pressures were negatively correlated with % HDL-C as shown in Supplementary Figure 3. Diastolic blood pressure and % HDL-C showed steeper slopes than systolic blood pressure, suggesting that % HDL-C was more closely associated with lowered diastolic blood pressure ($p = 0.0031$). The plump group showed 5–6 mmHg higher diastolic and systolic blood pressures than the slim group.

The plump group showed a remarkably high central augmentation pressure and index with an arterial stiffness reference age of 30 ± 13.9-years-old, whereas the slim group showed a reference age of 20.8 ± 2.3-years-old (**Table 1**).

Expression Level of apoA-I in HDL

To compare the expression level of apoA-I in HDL, the same amount of total proteins per individual HDL was loaded on each lane of a gel. As shown in **Figure 2**, the slim group showed 2.2- and 1.3-fold higher expression levels of apoA-I in HDL_2 and HDL_3, respectively, compared to the plump group as determined by SDS-PAGE. Based on Western blotting with an apoA-I antibody, the slim group showed 1.5- and 1.6-fold higher apoA-I levels in HDL_2 and HDL_3, respectively, compared to the plump group.

HDL_2 Particle Size and Cholesterol Efflux

The slim group showed a 15% larger HDL particle size and 1.9-fold higher number of particles than the plump group as shown in **Figure 3A** and a representative photo of **Figure 3** from TEM analysis. HDL_2 from the slim group showed significantly enhanced cholesterol efflux activity from macrophages (around 24 ± 2% efflux), whereas the plump group showed 21 ± 1% efflux ($p = 0.018$) during 24 h of incubation of each HDL as shown in **Figure 3B**.

Antioxidant Ability

Serum PON activity of the slim group was 1.3-fold higher than that of the plump group up to 60 min of incubation, as shown in **Figure 4A**. Serum FRAP ability was not significantly different between the groups, and the two groups showed saturated reduction potential at the same incubation time, as shown in **Figure 4B**. The slim group showed higher HDL-associated antioxidant enzyme activity, although their antioxidant potentials in serum were similar. This result suggests that HDL from the slim group showed enhanced functionality.

The slim group also showed higher HDL-associated antioxidant activity than the plump group (**Figure 5**). Regarding FRAP ability, the slim group showed 22% higher reduction potential than the plump group during 20 min of incubation (**Figure 5A**). Additionally, the slim group showed 1.7-fold higher PON activity than the plump group during 60 min of incubation (**Figure 5B**).

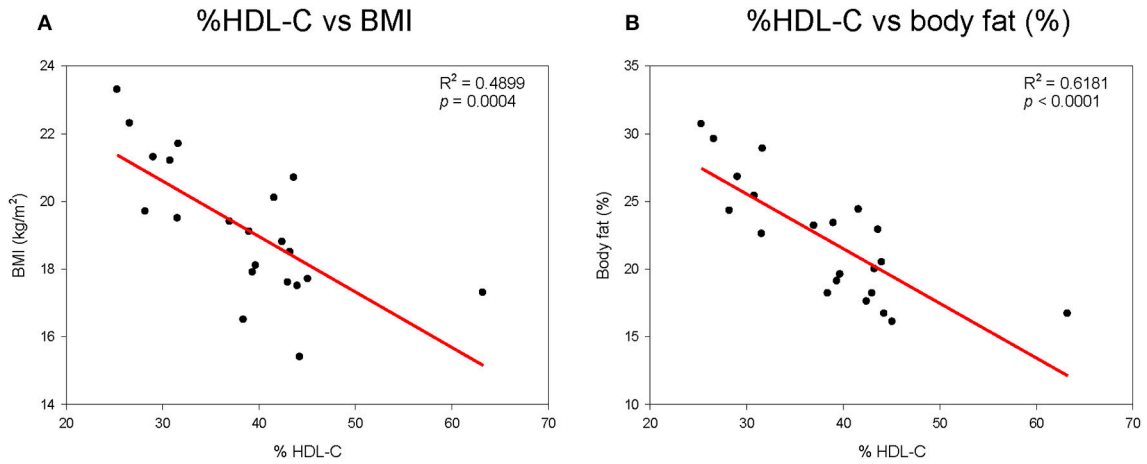

FIGURE 1 | Correlation of % HDL-C with body mass index **(A)** and body fat mass **(B)**.

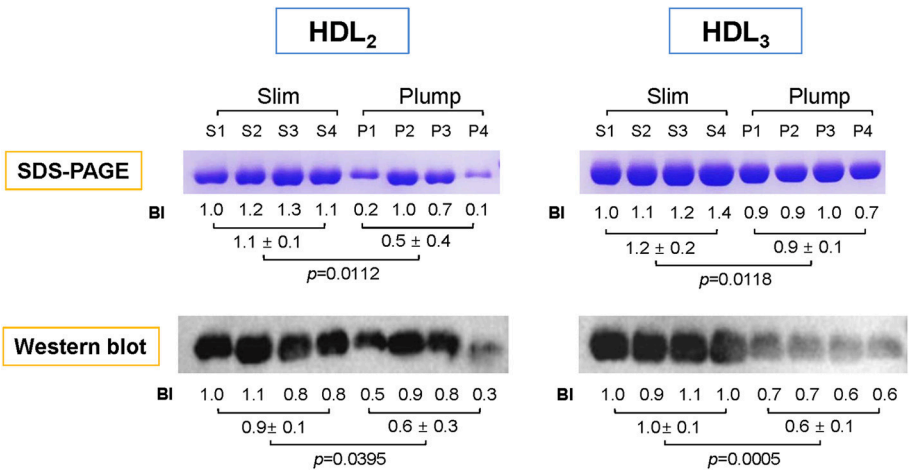

FIGURE 2 | Electrophoretic patterns of apolipoproteins in HDL_2 and HDL_3. The number indicates band intensity (BI) of apoA-I from densitometric analysis using Gel-Doc (Bio-Rad). The expression level of apoA-I was compared by Western blotting. BI was calculated using Chemi-Doc (Bio-Rad).

Compositions of Lipoproteins

As shown in **Figure 6A**, the plump group showed 1.9- and 1.3-fold higher protein contents in VLDL and LDL, respectively, but 20% lower protein content in the HDL_2 fraction. The lower protein content in HDL_2 from the plump group was strongly associated with reduced serum apoA-I content (**Table 2**). However, the plump group showed 10–13% higher glycation extent in all lipoproteins, especially VLDL and LDL (**Figure 6B**). At the same protein amount, the plump group showed 9% higher cholesterol content in VLDL and LDL (**Figure 6C**). However, the plump group showed 27% less cholesterol content in HDL_3, whereas there was no difference in HDL_2-C. Interestingly, the plump group showed elevated TG contents in all lipoprotein fractions, especially 1.3- and 1.2-fold higher TG contents in VLDL and HDL_3, respectively. HDL_3 from the plump group showed higher TG and lower cholesterol contents than the slim group (**Figure 6D**), suggesting functionality of lipoproteins may be impaired at the beginning of overweight status.

Modification of Lipoproteins

LDL from the plump group showed faster electromobility, as shown in **Figure 7A**, due to putative modifications such as oxidation and glycation. The plump group showed greater migration distance (1.3 ± 0.2 cm) than the slim group (0.9 ± 0.1 cm). TBARS assay was performed to determine oxidized products, showed all lipoproteins from the plump group showed higher MDA contents (**Figure 7B**). Especially, the plump group showed 45% more MDA content in HDL_2 compared to the slim group.

Cupric ion treatment revealed that the plump group was 1.3-fold more sensitive to oxidation than the slim group (**Figure 7C**) during 150 min of incubation. After incubation, Cu^{2+}-treated LDL from the plump group showed faster electromobility with

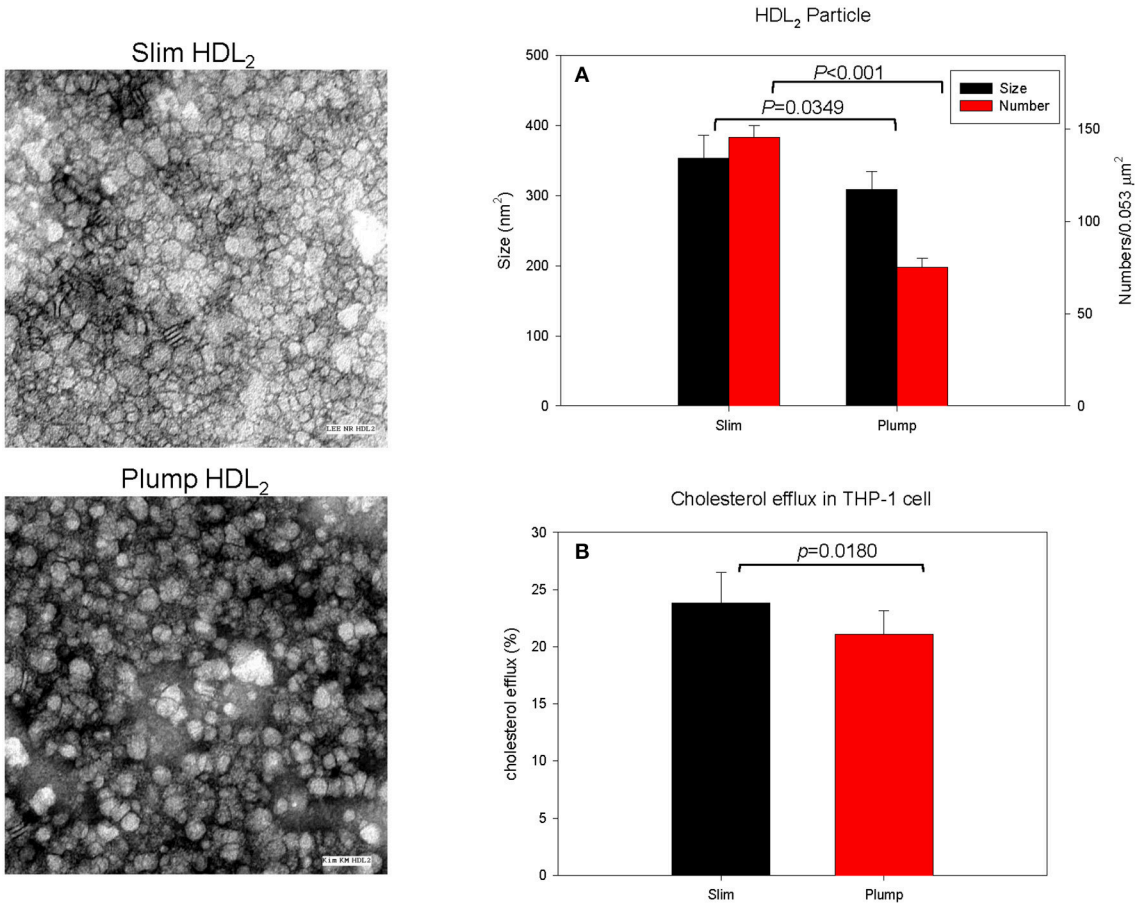

FIGURE 3 | Cholesterol efflux activity and a representative photo of negatively-stained HDL_2 and HDL_3 from slim and plump groups (electron microscopy). All micrographs are shown at a magnification of 40,000×. The scale bar corresponds to 100 nm. **(A)** Shows measured particle size of HDL and particle number in the designated area. **(B)** Shows cholesterol efflux activity from macrophages.

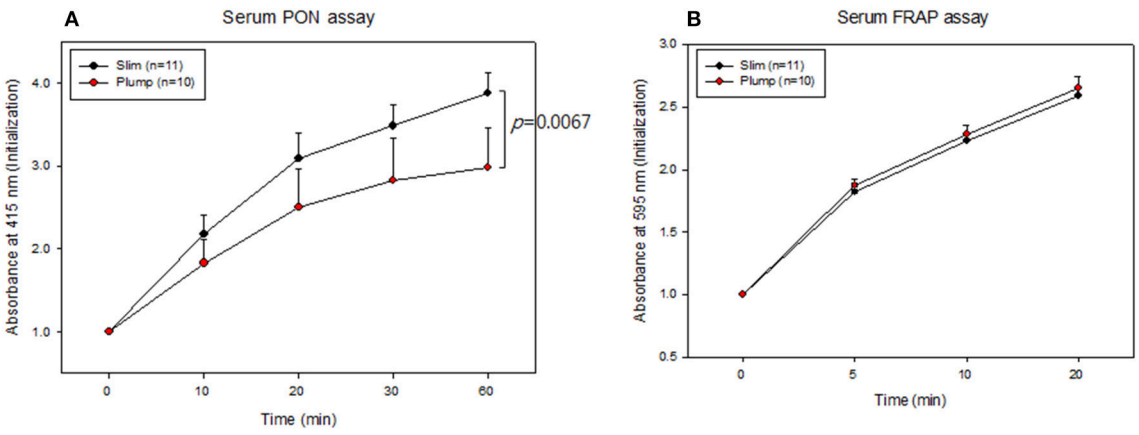

FIGURE 4 | Serum antioxidant activity. Paraoxonase activity **(A)** and ferric ion reduction ability **(B)**.

fainter band intensity as shown in the photo of **Figure 7C**, suggesting that LDL from the plump group was more susceptible to oxidation.

Uptake of LDL Into Macrophages

After 48 h of treatment with each LDL, the plump group showed 2-fold higher oil-red O-stained area than the slim group

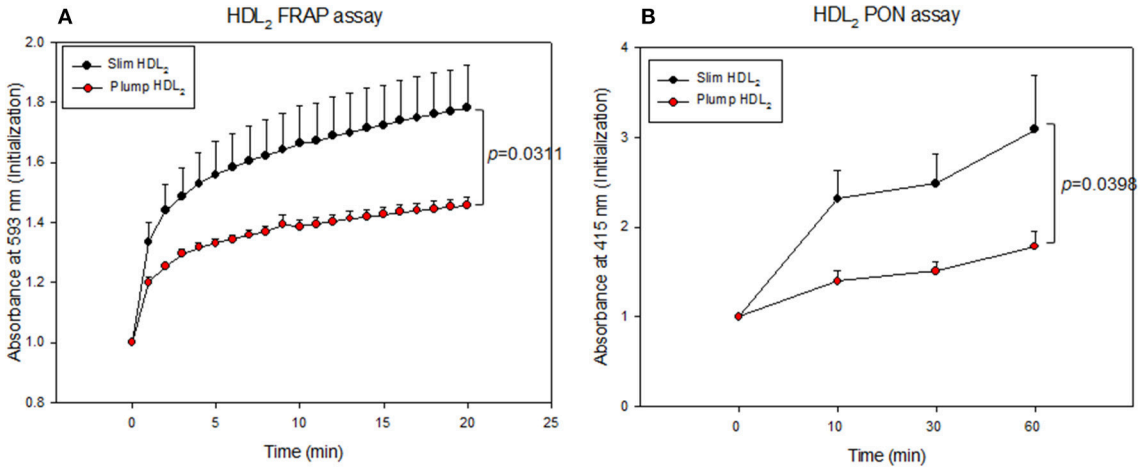

FIGURE 5 | Antioxidant activity of HDL_2-associated enzymes. Ferric ion reduction ability **(A)** and Paraoxonase activity **(B)**.

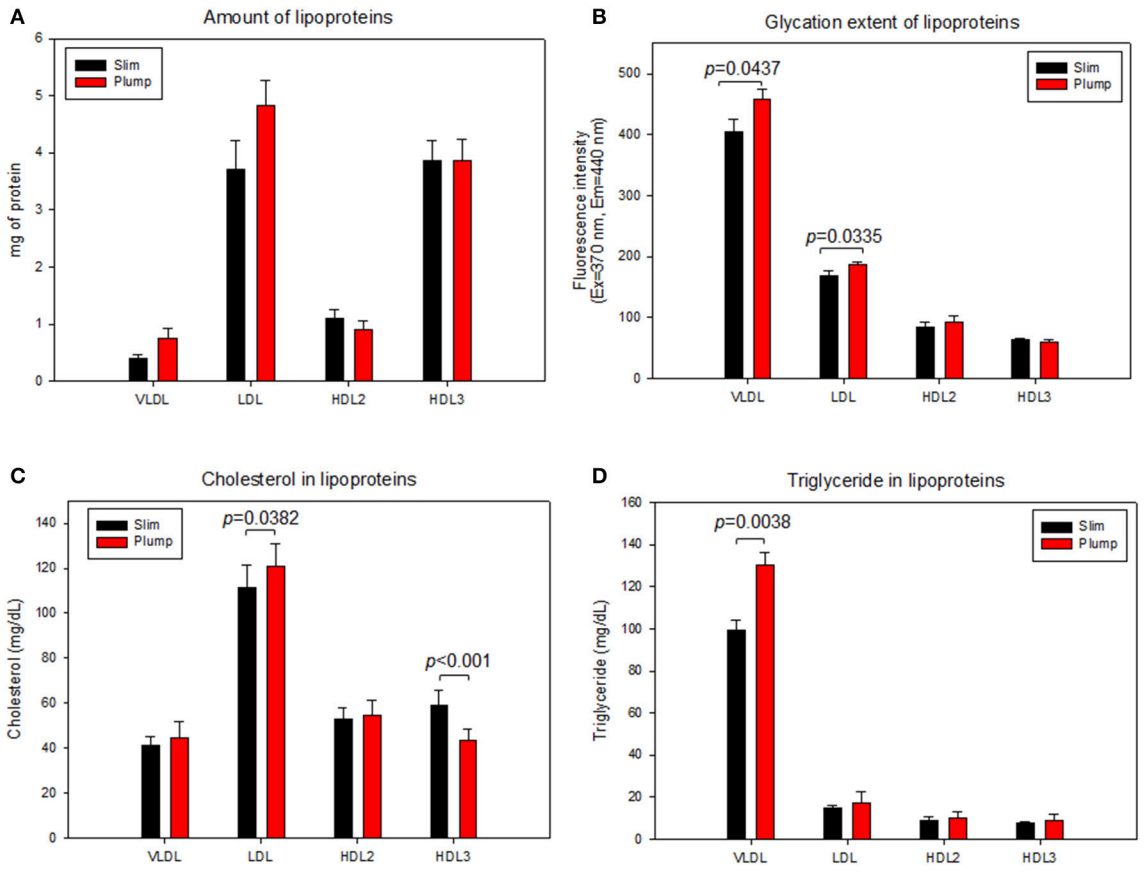

FIGURE 6 | Lipoprotein composition and glycation extent of slim and plump groups. Protein content **(A)** and glycation extent **(B)**. Lipoprotein composition and glycation extent of slim and plump groups. Cholesterol **(C)** and triglyceride content **(D)**.

(Supplementary Figure 4), suggesting that LDL from the plump group was taken up 2-fold more into macrophages. This result supports the earlier findings that LDL from the plump group was more glycated (**Figure 6B**) and oxidized (**Figure 7**), as modified LDL was more phagocytosed by macrophages to accelerate foam cell production.

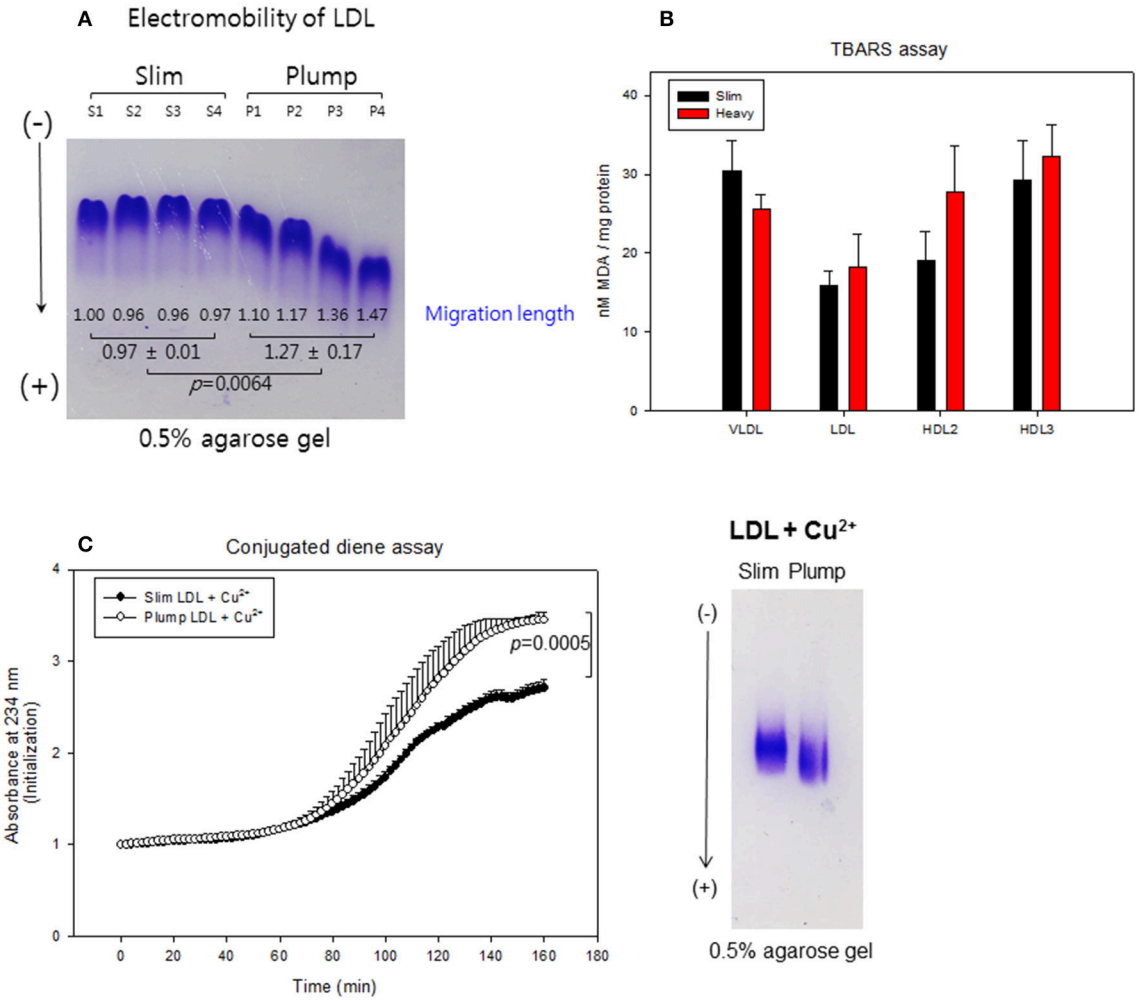

FIGURE 7 | Lipoprotein properties between slim and plump groups. Electromobility of LDL **(A)**, extent of oxidized species **(B)**. Susceptibility to cupric ion mediated oxidation **(C)**.

Embryo Survivability

Microinjection of LDL from the plump group caused the most severe embryo death up to 69% survival, whereas LDL from the slim group resulted in 75% embryo survival at 48 h post-injection, as shown in Supplementary Figure 5B. This difference in embryo survival can be attributed to more oxidized in LDL from the plump group (**Figure 7**). DHE staining revealed that plump LDL-injected embryos showed the strongest red intensity, suggesting the highest production of reactive oxygen species (Supplementary Figures 5A,C).

Injection of oxLDL caused the lowest embryo survival (around 44%), whereas PBS injection resulted in 84% survival, as shown in the graph of Supplementary Figure 6. In the presence of oxLDL, co-injection of HDL_3 from the slim group enhanced survival (around 70%), whereas HDL_3 from the plump group resulted in lower survivability (around 59%). oxLDL alone-injected embryos showed the strongest red fluorescence, which was 3-fold higher than PBS-injected embryos. However, HDL_3 from the slim and plump groups caused 25 and 16% reduction of red fluorescence, respectively, suggesting that HDL from the slim group was more effective in preventing embryonic death and ROS production mediated by oxLDL. Taken together, the plump group showed more dysfunctional HDL with smaller particle size, reduced antioxidant ability, greater atherogenic properties, such as higher CETP activity and mass with more inflammatory properties in human cells and zebrafish embryos.

DISCUSSION

To our knowledge, this is the first report demonstrating differences in lipoproteins and lipid levels between young women with slim and plump body weights. It has been well established that overweight and obese adolescents are worldwide epidemic issue (34) due to the prevalence of hypertension, cardiovascular disease, and metabolic syndrome, etc. However, there are few drugs capable of treating obesity long-term other than orlistat (Xenical) and lorcaserin (Belviq), which have several side effects such as physical and emotional disorders (35).

Elevated BP is the most frequent comorbidity identified in overweight adolescents (36). Our current results clearly show that % HDL-C was inversely correlated with body weight, body fat mass, and blood pressure (Supplementary Figures 1–3). However, there were no correlations with the amount of HDL-C (mg/dL), suggesting that % HDL-C in TC is a reliable biomarker to predict body fat mass and blood pressure (**Table 2**). There is little information about lipoprotein profiles and obesity in young women. Furthermore, there has been no report about the lipid and lipoprotein profiles of young women with a moderately plump body weight. Until now, there have been limitations in interpreting the physiological roles of HDL in health and beauty since most studies have focused on the quantity of HDL-C in order to explain its beneficial activities.

Recently, the importance of HDL functionality has been well investigated to prevent CVD and metabolic syndrome via protection of LDL from modification (37). In our study, the slim group showed enhanced antioxidant activity in both serum and HDL (**Figures 4**, **5**) with less oxidation of LDL (**Figure 7**). Although the plump group showed lower protein content in HDL_2, its proteins were more glycated and modified (**Figure 6**). Further, although the two groups showed a difference of 8.4 ± 2 kg in body weight and the plump group had a normal BMI, their lipid profiles and lipoprotein properties were distinctly different in terms of CETP mass and HDL functionality.

Elevated levels of CETP activity was found to be a major determinant of the atherogenic dyslipidemia, and atherosclerotic cardiovascular disease (38). Our study have also reported an elevated level of CETP mass and %CE-transfer in the plump group which was found to be significant when compared with the slim group. CETP is that enzyme accountable for moving cholesterol esters and triglycerides between, LDL, VLDL, and HDL. Lower level of CETP nurture HDL formation. Considering higher HDL levels are associated with lower risk of atherosclerosis, the elevated level of CETP is thought to play in promoting the disease by lowering in HDL-C (39). CETP mass activity was directly correlated with body weight and VFM (Supplementary Figure 2B), whereas apoA-I mass was inversely correlated with VFM (**Tables 1**, **2**). In a Japanese study, obese children showed increased plasma CETP activity as well as lower apoA-I content and higher serum TG levels (40). Another study on obese Japanese adults (BMI 33.1 kg/m^2) reported increased serum TG and reduced HDL-C levels via elevation of CETP activity (12). Further, obese women with BMIs around 35.1 ± 0.7 kg/m^2 showed 1.22-fold higher CETP content in serum compared to lean women (22.4 ± 0.3 kg/m^2) along with 1.7-fold higher serum TG and 23% lower HDL-C levels (41). These reports are in good agreement with our current results in terms of lowered HDL-C and increased TG serum levels via elevation of CETP mass, although subjects in the current study were not obese. The higher percentage of HDL-C in the slim group was associated with lower body fat and VFM contents. In both groups, the percentages of HDL-C and apoA-I contents were inversely correlated with blood pressure. VLDL and LDL from the plump group showed 13 and 30% more glycated end products and TG.

Injection of LDL from the slim group into zebrafish embryos resulted in 75% survival, whereas the overweight group showed 70% survival, indicating that LDL from the plump group had more inflammatory properties. The lowest embryo survivability (around 44%) was seen after injecting oxLDL while PBS injection lead to 84% survivability. The co-injection of HDL_3 and oxLDL in the slim group enhanced the survivability up to 70% in the zebrafish embryos, although the oxLDL and HDL_3 from the plump group resulted a lower survivability of 59%. The study observed that the HDL_3 from the slim and plump groups elicited 25 and 16% reduction in the red fluorescence that suggested a protective role of HDL extracted from slim group in the embryonic death and ROS production.

Further, the slim group showed 22% higher antioxidant activity in serum and HDL as well as 26% higher apoA-I content in HDL than the plump group. ApoA-I content in HDL from the slim group was 2-fold higher while LDL from the slim group was less oxidized compared to the plump group. LDL from the plump group showed 2-fold greater uptake into macrophages, whereas HDL from the plump group did not prevent ox-LDL phagocytosis by macrophages.

Although obese patients are often associated with low serum HDL-C and antioxidant activities, there has been no information about HDL particle number and size. The current results show that changes in obese status were associated with smaller HDL particle size and number as well as lowered apoA-I content. In addition to HDL, LDL showed a smaller particle size with increased susceptibility to oxidation. It is well known that PON-1 hydrolyzes lipid peroxides in order to prevent oxidation of LDL. Reduced HDL-associated PON-1 activity in the plump group (**Figure 5**) can explain the increase in LDL oxidation (**Figure 7**) and phagocytosis by macrophages (Supplementary Figure 4). Similar to our current results, obese patients displaying obstructive sleep apnea showed reduced serum PON-1 activities with elevated oxLDL levels, inflammation, and endothelia dysfunction (42). Impairment of antioxidant ability is well correlated with reduction of apoA-I content in HDL (43). It has been reported that obesity and metabolic syndrome are frequently associated with reduced apoA-I and elevated apoC-III contents in HDL along with decreased particle size (44). Plasma apoA-I level has been shown to be inversely associated with obesity in the Framingham Offspring Study conducted on 4,260 young adult men and women (45). Although apoA-I level was lower in the plump group in the current study, there was no difference in apoC-III level since the plump group was not obese.

In older men, diet-induced weight loss has been shown to be associated with increased HDL-C and apoA-I levels as well as reduced body fat mass and CETP activity. Among body fat mass areas, intra-abdominal fat (IAF) and abdominal subcutaneous fat (SQF) were shown to be inversely correlated with apoA-I content, suggesting that body fat mass and distribution are intimately associated with HDL functionality (46). Furthermore, older men showed an increased LDL particle size, whereas HDL particle size was not reported.

Obese subjects show smaller LDL and HDL particle sizes (47). In a Turkish study, obese children showed lower serum HDL-C

and higher TG levels than the control despite similar TC. They also showed lower PON activity, increased BMIs, and reduced HDL-C content (48), which are in good agreement with the current results. To prevent obesity progression, HDL should be functionally enhanced as well as increased in particle size via reduction of CETP activity. A cohort study studying the hearts of young overweight subjects (2,017 participants, aged 12–15-years-old) reported higher serum C-reactive protein, serum amyloid A, and CETP activities. Interestingly, the overweight group showed 1.3-fold higher HDL_2-associated CETP activity, whereas there was no difference in HDL_3-associated CETP activity (49), similar to our current results.

CONCLUSIONS

In conclusion, despite having normal BMIs, the plump group showed more atherogenic features in LDL and HDL as well as elevated oxidation and glycation with loss of antioxidant ability and apoA-I. Elevation in the CETP might be a key player in HDL metabolism during obesity progression, accumulating in visceral fat to impair the lipoprotein levels, antioxidant activity, and lipoprotein functionality. It is necessary to monitor the quality of HDL in terms of composition, structure and functional properties in order to increase the particle size and antioxidant activity.

ETHICS STATEMENT

Informed consent was obtained from all participants prior to enrollment in the study, and the Institutional Review Board at Yeungnam University (Gyeongsan, South Korea) approved the protocol (IRB #7002016-A-2015-003).

AUTHOR CONTRIBUTIONS

K-HP, DY, S-JK performed the experiments. J-RK analyzed the data. K-HC wrote the manuscript and supervised the whole project.

ACKNOWLEDGMENTS

This work was supported by a grant from the Medical Research Center Program (2015R1A5A2009124) through the National Research Foundation (NRF), funded by the Ministry of Science, ICT and Future Planning of Korea.

SUPPLEMENTARY MATERIAL

The Supplementary Material for this article can be found online at: https://www.frontiersin.org/articles/10.3389/fendo.2018.00406/full#supplementary-material

REFERENCES

1. Gordon T, Castelli WP, Hjortland MC, Kannel WB, Dawber TR. High density lipoprotein as a protective factor against coronary heart disease: the Framingham Study. *Am J Med.* (1977) 62:707–14. doi: 10.1016/0002-9343(77)90874-9
2. Nofer JR, Kehrel B, Fobker M, Levkau B, Assmann G, von Eckardstein A. HDL and arteriosclerosis: beyond reverse cholesterol transport. *Atherosclerosis* (2002) 161:1–16. doi: 10.1016/S0021-9150(01)00651-7
3. Aviram M, Rosenblat M, Bisgaier CL, Newton RS, Primo-Parmo SL, La Du BN. Paraoxonase inhibits high-density lipoprotein oxidation and preserves its functions. A possible peroxidative role for paraoxonase. *J Clin Invest.* (1998) 101:1581–90. doi: 10.1172/JCI1649
4. Zannis VI, Chroni A, Krieger M. Role of apoA-I, ABCA1, LCAT, and SR-BI in the biogenesis of HDL. *J Mol Med.* (2006) 84:276–94. doi: 10.1007/s00109-005-0030-4
5. Stefanick ML, Mackey S, Sheehan M, Ellsworth N, Haskell WL, Wood PD. Effects of diet and exercise in men and postmenopausal women with low levels of HDL cholesterol and high levels of LDL cholesterol. *N Engl J Med.* (1998) 339:12–20. doi: 10.1056/NEJM199807023390103
6. Wood PD, Stefanick ML, Williams PT, Haskell WL. The effects on plasma lipoproteins of a prudent weight-reducing diet, with or without exercise, in overweight men and women. *N Engl J Med.* (1991) 325:461–6. doi: 10.1056/NEJM199108153250703
7. Sammalkorpi K, Valtonen V, Kerttula Y, Nikkilä E, Taskinen MR. Changes in serum lipoprotein pattern induced by acute infections. *Metabolism* (1988) 37:859–65. doi: 10.1016/0026-0495(88)90120-5
8. Zappulla D. Environmental stress, erythrocyte dysfunctions, inflammation, and the metabolic syndrome: adaptations to CO_2 increases? *J Cardiometab Syndr.* (2008) 3:30–4. doi: 10.1111/j.1559-4572.2008.07263.x
9. Smith JD. Dysfunctional HDL as a diagnostic and therapeutic target. *Arterioscle Thromb Vasc Biol.* (2010) 30:151–5. doi: 10.1161/ATVBAHA.108.179226
10. Mooradian AD, Haas MJ, Wehmeier KR, Wong NC. Obesity-related changes in high-density lipoprotein metabolism. *Obesity* (2008) 16:1152–60. doi: 10.1038/oby.2008.202
11. Brown CD, Higgins M, Donato KA, Rohde FC, Garrison R, Obarzanek E, et al. Body mass index and the prevalence of hypertension and dyslipidemia. *Obesity* (2000) 8:605–19. doi: 10.1038/oby.2000.79
12. Arai T, Yamashita S, Hirano KI, Sakai N, Kotani K, Fujioka S, et al. Increased plasma cholesteryl ester transfer protein in obese subjects. A possible mechanism for the reduction of serum HDL cholesterol levels in obesity. *Arterioscler Thromb Vasc Biol.* (1994) 14:1129–36. doi: 10.1161/01.ATV.14.7.1129
13. Dullaart R, Sluiter W, Dikkeschei L, Hoogenberg K, Tol A. Effect of adiposity on plasma lipid transfer protein activities: a possible link between insulin resistance and high density lipoprotein metabolism. *Eur J Clin Invest.* (1994) 24:188–94. doi: 10.1111/j.1365-2362.1994.tb00987.x
14. Rye KA, Bursill CA, Lambert G, Tabet F, Barter PJ. The metabolism and anti-atherogenic properties of HDL. *J Lipid Res.* (2009) 50(Suppl.):S195–200. doi: 10.1194/jlr.R800034-JLR200
15. Haas MJ, Horani M, Mreyoud A, Plummer B, Wong NC, Mooradian AD. Suppression of apolipoprotein AI gene expression in HepG2 cells by TNF α and IL-1β. *Bioch Biophys Acta Gen. Sub.* (2003) 1623:120–8. doi: 10.1016/j.bbagen.2003.08.004
16. Beers A, Haas MJ, Wong NC, Mooradian AD. Inhibition of apolipoprotein AI gene expression by tumor necrosis factor α: roles for MEK/ERK and JNK signaling. *Biochemistry* (2006) 45:2408–13. doi: 10.1021/bi0518040
17. McGill HC, Jr., McMahan CA, Herderick EE, Zieske AW, Malcom GT, Tracy RE, et al. Obesity accelerates the progression of coronary atherosclerosis in young men. *Circulation* (2002) 105:2712–8. doi: 10.1161/01.CIR.0000018121.67607.CE
18. Yadav D, Kim SJ, Kim JR, Cho KH. Correlation among lipid parameters, pulse wave velocity and central blood pressure in young Korean population. *Clin Exp Hypertens* (2018). doi: 10.1080/10641963.2018.1441856. [Epub ahead of print].

19. Fok H, Guilcher A, Li Y, Brett S, Shah A, Clapp B, et al. Augmentation pressure is influenced by ventricular contractility/relaxation dynamics: novel mechanism of reduction of pulse pressure by nitrates. *Hypertension* (2014) 63:1050–5. doi: 10.1161/hypertensionaha.113.02955
20. Cho KH, Kim SJ, Yadav D, Kim JY, Kim JR. Consumption of cuban policosanol improves blood pressure and lipid profile via enhancement of HDL functionality in healthy women subjects: randomized, double-blinded, and placebo-controlled study. *Oxid Med Cell Longev.* (2018) 2018:4809525. doi: 10.1155/2018/4809525
21. Havel RJ, Eder HA, Bragdon JH. The distribution and chemical composition of ultracentrifugally separated lipoproteins in human serum. *J Clin Invest.* (1955) 34:1345–53. doi: 10.1172/JCI103182
22. Markwell MAK, Haas SM, Bieber L, Tolbert N. A modification of the Lowry procedure to simplify protein determination in membrane and lipoprotein samples. *Anal Biochem* (1978) 87:206–10. doi: 10.1016/0003-2697(78)90586-9
23. Blois MS. Antioxidant determinations by the use of a stable free radical. *Nature* (1958) 181:1199–200. doi: 10.1038/1811199a0
24. Park KH, Jang W, Kim KY, Kim JR, Cho KH. Fructated apolipoprotein AI showed severe structural modification and loss of beneficial functions in lipid-free and lipid-bound state with acceleration of atherosclerosis and senescence. *Biochem Biophys Res Commun.* (2010) 392:295–300. doi: 10.1016/j.bbrc.2009.12.179
25. Cho KH. Synthesis of reconstituted high density lipoprotein (rHDL) containing apoA-I and apoC-III: the functional role of apoC-III in rHDL. *Mol Cells* (2009) 27:291–7. doi: 10.1007/s10059-009-0037-8
26. Cho KH, Shin DG, Baek SH, Kim JR. Myocardial infarction patients show altered lipoprotein properties and functions when compared with stable angina pectoris patients. *Exp Mol Med.* (2009) 41:67–76. doi: 10.3858/emm.2009.41.2.009
27. Benzie IF, Strain JJ. The ferric reducing ability of plasma (FRAP) as a measure of "antioxidant power": the FRAP assay. *Anal Biochem.* (1996) 239:70–6. doi: 10.1006/abio.1996.0292
28. Eckerson HW, Wyte CM, La Du B. The human serum paraoxonase/arylesterase polymorphism. *Am J Hum Genet* (1983) 35:1126–1138.
29. Park KH, Shin DG, Kim JR, Hong JH, Cho KH. The functional and compositional properties of lipoproteins are altered in patients with metabolic syndrome with increased cholesteryl ester transfer protein activity. *Int J Mol Med.* (2010) 25:129–36. doi: 10.3892/ijmm_00000322
30. Low H, Hoang A, Sviridov D. Cholesterol efflux assay. *J Vis Exp* (2012) 61:e3810. doi: 10.3791/3810
31. Cho KH, Park SH, Park JE, Kim YO, Choi I, Kim JJ, et al. The function, composition, and particle size of high-density lipoprotein were severely impaired in an oliguric phase of hemorrhagic fever with renal syndrome patients. *Clin Biochem.* (2008) 41:56–64. doi: 10.1016/j.clinbiochem.2007.10.007
32. Park KH, Cho KH. A zebrafish model for the rapid evaluation of pro-oxidative and inflammatory death by lipopolysaccharide, oxidized low-density lipoproteins, and glycated high-density lipoproteins. *Fish Shellfish Immunol.* (2011) 31:904–10. doi: 10.1016/j.fsi.2011.08.006
33. Owusu-Ansah E, Yavari A, Mandal S, Banerjee U. Distinct mitochondrial retrograde signals control the G1-S cell cycle checkpoint. *Nat Genet.* (2008) 40:356–61. doi: 10.1038/ng.2007.50
34. Chung A, Backholer K, Wong E, Palermo C, Keating C, Peeters A. Trends in child and adolescent obesity prevalence in economically advanced countries according to socioeconomic position: a systematic review. *Obes Rev.* (2016) 17:276–95. doi: 10.1111/obr.12360
35. Yanovski SZ, Yanovski JA. Long-term drug treatment for obesity: a systematic and clinical review. *JAMA* (2014) 311:74–86. doi: 10.1001/jama.2013.281361
36. Kelly RK, Magnussen CG, Sabin MA, Cheung M, Juonala M. Development of hypertension in overweight adolescents: a review. *Adolesc. Health Med Ther.* (2015) 6:171–187. doi: 10.2147/AHMT.S55837
37. Rye KA, Barter PJ. Cardioprotective functions of HDLs. *J Lipid Res* (2014) 55:168–79doi: 10.1194/jlr.R039297
38. Rashid S, Sniderman A, Melone M, Brown PE, Otvos JD, Mente A, et al. Elevated cholesteryl ester transfer protein (CETP) activity, a major determinant of the atherogenic dyslipidemia, and atherosclerotic cardiovascular disease in South Asians. *Eur J Prev Cardiol.* (2015) 22:468–77. doi: 10.1177/2047487314528461
39. Assmann G, Gotto AM Jr. HDL cholesterol and protective factors in atherosclerosis. *Circulation* (2004) 109(23 Suppl. 1):III8–14. doi: 10.1161/01.cir.0000131512.50667.46
40. Hayashibe H, Asayama K, Nakane T, Uchida N, Kawada Y, Nakazawa S. Increased plasma cholesteryl ester transfer activity in obese children. *Atherosclerosis* (1997) 129:53–8. doi: 10.1016/S0021-9150(96)06014-5
41. Magkos F, Mohammed BS, Mittendorfer B. Plasma lipid transfer enzymes in non-diabetic lean and obese men and women. *Lipids* (2009) 44:459–64. doi: 10.1007/s11745-009-3285-7
42. Yadav R, France M, Aghamohammadzadeh R, Liu Y, Hama S, Kwok S, et al. Impairment of high-density lipoprotein resistance to lipid peroxidation and adipose tissue inflammation in obesity complicated by obstructive sleep apnea. *J Clin Endocrinol Metab.* (2014) 99:3390–8. doi: 10.1210/jc.2013-3939
43. Gu X, Huang Y, Levison BS, Gerstenecker G, DiDonato AJ, Hazen LB, et al. Identification of critical paraoxonase 1 residues involved in high density lipoprotein interaction. *J Biol Chem.* (2016) 291:1890–904. doi: 10.1074/jbc.M115.678334
44. Talayero B, Wang L, Furtado J, Carey VJ, Bray GA, Sacks FM. Obesity favors apolipoprotein E- and C-III-containing high density lipoprotein subfractions associated with risk of heart disease. *J Lipid Res.* (2014) 55:2167–77. doi: 10.1194/jlr.M042333
45. Garrison R, Wilson P, Castelli W, Feinleib M, Kannel W, McNamara P. Obesity and lipoprotein cholesterol in the Framingham offspring study. *Metabolism* (1980) 29:1053–60. doi: 10.1016/0026-0495(80)90216-4
46. Purnell JQ, Kahn SE, Albers JJ, Nevin DN, Brunzell JD, Schwartz RS. Effect of weight loss with reduction of intra-abdominal fat on lipid metabolism in older men. *J Clin Endocrinol Metab* (2000) 85:977–82. doi: 10.1210/jc.85.3.977
47. Makimura H, Feldpausch MN, Stanley TL, Sun N, Grinspoon SK. Reduced growth hormone secretion in obesity is associated with smaller LDL and HDL particle size. *Clin Endocrinol.* (2012) 76:220–7. doi: 10.1111/j.1365-2265.2011.04195.x
48. Agirbasli M, Tanrikulu A, Erkus E, Azizy M, Acar Sevim B, Kaya Z, et al. Serum paraoxonase-1 activity in children: the eff ects of obesity and insulin resistance. *Acta Cardiol.* (2014) 69:679–85. doi: 10.1080/AC.69.6.1000011
49. McEneny J, Blair S, Woodside JV, Murray L, Boreham C, Young IS. High-density lipoprotein subfractions display proatherogenic properties in overweight and obese children. *Pediatr Res.* (2013) 74:279–83. doi: 10.1038/pr.2013.93

Conflict of Interest Statement: The authors declare that the research was conducted in the absence of any commercial or financial relationships that could be construed as a potential conflict of interest.

frontiers in Endocrinology

CLINICAL TRIAL
published: 17 August 2018
doi: 10.3389/fendo.2018.00466

Twelve Weeks of Yoga or Nutritional Advice for Centrally Obese Adult Females

Shirley Telles, Sachin K. Sharma, Niranjan Kala, Sushma Pal, Ram K. Gupta and Acharya Balkrishna*

Patanjali Research Foundation, Haridwar, India

Background: Central obesity is associated with a higher risk of disease. Previously yoga reduced the BMI and waist circumference (WC) in persons with obesity. Additional anthropometric measures and indices predict the risk of developing diseases associated with central obesity. Hence the present study aimed to assess the effects of 12 weeks of yoga or nutritional advice on these measures. The secondary aim was to determine the changes in quality of life (QoL) given the importance of psychological factors in obesity.

Material and Methods: Twenty-six adult females with central obesity in a yoga group (YOG) were compared with 26 adult females in a nutritional advice group (NAG). Yoga was practiced for 75 min/day, 3 days/week and included postures, breathing practices and guided relaxation. The NAG had one 45 min presentation/week on nutrition. Assessments were at baseline and 12 weeks. Data were analyzed with repeated measures ANOVA and *post-hoc* comparisons. Age-wise comparisons were with *t*-tests.

Results: At baseline and 12 weeks NAG had higher triglycerides and VLDL than YOG. Other comparisons are within the two groups. After 12 weeks NAG showed a significant decrease in WC, hip circumference (HC), abdominal volume index (AVI), body roundness index (BRI), a significant increase in total cholesterol and LDL cholesterol. YOG had a significant decrease in WC, sagittal abdominal diameter, HC, BMI, WC/HC, a body shape index, conicity index, AVI, BRI, HDL cholesterol, and improved QoL. With age-wise analyses, in the 30–45 years age range the YOG showed most of the changes mentioned above whereas NAG showed no changes. In contrast for the 46–59 years age range most of the changes in the two groups were comparable.

Conclusions: Yoga and nutritional advice with a diet plan can reduce anthropometric measures associated with diseases related to central obesity, with more changes in the YOG. This was greater for the 30–45 year age range, where the NAG showed no change; while changes were comparable for the two groups in the 46–59 year age range. Hence yoga may be especially useful for adult females with central obesity between 30 and 45 years of age.

Trial registration: (CTRI/2018/05/014077).

Keywords: central obesity, anthropometry, anthropometric indices, risk of disease, yoga, nutritional advice

OPEN ACCESS

Edited by:
Deanne Helena Hryciw, Griffith University, Australia

Reviewed by:
Olivia Holland, Griffith University, Australia
Lannie O'Keefe, Victoria University, Australia

****Correspondence:***
Shirley Telles
shirleytelles@gmail.com

Specialty section:
This article was submitted to Obesity, a section of the journal Frontiers in Endocrinology

Received: *28 May 2018*
Accepted: *30 July 2018*
Published: *17 August 2018*

Citation:
Telles S, Sharma SK, Kala N, Pal S, Gupta RK and Balkrishna A (2018) Twelve Weeks of Yoga or Nutritional Advice for Centrally Obese Adult Females. Front. Endocrinol. 9:466. doi: 10.3389/fendo.2018.00466

BACKGROUND

The Indian Council of Medical Research-India Diabetes (ICMR-INDIAB) study is an ongoing cross sectional national study of the prevalence of obesity, diabetes, and hypertension across the Indian sub-continent (1). In Phase 1 of the study 16,000 individuals aged 20 years and above were sampled from the whole of India. Generalized, abdominal, and combined obesity (i.e., generalized as well as abdominal) were determined based on the BMI and waist circumference using the World Health Organization Asia Pacific Guidelines (2, 3). The ICMR-INDIAB study reported a higher prevalence of isolated abdominal obesity compared to generalized obesity across India. This finding was given importance considering the association independent of ethnicity, between central obesity and several chronic non-communicable diseases such as cardiovascular disease, type 2 diabetes mellitus and certain cancers (1).

Lifestyle changes which include increased physical activity, a healthy diet and a positive attitude have been recommended for the management of obesity (4). For people who are obese and physically less active, physical activity may seem challenging (5). This would prevent persons who are obese from initiating and adhering to increased physical activity. The practice of yoga has been adopted for weight control because of its increasing popularity and relative safety while supervised (6, 7). A systematic meta-analysis assessed the effects of yoga for weight related outcomes in overweight and obese persons assessed in randomized controlled trials (RCTs) (7). Thirty trials with a total of 2,173 participants from bibliographic databases such as MEDLINE, Scopus, and Cochrane Library were screened from their inception to March 2016. The risk of bias was assessed using the Cochrane risk of bias tool which demonstrated methodological drawbacks in the 30 trials. Nonetheless the authors of the meta-analysis concluded that yoga can be considered a safe and effective intervention to reduce the BMI in overweight and obese individuals.

A single study demonstrated a decrease in central obesity in 60 female participants after 12 weeks of yoga (8). This inference was based on the waist circumference. There are several other anthropometric measures and derived anthropometric indices which have been shown to predict the risk of developing diseases associated with central obesity (9).

The aim of this study was to determine if in adult females with central obesity a 12 week program of yoga or of nutritional advice could (i) alter anthropometric measurements associated with a risk of developing diseases associated with central obesity and (ii) positively influence the lipid profile and quality of life.

MATERIALS AND METHODS

Participants

Fifty two healthy Asian Indian adult females with central obesity with ages between 30 and 59 years (group average age ± SD; 43.98 ± 6.89 years) were recruited for the trial. The trial profile is provided in **Figure 1**. The sample size was determined from a previous study on centrally obese females (8). A required sample size ($n = 20$) was obtained using Cohen's formula for the effect size of 0.40 calculated from the mean and SD values of waist circumference which were changed significantly after 12 weeks of yoga, alpha at 0.05, powered at 0.90 using G power software (10). Participants were recruited through advertisements in local newspapers and flyers distributed in nearby residential areas and hospitals. Participation in the study was voluntary with no remuneration. The inclusion criteria were (i) waist circumference $\geq$ 80 cm (11), (ii) BMI $\geq$ 25 kg/m^2 (12), (iii) ages between 30 and 59 years, and (iv) willingness to take part in the study. The exclusion criteria were (i) obesity secondary to hormonal imbalance, medication such as steroids or secondary to any other medical condition, (ii) any physical or psychological disability which would have prevented the participants from taking part in the yoga program or attending the nutritional advice session, (iii) involvement in any other dietary or exercise program during the 12 months prior to, at the time of or during the study, and (iv) any co-morbidities associated with obesity such as cardiovascular disease, type-2 diabetes mellitus, or hypertension. No participant was excluded from the trial for the above mentioned reasons. The participants' written signed informed consent was taken. The baseline characteristics of the participants are given in **Table 1**.

Study Design

The present single blind comparative controlled trial was carried out between April and August 2016 where assessors were blinded to the group to which the participants belonged. The yoga group practiced yoga for 75 min/day, for 3 consecutive days in a week, over a 12 week period. Along with this they were given a diet plan for 1,900–2,000 Kcal/day developed based on the guidelines from the National Institute of Nutrition, India (13). The nutritional advice group was given lectures on nutrition (one 45 min lecture/week) and the same diet plan for 1,900–2,000 Kcal/day developed based on the guidelines from the National Institute of Nutrition, India (13). Adherence to yoga was based on the attendance in the yoga class noted by the yoga teacher. The compliance to the diet plan was based on the 24 h diet recall questionnaire which was administered at the start and end of the 12 week period. This did not cover the dietary intake during the rest of the time which is a limitation. Both groups were assessed for levels of physical activity using the International Physical Activity Questionnaire—Short Form administered at the beginning and end of 12 weeks. The study had the approval of the ethics committee of the institute, which was formed and based on the guidelines of the Indian Council of Medical Research and is in accordance with the Helsinki Declaration (Approval number: YRD/016/022). The trial is registered with the Clinical Trials Registry of India (CTRI/2018/05/014077). The present study is part of a larger nationwide trial of which the data are still being analyzed, comparing yoga with nutritional advice in different regions of India.

At the start of the trial an attempt was made to convince participants to be randomly allocated to yoga or nutritional advice groups. However participants had time and practical constraints. Hence based on their convenience they were assigned to either intervention. However several participants of the nutritional advice group mentioned that they were interested to learn yoga later on.

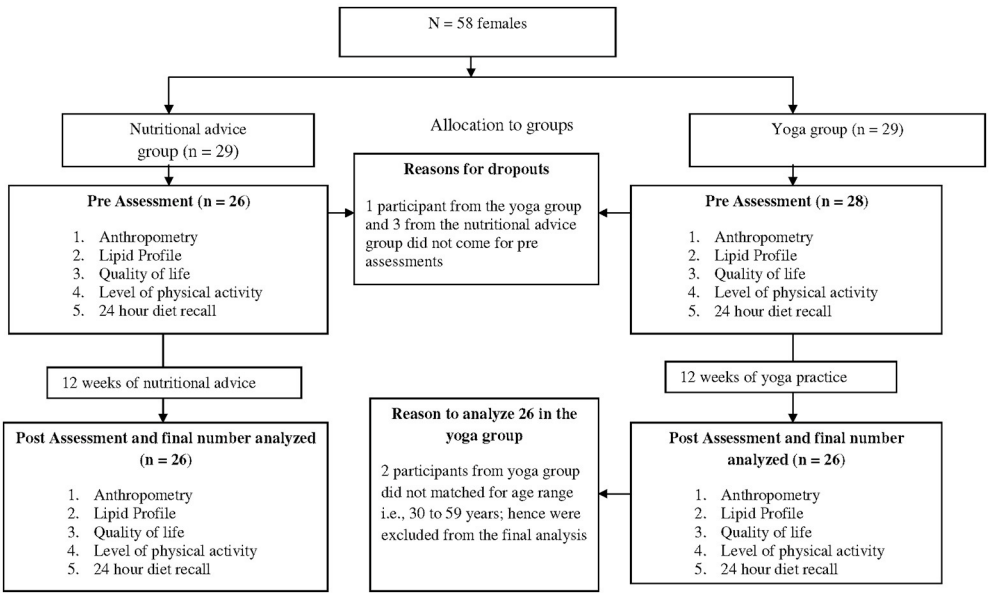

FIGURE 1 | Trial profile of the study.

TABLE 1 | The baseline characteristics of the participants.

Characteristics	Nutritional advice group	Yoga group
Number of participants (n)	26	26
Number of participants in 30–45 (years) age group	12	16
Number of participants in 46–59 (years) age group	14	10
Age in years (mean ± SD)	45.9 ± 7.4	42.5 ± 8.3
Weight in kg (mean ± SD)	74.62 ± 12.03	78.92 ± 12.03
BMI in kg/m^2 (mean ± SD)	31.75 ± 4.17	33.31 ± 4.71
Waist circumference in cm (mean ± SD)	100.77 ± 10.79	101.06 ± 8.56
Type of diet	Vegetarian	Vegetarian
Health	Normal	Normal
Taking any medication	No	No
Consumption of alcohol or nicotine in any form	No	No

Assessments

The following assessments were carried out by individuals who were blinded to the group to which the participants belonged.

Anthropometry

Waist Circumference (WC)

Participants were lightly clothed and asked to stand upright with their feet 25–30 cm apart and weight evenly distributed on both feet. The tape measure which was used for assessments (Gülick Anthropometric tape Model J00305, Lafayette Instrument, U.S.A.) was fitted around the abdomen without compressing soft tissue. The waist circumference was measured to the nearest 0.1 cm in a horizontal plane midway between the inferior costal margin and the iliac crest.

Sagittal Abdominal Diameter (SAD)

The participant was asked to lie supine on their back. The caliper used to measure the supine sagittal abdominal diameter has two arms attached to a vertical scale [Holtain-Kahn Abdominal Caliper 50 cm (98.609XL), U.K.]. The standard method was followed by which the lower arm of the caliper was placed under the participant (14). After a normal exhalation, the upper arm of the caliper was lowered to reach the mid-point between the inferior costal margin and the iliac crest. The lower arm was re-positioned if required. The reading on the vertical scale between the upper and lower arms of the caliper gave the supine sagittal abdominal diameter in cm.

Hip Circumference (HC)

The hip circumference was measured around the pelvis at the point of maximal protrusion of the buttocks. The ratio of the waist circumference to the hip circumference was derived and is a ratio of the fat stored centrally inside the abdomen (waist circumference) and fat stored peripherally (hip circumference).

Derived Anthropometric Indices

Seven anthropometric indices were derived from direct measurements using standardized formulae (9, 15–18). These indices are as follows.

Body Mass Index (BMI)

The body mass index (BMI) was calculated as the body weight (in kg), in light clothing and without footwear, divided by the height (in meters squared). The accuracy of the weighing machine

(Model DS 215 N, Essae-Teraoka Pvt. Ltd, Bengaluru, India) was up to 0.05 kg. The height was measured to the nearest 0.1 cm.

BMI = Weight (kg)/ Height ^{2}(m).

Waist-Hip Ratio (WHR)

WHR = WC (cm)/HC (cm).

A Body Shape Index (ABSI) (9)

ABSI = WC (m)/[BMI $^{2/3}$ (kg/m^2) Height ^{½} (m)]

where WC and height are expressed in m and BMI in kg/m^2.

Conicity Index (CI) (9)

CI = 0.109 $^{-1}$ WC (m) [Weight (kg) / Height (m)] $^{-1/2}$

where WC is measured in cm, weight in kg and height in m.

Abdominal Volume Index (AVI) (9)

AVI = [2WC^2 (cm) + 0.7 (WC - HC) ^{2} (cm)]/1000

where WC and HC (hip circumference) are expressed in cm.

Visceral Adiposity Index (VAI) (15)

VAI $_{\text{female}}$ = {WC (cm)/[36.58 +1.89BMI (kg/m^2)]} [TG (mmol/L)/0.81] [1.52/HDL (mmol/L)]

where WC is expressed in cm, BMI in kg/m^2, Triglycerides in mmol/L, and HDL in mmol/L.

Body Roundness Index (BRI) (9)

BRI = 364.2 – 365.5 [1 –π $^{-2}$ WC ^{2} (m) Height $^{-2}$ (m)] $^{1/2}$

where WC and height are expressed in m.

Biochemical Measures

Antecubital venous blood samples were collected under sterile conditions. Total cholesterol, triglycerides, high density, and low density lipoprotein cholesterol were estimated using appropriate enzymes followed by spectrophotometry.

24 h Diet Recall (Energy Intake/Day)

A structured interview was carried out to recall the food and fluids which the participants had consumed in the 24 h prior to the study. The method was as follows: participants were asked (i) to recall and list the foods they had consumed during the 24 h preceding the assessment, (ii) the method of preparation (e.g., raw, cooked, boiled, or baked), (iii) the size of utensils used, the interviewer had four types of utensils (i.e., a bowl, cup, glass, and spoon), each of which had four sizes. Participants were asked to indicate the size used by them. The volume of each of the utensils of different sizes had already been determined (19). The total energy intake/day as well as the amount of macronutrients was calculated based on norms for Indian foods (13, 19, 20).

Level of Physical Activity and Energy Expenditure/Day

Physical activity was assessed using the International Physical Activity Questionnaire Short Form (IPAQ) (21). Data obtained at the beginning and end of the 12 week period for both groups were extracted using the guidelines published by the IPAQ for data processing (22). From these data the basal metabolic rate of each participant was determined and energy expenditure/day was calculated using the Harris-Benedict equation (23).

Quality of Life

The Moorehead-Ardelt Quality of Life Questionnaire was used to assess six aspects of the quality of life (QoL) (24). These were general self-esteem, physical activity, social contacts, satisfaction concerning work, pleasure related to sexuality, and focus on eating behavior, with scores ranging from −0.5 to +0.5. The sum of these 6 scores provided a total QoL score. Each score was classified into 5 categories (very poor: −3.0 to −2.1; poor: −2.0 to −1.1; fair: −1.0 to +1.0; good: 1.1 to 2.0: and very good: 2.1 to 3.0).

Interventions

Nutritional Advice

Participants received a 45 min presentation on nutrition (1 presentation/week) for 12 weeks. The person who gave the presentation had a minimum of 12 years of education including 2 years of training in science. The presenter used slides made by the research institute conducting the trial. The 12 topics of the presentations were: (i) five basic food groups, (ii) vegetarian diet, (iii) proteins, (iv) fats, (v) carbohydrates, (vi) dietary fiber, (vii) vitamins, (viii) minerals, (ix) probiotics, (x) iron deficiency, (xi) calcium, and (xii) antioxidants.

Yoga

The yoga intervention consisted of (i) a universal prayer (3 min)[1], (ii) yoga postures *(asanas,* 42 min), (iii) voluntarily regulated breathing techniques (*pranayamas*, 24 min), and (iv) guided relaxation with meditation (6 min). Yoga classes were conducted on three successive days in a week between (i) 05:30 h and 06:45 h, during the 12 weeks. Attendance was noted in each yoga class by the yoga instructor. The instructor was also asked to note any adverse event during the classes. The yoga instructor had been teaching yoga for 5 years. All the participants in the yoga group attended at least 18 out of a total of 36 yoga classes. Details of the yoga intervention are given in **Table 2**.

Diet Plan

Participants of both groups were given a diet plan for a balanced diet of 1900–2000 Kcal/day. The diet plan included fruits, vegetables, lentils, complex carbohydrates, and dairy products. Hence it was a lacto-vegetarian diet. The ratio of carbohydrates, protein and fats in the diet was based on the guidelines for a balanced diet for an Indian population published by the National Institute of Nutrition, India (13), which states that a balanced Indian diet should have 10–15% of total calories from proteins, 20–30% of calories from fats and 50–60% of calories from carbohydrates. The total energy and nutritive values of the foods were determined from a database of Indian foods (20).

[1]May all be prosperous and happy
May all be free from illness
May all see what is uplifting
May no one suffer
Peace, peace, peace

TABLE 2 | Details of the yoga intervention.

Sl. no.		Name of the yoga practice	Duration of the practice
1	Universal prayer	*Sukhasana* (easy posture) + *Prathana mantra* (universal prayer)	3 min
2	*Pranayama* (voluntarily regulated yoga breathing)	1. *Bhastrika* (bellows yoga breathing)	3 min
		2. *Kapalabhati* (high frequency yoga breathing)	6 min
		3. *Ujjayi* (victorious breathing)	3 min
		4. *Anulom-vilom* (alternate nostril yoga breathing)	6 min
		5. *Bhramari* (bumble bee breathing)	3 min
		6. *Udgeeth* (OM chanting)	3 min
3	*Asanas* Standing postures	1. *Tirryaktadasana* (swaying palm tree pose) (right side, left side with 10 repetitions; normal breathing and eyes closed)	3 min
		2. *Trikonasana* (triangle pose) (right side followed by left side; the posture is sustained for at least 15 s on either side with eyes closed and normal breathing)	3 min
		3. *Konasana* (angle pose) (right side followed by left side; the posture is sustained for at least 15 s on either side with eyes closed and normal breathing)	3 min
		4. *Padahastasana* (hand to foot pose) (remaining in the posture for at least 15 s with normal breathing and eyes closed)	1 min
4	*Asanas* Sitting postures	1.*Chakkiasana* (mill churning pose) seated with legs extended, hands stretched out and fingers interlaced. Each movement would involve forward bending and making circles with the extended arms keeping the spine erect (15 rounds, clockwise; 15 rounds anti-clockwise with normal breathing and eyes closed)	3 min
		2. *Sthitta konaasana* (static angle pose) Extending both legs and keeping them one forearm span apart while seated, then holding the left big toe with the right hand while the left arm is extended upward. The person should face the extended left arm keeping the spine erect. During the practice there should be normal breathing and eyes closed. The posture should be maintained for at least 15 s. The practice is repeated on the opposite side.	3 min
		3. *Paschimottanasana* (seated forward bend pose) (remaining in the posture for at least 15 s with normal breathing and eyes closed)	1 min
5	*Asanas* Supine postures	1. *Ardhahalasana* (half plow pose) raising both legs to form a right angle, keeping the legs straight at the knee, repetitive (10 times with eyes closed and normal breathing)	3 min
		2. *Padavrttasana* (cyclical leg pose) raising the right leg extended at the knee and making circles in the air, rotating the leg (10 rounds clockwise and 10 rounds anticlockwise with normal breathing and eyes closed). The practice is repeated with the left leg with 10 rounds clockwise and 10 rounds anticlockwise.	6 min
		3. *Dwicakriasana* (cycling pose) repetitive (10 times with eyes closed and normal breathing)	3 min
		4. *Markatasana* (monkey pose) this is a spinal twist (right side, left side with 10 repetitions; normal breathing and eyes closed)	6 min
6	*Asanas* Prone postures	*1. Bhujangaasana* (cobra pose) two methods are followed. Method1—Lie prone with extended elbows and the palms near the chest, flat on the ground. Then the upper part of the body till the waist is raised while looking upwards and forwards. The weight of the upper parts of the body should be evenly distributed on both hands. The procedure is repeated 10 times with eyes closed and normal breathing. The second method is almost the same except that the hands are not kept apart but with the right palm over the left palm. The rest of the procedure is the same. This method is also repeated 10 times with normal breathing and eyes closed.	6 min
		2. *Salabhasana* (locust pose) (remaining in the posture for at least 15 s with normal breathing and eyes closed)	1 min
7	Guided relaxation	*Shavasana* (corpse pose) with breath awareness	6 min
		Total duration	75 min

Those practices which are commonly used are not detailed.

Data Analysis

Group as a Whole

The data obtained at the beginning and end of the 12 week period for the two groups were compared with a repeated measures analysis of variance (ANOVA) followed by multiple *post-hoc* comparisons which were Bonferroni adjusted. The ANOVA had one Within subjects factor i.e., States, with two levels (pre and post) and one Between subjects factor i.e., Groups which were (i)

TABLE 3 | Anthropometric variables.

Variables	Nutritional advice ($n = 26$)					Yoga ($n = 26$)				
	Pre	Post	Cohen's d	95% CI		Pre	Post	Cohen's d	95% CI	
				Lower	Upper				Lower	Upper
Waist circumference (cm)	100.8 ± 10.8	97.9 ± 8.6*	0.30	0.72	5.00	101.1 ± 8.6	94.8 ± 7.1***	0.81	4.14	8.41
SAD (cm)	23.5 ± 2.8	23.3 ± 2.3	0.08	−0.35	0.73	24.1 ± 2.6	23.1 ± 2.6**	0.39	0.45	1.52
Hip circumference (cm)	111.7 ± 7.4	109.2 ± 6.8**	0.36	0.79	4.16	112.3 ± 10.4	107.8 ± 9.3***	0.46	2.79	6.16
BMI (kg/m^2)	31.8 ± 4.2	31.3 ± 4.1	0.12	−0.10	1.06	33.3 ± 4.7	32.2 ± 5.4***	0.22	0.52	1.68
Waist/hip ratio	0.9 ± 0.1	0.9 ± 0.1	0.17	−0.01	0.03	0.9 ± 0.1	0.9 ± 0.1*	0.31	0.00	0.04
A body shape index	0.081 ± 0.01	0.079 ± 0.01$^{@}$	0.22	−0.02	0.29	0.079 ± 0.01	0.06 ± 0.01*	0.21	0.04	0.35
Conicity index	1.3 ± 0.1	1.3 ± 0.1	0.21	−0.00	0.05	1.3 ± 0.2	1.3 ± 0.1**	0.28	0.01	0.06
Abdominal volume index	20.7 ± 4.3	19.4 ± 3.4**	0.33	0.44	2.02	21.2 ± 6.1	19.3 ± 5.6***	0.33	1.08	2.65
Visceral adiposity index	2.9 ± 1.4$^{\#}$	3.0 ± 2.1	0.02	−0.51	0.44	2.2 ± 1.1	2.3 ± 0.9	0.07	−0.51	0.37
Body roundness index	6.9 ± 2.0	6.4 ± 1.5**	0.30	0.18	0.84	7.0 ± 2.4	6.3 ± 2.2***	0.33	0.40	1.06

Values are group mean± SD.

**p < 0.05; **p < 0.01; ***p < 0.001, post-hoc analyses with Bonferroni adjustment, post values compared with pre.*

$^{\#}$p < 0.05, post-hoc analyses with Bonferroni adjustment, pre values compared with pre.

$^{@}$p < 0.05, post-hoc analyses with Bonferroni adjustment, post values compared with post.

BMI, Body mass index; SAD, Sagittal abdominal diameter.

TABLE 4 | Lipid profile.

Variables	Nutritional advice ($n = 26$)					Yoga ($n = 26$)				
	Pre	Post	Cohen's d	95% CI		Pre	Post	Cohen's d	95% CI	
				Lower	Upper				Lower	Upper
Total cholesterol (mmol/L)	4.6 ± 0.8	5.0 ± 0.8**	0.54	−0.7	−0.15	4.6 ± 0.8	4.6 ± 1.0	0.02	−0.3	0.23
Triglycerides (mmol/L)	1.72 ± 0.7$^{\#}$	1.7 ± 0.7$^{@@}$	0.01	−0.21	0.19	1.35 ± 0.5	1.30 ± 0.42	0.18	−0.11	0.27
LDL cholesterol (mmol/L)	2.8 ± 0.6	3.0 ± 0.6*	0.41	−0.44	−0.02	3.1 ± 0.6	3.0 ± 0.7	0.15	−0.08	0.27
HDL cholesterol(mmol/L)	1.2 ± 0.3	1.3 ± 0.3	0.13	−0.14	0.06	1.23 ± 0.24	1.1 ± 0.3*	0.50	0.03	0.22
VLDL (mmol/L)	0.77 ± 0.3$^{\#}$	0.78 ± 0.29$^{@@}$	0.04	−0.10	0.08	0.58 ± 0.24	0.56 ± 0.15	0.12	−0.06	0.11

Values are group mean ± SD.

**p < 0.05; **p < 0.01, post-hoc analyses with Bonferroni adjustment, post values compared with pre.*

$^{@@}$p < 0.01, post-hoc analyses with Bonferroni adjustment, post values compared with post.

$^{\#}$p < 0.05, post-hoc analyses with Bonferroni adjustment, pre values compared with pre.

TABLE 5 | Estimated energy intake/day based on 24 h diet recall questionnaire.

Variables	Nutritional advice ($n = 26$)					Yoga ($n = 26$)				
	Pre	Post	Cohen's d	95% CI		Pre	Post	Cohen's d	95% CI	
				Lower	Upper				Lower	Upper
Protein (gm)/day	53.8 ± 17.4	55.7 ± 10.3	0.13	−9.15	5.44	59.0 ± 14.0	50.7 ± 10.4	0.68	1.24	15.23
Fat (gm)/day	47.5 ± 19.6	46.9 ± 18.5	0.03	−8.87	10.03	39.2 ± 14.1	41.4 ± 16.7	0.15	−11.88	7.39
Carbohydrates (gm)/day	193.6 ± 76.9	222.0 ± 77.5	0.38	−79.07	22.12	216.5 ± 55.4	248.7 ± 114.2	0.37	−82.78	18.42
Energy intake (Kcal)/day	1625.9 ± 395.4	1716.3 ± 384.6	0.24	−320.57	139.89	1753.5 ± 423.5	1590.6 ± 366.0	0.42	−67.33	393.13

Values are group mean ± SD.

nutritional advice group with a diet plan of 1900–2000 Kcal/day and (ii) yoga group who had a similar diet plan of 1900–2000 Kcal/day, as the nutritional advice group.

Analysis Based on Age

Both nutritional advice and yoga groups were subdivided based on age as (i) participants between 30 and 45 years and (ii) those who were 46 years and above.

For (i) and (ii) there were separate between group comparisons of values at baseline and after 12 weeks using *t*-tests for unpaired data. Within the groups baseline data and date at 12 weeks were compared with *t*-tests for paired data.

RESULTS

None of the participants reported any adverse events during the trial. At baseline the visceral adiposity index (VAI), levels of triglycerides and of VLDL differed significantly between the nutritional advice and yoga groups. The group mean values ±

TABLE 6 | Estimated energy expenditure/day based on (i) International Physical Activity Questionnaire—Short Form and (ii) Harris-Benedict equation to determine the basal metabolic rate.

Variable	Nutritional advice ($n = 26$)					Yoga ($n = 26$)				
	Pre	Post	Cohen's d	95% CI		Pre	Post	Cohen's d	95% CI	
				Lower	Upper				Lower	Upper
Total energy (Kcal) spent/day	2022.6 ± 238.7	1995.6 ± 205.7	0.12	−87.79	141.78	2158.8 ± 322.6	2019.5 ± 219.8	0.52	24.10	253.67

Values are group mean ± SD.

TABLE 7 | Quality of life.

Variables	Nutritional advice ($n = 26$)					Yoga ($n = 26$)				
	Pre	Post	Cohen's d	95% CI		Pre	Post	Cohen's d	95% CI	
				Lower	Upper				Lower	Upper
General self-esteem	0.22 ± 0.27	0.3 ± 0.16	0.37	−0.185	0.015	0.22 ± 0.25	0.30 ± 0.16	0.39	−0.188	0.012
Physical activity	0.25 ± 0.23	0.32 ± 0.15	0.37	−0.165	0.026	0.24 ± 0.23	0.25 ± 0.22	0.05	−0.130	0.61
Social contacts	0.22 ± 0.29	0.30 ± 0.15	0.35	−0.104	0.081	0.24 ± 0.23	0.30 ± 0.17	0.30	−0.130	0.168
Satisfaction concerning work	0.32 ± 0.14	0.35 ± 0.12	0.24	−0.108	0.046	0.29 ± 0.25	0.29 ± 0.22	0.00	−0.085	0.069
Pleasure related to sexuality	0.04 ± 0.31	0.14 ± 0.31	0.33	−0.196	0.034	0.07 ± 0.31	0.14 ± 0.25	0.25	−0.184	0.046
Focus on eating behavior	0.29 ± 0.22	0.27 ± 0.21	0.09	−0.072	0.110	0.2 ± 0.3	0.29 ± 1.9*	0.07	−0.183	−0.001
Total quality of life	1.34 ± 0.93	1.67 ± 0.78	0.39	−0.675	0.014	1.23 ± 1.06	1.58 ± 0.87*	0.37	−0.690	−0.002

Values are group mean ± SD.
$p < 0.05$, post-hoc analyses with Bonferroni adjustment, post values compared with pre.

SD for the (i) anthropometric measures and anthropometric indices, (ii) lipid profile, (iii) energy intake/day and energy expenditure/day, and (iv) quality of life are given in **Tables 3**–**7**.

Repeated Measures Analysis of Variance (RM-ANOVA)

The ANOVA values for the Within-Subjects factor (States), Between-Subjects factor (Groups) and interaction between the two are given below. The details of the ANOVA are available in the **Supplementary Material**.

Within-Subjects Factor (States)

There were significant differences between post and pre states for waist circumference ($F = 36.92$, $p < 0.001$), sagittal abdominal diameter ($F = 9.66$, $p < 0.01$), hip circumference ($F = 34.41$, $p < 0.001$), BMI ($F = 14.88$, $p < 0.001$), a body shape index ($F = 20.77$, $p < 0.01$), conicity index ($F = 13.09$, $p < 0.001$), abdominal volume index ($F = 31.05$, $p < 0.001$), body roundness index ($F = 28.78$, $p < 0.001$), total cholesterol ($F = 5.71$, $p < 0.05$), general self-esteem ($F = 6.05$, $p < 0.05$), and total quality of life ($F = 7.80$, $p < 0.01$). For all comparisons mentioned above the condition of sphericity was met and value of epsilon (Huynh-Feldt, Greenhouse-Geisser) was 1. The degrees of freedom for all variables were 1,50.

Between-Subjects Factors (Groups)

There were significant differences between the groups in a body shape index ($F = 4.10$, $p < 0.05$), triglycerides ($F = 8.23$, $p < 0.01$), and VLDL ($F = 9.94$, $p < 0.01$). The condition of sphericity was met for the comparisons and value of epsilon (Huynh-Feldt, Greenhouse- Geisser) was 1. The degrees of freedom for all variables were 1,50.

Interaction Between States and Groups

Interaction between States and Groups was significant for waist circumference ($F = 5.11$, $p < 0.05$), total cholesterol ($F = 4.69$, $p < 0.05$), LDL cholesterol ($F = 5.77$, $p < 0.05$), and HDL cholesterol ($F = 5.44$, $p < 0.05$). A significant interaction between States and Groups suggests that the effects of the two factors are interdependent. For all comparisons the condition of sphericity was met and value of epsilon (Huynh-Feldt, Greenhouse-Geisser) was 1. The degrees of freedom for all variables were 1, 50 (States) x 50 (Groups).

Post-hoc Analyses

There were two *post-hoc* comparisons: (i) Between groups [at baseline (pre) and at 12 weeks (post)] and (ii) Within groups, comparing values obtained at 12 weeks (post) with those at baseline (pre).

Post-hoc Between Groups Comparisons

At baseline (pre) the visceral adiposity index (VAI, $p < 0.05$), VLDL ($p < 0.05$) and triglyceride levels ($p < 0.05$) were significantly higher in the nutritional advice group compared to the yoga group. After 12 weeks (post) a body shape index ($p < 0.01$), the triglyceride levels ($p < 0.01$), and VLDL ($p < 0.01$) levels were higher in the nutritional advice group compared to the yoga group.

TABLE 8 | Anthropometric variables and derived indices for two age range i.e., 30-45 and 46-59 year.

Variables	Nutritional advice				Yoga			
	Pre	Post	*t* value	Cohen's d	Pre	Post	*t* value	Cohen's d
Age range	**30–45 Years age range**							
Number of participants (n)	12				16			
Waist circumference (cm)	97.3 ± 12.3	98.0 ± 10.6	0.52	0.07	101.6 ± 9.3	95.3 ± 8.4***	5.77	0.71
SAD (cm)	22.0 ± 2.7	22.6 ± 2.5	1.25	0.25	24.0 ± 2.6	23.1 ± 2.8**	3.34	0.34
Hip circumference (cm)	110.8 ± 9.5	109.7 ± 9.0	0.70	0.12	113.2 ± 11.8	108.9 ± 9.8**	4.25	0.40
BMI (kg/m^2)	30.5 ± 4.8	30.6 ± 4.5	0.20	0.02	33.1 ± 4.9	32.0 ± 4.7**	4.08	0.24
Waist/hip ratio	0.9 ± 0.1	0.9 ± 0.1	0.88	0.17	0.9 ± 0.1	0.9 ± 0.1	1.98	0.25
A body shape index	0.1 ± 0.0	0.1 ± 0.0	0.368	0.00	0.08 ± 0.0	0.08 ± 0.0**	4.0	0.31
Conicity index	1.3 ± 0.1	1.3 ± 0.1	0.75	0.10	1.3 ± 0.2	1.3 ± 0.2*	2.68	0.18
Abdominal volume index	19.4 ± 4.9	19.5 ± 4.2	0.31	0.04	22.3 ± 7.3	20.5 ± 6.7***	4.48	0.27
Visceral adiposity index	2.9 ± 1.4	2.6 ± 1.3	0.92	0.26	2.1 ± 1.0	2.3 ± 0.8	1.65	0.28
Body roundness index	6.2 ± 2.1	6.3 ± 1.8	0.35	0.04	7.4 ± 2.9	6.7 ± 2.6**	4.01	0.26
Age range	**46–59 Years**							
Number of participants (n)	14				10			
Waist circumference (cm)	103.8 ± 8.7$^{\#}$	97.9 ± 6.8***	3.26	0.79	100.2 ± 7.7	93.9 ± 4.8**	3.33	1.03
SAD (cm)	24.8 ± 2.3	23.9 ± 2.0**	4.64	0.42	24.2 ± 2.7	23.1 ± 2.3*	2.99	0.46
Hip circumference (cm)	112.5 ± 5.2	108.8 ± 4.4**$^{@}$	3.30	0.80	110.8 ± 8.1	106.2 ± 8.7**	4.59	0.59
BMI (kg/m^2)	32.9 ± 3.4	31.9 ± 3.7	2.15	0.28	33.6 ± 4.6	32.6 ± 4.1*	2.36	0.24
Waist/hip ratio	0.9 ± 0.1	0.9 ± 0.1*	2.19	0.32	0.9 ± 0.0	0.9 ± 0.0	1.07	0.30
A body shape index	0.08 ± 0.0	0.08 ± 0.0**	3.43	0.10	0.08 ± 0.0	0.1 ± 0.0*	2.94	0.42
Conicity index	1.4 ± 0.1	1.3 ± 0.1**	4.18	0.77	1.3 ± 0.1	1.2 ± 0.1	2.01	0.55
Abdominal volume index	21.8 ± 3.5	19.4 ± 2.6***	4.61	0.82	19.4 ± 2.7	17.4 ± 2.2**	3.30	0.82
Visceral adiposity index	2.9 ± 1.4	3.3 ± 2.6	0.79	0.20	2.4 ± 1.2	2.2 ± 1.0	1.11	0.19

Values are group mean ± SD.

**p < 0.05; **p < 0.01; ***p < 0.001, paired t-test, post values compared with pre.*

$^{@}$p < 0.05, Unpaired t-test, post values compared with post.

$^{\#}$p < 0.05, Unpaired t-test, pre values compared with pre.

BMI, Body mass index; SAD, Sagittal abdominal diameter.

Post-hoc Comparisons Within a Group (Post-Pre)

The nutritional advice group showed a significant decrease in the waist circumference ($p < 0.05$), hip circumference ($p < 0.01$), abdominal volume index ($p < 0.01$), body roundness index ($p < 0.01$), a significant increase in total cholesterol ($p < 0.01$), and LDL cholesterol ($p < 0.05$).

The yoga group had a significant decrease in waist circumference ($p < 0.001$), sagittal abdominal diameter ($p < 0.01$), hip circumference ($p < 0.001$), BMI ($p < 0.001$), waist/hip ratio ($p < 0.05$), a body shape index ($p < 0.05$), conicity index ($p < 0.01$), abdominal volume index ($p < 0.001$), body roundness index ($p < 0.001$), HDL cholesterol ($p < 0.05$), improved quality of life, i.e., focus on eating behavior ($p < 0.05$) and total quality of life ($p < 0.05$).

Age Wise Analysis (*t*-Tests)

The participants of both groups were divided as two groups based on age, viz., 30–45 years and 46–59 years. For each age group, comparisons were made between nutritional advice and yoga groups using *t*-tests for unpaired data and within each group using *t*-tests for paired data. The age wise group mean values ± SD for the (i) anthropometric measures and anthropometric indices, (ii) lipid profile, (iii) energy intake/day and energy expenditure/day, and (iv) quality of life are given in **Tables 8–12**.

Age Group 30–45 Years

Between Groups

At baseline the triglyceride levels and the focus on eating behavior (an aspect of the quality of life) were lower in the yoga group ($p < 0.05$, both cases) compared to the nutritional advice group. There were no differences at 12 weeks between groups.

Within Groups

There were no significant changes in the nutritional advice group. In the yoga group there was a decrease in waist circumference, sagittal abdominal diameter, hip circumference, BMI, a body shape index, conicity index, abdominal volume index, and body roundness index ($p < 0.05$ in all cases).

TABLE 9 | Lipid profile for two age range i.e., 30–45 and 46–59 year.

Variables	Nutritional advice				Yoga			
	Pre	Post	*t* value	Cohen's d	Pre	Post	*t* value	Cohen's d
Age range	**(30–45 Years)**							
Number of participants (n)	12				16			
Total cholesterol (mmol/L)	4.58 ± 0.78	5.43 ± 0.62	3.71	1.26	4.34 ± 0.77	4.20 ± 0.74	1.59	0.19
Triglycerides (mmol/L)	1.75 ± 0.80[#]	1.64 ± 0.52	0.55	0.17	1.22 ± 0.36	1.24 ± 0.34	0.39	0.07
LDL cholesterol (mmol/L)	2.95 ± 0.49	3.41 ± 0.48	3.37	0.98	2.89 ± 0.59	2.76 ± 0.62	1.72	0.22
HDL cholesterol (mmol/L)	1.17 ± 0.19	1.33 ± 0.24	1.60	0.74	1.22 ± 0.22	1.08 ± 0.20	3.33	0.68
VLDL (mmol/L)	0.75 ± 0.32	0.72 ± 0.20	0.39	0.13	0.54 ± 0.17	0.54 ± 0.13	0.20	0.05
Age range	**(46–59 Years)**							
Number of participants (n)	14				10			
Total cholesterol (mmol/L)	4.55 ± 0.84	4.54 ± 0.78	0.04	0.01	5.08 ± 0.55	5.35 ± 0.86	1.14	0.39
Triglycerides (mmol/L)	1.70 ± 0.56	1.82 ± 0.79	0.78	0.19	1.56 ± 0.62	1.32 ± 0.42	1.59	0.48
LDL cholesterol (mmol/L)	2.65 ± 0.60	2.62 ± 0.43	0.19	0.05	3.36 ± 0.42	3.31 ± 0.83	0.25	0.07
HDL cholesterol (mmol/L)	1.28 ± 0.40	1.20 ± 0.32	1.09	0.23	1.28 ± 0.28	1.18 ± 0.35	1.78	0.33
VLDL (mmol/L)	0.78 ± 0.26	0.84 ± 0.38	0.78	0.19	0.66 ± 0.31	0.60 ± 0.19	0.88	0.25

Values are group mean ± SD.
[#]$p < 0.05$, Unpaired t-test, pre values compared with pre.

TABLE 10 | Estimated energy intake/day based on 24 h diet recall questionnaire for two different age range i.e., 30–45 and 46–59 year.

Variables	Nutritional advice				Yoga			
	Pre	Post	*t* value	Cohen's d	Pre	Post	*t* value	Cohen's d
Age range	**(30–45 Years)**							
Number of participants (n)	12				16			
Protein (gm)/day	51.9 ± 19.3	55.9 ± 12.0	0.54	0.26	64.5 ± 13.5	53.6 ± 8.9	2.79	0.98
Fat (gm)/day	52.3 ± 22.1	54.9 ± 17.5	0.34	0.17	37.8 ± 13.2	42.7 ± 17.8	0.77	0.32
Carbohydrates (gm)/day	198.0 ± 76.9	216.8 ± 60.8	0.68	0.28	238.2 ± 45.5	251.1 ± 97.6	0.43	0.18
Energy intake (Kcal)/day	1601.4 ± 447.1	1738.8 ± 292.3	0.83	0.38	1744.6 ± 299.8	1679.9 ± 425.1	0.49	0.18
Age range	**(46–59 Years)**							
Number of participants (n)	14				10			
Protein (gm)/day	55.9 ± 15.7	55.5 ± 8.6	0.09	0.03	50.7 ± 9.9	46.4 ± 11.5	1.03	0.42
Fat (gm)/day	43.4 ± 16.9	40.1 ± 16.9	0.53	0.20	41.7 ± 16.0	39.2 ± 15.3	0.37	0.17
Carbohydrates (gm)/day	189.8 ± 79.5	226.5 ± 91.5	1.09	0.45	181.8 ± 53.8	244.7 ± 142.6	1.12	0.62
Energy intake (Kcal)/day	1646.9 ± 361.3	1696.9 ± 459.6	0.29	0.13	1767.8 ± 589.9	1447.7 ± 184.8	1.58	0.77

Values are group mean ± SD.

Age Group 46–59 Years

Between Groups

At baseline the waist circumference and satisfaction concerning work (of the quality of life scale) were higher in the nutritional advice group compared to the yoga group ($p < 0.05$). At 12 weeks the hip circumference and satisfaction concerning work remained higher in the nutritional advice group compared to the yoga group ($p < 0.05$ both cases).

Within Groups

The nutritional advice group showed a decrease in waist circumference, sagittal abdominal diameter, hip circumference, waist-hip ratio, a body shape index, conicity index, abdominal volume index, and body roundness index ($p < 0.05$ in all cases). The yoga group had a significant decrease in waist circumference, sagittal abdominal diameter, hip circumference, BMI, a body shape index, abdominal volume index, body roundness index, and total quality of life ($p < 0.05$ in all cases). The significant results have been summarized in the **Supplementary Material**.

DISCUSSION

Following 12 weeks of nutritional advice there was a significant decrease in waist circumference, hip circumference, abdominal

TABLE 11 | Estimated energy expenditure/day based on (i) International Physical Activity Questionnaire—Short Form and (ii) Harris-Benedict equation to determine the basal metabolic rate for two different age range i.e., 30-45 and 46-59 years.

Variables	Nutritional advice ($n = 12$)				Yoga ($n = 16$)			
	Pre	Post	*t* value	Cohen's d	Pre	Post	*t* value	Cohen's d
Age range	**(30–45 Years)**							
Number of participants (n)	12				16			
Total energy (Kcal) spent/day	2027.8 ± 275.2	2035.0 ± 233.8	0.07	0.03	2173.0 ± 299.5	2007.1 ± 226.9	2.40	0.65
Age range	**(46–59 Years)**							
Number of participants (n)	14				10			
Total energy (Kcal) spent/day	2018.2 ± 213.2	1961.9 ± 180.0	0.75	0.30	2136.2 ± 372.5	2040.6 ± 218.3	1.00	0.33

Values are group mean ± SD.

TABLE 12 | Quality of life for two different age range i.e., 30–45 and 46–59 years.

Variables	Nutritional advice				Yoga			
	Pre	Post	*t* value	Cohen's d	Pre	Post	*t* value	Cohen's d
Age range	**(30–45 Years)**							
Number of participants (n)	12				16			
General self-esteem	0.3 ± 0.2	0.29 ± 0.19	0.15	0.06	0.2 ± 0.3	0.3 ± 0.2	0.99	0.28
Physical activity	0.3 ± 0.2	0.3 ± 0.2	0.24	0.06	0.3 ± 0.2	0.3 ± 0.2	0.11	0.00
Social contacts	0.2 ± 0.3	0.3 ± 0.2	1.27	0.60	0.2 ± 0.3	0.3 ± 0.2	0.63	0.23
Satisfaction concerning work	0.3 ± 0.2	0.3 ± 0.1	0.0	0.00	0.4 ± 0.2	0.3 ± 0.2	0.48	0.17
Pleasure related to sexuality	0.1 ± 0.3	0.1 ± 0.3	0.14	0.04	0.2 ± 0.2	0.2 ± 0.2	0.89	0.30
Focus on eating behavior	0.3 ± 0.2$^{\#}$	0.2 ± 0.2	0.89	0.33	0.2 ± 0.3	0.3 ± 0.2	1.23	0.44
Total quality of life	1.4 ± 0.7	1.5 ± 0.9	0.36	0.09	1.5 ± 0.9	1.8 ± 0.8	1.15	0.32
Age range	**(46-59 Years)**							
Number of participants (n)	14				10			
General self-esteem	0.2 ± 0.4	0.3 ± 0.1	1.93	0.58	0.2 ± 0.3	0.3 ± 0.1	1.59	0.65
Physical activity	0.2 ± 0.3	0.4 ± 0.1	1.97	0.74	0.1 ± 0.3	0.2 ± 0.2	1.27	0.34
Social contacts	0.3 ± 0.3	0.3 ± 0.2	0.60	0.17	0.3 ± 0.2	0.2 ± 0.2	0.16	0.05
Satisfaction concerning work	0.3 ± 0.1$^{\#}$	0.4 ± 0.1$^{@}$	1.37	0.72	0.2 ± 0.3	0.2 ± 0.3	1.21	0.25
Pleasure related to sexuality	−0.0 ± 0.3	0.1 ± 0.3	1.58	0.44	−0.1 ± 0.4	0.0 ± 0.3	0.85	0.29
Focus on eating behavior	0.3 ± 0.3	0.3 ± 0.2	0.38	0.10	0.2 ± 0.3	0.3 ± 0.1	1.72	0.63
Total quality of life	1.3 ± 1.1	1.8 ± 0.7	1.87	0.62	0.8 ± 1.2	1.3 ± 1.0*	2.57	0.47

Values are group mean±SD.

$^{*}p < 0.05$, Paired t-test, post values compared with pre.

$^{@}p < 0.05$, Unpaired t-test, post values compared with post.

$^{\#}p < 0.05$, Unpaired t-test, pre values compared with pre.

volume index, and increase in total cholesterol and LDL cholesterol. The yoga group at the end of 12 weeks showed a decrease in waist circumference, sagittal abdominal diameter, hip circumference, BMI, waist-hip ratio, a body shape index, conicity index, abdominal volume index, body roundness index, HDL cholesterol, and better total quality of life. When both groups were considered as two age ranges (i.e., 30–45 and 46–59 years), the results were different. For the 30–45 years age group the nutritional advice group showed no change after 12 weeks whereas the yoga group showed most of the changes mentioned above for the group as a whole. In contrast to this for the 46–59 year age group, the nutritional advice and yoga groups showed comparable benefits with reduction in most-anthropometric measures and indices at 12 weeks. Hence yoga may be especially useful for adult females between 30 and 45 years of age.

The waist circumference, hip circumference, abdominal volume index, and body roundness decreased in both groups irrespective of age. The waist circumference correlates with increased risk of cardiovascular disease (25), the abdominal volume index has been correlated with impaired glucose tolerance and higher incidence of type 2 DM and metabolic syndrome (26). Body roundness index was associated with higher occurrence of non-alcoholic fatty liver disease (27). Hence the risk of these conditions could be considered to be lower in both groups at 12 weeks. The other changes in the yoga group also suggest a reduction in the risk of

developing obesity associated diseases such as carotid artery stiffness (28) and insulin resistance (29), based on a decrease in SAD, cardiovascular disease (based on reduction in waist-hip ratio and conicity index (30), and cardiometabolic disease (based on reduced a body shape index and BMI) (31). Hence these risk factors reduced in the yoga group irrespective of age.

The serum lipid profile was assessed using quantitative methods. The yoga group showed a significant decrease in HDL cholesterol. This reduction in HDL cholesterol has been seen in two other studies, in which obese participants received yoga for 6 days and 15 days (32, 33). In both studies participants consumed a plant based lacto vegetarian diet comparable to that of the present study. In another study, 12 weeks of yoga practice resulted in a significant decrease in total cholesterol, triglycerides and LDL levels with a non-significant increase in HDL levels (34). The participants' diet was not described. It has been observed that those diets which are most effective in reducing the risk of atherosclerosis are usually associated with the greatest decrease in protective HDL cholesterol levels (35–37). These diets are typically plant based high fiber low fat diets. However this reduction in protective HDL cholesterol levels following such diets need not necessarily be harmful as separate studies have shown that even if HDL levels decrease, the anti-inflammatory efficacy of HDL cholesterol may be enhanced despite reduction in absolute levels of HDL (38, 39).

In the nutritional advice group there was a significant increase in total cholesterol, and LDL levels. The explanation for this increase is not clear as the nutritional advice group was given the same dietary instructions as the yoga group. Mental stress levels have a positive correlation with total cholesterol, triglycerides and LDL cholesterol levels (40–42). Practicing yoga is one of the methods for stress reduction. Even though the stress levels were not measured in the present study it may be speculated that in the absence of yoga intervention the nutritional advice group continued to experience higher stress levels which contributed to the increase in total cholesterol, and LDL cholesterol levels. Though this is a speculation it is supported by the results of the participants' response to the six items of the Moorehead-Ardelt Quality of Life Questionnaire.

The yoga group showed significantly higher scores in focus on eating behavior (an aspect of quality of life) and total quality of life after 12 weeks. Previously the Moorehead-Ardelt Quality of Life Questionnaire has been used to compare the quality of life in obese persons who were experienced in yoga compared to those without any yoga experience and demonstrated a better quality of life in the group with prior yoga experience (43). These findings are of importance as psychological wellbeing is important for the long term successful management of obesity (44).

The centrally obese participants of the present trial showed no differences in their energy intake or energy expenditure after 12 weeks irrespective of the group to which they belonged. Energy intake was derived from the 24 h diet recall questionnaire which does not give an accurate idea of the diet during the 12 week period. Hence though the present results suggest that the energy intake in a day did not differ significantly with the energy expenditure in a day, between groups after 12 weeks it must be emphasized that both energy intake/day and energy expenditure/day were assessed by qualitative methods which lack the accuracy and objectivity of quantitative assessments.

The main limitations of the present findings are the study design and small sample size. Both the yoga and nutritional advice groups were given their intervention based on convenience, though the nutritional advice group did express an interest to learn yoga at some stage after the trial. The ideal design would have been a randomized controlled trial but after recruitment it was clear that though the participants were motivated to learn yoga, for personal reasons such as time constraints they were unable to state that they could complete 12 weeks of yoga practice successfully. This point demonstrates the practical difficulties a person may have in learning and practicing any intervention. Apart from this, though the supine sagittal abdominal diameter through anthropometry is an acceptable method to measure visceral adipose tissue, magnetic resonance imaging (MRI), dual-energy x-ray absorptiometry (DEXA), and computed tomography (CT) scans would be more accurate (30). To distinguish between types of adipose tissue in central obesity these methods are essential. The other limitations include the lack of quantitative measures to assess energy expenditure/day and energy intake/day. Also the present sample included females alone, all of whom were generational vegetarians. Hence generalizing the findings cannot be done.

CONCLUSIONS

Yoga and nutritional advice with a diet plan can reduce anthropometric measures associated with diseases related to central obesity, with more changes in the yoga group. This difference was greater for the 30–45 years age range, where the nutritional advice group showed no change; while changes were comparable for the two groups in the 46–59 year age range. Hence yoga may be especially useful for adult females with central obesity between 30 and 45 years of age.

AUTHOR CONTRIBUTION

ST, SS, and AB designed the study. NK and SP performed data collection and analyses. ST and SS wrote the manuscript. NK, SP, and RG prepared the manuscript. ST, SS, NK, SP, RG, and AB proofread the manuscript.

FUNDING

The study was funded by Patanjali Research Foundation (Trust), Haridwar, India.

ACKNOWLEDGMENTS

The authors gratefully acknowledge the help of Dr. Jaideep Arya, Chief Central Coordinator of Patanjali Yog Samiti, Haridwar,

Uttarakhand, India. The meticulous work of slide preparation for the nutritional advice group and the arrangement of data by Deepshikha Tyagi, Babita Vishwakarma, Kumar Gandharva, Savita Agnihotri, Alok Singh, Sadhna Verma, Deepak Pal, and Ankit Gupta was an important and indispensable contribution.

SUPPLEMENTARY MATERIAL

The Supplementary Material for this article can be found online at: https://www.frontiersin.org/articles/10.3389/fendo.2018.00466/full#supplementary-material

REFERENCES

1. Pradeepa R, Anjana RM, Joshi SR, Bhansali A, Deepa M, Joshi PP, et al. Prevalence of generalized & abdominal obesity in urban & rural India- the ICMR - INDIAB Study (Phase-I) [ICMR-INDIAB-3]. *Indian J Med Res.* (2015) 142:139–50. doi: 10.4103/0971-5916.164234
2. World Health Organization. *The Asia-Pacific Perspective: Redefining Obesity and its Treatment*. St Leonards, NSW: Health Communications Australia Pty Limited (2000).
3. Harrison GG, Buskirk ER, Carter L, Johnston FE, Lohman TG, Pollock ML, et al. Skinfold thickness and measurement technique. In: Lohman TG, Roche AF, Martorell R, editors. *Anthropometric Standardization Reference Manual*. Champaign, IL: Human Kinetics Books (1988). p. 55–60.
4. Jensen MD, Ryan DH, Apovian CM, Ard JD, Comuzzie AG, Donato KA, et al. 2013 AHA/ACC/TOS guideline for the management of overweight and obesity in adults: a report of the American College of Cardiology/American Heart Association task force on practice guidelines and the obesity society. *Circulation* (2014) 63:2985–3023. doi: 10.1161/01.cir.0000437739.71477.ee
5. Ball K, Crawford D, Owen N. Too fat to exercise? Obesity as a barrier to physical activity. *Aust N Z J Public Health* (2000) 24:331–3. doi: 10.1111/j.1467-842X.2000.tb01579.x
6. Naveen GH, Varambally S, Thirthalli J, Rao M, Christopher R, Gangadhar BN. Serum cortisol and BDNF in patients with major depression—effect of yoga. *Int Rev Psychiatry* (2016) 28:273–8. doi: 10.1080/09540261.2016.1175419
7. Lauche R, Langhorst J, Lee MS, Dobos G, Cramer H. A systematic review and meta-analysis on the effects of yoga on weight-related outcomes. *Prev Med.* (2016) 87: 213–32. doi: 10.1016/j.ypmed.2016.03.013
8. Cramer H, Thoms MS, Anheyer D, Lauche R, Dobos G. Yoga in women with abdominal obesity: a randomized controlled trial. *Dtsch Arztebl Int.* (2016) 113:645–52. doi: 10.3238/arztebl.2016.0645
9. Wang H, Liu A, Zhao T, Gong X, Pang T, Zhou Y, et al. Comparison of anthropometric indices for predicting the risk of metabolic syndrome and its components in Chinese adults: a prospective, longitudinal study. *BMJ Open* (2017) 7:e016062. doi: 10.1136/bmjopen-2017-016062
10. Erdfelder, E, Faul, F, Buchner, A. GPOWER: A general power analysis program. *Behav Res Methods Instrum Comput* (1996) 28:1–11.
11. International Diabetes Federation. *The IDF Consensus Worldwide Definition of the Metabolic Syndrome*. (2006). Available online at: https://www.idf.org/our-activities/advocacy-awareness/resources-and-tools/60:idfconsensus-worldwide-definitionof-the-metabolic-syndrome.html
12. I Government Health. *India Reworks Obesity Guidelines, BMI Lowered*. (2010). Available online at: http://www.igovernment.in/articles/26259/india-reworks-obesity-guidelines-bmi-lowered
13. National Institute of Nutrition. *Dietary Guidelines for Indians-A Manual*. Hyderabad: National Institute of Nutrition (2011).
14. Yim JY, Kim D, Lim SH, Park MJ, Choi SH, Lee CH, et al. Sagittal abdominal diameter is a strong anthropometric measure of visceral adipose tissue in the Asian general population. *Diabetes Care* (2010) 33:2665–70. doi: 10.2337/dc10-0606
15. Amato MC, Giordano C, Galia M, Criscimanna A, Vitabile S, Midiri M, et al. Visceral adiposity index: a reliable indicator of visceral fat function associated with cardiometabolic risk. *Diabetes Care* (2010) 33:920–22. doi: 10.2337/dc09-1825
16. Zhang ZQ, Deng J, He LP, Ling WH, Su YX, Chen YM. Comparison of various anthropometric and body fat indices in identifying cardiometabolic disturbances in Chinese men and women. *PLoS ONE* (2013) 8:e70893. doi: 10.1371/journal.pone.0070893
17. Kang SH, Cho KH, Park JW, Do JY. Comparison of waist to height ratio and body indices for prediction of metabolic disturbances in the Korean population: the Korean National Health and Nutrition Examination Survey 2008-2011. *BMC Endocr Disord.* (2015) 15:79. doi: 10.1186/s12902-015-0075-5
18. Tripolino C, Irace C, Carallo C, Scavelli FB, Gnasso A. Body fat and blood rheology: evaluation of the association between different adiposity indices and blood viscosity. *Clin Hemorheol Microcirc* (2017) 65:241–48. doi: 10.3233/CH-16172
19. Telles S, Bhardwaj AK, Gupta RK, Kumar A, Balkrishna A. Development of a food frequency questionnaire to assess dietary intake for the residents of the Northern Region of India. *IJAMY* (2016) 9:139–47. doi: 10.21088/ijamy.0974.6986.9416.2
20. Medindia. *Calories in Indian Food*. Available online at: https://www.medindia.net/calories-in-indian-food/index.asp
21. Craig CL, Marshall AL, Sjöström M, Bauman AE, Booth ML, Ainsworth BE, et al. International physical activity questionnaire: 12-country reliability and validity. *Med Sci Sports Exerc.* (2003) 35:1381–95. doi: 10.1249/01.MSS.0000078924.61453.FB
22. IPAQ Research Committee. *Guidelines for Data Processing and Analysis of the International Physical Activity Questionnaire (IPAQ)–Short and Long Forms*. (2005). Available online at: www.ipaq.ki.se
23. Mifflin MD, St Jeor ST, Hill LA, Scott BJ, Daugherty SA, Koh YO. A new predictive equation for resting energy expenditure in healthy individuals. *Am J Clin Nutr.* (1990) 51:241–47. doi: 10.1093/ajcn/51.2.241
24. Myers JA, Clifford JC, Sarker S, Primeau M, Doninger GL, Shayani V. Quality of life after laparoscopic adjustable gastric banding using the Baros and Moorehead-Ardelt quality of life questionnaire II. *JSLS* (2006) 10:414–20.
25. Goh LG, Dhaliwal SS, Welborn TA, Lee AH, Della PR. Anthropometric measurements of general and central obesity and the prediction of cardiovascular disease risk in women: a cross-sectional study. *BMJ Open* (2014) 4:e004138. doi: 10.1136/bmjopen-2013-004138
26. Guerrero-Romero F, Rodríguez-Morán M. Abdominal volume index. An anthropometry-based index for estimation of obesity is strongly related to impaired glucose tolerance and type 2 diabetes mellitus. *Arch Med Res.* (2003) 34:428–32. doi: 10.1016/S0188-4409(03)00073-0
27. Motamed N, Rabiee B, Hemasi GR, Ajdarkosh H, Khonsari MR, Maadi M, et al. Body roundness index and waist-to-height ratio are strongly associated with non-alcoholic fatty liver disease: a population-based study. *Hepat Mon* (2016) 16:e39575. doi: 10.5812/hepatmon.39575
28. Lefferts WK, Sperry SD, Jorgensen RS, Kasprowicz AG, Skilton MR, Figueroa A, et al. Carotid stiffness, extra-media thickness and visceral adiposity in young adults. *Atherosclerosis* (2017) 265:140–6. doi: 10.1016/j.atherosclerosis.2017.08.033
29. Vasques AC, Cassani RS, Forti AC, Vilela BS, Pareja JC, Tambascia MA, et al. Sagittal abdominal diameter as a surrogate marker of insulin resistance in an admixtured population–brazilian metabolic syndrome study (BRAMS). *PLoS ONE* (2015) 10:e0125365. doi: 10.1371/journal.pone.0125365
30. Motamed N, Perumal D, Zamani F, Ashrafi H, Haghjoo M, Saeedian FS, et al. Conicity Index and waist-to-hip ratio are superior obesity indices in predicting 10-Year cardiovascular risk among men and women. *Clin Cardiol* (2015) 38:527–34. doi: 10.1002/clc.22437
31. Bertoli S, Leone A, Krakauer NY, Bedogni G, Vanzulli A, Redaelli VI, et al. Association of Body Shape Index (ABSI) with cardio-metabolic risk factors: a cross-sectional study of 6081 Caucasian adults. *PLoS ONE* (2017)12:e0185013. doi: 10.1371/journal.pone.0185013
32. Telles S, Naveen VK, Balkrishna A, Kumar S. Short term health impact of a yoga and diet change program on obesity. *Med Sci Monit.* (2010) 16:CR35–40.
33. Telles S, Sharma SK, Yadav A, Singh N, Balkrishna A. A comparative controlled trial comparing the effects of yoga and walking for overweight

and obese adults. *Med Sci Monit.* (2014) 20:894–904. doi: 10.12659/MSM.889805
34. Shantakumari N, Sequeira S. Effects of a yoga intervention on lipid profiles of diabetes patients with dyslipidemia. *Indian Heart J.* (2013) 65:127–31. doi: 10.1016/j.ihj.2013.02.010
35. Schaefer EJ, Levy RI, Ernst ND, Van Sant FD, Brewer HB Jr. The effects of low cholesterol, high polyunsaturated fat, and low fat diets on plasma lipid and lipoprotein cholesterol levels in normal and hypercholesterolemic subjects. *Am J Clin Nutr.* (1981) 34:1758–63.
36. Zanni EE, Zannis VI, Blum CB, Herbert PN, Breslow JL. Effect of egg cholesterol and dietary fats on plasma lipids, lipoproteins, and apoproteins of normal women consuming natural diets. *J Lipid Res.* (1987) 28:518–27.
37. Ehnholm C, Huttunen JK, Pietinen P, Leino U, Mutanen M, Kostiainen E, et al. Effect of diet on serum lipoproteins in a population with a high risk of coronary heart disease. *N Engl J Med.* (1982) 307:850–5. doi: 10.1056/NEJM198209303071403
38. Kent L, Morton D, Rankin P, Ward E, Grant R, Gobble J, et al. The effect of a low-fat, plant-based lifestyle intervention (CHIP) on serum HDL levels and the implications for metabolic syndrome status - a cohort study. *Nutr Metab.* (2013) 10:58. doi: 10.1186/1743-7075-10-58
39. Roberts CK, Barnard RJ. Effects of exercise and diet on chronic disease. *J Appl Physiol.* (2005) 98:3–30. doi: 10.1152/japplphysiol.00852.2004
40. Grundy SM, Griffin AC. Effects of periodic mental stress on serum cholesterol levels. *Circulation* (1959) 19:496–8. doi: 10.1161/01.CIR.19.4.496
41. Siegrist J, Matschinger H, Cremer P, Seidel D. Atherogenic risk in men suffering from occupational stress. *Atherosclerosis* (1988) 69:211–18.
42. Grundy SM, Griffin AC. Relationship of periodic mental stress to serum lipoprotein and cholesterol levels. *JAMA* (1959) 171:1794–96. doi: 10.1001/jama.1959.03010310026007
43. Sharma SK, Kala N, Telles S, Arya J, Balkrishna A. A comparison of the quality of life in obese persons based on experience of yoga practice. *IJTK* (2016) 16:17–20. Available online at: http://nopr.niscair.res.in/handle/123456789/42287
44. Ross A, Brooks A, Leonard KT, Wallen G. A different weight loss experience: a qualitative study exploring the behavioral, physical, and psychosocial changes associated with yoga that promote weight loss. *Evid Based Complement Alternat Med.* (2016) 2016:1–11. doi: 10.1155/2016/2914745

Conflict of Interest Statement: The authors declare that the research was conducted in the absence of any commercial or financial relationships that could be construed as a potential conflict of interest.

The reviewer OH and handling Editor declared their shared affiliation.

Advantages of publishing in Frontiers

OPEN ACCESS
Articles are free to read for greatest visibility and readership

FAST PUBLICATION
Around 90 days from submission to decision

HIGH QUALITY PEER-REVIEW
Rigorous, collaborative, and constructive peer-review

TRANSPARENT PEER-REVIEW
Editors and reviewers acknowledged by name on published articles

Frontiers
Avenue du Tribunal-Fédéral 34
1005 Lausanne | Switzerland

Visit us: www.frontiersin.org
Contact us: info@frontiersin.org | +41 21 510 17 00

REPRODUCIBILITY OF RESEARCH
Support open data and methods to enhance research reproducibility

DIGITAL PUBLISHING
Articles designed for optimal readership across devices

FOLLOW US
@frontiersin

IMPACT METRICS
Advanced article metrics track visibility across digital media

EXTENSIVE PROMOTION
Marketing and promotion of impactful research

LOOP RESEARCH NETWORK
Our network increases your article's readership